September 2015

Revision 15A

MAGNATRAN

(**M**odular **A**dvanced **G**eneration **N**uclear **A**ll-purpose **TRANsport**)

MAGNATRAN RAI Response Package Submittal

Book 1 of 1

NON-PROPRIETARY VERSION

Docket No. 71-9356

NAC INTERNATIONAL

Atlanta Corporate Headquarters: 3930 East Jones Bridge Road, Norcross, Georgia 30092 USA
Phone 770-447-1144, Fax 770-447-1797, www.nacintl.com

Enclosure 1

RAI Responses

No. 71-9356 for the MAGNATRAN Cask

MAGNATRAN SAR, Revision 15A

NAC INTERNATIONAL

RESPONSE TO THE

UNITED STATES
NUCLEAR REGULATORY COMMISSION

REQUEST FOR ADDITIONAL INFORMATION
(PROPRIETARY REQUESTS)

June 2015

FOR REVIEW OF THE CERTIFICATE OF COMPLIANCE NO. 9356, MAGNATRAN TRANSPORATION PACKAGE

(CoC NO. 9356 DOCKET NO. 71-9356)

September 2015

Table of Contents

GENERAL INFORMATION EVALUATION 3
STRUCTURAL EVALUATION 4
MATERIALS EVALUATION 5
THERMAL EVALUATION 5
CONTAINMENT EVALUATION 12
SHIELDING EVALUATION 13
CRITICALITY EVALUATION 14
OPERATING PROCEDURES EVALUATION 18
ACCEPTANCE AND MAINTENANCE TESTS EVALUATION 19

NAC INTERNATIONAL RESPONSE TO REQUEST FOR ADDITIONAL INFORMATION

GENERAL INFORMATION EVALUATION

All questions are non-proprietary. See non-proprietary RAI responses.

NAC INTERNATIONAL RESPONSE TO REQUEST FOR ADDITIONAL INFORMATION

STRUCTURAL EVALUATION

All questions are non-proprietary. See non-proprietary RAI responses.

NAC INTERNATIONAL RESPONSE TO REQUEST FOR ADDITIONAL INFORMATION

MATERIALS EVALUATION

All questions are non-proprietary. See non-proprietary RAI responses.

NAC INTERNATIONAL RESPONSE TO REQUEST FOR ADDITIONAL INFORMATION

THERMAL EVALUATION

3-1 See non-proprietary RAI responses.

NAC INTERNATIONAL RESPONSE TO REQUEST FOR ADDITIONAL INFORMATION

THERMAL EVALUATION

3-2P [redacted]

This information is needed to confirm compliance with Title 10 of the *Code of Federal Regulations* (10 CFR) 71.73.

NAC International Response to Thermal Evaluation RAI 3-2P:

[redacted]

NAC INTERNATIONAL RESPONSE TO REQUEST FOR ADDITIONAL INFORMATION

THERMAL EVALUATION

3-3 See non-proprietary RAI responses.

NAC INTERNATIONAL RESPONSE TO REQUEST FOR ADDITIONAL INFORMATION

THERMAL EVALUATION

3-4 See non-proprietary RAI responses.

NAC INTERNATIONAL RESPONSE TO REQUEST FOR ADDITIONAL INFORMATION

THERMAL EVALUATION

3-5P [redacted]

This information is needed to determine compliance with 10 CFR 71.73.

NAC International Response to Thermal Evaluation RAI 3-5P:

[redacted]

NAC INTERNATIONAL RESPONSE TO REQUEST FOR ADDITIONAL INFORMATION

THERMAL EVALUATION

3-6 thru 3-15, see non-proprietary RAI responses.

NAC INTERNATIONAL RESPONSE TO REQUEST FOR ADDITIONAL INFORMATION

CONTAINMENT EVALUATION

No questions.

NAC INTERNATIONAL RESPONSE TO REQUEST FOR ADDITIONAL INFORMATION

SHIELDING EVALUATION

All questions are non-proprietary. See non-proprietary RAI responses.

NAC INTERNATIONAL RESPONSE TO REQUEST FOR ADDITIONAL INFORMATION

CRITICALITY EVALUATION

6-1P [redacted]

This information is needed to confirm compliance with 71.55(b).

NAC International Response to Criticality Evaluation RAI 6-1P:

[redacted]

[redacted]

NAC INTERNATIONAL RESPONSE TO REQUEST FOR ADDITIONAL INFORMATION

CRITICALITY EVALUATION

6-2P [redacted]

This information is needed to determine compliance with 10 CFR 71.55(b).

NAC International Response to Criticality Evaluation RAI 6-2P:

[redacted]

NAC INTERNATIONAL RESPONSE TO REQUEST FOR ADDITIONAL INFORMATION

CRITICALITY EVALUATION

6-3 thru 6-7, see non-proprietary RAI responses.

NAC INTERNATIONAL RESPONSE TO REQUEST FOR ADDITIONAL INFORMATION

OPERATING PROCEDURES EVALUATION

All questions are non-proprietary. See non-proprietary RAI responses.

NAC INTERNATIONAL RESPONSE TO REQUEST FOR ADDITIONAL INFORMATION

ACCEPTANCE AND MAINTENANCE TESTS EVALUATION

All questions are non-proprietary. See non-proprietary RAI responses.

NAC INTERNATIONAL

RESPONSE TO THE

UNITED STATES
NUCLEAR REGULATORY COMMISSION

REQUEST FOR ADDITIONAL INFORMATION
(NON-PROPRIETARY REQUESTS)

June 2015

FOR REVIEW OF THE CERTIFICATE OF COMPLIANCE NO. 9356, MAGNATRAN TRANSPORATION PACKAGE

(CoC NO. 9356 DOCKET NO. 71-9356)

September 2015

Table of Contents

GENERAL INFORMATION EVALUATION 3
STRUCTURAL EVALUATION 11
THERMAL EVALUATION 17
CONTAINMENT EVALUATION 62
SHIELDING EVALUATION 63
CRITICALITY EVALUATION 70
OPERATING PROCEDURES EVALUATION 79
ACCEPTANCE AND MAINTENANCE EVALUATION 86

NAC INTERNATIONAL RESPONSE TO REQUEST FOR ADDITIONAL INFORMATION

GENERAL INFORMATION EVALUATION

1-1 Provide the following information:

a. Revise Section 1.3.2, "Contents" to ensure that the description of the contents is consistent with the rest of the SAR. Item 12.i. on page 1.3-28 states "Spent fuel content shall be loaded in accordance with the loading tables in Chapter 5, Section 5.8.10 and Table 5.8-49 of this SAR." Section 5.8.10, does not appear to contain any loading tables.

b. Specification regarding application of the specific activity limit for greater than class C (GTCC) waste contents. While a package may be loaded with material that may have the allowable specific activity when averaged over the entire contents; this averaging allows potentially significant variations in specific activity in the contents. This variation could result in much higher dose rates than analyzed. Thus, the specific activity limits should include limits on potential variability of GTCC activity.

c. Specification of replacement rods for boiling-water reactor (BWR) fuel as solid, unirradiated rods, or, with appropriate analysis, the applicant could provide a specification similar to that for pressurized- water reactor (PWR) fuel. The PWR content limits include a restriction on the number of irradiated steel replacement rods in an assembly, their exposure and cooling time, and the number of assemblies in the package with these rods. The current application only appears to support use of solid, unirradiated replacement rods for BWR contents.

d. Maximum exposure and minimum cooling time limits for Combustion Engineering (CE) neutron source assemblies. No specifications are currently provided, and it is not clear that control element assemblies (CEAs) bound neutron source assemblies (NSAs) since NSAs have steel/Inconel components in the active fuel zone whereas CEAs do not.

e. Clarification of the cooling times for PWR assemblies with irradiated steel replacement rods. It appears that PWR assemblies with irradiated steel replacement rods must be cooled an additional year, but also have minimum cooling times not less than 20 years.

f. Minimum density and hydrogen content for the neutron shield (Drawing Nos. 71160-502-3P and 71160-502-3NP). These specifications, together with the B_4C content limit (already included on the drawing), are important for the shield's performance.

g. Confirmation that damaged Combustion Engineering (CE) 16x16 fuel (fuel type 16a) is not an allowable package content. The calculation package 71160-5508, Revision 0, indicates that damaged CE 16x16 fuel is not an allowed content; however, the application does not clearly indicate one way or the other.

h. Clarification of the additional cooling time requirements for fuel in damaged fuel transportable storage canisters (DF TSCs). It appears that the additional cooling time applies to all assemblies (damaged and undamaged) in the DF TSC when damaged fuel is present and that this cooling time is, for undamaged assemblies, in addition to any cooling time that must be added for loading of non-fuel hardware.

i. Clarification that CE burnable poison rod assemblies (BPRAs) and thimble plug devices (TPDs) are not allowed contents. The shielding analysis (application Section 5.8.5) does not include CE BPRAs or TPDs as contents. However, per Section 5.8.10.2, Table 5.8-49 includes additional cooling time requirements for CE 14x14 assemblies with BPRAs or TPDs when these assemblies are loaded with damaged fuel in the DF TSC.

j. Clarification whether damaged fuel with enrichments as low as 1.3 weight percent are allowed contents. It is not clear that the damaged fuel shielding analysis covers these low enrichments.

k. Clarification that the added cooling times applied to DF TSC contents when damaged fuel is loaded also apply when high burnup fuel is loaded. Since high burnup fuel is treated as damaged fuel regardless of its actual physical condition at loading, the contents specifications should state that contents requirements for the DF TSC when loaded with damaged fuel also apply when the TSC is loaded with high burnup fuel.

l. Tolerances on the technical drawings for items relied on in the shielding analysis. It is not clear that the drawings include the tolerances for items important to shielding (e.g., thickness of the package's lead shielding, steel inner and outer shells, neutron shield assembly components, lid, and base). It is also unclear that the dimensions in the shielding analysis are consistent with the package's tolerances.

Shielding analyses should be modified, as necessary, to support the proposed contents specifications and package tolerances.

This information is needed to confirm compliance with 10 CFR 71.33 and 71.35(a).

NAC International Response to General Information Evaluation RAI 1-1:

a. Table 5.8-49 in Section 5.8.10 lists the fuel cool time increase (delta cool time from undamaged) required for loading fuel assembly contents into a TSC with DF Basket when DF material is present. Item 12.i is updated to reflect the purpose of Table 5.8-49 and includes the reference to the baseline undamaged fuel load tables (Section 5.3) modified by this information.
b. GTCC activity limits (as seen in Section 1.3.2, item 7) are on a per pound basis, restricting the potential of significant variations in specific activity and higher than calculated dose rates.
c. The reviewer is correct with the observation; the PWR fuel assembly expanded definition of replacement rods is not adopted for BWR assemblies. The SAR contains no justification, and therefore, no allowance for the PWR definition to be applicable to BWR fuel. Section 1.3.2, Item 13.m, which states that a BWR assembly may contain solid filler rods, is revised to clarify that these rods must be "unirradiated."
d. NSAs are removed as a possible payload for CE type (CE14 and CE16) fuel assemblies. Table 1.3-16 is revised to remove the additional fuel time indicated for loading in the CE14 and CE16 fuel types. Section 1.3.2, items 11.m. and 12.p are revised to clarify which assembly types may contain NSAs. Section 5.8.5 is revised to state that CE14 and CE16 fuel types are not allowed to be loaded with NSAs.
e. The reviewer is correct. A 20-year cool time was used in the cobalt source generation and the analysis documented an additional year cool time required on the fuel assembly containing the activated rods to compensate for the additional source. This leads to a minimum 21-year requirement for fuel containing activated stainless replacement rods. Section 1.3.2, item 11.n is updated to clarify the appropriate cool time for assemblies with activated steel replacement rods, i.e., a minimum 21 years or cool time table documented value plus one year, whichever is greater.
f. The evaluated hydrogen content of the neutron shield is 6 weight percent (0.0979 g/cm^3) with an overall shield material density of 1.632 g/cm^3. NS-4-FR neutron shield hydrogen content and overall material minimum density are added to drawings 71160-502-3P and 71160-502-3NP.
g. Note Section 1.3.2, item 12.t is added (page 1.3-31) to clarify that damaged CE 16×16 is not allowed content in the MAGNATRAN system. Correspondingly, as this application treats HBU fuel (>45 GWd/MTU) as damaged, HBU CE 16×16 is not allowed content in the MAGNATRAN system.
h. The additional cool time required to load damaged fuel applies to the entire payload. Section 1.3.2, Item 12.i is updated to clarify additional cool applies to all assemblies in the DF TSC.
i. The reviewer is correct with the observation, CE BPRAs and TPs are not evaluated. Table 5.8-49 contains additional cool time to load damaged fuel. It is applicable to fuel assemblies regardless of NFHW content. In the case of the CE assemblies, it means it is applicable to damaged fuel with no NFHW. Section 5.8.10.2 is updated to clarify the contents of Table 5.8-49. A note is added to Section 1.3.2, item 11.i and 12.l to indicate

that CE14 and CE16 fuel types are not permitted to be loaded with BPRA or TP nonfuel hardware.

j. Low enrichment damaged fuel is allowed. Damaged PWR fuel uses the non-damaged loading tables with the augmented additional cool time from Table 5.8-49 when applicable. Low enrichment and low burnup PWR fuel loading are shown in Table 5.8-14b. No additional cool time (Table 5.8-49) is needed for low burnup PWR fuel when transporting damaged fuel. Section 5.8.10.2 is revised throughout to clarify that the low burnup tables are applicable to damaged fuel.
k. Section 1.3.2, item 12.i is updated to clarify that the additional cool time from Table 5.8-49 applies to HBU loadings, as HBU material is treated as damaged within the application.
l. Tolerances are on the technical drawings.

NAC INTERNATIONAL RESPONSE TO REQUEST FOR ADDITIONAL INFORMATION

GENERAL INFORMATION EVALUATION

1-2 Specify on Drawing No. 71160-505 (sheet 1 of 4) the type of metallic seal and the materials of construction of the seal. Provide justification for the lower temperature use for the metallic O-ring specified on the drawing.

NRC's request for additional information (RAI) question 3-5c, in the non-proprietary enclosure to NRC letter dated September 10, 2013 (Agencywide Documents Access and Management System (ADAMS) Accession No. ML13254A109) asked for references for the minimal acceptable operating temperature for normal conditions of transport "Cold" at -40°F for the components in the table in Section 3.3.2 of the SAR. Note that the safe operating range of the metallic O-rings is obtained from the technical information presented in section 4.5.2 of the SAR. This section is Helicoflex literature which only specifies the upper operating temperature. The lower operating temperature is not provided. NRC's question 1-5c in the non-proprietary enclosure to NRC letter dated September 10, 2013, stated that Drawing No. 71160-505 (sheet 1 of 4) lists the metallic O-ring and EPDM O-ring as commercial, but there are many different construction and materials used in the metallic O-rings that are "commercial," which may affect the ability of these components to work properly within the specified temperature range.

The response to NRC's question 3-5c referred to a manufacturers catalogue of specifications. There are many configurations of metallic O-rings but since only the section dealing with Helicoflex was provided, NRC staff assumes that Helicoflex will be the metallic O-ring used in the MAGNATRAN packaging. This should be stated on the governing drawings. The catalogue further indicated on page 0 that there were a variety of materials that could be used in the seals and the maximum temperature of use depended on the size of the O-ring and material used. Neither was specified on the drawing or the SAR. Some of these temperatures could be below the temperatures specified in the Table in SAR Section 3.3.2.

The only mention of lower usable temperatures was a general note i,e., [sic] "General characteristics – temperatures from -172°C up to 800°C." No mention was made of which O-ring designs these temperatures applied to. The NRC can only assume that this temperature range brackets all Helicoflex O-rings and materials used. It could also be assumed that particular O-ring sizes and materials would have a more limited range.

This information is needed to confirm compliance with 10 CFR 71.52, 10 CFR 71.71, and 10 CFR 71.73.

NAC International Response to General Information Evaluation RAI 1-2:

Specific part numbers are added to the 71160-505 license drawing for the metal O-ring seals for the lid and port cover. Manufacturer drawings detail the significant material and performance attributes of the O-rings. As detailed, the specified seals have a working temperature range inclusive of -40°F to 550°F. These are exemplar seals in that they meet the application requirements and have a compression force enveloped by the structural evaluation and the bolt preload.

NAC INTERNATIONAL RESPONSE TO REQUEST FOR ADDITIONAL INFORMATION

GENERAL INFORMATION EVALUATION

1-3 Specify on the drawings that the bolts will be procured in accordance with the American Society of Mechanical Engineers materials specification SB-637.

The bolts that are used to fasten the MAGNATRAN lid to the top forging of the packaging body are fabricated from ASME SB-637, Grade N07718, nickel alloy (see SAR Section 2.1.2.2). The ductile-to-brittle transition temperature of this steel is below the expected operating temperatures, so brittle fracture of the bolts is not expected. Procurement of the bolts in accordance with the ASME SB 637 specification will ensure that the material receives the proper heat treatment and possesses the required mechanical propertied

This information is needed to determine compliance with 10 CFR Part 71.

NAC International Response to General Information Evaluation RAI 1-3:

License Drawing 71160-504, Rev. 1 details the material of the bolts is ASME SB637, Grade N07718 as noted. Therefore, no changes are required.

NAC INTERNATIONAL RESPONSE TO REQUEST FOR ADDITIONAL INFORMATION

GENERAL INFORMATION EVALUATION

1-4 Indicate on Drawing No. 71160-502, sheets 7 and 8, that note Δ12 (regarding the dye penetrate test) applies the closure welds on the stainless steel cladding of the neutron shields not only the attachment of the neutron shields to the cask body.

NRC question 2-11 in the non-proprietary enclosure to NRC letter dated September 10, 2013, requested the applicant to provide the applicable standards and codes, such as those presented in the MAGNASTOR SAR (Docket No. 72-1031), for the neutron shielding fabrication, examinations of the welds, and qualifications of the personnel. A liquid penetrant inspection of the neutron shield assembly welds with Note Δ12 as follows: "PT Final pass. Examined per ASME Section V, Article 6 with acceptance per Section III, Article NF-5350," was added to NAC drawing 71160-502, Revision 2P. The note was added for the welds of the neutron shield assembly to the cask body and not to the fabrication welds that sealed the stainless steel shell around the neutron absorber. This seal is necessary as it prevents the intrusion of water into the neutron shields material, which prevents degradation of the shield material.

This information is needed to determine compliance with 10 CFR Part 71.47(a).

NAC International Response to General Information Evaluation RAI 1-4:

Delta Note 15, "PT Final, Pass, Examine Per ASME Section V, Article 6. Acceptance Per ASME Section III, Article NF-5350," applies to the welds in question as indicated on sheet 6 of 8 of license drawing no. 71160-502 Rev. 4P. Therefore, no changes are required.

NAC INTERNATIONAL RESPONSE TO REQUEST FOR ADDITIONAL INFORMATION

STRUCTURAL EVALUATION

2-1 Revise the impact limiter dimension description on page 1.3-7 of the application.

On page 1.3-7 of the application, the impact limiter dimension description is "81 inches deep." The impact limiter dimension description should be consistent with that depicted in Drawing No. 71160-531, Rev. 1P, "66 inches deep."

This information is needed to confirm compliance with 10 CFR 71.33(a)(5).

NAC International Response to Structural Evaluation RAI 2-1:

The dimension has been revised on SAR page 1.3-7 to state the correction dimension of 66 inches.

NAC INTERNATIONAL RESPONSE TO REQUEST FOR ADDITIONAL INFORMATION

STRUCTURAL EVALUATION

2-2 Revise the following statement in Section 2.6.7.5 of the application, as appropriate, to recognize the use of a half-symmetry finite element analysis (FEA) model for evaluating the package subject to a side drop event.

Section 2.6.7.5 of the application states: "[T]he side drop simulations were performed using a quarter-symmetry model with a quarter of the package assembly in the finite element model..."

The staff notes that the boundary conditions associated with the inertia effects of a side drop cannot be properly modeled using only a quarter of the package in a FEA model.

This information is needed to confirm compliance with 10 CFR 71.33(a)(5).

NAC International Response to Structural Evaluation RAI 2-2:

The side drop simulations were performed using a quarter-symmetry model as shown in figure below. The description of the finite element models on SAR Page 2.6.7.5-8 has been clarified. SAR Figure 2.6.7-3 has been updated to include the quarter symmetry model.

The MAGNATRAN has identical impact limiters on both top and bottom ends. The geometric dimensions/ weights of both the impact limiters are the same. The size of metal structures, red woods and balsa woods in both top and bottom impact limiters are identical.

The total length of the transport ready cask with impact limiters is equal to 322 inch and its geometric center is at a distance of 161 inch from the ends of the impact limiters.

The center of gravity (CG) of the transport ready cask with impact limiters is located at a distance of 106 in (or 105 in, depending on the fuel type) from the base of the TSC. The distance of CG of the transport ready cask with impact limiters from the bottom end of the bottom impact limiter is equal to160 inch (or 159 inch, depending on the fuel type).

The maximum distance between the CG and the geometric center (eccentricity) is equal to 2 inch, which is equal to 0.6% of the overall length (322 inch) of the MAGNATRAN. This eccentricity is very small and does not affect the behavior of the MAGNATRAN during the side drop.

The details of the symmetry plane considered in the side drop is as shown in the Figure given below. One plane passes through the center of the package along the axial direction and another plane passes through the mid-height of the package in the transverse direction. The resulting model captures the behavior of the package during side drop event.

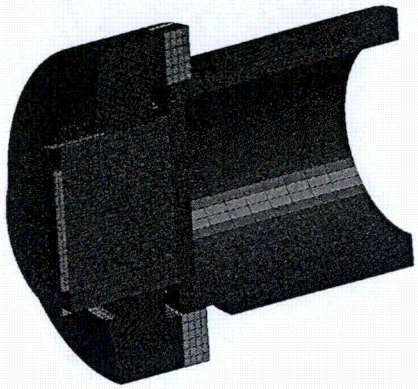

Quarter-Symmetry Model for Side Drop

NAC INTERNATIONAL RESPONSE TO REQUEST FOR ADDITIONAL INFORMATION

STRUCTURAL EVALUATION

2-3 Provide NAC Calculation No. 71160-2121, Rev. 0, "Gap Between the Lead and Steel Shells of the Transport Cask."

In its December 1, 2014, response to NRC's request for additional information (RAI), NAC introduces Revision 3 to Calculation No. 71160-2018, which changes the previously calculated lead slump of 2.33 inches to 0.87 inches at the top of the lead annulus. Section 6.1.5.3 of Calculation No. 71160-2018, Rev. 3, refers to Calculation No. 71160-2121, Rev. 0, for the calculation to which this new calculated lead slump is attributed. The subject calculation is not available to determining the shielding performance of the package associated with the package hypothetical accident condition free drop tests.

This information is needed to confirm compliance with 10 CFR 71.73(C)(1).

NAC International Response to Structural Evaluation RAI 2-3:

The calculation is being provided in the calculations enclosure of this submittal package.

NAC INTERNATIONAL RESPONSE TO REQUEST FOR ADDITIONAL INFORMATION

STRUCTURAL EVALUATION

2-4 Either 1) provide assurance that the neutron absorber plates have not degraded during storage to a condition where they cannot meet all regulatory requirements during transport or, 2) place a step in the operating procedure requiring, prior to loading stating "that using either operational experience, experimental data, or reference to an NRC approved calculation or guidance that option 1 is met."

NRC's question 6-1c in the non-proprietary enclosure to NRC letter dated September 10, 2013, asked the applicant to demonstrate that any material used as poison plates meets the assumptions used in the criticality safety analyses under all conditions specified in 10 CFR 71.71 and 10 CFR 71.73. The applicant's response was "Chapter 6 contains the criticality analysis of the poison plates. Chapter 8 contains the thermal and structural analyses of the poison plates. Section 8.1.5.1.3 contains acceptance testing, including the neutron attenuation capability related testing of the materials, and thermal and structural values, and states which poison plate material has what credit applied." The acceptance testing was prior to loading when the absorber plates were new. The thermal and structural analysis assumes that the absorber plates are in the as-manufactured condition. The canisters being loaded into the MAGNATRAN packaging were previously stored for an undetermined length of time stored in the MAGNASTOR storage cask. The analysis must account for any degradation in the absorber plates during the storage duration.

This information is needed to determine compliance with 10 CFR 71.55 and 10 CFR 71.59.

<u>NAC International Response to Materials Evaluation RAI 2-4:</u>

For loaded canisters affected by 10 CFR Part 72 "license renewal" actions, the operating procedure currently requires, prior to loading, a system specific review and assessment to ensure that the MAGNATRAN packaging certified content conditions are validated. This review would include verification that the neutron absorber plates have not degraded during storage to a condition where they cannot meet all regulatory requirements during transport. See SAR page 7.1-6, last sentence or top paragraph.

NAC INTERNATIONAL RESPONSE TO REQUEST FOR ADDITIONAL INFORMATION

STRUCTURAL EVALUATION

2-5 Provide reference(s) for all specified material properties, including emissivity, used as design basis throughout the SAR.

The application must include a description of the proposed package in sufficient detail to identify the package accurately and provide a sufficient basis for evaluation of the package.

This information is needed to determine compliance with 10 CFR 71.33.

NAC International Response to Materials Evaluation RAI 2-5:

NAC proprietary Calculation No. 71160-2101 Rev. 7 "Structural and Thermal Material Properties – MAGNASTOR/MAGNATRAN Cask Systems" is provided. All material properties used in the SAR, including references, are documented in this calculation.

NAC INTERNATIONAL RESPONSE TO REQUEST FOR ADDITIONAL INFORMATION

THERMAL EVALUATION

3-1 Provide energy balance calculations on the personnel barrier to determine its maximum temperature.

The NAC response to NRC's question 3-15 in letter dated January 13, 2015, stated that the personnel barrier temperature is an output from the FLUENT analysis. However, the reported temperature is a value at a certain location in the flowfield; the barrier was not modeled. Therefore, the reported temperature does not consider the influence of radiation heat transfer from the package's hot surface, etc. The energy balance calculation should be provided and assumptions used in the calculation justified, considering there is less than 20°F margin from the exclusive use, maximum temperature in the regulations.

This information is needed to confirm compliance with 10 CFR 71.43(g) and 10 CFR 71.71.

NAC International Response to Thermal Evaluation RAI 3-1:

A calculation was performed to determine the personnel barrier temperature increase due to radiation from the cask surface and from solar insolance. This results in a change of 1.25°F in the maximum temperature of the personnel barrier. Therefore, the maximum temperature of the personnel barrier is 163°F, which is within the maximum temperature of 185°F allowed for exclusive use.

The detailed calculations are documented in Appendix M of NAC calculation 71160-3045, Rev. 2.

NAC INTERNATIONAL RESPONSE TO REQUEST FOR ADDITIONAL INFORMATION

THERMAL EVALUATION

3-2 See proprietary RAI responses.

NAC INTERNATIONAL RESPONSE TO REQUEST FOR ADDITIONAL INFORMATION

THERMAL EVALUATION

3-3 Modify the thermal analysis for hypothetical accident conditions to take into account the thermal inertia effects or justify that the thermal methodology for hypothetical accident conditions will generate accurate, or bounding, component temperatures, considering that the thermal inertia of the TSC and contents are not taken into account.

The NAC response to question 3-21 and previous NRC's questions (letter dated February 28, 2013, see ADAMS Accession No. ML13059A711) indicated the staff's concern with the hypothetical accident conditions methodology and its results. Rather than model the thermal inertia of the TSC/contents, the non-physical methodology mixes separate analyses for normal conditions of transport and hypothetical accident conditions by relying on the addition of a "delta_T" parameter to the temperature of the package inner surface for normal conditions of transport. Contrary to the NAC response to NRC's question 3-7(f), there is potential for the current methodology to produce non-conservative results for content with certain masses. A confirmatory analysis, which included the thermal inertia effects, was used to understand the behavior of the "delta_T" parameter, with the result shown in the figure below. As can be seen in the figure, the NAC hypothetical accident conditions methodology results in a constant "delta_T" parameter throughout the hypothetical accident conditions transient, compared to the varying temperature parameter from the physical reality-based NRC confirmatory analysis. The results in the figure demonstrate the inadequacy of the hypothetical accident conditions methodology to model physical behavior and therefore, show there is uncertainty that the hypothetical accident conditions methodology produces accurate, or bounding, temperatures.

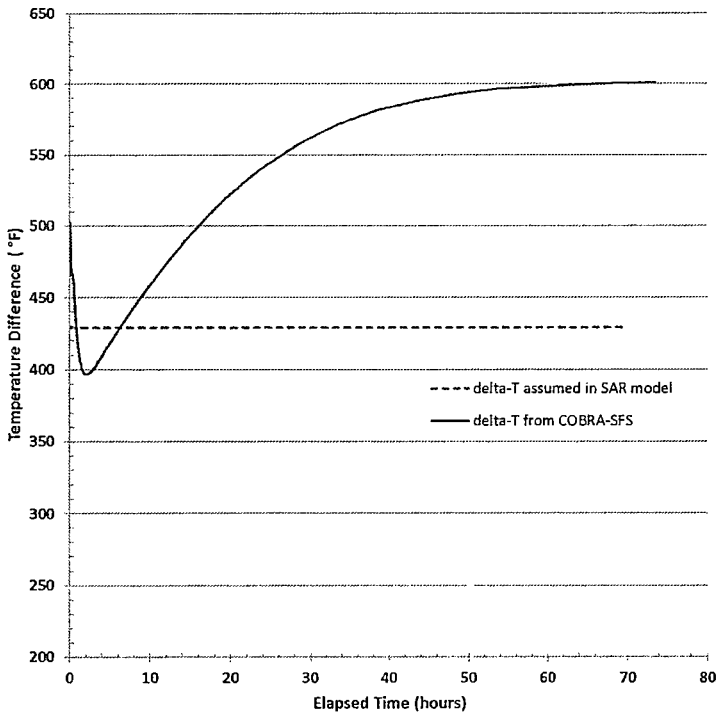

This information is needed to confirm compliance with 10 CFR 71.73.

NAC International Response to Thermal Evaluation RAI 3-3:

The delta T (ΔT) used in the transient evaluation is the temperature difference between the basket/fuel assembly center and the inner shell surface for the normal operation steady state condition. This normal steady state condition is also required to be the initial condition for the fire condition. The fire condition is applied instantaneously to the cask surface. The temperature of the inner shell inner surface does not instantaneously increase due to the conductivity and thermal mass of the intervening shells. When the temperature of the surface of the inner shell does increase, the temperature increase at the inner shell is not transmitted instantaneously to the basket center due to the conductivity and thermal mass of the intervening fuel assemblies and basket. The only possible means to permit the basket center temperature to track with the inner shell surface temperature is to treat the basket and fuel assemblies as having an infinite thermal diffusivity. The use of the ΔT could appear to be a non-physical methodology, because the non-physical nature is due to the treatment of the thermal diffusivity as being infinite, whereas the basket and fuel assemblies have a limited diffusivity due to the large mass and limited conductivity.

In reviewing the temperature time history contained in the RAI, it is assumed that the ΔT is between the same two points in the model (basket and inner shell). It appears that the ΔT is decreasing during the fire, which is not possible since heat is being infused into the inner shell, and there is no means to reject heat from the basket except through the shells. Also, there is no mechanism to alter the conductivity or thermal mass of the basket or inner shell during the fire or

after the fire. After the fire, the ΔT in the plot should return to essentially the initial value, since the fuel heat has not changed. Since the copper fins remain intact and are functional, the heat rejection capability is affected only in a limited means due to the removal of the aluminum surface. The temperature time history does not reflect this.

To further confirm the conservatism of the ΔT approach, a thermal analysis was performed and documented in Appendix F of NAC calculation 71160-3015, which was previously submitted. The analysis documented in Appendix F considered the diffusivity (conductivity and thermal mass) of the contents. The maximum fuel temperature is 814°F from the transient analysis, which is 79°F lower than the maximum content center temperature using the ΔT approach. Therefore, treatment of the contents as having infinite diffusivity as embedded in the ΔT approach provides bounding maximum basket and fuel assembly temperatures for the fire condition.

NAC INTERNATIONAL RESPONSE TO REQUEST FOR ADDITIONAL INFORMATION

THERMAL EVALUATION

3-4 Provide the pressure spreadsheet discussed in NAC's response to question 3-14 in letter dated January 13, 2015, and include/confirm the volume of tubes in the pressure calculation of Calculation Package 71160-3022, Rev. 1.

a. The pressure calculation mentions a spreadsheet, but it was not included and therefore a review cannot be performed.

b. Section 6.1.3.2 includes an equation for V_{tubes} that should be clarified/confirmed within the calculation package text and the spreadsheet; the equation does not appear to be correct.

NAC International Response to Thermal Evaluation RAI 3-4:

a. Spreadsheet is attached to the responses as a proprietary attachment

b. The calculation (71160-3022) has an editorial error in the guide tube volume equation in Section 6.1.3.2 of the calculation. An additional square (^{2}) is incorrectly shown in the first line of the equation. The correct formula was applied in the excel calculation (see row 51 of the "Fuel" sheet). Note that while it is certainly important to correctly apply the volume calculation of the guide tubes the actual volume associated with the guide tubes is so small that it is inconsequential to system performance.

UMS Fuel Assembly Descriptions		PWR Fuel Assembly Descriptions														PWR Fuel Assembly Descri	
Fuel ID		ce14a	ce14b	ex14b	we14d	ex14a	ex14c	we14a	we14b	we14c	hy14a	hy14b	ex15a	we15a	we15b	we15c	hy15a
Fuel Class		1	1	1	1	1	1	1	1	1	1	1	1	1	1	1	1
Reactor		PWR	PWR	PWR	PWR	PWR	PWR	PWR	PWR	PWR	PWR	PWR	PWR	PWR	PWR	PWR	PWR
Vendor		CE	CE	Ex/ANF	WE	Ex/ANF	Ex/ANF	WE	WE	WE	Holtec	Holtec	Ex/ANF	WE	WE	WE	Holtec
Array		14	14	14	14	14	14	14	14	14	14	14	15	15	15	15	15
Version		Std.	Ft Cal.	CE	CE Model	WE	Prairie Isl.	Std/ZCA	OFA	Std/ZCB	A	B	WE	Std	Std/ZC	OFA	A
Min MTU	[MTU]	#NAME?	#NAME?	#NAME?	#NAME?	#NAME?	#NAME?	#NAME?	#NAME?	#NAME?	#NAME?	#NAME?	#NAME?	#NAME?	#NAME?	#NAME?	#NAME?
Max MTU	[MTU]	#NAME?	#NAME?	#NAME?	#NAME?	#NAME?	#NAME?	#NAME?	#NAME?	#NAME?	#NAME?	#NAME?	#NAME?	#NAME?	#NAME?	#NAME?	#NAME?
Number of Fuel Rods		176	176	176	176	179	179	179	179	179	179	179	204	204	204	204	204
Min Pitch	[in]	0.580	0.580	0.580	0.580	0.556	0.556	0.556	0.556	0.556	0.556	0.556	0.563	0.563	0.563	0.563	0.550
Max Pitch	[in]	0.580	0.580	0.580	0.580	0.556	0.556	0.556	0.556	0.556	0.556	0.556	0.563	0.563	0.563	0.563	0.550
Min Rod Diameter	[in]	0.440	0.440	0.440	0.440	0.424	0.417	0.422	0.400	0.422	0.400	0.417	0.424	0.422	0.422	0.422	0.418
Max Rod Diameter	[in]	0.440	0.440	0.440	0.440	0.424	0.417	0.422	0.400	0.422	0.4000	0.4170	0.424	0.422	0.422	0.422	0.4180
Min Clad Thickness	[in]	0.026	0.026	0.031	0.026	0.030	0.030	0.023	0.024	0.023	0.024	0.022	0.030	0.024	0.024	0.024	0.026
Max Clad Thickness	[in]	0.028	0.028	0.031	0.026	0.030	0.030	0.023	0.024	0.023	0.0243	0.0218	0.030	0.024	0.024	0.024	0.0260
Min Pellet Diameter	[in]	0.3765	0.3765	0.3700	0.3805	0.3505	0.3505	0.3674	0.3444	0.3674	0.3444	0.3659	0.3565	0.3659	0.3659	0.3659	0.3580
Max Pellet Diameter	[in]	0.3765	0.3815	0.3700	0.3805	0.3505	0.3505	0.3674	0.3444	0.3674	0.3444	0.3659	0.3565	0.3669	0.3669	0.3659	0.3580
Min Active Length	[in]	137.00	128.00	134.00	136.70	142.00	144.00	145.20	144.00	145.20	144.00	144.00	144.00	144.00	144.00	144.00	132.00
Max Active Length	[in]	137.00	128.00	136.70	136.70	142.00	144.00	145.20	144.00	145.20	144.00	144.00	144.00	144.00	144.00	144.00	132.00
Fuel Assembly Height	[in]	157.000	148.835	156.700	157.238	160.130	160.130	161.100	159.710	159.710	159.710	160.130	159.710	160.100	160.100	159.765	149.100
Fuel Assembly Width	[in]	8.250	8.250	8.110	8.030	7.763	7.763	7.763	7.763	7.763	7.763	7.763	8.430	8.449	8.449	8.424	8.336
Top End-Cap Height	[in]	0.399	0.433	0.500	0.685	0.500	0.500	0.685	0.685	0.685	0.685	0.500	0.500	0.685	0.685	0.685	1.000
Bottom End-Cap Height	[in]	1.247	1.247	0.700	0.685	0.700	0.700	0.685	0.685	0.685	0.685	0.700	0.700	0.685	0.685	0.685	1.247
Lower Plenum Region Height	[in]	0.000	0.000	0.000	0.000	0.000	0.000	0.000	0.000	0.000	0.000	0.000	0.000	0.000	0.000	0.000	0.000
Upper Plenum Region Height	[in]	8.625	7.010	8.600	8.418	5.900	3.900	5.790	6.473	5.790	6.473	3.900	6.800	5.010	7.386	6.480	7.442
Lower Nozzle Height	[in]	3.625	5.438	2.677	3.312	2.600	2.600	3.188	2.738	2.738	2.738	2.600	2.720	2.738	2.738	2.738	4.271
Upper Nozzle Height	[in]	4.937	5.340	4.937	5.763	6.865	6.865	3.500	3.480	3.500	3.480	6.865	3.480	3.480	3.480	3.550	3.140
Gap Fuel Rod To Bottom Nozzle	[in]	0.063	0.300	0.000	0.200	0.782	0.782	0.000	0.821	0.000	0.821	0.782	0.658	0.000	0.000	0.813	0.000
Gap Fuel Rod To Top Nozzle	[in]	1.201	1.057	1.293	1.475	0.782	0.782	1.037	0.821	1.037	0.821	0.782	0.852	1.037	1.037	0.813	0.000
Fuel Rod Height	[in]	147.174	136.700	146.500	146.488	149.100	149.100	152.360	151.850	152.360	151.850	149.100	152.000	152.756	152.756	151.850	141.689
Number of Water Rods		0	0	0	0	0	0	0	0	0	0	0	0	0	0	0	0
Water Rod OD	[in]	0.000	0.000	0.000	0.000	0.000	0.000	0.000	0.000	0.000	0.000	0.000	0.000	0.000	0.000	0.000	0.000
Water Rod Thickness	[in]	0.000	0.000	0.000	0.000	0.000	0.000	0.000	0.000	0.000	0.000	0.000	0.000	0.000	0.000	0.000	0.000
Channel Inner Dimension	[in]	0.000	0.000	0.000	0.000	0.000	0.000	0.000	0.000	0.000	0.000	0.000	0.000	0.000	0.000	0.000	0.000
Min Channel Thickness	[in]	0.000	0.000	0.000	0.000	0.000	0.000	0.000	0.000	0.000	0.000	0.000	0.000	0.000	0.000	0.000	0.000
Max Channel Thickness	[in]	0.000	0.000	0.000	0.000	0.000	0.000	0.000	0.000	0.000	0.000	0.000	0.000	0.000	0.000	0.000	0.000
Number of Guide Tubes		4	4	4	4	16	16	16	16	16	16	16	20	20	20	20	20
Guide Tube OD	[in]	1.115	1.135	1.115	1.115	0.481	0.481	0.481	0.481	0.481	0.481	0.481	0.544	0.484	0.484	0.484	0.414
Guide Tube Thickness	[in]	0.040	0.026	0.036	0.040	0.034	0.034	0.034	0.034	0.034	0.017	0.017	0.017	0.015	0.015	0.015	0.0165
Number of Instrument Tubes		1	1	1	1	1	1	1	1	1	1	1	1	1	1	1	1
Instrument Tube OD	[in]	1.115	1.135	1.115	1.115	0.481	0.481	0.481	0.481	0.481	0.481	0.481	0.544	0.484	0.484	0.484	0.414
Instrument Tube Thickness	[in]	0.040	0.026	0.036	0.040	0.034	0.034	0.034	0.034	0.034	0.017	0.017	0.017	0.015	0.015	0.015	0.0165
Total Assembly Weight	[kg]	581.1	558.4	580.0	582.0	576.6	576.6	573.0	533.9	573.0			644.0	657.0	657.0	661.8	
Lower Nozzle SS Mass	[kg]	5.0000	3.1800	6.0800	5.4400	4.7600	4.7600	7.8930	5.4430	7.8930	5.4430	4.7600	5.6800	5.4430	5.4400	5.4400	5.4000
Upper Nozzle SS Mass	[kg]	6.1800	6.3200	11.5498	9.5460	9.3384	6.5800	9.8880	7.0260	9.8880	7.0260	6.5800	6.7892	11.8030	11.8400	7.8500	4.5000
Upper Plenum Spring Mass (Max)	[kg]	7.9800	7.9800	4.0700	3.1100	3.4900	5.3600	5.6800	3.2500	5.6836	3.2500	5.3600	3.6100	4.0700	4.0700	3.6800	4.6278
Upper Plenum Spring Mass (Min)	[kg]	7.9800	7.9800	4.0700	3.1100	3.4900	5.3600	5.6800	3.2500	5.6836			3.6100	4.0700	4.0700	3.6800	
Upper Plenum Grid Mass	[kg]	0.0000	0.0000	0.0682	0.7700	0.0518	0.0500	0.6800	0.9500	0.6800	0.9500	0.0500	0.0490	1.0700	1.0660	0.9070	0.0000
Lower Plenum Spring SS Mass	[kg]	0.0000	0.0000	0.0000	0.0000	0.0000	0.0000	0.0000	0.0000	0.0000	0.0000	0.0000	0.0000	0.0000	0.0000	0.0000	0.0000
Incore Hardware SS Mass	[kg]	0.0000	0.0000	0.0000	0.6580	0.0000	0.0000	8.1200	0.0000	0.0000	0.0000	0.0000	0.0000	10.6370	0.0000	0.0000	0.0000
Incore Hardware Inconel Mass	[kg]	1.3600	1.3600	0.5681	6.7590	0.4158	0.3100	5.3700	0.8620	5.3700	0.8620	0.3100	0.3052	6.8080	8.0500	1.0300	0.8200
Upper Plenum Zircaloy	[kg]	0.6800	0.6800	0.5518	0.0000	0.6882		0.0000	0.0000	0.0000	0.0000	0.0000	0.6510	0.0000	0.0000	0.0000	0.8100
Incore Zircaloy	[kg]	4.7600	4.7600	4.3719	0.0000	5.5242		0.0000	9.2080	0.0000	9.2080	0.0000	4.0548	0.0000	0.0000	7.9600	6.4500
		Done	Done	Done	Done	Done	No Data	Done	Done	Done			Done	Done	Done	Done	

UMS Fuel Assembly Descriptions		ptions												PWR Fuel Assembly Descriptions				
Fuel ID		hy15c	ce15a	ce15b	ex15b	ce16a	ex17a	we17a	we17b	we17c	hy17a	hy17b	bw15a	bw15b	hy15d	hy15e	hy15f	hy15h
Fuel Class		1	1	1	1	1	1	1	1	1	1	1	2	2	2	2	2	2
Reactor		PWR	PWR	PWR	PWR	PWR	PWR	PWR	PWR	PWR	PWR	PWR	PWR	PWR	PWR	PWR	PWR	PWR
Vendor		Holtec	CE	CE	Ex/ANF	CE	Ex/ANF	WE	WE	WE	Holtec	Holtec	B&W	B&W	Holtec	Holtec	Holtec	Holtec
Array		15	15	15	15	16	17	17	17	17	17	17	15	15	15	15	15	15
Version		C	Palis.	Palis.	Palis	Lucie 2	WE	Std	OFA	Vant 5	A	B	Mark B	Mark BZ	D	E	F	H
Min MTU	[MTU]	#NAME?	#NAME?	#NAME?	#NAME?	#NAME?	#NAME?	#NAME?	#NAME?	#NAME?	#NAME?	#NAME?	#NAME?	#NAME?	#NAME?	#NAME?	#NAME?	#NAME?
Max MTU	[MTU]	#NAME?	#NAME?	#NAME?	#NAME?	#NAME?	#NAME?	#NAME?	#NAME?	#NAME?	#NAME?	#NAME?	#NAME?	#NAME?	#NAME?	#NAME?	#NAME?	#NAME?
Number of Fuel Rods		204	216	216	216	236	264	264	264	264	264	264	208	208	208	208	208	208
Min Pitch	[in]	0.563	0.550	0.550	0.550	0.506	0.496	0.496	0.496	0.496	0.496	0.496	0.568	0.568	0.568	0.568	0.568	0.568
Max Pitch	[in]	0.563	0.550	0.550	0.550	0.506	0.496	0.496	0.496	0.496	0.496	0.496	0.568	0.568	0.568	0.568	0.568	0.568
Min Rod Diameter	[in]	0.417	0.418	0.418	0.415	0.382	0.360	0.374	0.360	0.360	0.360	0.372	0.430	0.430	0.430	0.428	0.428	0.414
Max Rod Diameter	[in]	0.4170	0.418	0.418	0.417	0.382	0.360	0.374	0.360	0.360	0.3600	0.3720	0.430	0.430	0.4300	0.4280	0.4280	0.4140
Min Clad Thickness	[in]	0.027	0.024	0.026	0.028	0.025	0.025	0.023	0.023	0.023	0.023	0.021	0.027	0.027	0.025	0.025	0.023	0.022
Max Clad Thickness	[in]	0.0265	0.026	0.026	0.030	0.025	0.025	0.0225	0.023	0.023	0.0225	0.0205	0.027	0.027	0.0250	0.0245	0.0230	0.0220
Min Pellet Diameter	[in]	0.3570	0.3580	0.3580	0.3430	0.3250	0.3030	0.3225	0.3088	0.3088	0.3088	0.3232	0.3686	0.3686	0.3735	0.3707	0.3742	0.3622
Max Pellet Diameter	[in]	0.3570	0.3590	0.3580	0.3430	0.3250	0.3030	0.3225	0.3088	0.3088	0.3088	0.3232	0.3686	0.3686	0.3735	0.3707	0.3742	0.3622
Min Active Length	[in]	144.00	132.00	132.00	131.80	136.70	144.00	144.00	144.00	144.00	144.00	144.00	144.00	144.00	144.00	144.00	144.00	144.00
Max Active Length	[in]	144.00	132.00	132.00	131.80	136.70	144.00	144.00	144.00	144.00	144.00	144.00	144.00	144.00	144.00	144.00	144.00	144.00
Fuel Assembly Height	[in]	159.765	149.100	149.125	148.852	158.129	159.710	159.800	159.800	160.100	160.100	159.800	165.625	165.625	165.625	165.625	165.625	165.625
Fuel Assembly Width	[in]	8.424	8.336	8.200	8.250	8.100	8.430	8.426	8.426	8.426	8.426	8.426	8.536	8.536	8.536	8.536	8.536	8.656
Top End-Cap Height	[in]	0.685	1.000	1.000	0.500	0.750	0.500	0.685	0.685	0.685	0.685	0.685	0.685	0.685	0.685	0.685	0.685	0.685
Bottom End-Cap Height	[in]	0.685	1.247	1.247	0.720	0.891	0.700	0.685	0.685	0.895	0.895	0.685	0.685	0.685	0.685	0.685	0.685	0.685
Lower Plenum Region Height	[in]	0.000	0.000	0.000	0.000	0.000	0.000	0.000	0.000	0.000	0.000	0.000	4.563	4.563	0.000	0.000	0.000	4.563
Upper Plenum Region Height	[in]	6.480	7.442	7.442	6.480	8.158	6.800	6.260	6.260	6.720	6.720	6.260	4.563	4.563	4.563	4.563	4.563	4.563
Lower Nozzle Height	[in]	2.738	4.271	4.833	4.833	3.821	2.720	2.700	2.700	2.738	2.738	2.700	2.000	2.000	2.000	2.000	2.000	2.000
Upper Nozzle Height	[in]	3.550	3.140	3.140	3.140	6.821	3.480	3.670	3.670	3.480	3.480	3.670	8.875	9.875	9.875	9.875	9.875	9.875
Gap Fuel Rod To Bottom Nozzle	[in]	0.813	0.000	0.000	0.000	0.000	0.658	0.000	0.000	0.791	0.791	0.000	0.000	0.000	0.000	0.000	0.000	0.000
Gap Fuel Rod To Top Nozzle	[in]	0.813	0.000	1.152	1.427	0.997	0.852	1.300	1.300	0.791	0.791	1.300	1.625	0.625	0.625	0.625	0.625	0.625
Fuel Rod Height	[in]	151.850	141.689	140.000	139.423	146.499	152.000	151.630	151.630	152.300	152.300	151.630	153.125	153.125	153.125	153.125	153.125	153.125
Number of Water Rods		0	0	0	0	0	0	0	0	0	0	0	0	0	0	0	0	0
Water Rod OD	[in]	0.000	0.000	0.000	0.000	0.000	0.000	0.000	0.000	0.000	0.000	0.000	0.000	0.000	0.000	0.000	0.000	0.000
Water Rod Thickness	[in]	0.000	0.000	0.000	0.000	0.000	0.000	0.000	0.000	0.000	0.000	0.000	0.000	0.000	0.000	0.000	0.000	0.000
Channel Inner Dimension	[in]	0.000	0.000	0.000	0.000	0.000	0.000	0.000	0.000	0.000	0.000	0.000	0.000	0.000	0.000	0.000	0.000	0.000
Min Channel Thickness	[in]	0.000	0.000	0.000	0.000	0.000	0.000	0.000	0.000	0.000	0.000	0.000	0.000	0.000	0.000	0.000	0.000	0.000
Max Channel Thickness	[in]	0.000	0.000	0.000	0.000	0.000	0.000	0.000	0.000	0.000	0.000	0.000	0.000	0.000	0.000	0.000	0.000	0.000
Number of Guide Tubes		20	8	8	8	4	24	24	24	24	24	24	16	16	16	16	16	16
Guide Tube OD	[in]	0.484	0.414	0.417	0.417	1.115	0.480	0.482	0.482	0.482	0.482	0.482	0.493	0.493	0.493	0.493	0.493	0.493
Guide Tube Thickness	[in]	0.0170	0.024	0.027	0.027	0.026	0.016	0.015	0.015	0.015	0.016	0.014	0.016	0.016	0.015	0.014	0.014	0.014
Number of Instrument Tubes		1	1	1	1	1	1	1	1	1	1	1	1	1	1	1	1	1
Instrument Tube OD	[in]	0.484	0.414	0.417	0.417	1.115	0.480	0.482	0.482	0.482	0.482	0.482	0.493	0.493	0.493	0.493	0.493	0.493
Instrument Tube Thickness	[in]	0.0170	0.024	0.027	0.027	0.026	0.016	0.015	0.015	0.015	0.016	0.014	0.016	0.016	0.015	0.014	0.014	0.014
Total Assembly Weight	[kg]		612.9	616.9	612.0	589.7	620.0	665.0	665.0	619.2			687.2	687.2				689.0
Lower Nozzle SS Mass	[kg]	5.4400	5.4000	5.4000	4.7700	5.4000	5.7500	5.9000	5.8970	5.8970	5.8970	5.9000	9.6100	9.6100	9.6100	9.6100	9.6100	9.6100
Upper Nozzle SS Mass	[kg]	7.8500	4.5000	4.5000	4.4492	11.3000	7.3205	7.8500	7.8500	7.8500	7.8500	7.8500	10.7600	10.7600	10.7600	10.7600	10.7600	10.7600
Upper Plenum Spring Mass (Max)	[kg]	3.6800	4.9000	4.9000	3.3300	10.7000	2.9900	4.4300	3.5900	3.5900	3.5900	4.4300	1.9800	1.9800	1.9800	1.9800	1.9800	1.9800
Upper Plenum Spring Mass (Min)	[kg]		4.9000	4.9000	3.3300	10.7000	2.9900	4.4300	3.5900	3.5900			1.9800	1.9800				
Upper Plenum Grid Mass	[kg]	0.9070	0.0000	0.0000	0.1008	0.0000	0.1568	0.8840	0.9760	0.9760	0.9760	0.8840	1.0400	1.0400	1.0400	1.0400	1.0400	1.0400
Lower Plenum Spring SS Mass	[kg]	0.0000	0.0000	0.0000	0.0000	0.0000	0.0000	0.0000	0.0000	0.0000	0.0000	0.0000	1.9800	1.9800	1.9800	1.9800	1.9800	1.9800
Incore Hardware SS Mass	[kg]	0.0000	0.0000	0.0000	0.0000	0.0000	0.0000	0.5400	0.0910	0.0910	0.0910	0.5400	0.0000	0.0000	0.0000	0.0000	0.0000	0.0000
Incore Hardware Inconel Mass	[kg]	1.0300	0.8200	0.8200	0.9093	1.3600	1.0976	4.9000	0.9250	0.9250	0.9250	4.9000	4.9000	0.0000	0.0000	0.0000	0.0000	0.0000
Upper Plenum Zircaloy	[kg]	0.0000	0.8100	0.8100	0.3792	0.8100	0.9632	0.0000	0.0000	0.0000	0.0000	0.0000	0.0000	0.0000	0.0000	0.0000	0.0000	0.0000
Incore Zircaloy	[kg]	7.9600	6.4500	6.4500	3.4207	6.4500	6.7424	0.0000	7.0220	7.0220	7.0220	0.0000	0.6400	5.5400	5.5400	5.5400	5.5400	5.5400
			Done	Done	Done	Done	Done	Done	Done	Done			Done	Done				

UMS Fuel Assembly Descriptions							BWR Fuel Assembly Descriptions											
Fuel ID		bw17a	hy17c	ce16b	ce16c	ce16d	ex07a	ge07a	ge07b	ge07c	ge08a	ge08b	ge08c	ge08d	ge08d	ex08a	ge08e	ex09a
Fuel Class		2	2	3	3	3	4	4	4	4	4	4	4	4	4	4	4	4
Reactor		PWR	PWR	PWR	PWR	PWR	BWR	BWR	BWR	BWR	BWR	BWR	BWR	BWR	BWR	BWR	BWR	BWR
Vendor		B&W	Holtec	CE	CE	CE	Ex/ANF	GE	GE	GE	GE	GE	GE	GE	GE	Ex/ANF	GE	Ex/ANF
Array		17	17	16	16	16	7	7	7	7	8	8	8	8	8	8	8	9
Version		Mark C	C	Sono 2&3	ANO2	SYS80	GE	GE-2a	GE-2b	GE-3	GE-8	GE-10	GE-5	GE-6 (prep)	GE-7 (barr)	JP-3	GE-4	JP-3
Min MTU	[MTU]	#NAME?	#NAME?	#NAME?	#NAME?	#NAME?	#NAME?	#NAME?	#NAME?	#NAME?	#NAME?	#NAME?	#NAME?	#NAME?	#NAME?	#NAME?	#NAME?	#NAME?
Max MTU	[MTU]	#NAME?	#NAME?	#NAME?	#NAME?	#NAME?	#NAME?	#NAME?	#NAME?	#NAME?	#NAME?	#NAME?	#NAME?	#NAME?	#NAME?	#NAME?	#NAME?	#NAME?
Number of Fuel Rods		264	264	236	236	236	48	49	49	49	60	60	62	62	62	63	63	79
Min Pitch	[in]	0.502	0.502	0.506	0.506	0.506	0.738	0.738	0.738	0.738	0.638	0.638	0.640	0.640	0.640	0.641	0.640	0.572
Max Pitch	[in]	0.502	0.502	0.506	0.506	0.506	0.738	0.738	0.738	0.738	0.640	0.640	0.640	0.640	0.640	0.641	0.640	0.572
Min Rod Diameter	[in]	0.379	0.377	0.382	0.382	0.382	0.570	0.570	0.563	0.563	0.484	0.484	0.483	0.483	0.483	0.484	0.493	0.424
Max Rod Diameter	[in]	0.379	0.3770	0.382	0.382	0.382	0.570	0.570	0.563	0.563	0.484	0.484	0.483	0.483	0.483	0.484	0.493	0.424
Min Clad Thickness	[in]	0.024	0.022	0.025	0.025	0.025	0.036	0.032	0.032	0.037	0.032	0.032	0.032	0.032	0.032	0.036	0.034	0.030
Max Clad Thickness	[in]	0.024	0.0220	0.025	0.025	0.025	0.036	0.036	0.032	0.037	0.032	0.032	0.032	0.032	0.032	0.036	0.034	0.030
Min Pellet Diameter	[in]	0.3232	0.3252	0.3250	0.3250	0.3250	0.4900	0.4880	0.4870	0.4770	0.4095	0.4095	0.4100	0.4100	0.4100	0.4045	0.4160	0.3565
Max Pellet Diameter	[in]	0.3240	0.3252	0.3250	0.3250	0.3250	0.4900	0.4880	0.4870	0.4770	0.4100	0.4100	0.4100	0.4100	0.4100	0.4045	0.4160	0.3565
Min Active Length	[in]	143.00	144.00	150.00	150.00	150.00	144.00	144.00	144.00	144.00	145.20	145.20	145.20	145.20	145.20	145.20	144.00	145.20
Max Active Length	[in]	143.00	144.00	150.00	150.00	150.00	144.00	144.00	144.00	144.00	145.20	145.20	145.20	145.20	145.20	145.24	144.00	145.24
Fuel Assembly Height	[in]	165.719	166.719	176.803	176.803	178.300	171.250	171.125	171.125	171.125	171.125	171.125	171.125	171.125	171.125	171.290	171.125	171.290
Fuel Assembly Width	[in]	8.536	8.536	8.100	8.250	8.250	5.247	5.518	5.470	5.518	5.518	5.518	5.518	5.518	5.518	5.251	5.518	5.251
Top End-Cap Height	[in]	0.685	0.685	0.500	0.500	0.500	0.355	0.160	0.435	0.160	0.435	0.435	0.435	0.435	0.435	0.355	0.440	0.345
Bottom End-Cap Height	[in]	0.685	0.685	0.891	0.891	0.891	0.355	0.625	0.625	0.625	0.625	0.625	0.625	0.625	0.625	0.355	0.625	0.355
Lower Plenum Region Height	[in]	4.844	0.000	0.000	0.000	0.000	0.000	0.000	0.000	0.000	0.000	0.000	0.000	0.000	0.000	0.000	0.000	0.000
Upper Plenum Region Height	[in]	4.844	4.844	9.527	9.527	9.527	10.200	11.240	10.965	11.240	9.765	9.765	9.765	9.765	9.765	10.020	10.965	9.580
Lower Nozzle Height	[in]	2.000	2.000	3.812	3.812	3.812	6.750	6.760	6.760	6.760	6.760	6.760	6.760	6.760	6.760	6.650	6.760	6.940
Upper Nozzle Height	[in]	9.406	9.406	9.723	10.141	11.047	8.690	7.500	7.500	7.500	7.500	7.500	7.500	7.500	7.500	7.770	7.500	7.500
Gap Fuel Rod To Bottom Nozzle	[in]	0.000	0.000	0.000	0.000	0.000	0.000	0.000	0.000	0.000	0.000	0.000	0.000	0.000	0.000	0.000	0.000	0.000
Gap Fuel Rod To Top Nozzle	[in]	1.625	1.625	2.100	1.532	1.532	0.900	0.840	0.840	0.840	0.840	0.840	0.840	0.840	0.840	0.900	0.840	1.330
Fuel Rod Height	[in]	152.688	153.688	161.168	161.318	161.318	154.910	156.025	156.025	156.025	156.025	156.025	156.025	156.025	156.025	155.970	156.025	155.520
Number of Water Rods		0	0	0	0	0	1	0	0	0	4	1	2	2	2	1	1	2
Water Rod OD	[in]	0.000	0.000	0.000	0.000	0.000	0.570	0.000	0.000	0.000	0.484	1.260	0.591	0.591	0.591	0.484	0.493	0.424
Water Rod Thickness	[in]	0.000	0.000	0.000	0.000	0.000	0.000	0.000	0.000	0.000	0.031	0.039	0.030	0.030	0.030	0.036	0.034	0.030
Channel Inner Dimension	[in]	0.000	0.000	0.000	0.000	0.000	5.278	5.278	5.278	5.278	5.278	5.278	5.278	5.278	5.278	5.278	5.278	5.278
Min Channel Thickness	[in]	0.000	0.000	0.000	0.000	0.000	0.080	0.080	0.080	0.080	0.080	0.080	0.080	0.080	0.080	0.080	0.080	0.080
Max Channel Thickness	[in]	0.000	0.000	0.000	0.000	0.000	0.120	0.120	0.120	0.120	0.120	0.120	0.120	0.120	0.120	0.120	0.120	0.120
Number of Guide Tubes		24	24	4	4	4	0	0	0	0	0	0	0	0	0	0	0	0
Guide Tube OD	[in]	0.420	0.420	0.970	0.970	0.980	0.000	0.000	0.000	0.000	0.000	0.000	0.000	0.000	0.000	0.000	0.000	0.000
Guide Tube Thickness	[in]	0.018	0.020	0.035	0.035	0.035	0.000	0.000	0.000	0.000	0.000	0.000	0.000	0.000	0.000	0.000	0.000	0.000
Number of Instrument Tubes		1	1	1	1	1	0	0	0	0	0	0	0	0	0	0	0	0
Instrument Tube OD	[in]	0.420	0.420	0.970	0.970	0.980	0.000	0.000	0.000	0.000	0.000	0.000	0.000	0.000	0.000	0.000	0.000	0.000
Instrument Tube Thickness	[in]	0.015	0.020	0.025	0.025	0.025	0.000	0.000	0.000	0.000	0.000	0.000	0.000	0.000	0.000	0.000	0.000	0.000
Total Assembly Weight	[kg]	682.7		648.6	659.5	648.6	280.8		279.0							255.1	279.0	252.6
Lower Nozzle SS Mass	[kg]	6.8700	6.8700	5.4000	5.4000	7.3000	4.220	4.700	4.700	4.700	4.700	4.700	4.700	4.700	4.700	3.940	4.700	4.530
Upper Nozzle SS Mass	[kg]	18.1300	18.1300	16.8000	13.4000	15.9000	3.520	2.080	2.080	2.080	2.080	2.080	2.080	2.080	2.080	1.690	2.080	2.000
Upper Plenum Spring Mass (Max)	[kg]	1.5600	1.5600	10.7000	10.7000	10.7000	2.830	1.848	1.848	1.848	1.793	1.793	1.853	1.853	1.853	2.858	1.883	1.684
Upper Plenum Spring Mass (Min)	[kg]	1.5600		10.7000	10.7000	10.7000	2.830	1.848	1.848	1.848	1.064	1.064	1.100	1.100	1.100	2.858	1.118	1.684
Upper Plenum Grid Mass	[kg]	1.3000	1.3000	0.0000	0.0000	0.0000	0.000	0.000	0.000	0.000	0.000	0.000	0.000	0.000	0.000	0.000	0.000	0.000
Lower Plenum Spring SS Mass	[kg]	1.5600	1.5600	0.0000	0.0000	0.0000	0.000	0.000	0.000	0.000	0.000	0.000	0.000	0.000	0.000	0.000	0.000	0.000
Incore Hardware SS Mass	[kg]	0.0000	0.0000	0.0000	0.0000	0.0000	0.000	0.000	0.000	0.000	0.000	0.000	0.000	0.000	0.000	0.000	0.000	0.000
Incore Hardware Inconel Mass	[kg]	4.2700	4.2700	1.3600	1.3600	1.3600	0.326	2.030	0.320	0.320	0.290	0.290	0.330	0.330	0.330	0.216	0.330	0.245
Upper Plenum Zircaloy	[kg]	0.0000	0.0000	0.8200	0.8200	0.8200												
Incore Zircaloy	[kg]	0.5400	0.5400	7.3500	8.2000	7.3500												
		Done		Done	Done	Done												

UMS Fuel Assembly Descriptions				BWR Fuel Assembly Descriptions														BWR Fuel As
Fuel ID		ge07f	ge07g	ge07h	hy07a	hy08a	ge08i	hy08b	hy08c	ex08b	ge08j	ge08k	ge08l	hy08d	ge08m	ge08n	hy08e	hy08f
Fuel Class		5	5	5	5	5	5	5	5	5	5	5	5	5	5	5	5	5
Reactor		BWR	BWR	BWR	BWR	BWR	BWR	BWR	BWR	BWR	BWR	BWR	BWR	BWR	BWR	BWR	BWR	BWR
Vendor		GE	GE	GE	Holtec	Holtec	GE	Holtec	Holtec	Ex/ANF	GE	GE	GE	Holtec	GE	GE	Holtec	Holtec
Array		7	7	7	7	8	8	8	8	8	8	8	8	8	8	8	8	8
Version		GE-2	GE-3a	GE-3b	B	E	GE-10	D1	D2	JP-4,5	GE-5	GE-6 (prep)	GE-7 (barr)	C	GE-4a	GE-4b	B1	B2
Min MTU	[MTU]	#NAME?	#NAME?	#NAME?	#NAME?	#NAME?	#NAME?	#NAME?	#NAME?	#NAME?	#NAME?	#NAME?	#NAME?	#NAME?	#NAME?	#NAME?	#NAME?	#NAME?
Max MTU	[MTU]	#NAME?	#NAME?	#NAME?	#NAME?	#NAME?	#NAME?	#NAME?	#NAME?	#NAME?	#NAME?	#NAME?	#NAME?	#NAME?	#NAME?	#NAME?	#NAME?	#NAME?
Number of Fuel Rods		49	49	49	49	59	60	60	61	62	62	62	62	62	63	63	63	64
Min Pitch	[in]	0.738	0.738	0.738	0.738	0.640	0.640	0.640	0.640	0.641	0.640	0.640	0.640	0.641	0.640	0.640	0.642	0.642
Max Pitch	[in]	0.738	0.738	0.738	0.738	0.640	0.642	0.640	0.640	0.641	0.642	0.642	0.642	0.641	0.640	0.640	0.642	0.642
Min Rod Diameter	[in]	0.563	0.563	0.563	0.563	0.493	0.484	0.483	0.483	0.484	0.483	0.483	0.483	0.483	0.493	0.493	0.484	0.484
Max Rod Diameter	[in]	0.563	0.563	0.563	0.5630	0.4930	0.484	0.4830	0.4830	0.484	0.484	0.484	0.484	0.4830	0.493	0.493	0.4840	0.4840
Min Clad Thickness	[in]	0.032	0.037	0.037	0.032	0.034	0.032	0.030	0.030	0.036	0.032	0.032	0.032	0.029	0.034	0.034	0.027	0.027
Max Clad Thickness	[in]	0.032	0.037	0.037	0.0320	0.0340	0.032	0.0300	0.0300	0.036	0.032	0.032	0.032	0.0290	0.034	0.034	0.0273	0.0273
Min Pellet Diameter	[in]	0.4870	0.4770	0.4770	0.4910	0.4160	0.4100	0.4140	0.4140	0.4045	0.4100	0.4100	0.4100	0.4160	0.4160	0.4160	0.4195	0.4195
Max Pellet Diameter	[in]	0.4870	0.4770	0.4770	0.4910	0.4160	0.4110	0.4140	0.4140	0.4045	0.4110	0.4110	0.4110	0.4160	0.4160	0.4160	0.4195	0.4195
Min Active Length	[in]	144.00	144.00	146.00	150.00	150.00	150.00	150.00	150.00	150.00	150.00	150.00	150.00	150.00	144.00	146.00	150.00	150.00
Max Active Length	[in]	144.00	144.00	146.00	150.00	150.00	150.00	150.00	150.00	150.00	150.00	150.00	150.00	150.00	144.00	146.00	150.00	150.00
Fuel Assembly Height	[in]	176.160	176.160	176.160	176.200	176.200	176.161	176.200	176.200	176.050	176.160	176.160	176.160	176.200	176.160	176.160	176.200	176.200
Fuel Assembly Width	[in]	5.518	5.518	5.518	5.518	5.518	5.518	5.518	5.518	5.251	5.518	5.518	5.518	5.518	5.518	5.518	5.518	5.518
Top End-Cap Height	[in]	0.305	0.305	0.435	0.435	0.346	0.346	0.346	0.346	0.355	0.345	0.345	0.345	0.346	0.440	0.435	0.346	0.346
Bottom End-Cap Height	[in]	0.625	0.625	0.625	0.625	0.625	0.625	0.625	0.625	0.355	0.625	0.625	0.625	0.625	0.625	0.625	0.625	0.625
Lower Plenum Region Height	[in]	0.000	0.000	0.000	0.000	0.000	0.000	0.000	0.000	0.000	0.000	0.000	0.000	0.000	0.000	0.000	0.000	0.000
Upper Plenum Region Height	[in]	16.130	16.130	14.000	14.000	9.580	9.580	9.580	9.580	10.024	9.580	9.580	9.580	9.580	15.995	14.000	9.580	9.580
Lower Nozzle Height	[in]	6.760	6.760	6.760	6.760	6.760	6.760	6.760	6.760	6.650	6.760	6.760	6.760	6.760	6.760	6.760	6.760	6.760
Upper Nozzle Height	[in]	7.500	7.500	7.500	7.500	7.500	7.500	7.500	7.500	7.766	7.500	7.500	7.500	7.500	7.500	7.500	7.500	7.500
Gap Fuel Rod To Bottom Nozzle	[in]	0.000	0.000	0.000	0.000	0.000	0.000	0.000	0.000	0.000	0.000	0.000	0.000	0.000	0.000	0.000	0.000	0.000
Gap Fuel Rod To Top Nozzle	[in]	0.840	0.840	0.840	0.840	1.350	1.350	1.350	1.350	0.900	1.350	1.350	1.350	1.350	0.840	0.840	1.350	1.350
Fuel Rod Height	[in]	156.120	156.120	161.060	161.060	160.551	160.551	160.551	160.551	160.734	160.550	160.550	160.550	160.551	161.060	161.060	160.551	160.551
Number of Water Rods		0	0	0	0	5	1	4	3	2	2	2	2	2	1	1	1	0
Water Rod OD	[in]	0.000	0.000	0.000	0.000	0.493	1.260	0.483	0.483	0.484	0.591	0.591	0.591	0.483	0.493	0.493	0.484	0.000
Water Rod Thickness	[in]	0.000	0.000	0.000	0.000	0.034	0.039	0.000	0.000	0.036	0.030	0.030	0.030	0.000	0.034	0.034	0.034	0.000
Channel Inner Dimension	[in]	5.278	5.278	5.278	5.278	5.278	5.278	5.278	5.278	5.278	5.278	5.278	5.278	5.278	5.278	5.278	5.278	5.278
Min Channel Thickness	[in]	0.080	0.080	0.080	0.080	0.080	0.080	0.080	0.080	0.080	0.080	0.080	0.080	0.080	0.080	0.080	0.080	0.080
Max Channel Thickness	[in]	0.120	0.120	0.120	0.120	0.120	0.120	0.120	0.120	0.120	0.120	0.120	0.120	0.120	0.120	0.120	0.120	0.120
Number of Guide Tubes		0	0	0	0	0	0	0	0	0	0	0	0	0	0	0	0	0
Guide Tube OD	[in]	0.000	0.000	0.000	0.000	0.000	0.000	0.000	0.000	0.000	0.000	0.000	0.000	0.000	0.000	0.000	0.000	0.000
Guide Tube Thickness	[in]	0.000	0.000	0.000	0.000	0.000	0.000	0.000	0.000	0.000	0.000	0.000	0.000	0.000	0.000	0.000	0.000	0.000
Number of Instrument Tubes		0	0	0	0	0	0	0	0	0	0	0	0	0	0	0	0	0
Instrument Tube OD	[in]	0.000	0.000	0.000	0.000	0.000	0.000	0.000	0.000	0.000	0.000	0.000	0.000	0.000	0.000	0.000	0.000	0.000
Instrument Tube Thickness	[in]	0.000	0.000	0.000	0.000	0.000	0.000	0.000	0.000	0.000	0.000	0.000	0.000	0.000	0.000	0.000	0.000	0.000
Total Assembly Weight	[kg]	279.0					269.0			266.6					279.0			
Lower Nozzle SS Mass	[kg]	4.700	4.700	4.700	4.700	4.700	4.700	4.700	4.700	3.940	4.700	4.700	4.700	4.700	4.700	4.700	4.700	4.700
Upper Nozzle SS Mass	[kg]	2.080	2.080	2.080	2.080	2.080	2.080	2.080	2.080	1.690	2.080	2.080	2.080	2.080	2.080	2.080	2.080	2.080
Upper Plenum Spring Mass (Max)	[kg]	1.848	1.848	1.848	1.848	1.763	1.793	1.793	1.823	2.812	1.853	1.853	1.853	1.853	1.883	1.883	1.883	1.913
Upper Plenum Spring Mass (Min)	[kg]	1.848	1.848	1.848			1.064			2.812	1.100	1.100	1.100		1.118	1.118		
Upper Plenum Grid Mass	[kg]	0.000	0.000	0.000	0.000	0.000	0.000	0.000	0.000	0.000	0.000	0.000	0.000	0.000	0.000	0.000	0.000	0.000
Lower Plenum Spring SS Mass	[kg]	0.000	0.000	0.000	0.000	0.000	0.000	0.000	0.000	0.000	0.000	0.000	0.000	0.000	0.000	0.000	0.000	0.000
Incore Hardware SS Mass	[kg]	0.000	0.000	0.000	0.000	0.000	0.000	0.000	0.000	0.000	0.000	0.000	0.000	0.000	0.000	0.000	0.000	0.000
Incore Hardware Inconel Mass	[kg]	0.320	0.320	0.320	0.320	0.290	0.290	0.290	0.290	0.216	0.330	0.330	0.330	0.290	0.330	0.320	0.290	0.290
Upper Plenum Zircaloy	[kg]																	
Incore Zircaloy	[kg]																	

UMS Fuel Assembly Descriptions		sembly Descriptions												
Fuel ID		hy08g	hy09a	ex09b	ge09a	sp09a	hy09b	ex09c	ge09b	hy09c	hy10a	hy10b	hy10c	hy10d
Fuel Class		5	5	5	5	5	5	5	5	5	5	5	5	5
Reactor		BWR	BWR	BWR	BWR	BWR	BWR	BWR	BWR	BWR	BWR	BWR	BWR	BWR
Vendor		Holtec	Holtec	Ex/ANF	GE	SPC	Holtec	Ex/ANF	GE	Holtec	Holtec	Holtec	Holtec	ABB
Array		8	9	9	9	9	9	9	9	9	10	10	10	10
Version		F	B	JP-4,5	GE-11	9x9-5	E	JP-4,5	GE-11	C	B	A	C	SVEA-100
Min MTU	[MTU]	#NAME?	#NAME?	#NAME?	#NAME?	#NAME?	#NAME?	#NAME?	#NAME?	#NAME?	#NAME?	#NAME?	#NAME?	#NAME?
Max MTU	[MTU]	#NAME?	#NAME?	#NAME?	#NAME?	#NAME?	#NAME?	#NAME?	#NAME?	#NAME?	#NAME?	#NAME?	#NAME?	#NAME?
Number of Fuel Rods		64	72	74	74	76	76	79	79	80	91	92	96	100
Min Pitch	[in]	0.609	0.572	0.572	0.566	0.572	0.572	0.572	0.566	0.572	0.510	0.510	0.488	0.488
Max Pitch	[in]	0.609	0.572	0.572	0.567	0.572	0.572	0.572	0.567	0.572	0.510	0.510	0.488	0.488
Min Rod Diameter	[in]	0.458	0.433	0.424	0.441	0.443	0.417	0.424	0.441	0.423	0.396	0.404	0.378	0.378
Max Rod Diameter	[in]	0.4576	0.4330	0.424	0.441	0.4430	0.4170	0.424	0.441	0.4230	0.3957	0.4040	0.3780	0.3780
Min Clad Thickness	[in]	0.029	0.026	0.030	0.028	0.031	0.027	0.030	0.028	0.030	0.024	0.026	0.024	0.024
Max Clad Thickness	[in]	0.0290	0.0260	0.030	0.028	0.0310	0.0265	0.030	0.028	0.0295	0.0239	0.0260	0.0243	0.0243
Min Pellet Diameter	[in]	0.3913	0.3740	0.3565	0.3760	0.3750	0.3530	0.3565	0.3760	0.3565	0.3420	0.3455	0.3224	0.3224
Max Pellet Diameter	[in]	0.3913	0.3740	0.3565	0.3760	0.3750	0.3530	0.3565	0.3760	0.3565	0.3420	0.3455	0.3224	0.3224
Min Active Length	[in]	150.00	150.00	150.00	150.00	150.00	150.00	150.00	150.00	150.00	150.00	150.00	150.00	150.00
Max Active Length	[in]	150.00	150.00	150.00	150.00	150.00	150.00	150.00	150.00	150.00	150.00	150.00	150.00	150.00
Fuel Assembly Height	[in]	176.200	176.200	176.058	176.161	176.200	176.200	176.058	176.161	176.200	176.200	176.200	176.200	176.200
Fuel Assembly Width	[in]	5.518	5.518	5.251	5.518	5.518	5.518	5.251	5.518	5.518	5.518	5.518	5.518	5.518
Top End-Cap Height	[in]	0.346	0.346	0.355	0.346	0.346	0.346	0.355	0.346	0.346	0.346	0.346	0.346	0.346
Bottom End-Cap Height	[in]	0.625	0.625	0.355	0.625	0.625	0.625	0.355	0.625	0.625	0.625	0.625	0.625	0.625
Lower Plenum Region Height	[in]	0.000	0.000	0.000	0.000	0.000	0.000	0.000	0.000	0.000	0.000	0.000	0.000	0.000
Upper Plenum Region Height	[in]	9.580	9.580	9.578	9.580	9.580	9.580	9.578	9.580	9.580	9.580	9.580	9.580	9.580
Lower Nozzle Height	[in]	6.760	6.760	6.940	6.760	6.760	6.760	6.940	6.760	6.760	6.760	6.760	6.760	6.760
Upper Nozzle Height	[in]	7.500	7.500	7.500	7.500	7.500	7.500	7.500	7.500	7.500	7.500	7.500	7.500	7.500
Gap Fuel Rod To Bottom Nozzle	[in]	0.000	0.000	0.000	0.000	0.000	0.000	0.000	0.000	0.000	0.000	0.000	0.000	0.000
Gap Fuel Rod To Top Nozzle	[in]	1.350	1.350	1.330	1.350	1.350	1.350	1.330	1.350	1.350	1.350	1.350	1.350	1.350
Fuel Rod Height	[in]	160.551	160.551	160.288	160.551	160.551	160.551	160.288	160.551	160.551	160.551	160.551	160.551	160.551
Number of Water Rods		1	1	2	2	5	5	2	2	1	1	2	5	1
Water Rod OD	[in]	Cross	1.716	0.984	0.984	0.443	0.417	0.424	0.441	0.423	1.530	0.808	Diamond+	Cross
Water Rod Thickness	[in]	0.032	0.000	0.028	0.028	0.012	0.012	0.030	0.028	0.020	0.000	0.030	0.031	0.034
Channel Inner Dimension	[in]	5.278	5.278	5.278	5.278	5.278	5.278	5.278	5.278	5.278	5.278	5.278	5.278	5.278
Min Channel Thickness	[in]	0.080	0.080	0.080	0.080	0.080	0.080	0.080	0.080	0.080	0.080	0.080	0.080	0.080
Max Channel Thickness	[in]	0.120	0.120	0.120	0.120	0.120	0.120	0.120	0.120	0.120	0.120	0.120	0.120	0.120
Number of Guide Tubes		0	0	0	0	0	0	0	0	0	0	0	0	0
Guide Tube OD	[in]	0.000	0.000	0.000	0.000	0.000	0.000	0.000	0.000	0.000	0.000	0.000	0.000	0.000
Guide Tube Thickness	[in]	0.000	0.000	0.000	0.000	0.000	0.000	0.000	0.000	0.000	0.000	0.000	0.000	0.000
Number of Instrument Tubes		0	0	0	0	0	0	0	0	0	0	0	0	0
Instrument Tube OD	[in]	0.000	0.000	0.000	0.000	0.000	0.000	0.000	0.000	0.000	0.000	0.000	0.000	0.000
Instrument Tube Thickness	[in]	0.000	0.000	0.000	0.000	0.000	0.000	0.000	0.000	0.000	0.000	0.000	0.000	0.000
Total Assembly Weight	[kg]			261.0	256.0	261.0		261.0	256.0					
Lower Nozzle SS Mass	[kg]	4.700	4.740	4.530	4.740	4.740	4.740	4.530	4.740	4.740	4.740	4.740	4.740	4.740
Upper Nozzle SS Mass	[kg]	2.080	2.080	1.950	2.080	2.080	2.080	1.950	2.080	2.080	2.080	2.080	2.080	2.080
Upper Plenum Spring Mass (Max)	[kg]	1.913	1.535	1.578	1.578	1.620	1.620	1.684	1.684	1.706	1.940	1.961	2.047	2.132
Upper Plenum Spring Mass (Min)	[kg]			1.578	1.578			1.684	1.684					
Upper Plenum Grid Mass	[kg]	0.000	0.000	0.000	0.000	0.000	0.000	0.000	0.000	0.000	0.000	0.000	0.000	0.000
Lower Plenum Spring SS Mass	[kg]	0.000	0.000	0.000	0.000	0.000	0.000	0.000	0.000	0.000	0.000	0.000	0.000	0.000
Incore Hardware SS Mass	[kg]	0.000	0.000	0.000	0.000	0.000	0.000	0.000	0.000	0.000	0.000	0.000	0.000	0.000
Incore Hardware Inconel Mass	[kg]	0.290	0.120	0.246	0.120	0.120	0.120	0.246	0.120	0.120	0.120	0.120	0.120	0.120
Upper Plenum Zircaloy	[kg]													
Incore Zircaloy	[kg]													

tblFuelData

Revision History		
Pressure & Fuel Data Versions	revFuel	v1.0

Linked Workbooks		
Fuel	wkbFuel	ms_fueldata_v31z xls

Conversion Factors			
Conversion	Unit	Name	Value
in to cm	[cm/in]	in2cm	2.54
in3 to cm3	[cm3/in3]	inc2cmc	16.387064
GW to W	[W/GW]	GW2W	1.E+09
Avogadro constant		avogadro	6.0E+23
Ideal Gas Constant	[(l-atm)/(mol-K)]	gasconst	0.08205
MeV to Joules (W-sec)	[J/MeV]	MeV2J	1.602E-13
Fission to MeV	[MeV/Fission]	Fisssion2MeV	200
Day to Seconds	[sec/day]	day2sec	8.64E+04
Pound to kilogram	[kg/lb]	lb2kg	0.4535924
Kelvin to Celsius		KtoC	273.15
in3 to liters	[l/in3]	inc2l	0.016387064

Parameters	Unit	Name	Value
Number Assy PWR		numAssyPWR	37
Number Assy BWR		numAssyBWR	87
Number CEA		numCEA	9
Number DFC		numDFC	4
Number DFC Spacer		numDFCSpacer	4
Density SS	g/cm3	rhoSS	7.94
Density Zircaloy	g/cm3	rhoZirc	6.56
Density Inconel	g/cm3	rhoInconel	8.3
Density Silver	g/cm3	rhoSilver	10.5
Density Hafnium	g/cm3	rhoHafnium	13.31
B10 Abundance	%	gB10gB	0.203
B10 Atomic Mass	amu	B10amu	10.013
Boron Atomic Mass	amu	Bamu	10.811
Carbon Atomic Mass	amu	Camu	12.0107
Moles of He / Moles of B10	%	B102He	100%
WABA B10 Liner Concnetration Factor	%	WABAB10Factor	100%
Denisty B4C	g/cm3	rhoB4c	2.52

Parameters Specific to Pressure Calculation			
Parameters	Unit	Name	Value
Pressure Conv. 1	psi/Mpa	pconv1	0.0069684
Pressure Conv. 2	[psi/atm]	atm2psi	14.7
Fission Gas	atoms/fission	atomperfiss	0.3125
PWR Rod Backfill Pressure	psig	pbackfillpress	500
BWR Rod Backfill Pressure	psig	bbackfillpress	132
Rod Backfill Temp	K	tbackfill	293.15
VCC Norm Fuel Rod Failure Fraction	%	vccnormfuelfail	1%
VCC Off-Norm Fuel Rod Failure Fraction	%	vccoffnormfuelfail	10%
100% Fuel Rod Failure Fraction	%	allfuelfail	100%
Fission & Actinide Decay Gas Release Fraction	% (per failed rod)	fuelgasrelease	30%
Rod Backfill Gas Release Fraction	% (per failed rod)	rodbackfillgasrelease	100%
BPRA Gas Release Fraction	% (per failed rod)	BPRAgasrelease	100%
Transfer Norm Bulk Ave Gas Temp	°F	tfrnormtemp	477
Transfer Off-Norm Bulk Ave Gas Temp	°F	tfroffnormtemp	502
Transfer Accident Bulk Ave Gas Temp	°F	tfracctemp	677
Transport Norm Bulk Ave Gas Temp	°F	trnnormtemp	515
Transport Accident Bulk Ave Gas Temp	°F	trnacctemp	670

508
662

F	K	atm	psig
468	515.372	8.01	103.0
666	625.37	9.72	128.1

NAC INTERNATIONAL RESPONSE TO REQUEST FOR ADDITIONAL INFORMATION

THERMAL EVALUATION

3-5 See proprietary RAI responses.

NAC INTERNATIONAL RESPONSE TO REQUEST FOR ADDITIONAL INFORMATION

THERMAL EVALUATION

3-6 Clarify the meaning of an "area-weighted" y+ value so that a review of the FLUENT fin model can be performed

NAC's response to NRC question 3-1 in letter dated January 13, 2015, states that the area-weighted y+ value of 0.55 is appropriate for the model. Confirm that all of the local grid/nodes have an appropriate y+ value, recognizing that y+ values should be determined locally at each grid node near the surface and not determined as an average over a surface.

This information is needed to confirm compliance with 10 CFR 71.35, 10 CFR 71.71, and 10 CFR 71.73.

NAC International Response to Thermal Evaluation RAI 3-6:

The area-weighted average y^+ is the cell surface area weighted average on model surfaces.

Figure 1 is the contour plot of y^+ across all solid surfaces facing the air for the full range of y^+ values determined by the solution. For the entire cask surface, in considering all the cells, $0.0065 < y^+ < 3.2$. It is observed that more than 99% of the surface area has a $y^+<2$. Acceptable values of y^+ for resolving the sublayer is for $y^+ \sim O(1)$. Therefore, the near-wall mesh resolves the sub-layer by accurately capturing the wall velocity and temperature gradients.

Figure 1 – Contour plot of y^+ across solid surfaces facing air zones, for full range of y^+.

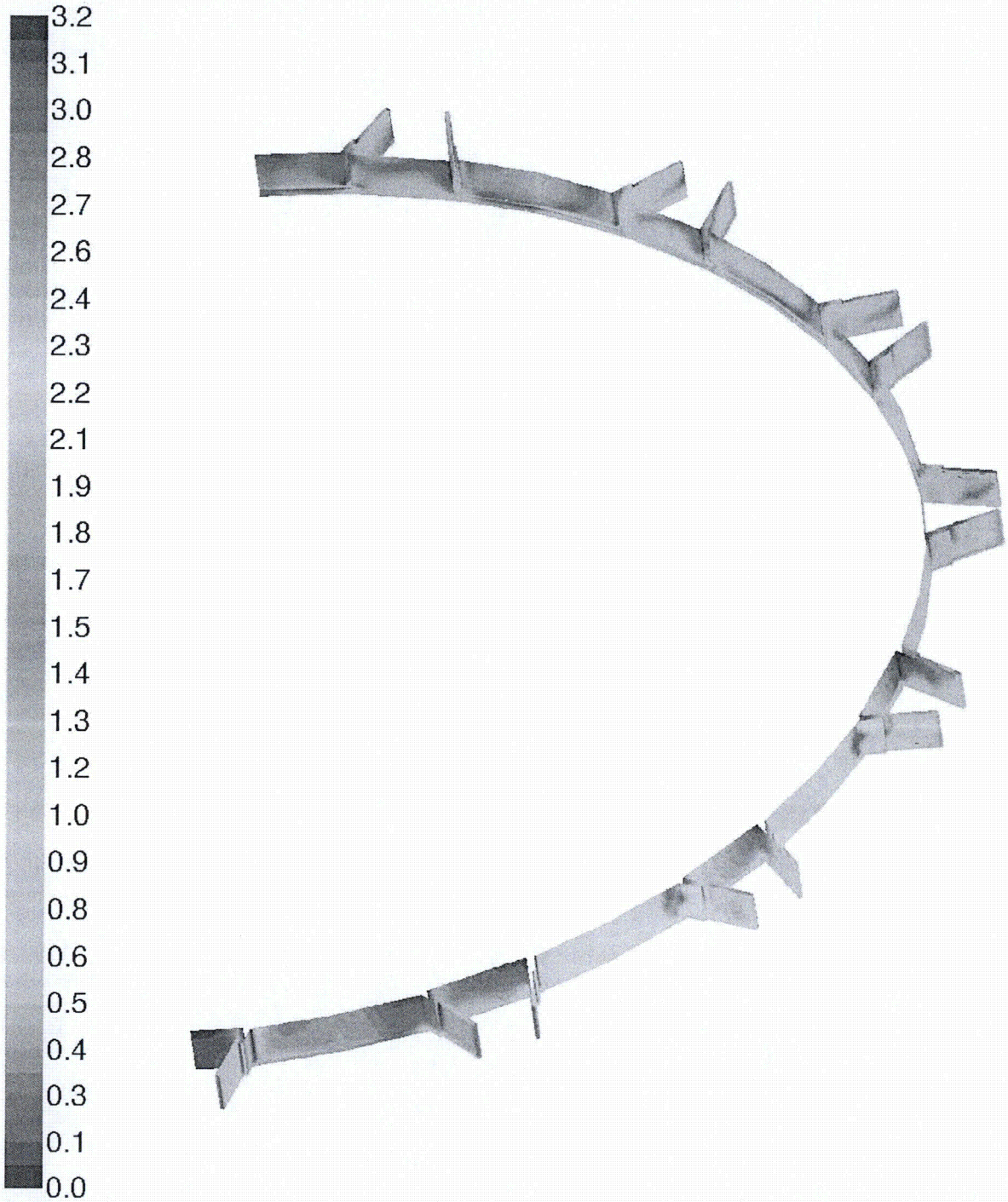

NAC INTERNATIONAL RESPONSE TO REQUEST FOR ADDITIONAL INFORMATION

THERMAL EVALUATION

3-7 Provide a more accurate package boundary condition heat transfer coefficient during the fire analysis that recognizes fins tend to augment heat transfer (including the contribution due to convection from the fire) or provide a bounding boundary condition.

a. According to NAC's response to question 3-1 in letter dated January 13, 2015, the MAGNATRAN® fin effectiveness is 3.1. However, NAC's response to question 3-12 did not address the effect of fins, which augment heat transfer from the fire's forced convection, during the thermal test for hypothetical accident conditions. Rather, the hypothetical accident conditions thermal model relies on input from a reference that describes a thermal analysis for hypothetical accident conditions from a package that is unfinned. A more accurate heat transfer coefficient, or a bounding boundary condition (i.e., 800 °C temperature), should be modeled.

b. Explain how the radiation thermal input from the fire is imposed on the model. It is understood that currently, a heat transfer coefficient boundary condition of 0.01833 Btu/hr in^2-°F is imposed during the fire.

c. NAC's response to question 3-12 in letter dated January 13, 2015, indicates a 171 Btu/hr-in^2 average total peak flux. Define "average total peak" heat flux (average versus peak) and show how it is calculated and imposed on the model to achieve the current convection coefficient of 0.01833 Btu/hr- in^2-°F. Clarify whether it is the portion attributed only to convection effects.

This information is needed to confirm compliance with 10 CFR 71.73.

<u>NAC International Response to Thermal Evaluation RAI 3-7:</u>

A. Fins are used to increase the heat transfer from a surface by increasing the effective surface area. The fin effectiveness is defined as the ratio of the fin heat transfer rate to the heat transfer rate that would exist without the fin. The fin effectiveness is 3.1 for the MAGNATRAN cask, which means 3.1 times of heat is transferred into the cask during the fire than the cask without the fin.

The surface area of the cask has been increased significantly compared with the area that would exist without the fin. In the MAGNATRAN thermal analyses, the effect of fins during the fire accident is considered by applying the fire boundary condition (convection and radiation) to all cask outer surfaces, including both sides of all the fin surfaces that are exposed to the fire, which results in the 3.1 times of heat being transferred to the cask during the fire than the cask without the fins.

As shown in the NAC's response to question 3-12 in letter dated January 13, 2015, the radiation from the fire plus the convection during the fire in the MAGNATRAN analysis provided adequate heat flux as compared with the test data (from the paper which the NRC recommended to NAC).

B. The radiation during the fire is applied by combining it with the convection film coefficient of h_c of 0.01833 Btu/hr in^2-°F. Radiation heat transfer on the surface of the cask is incorporated in the boundary condition applied to the model by modifying the convection coefficient. This derivation is presented in Section 3.2.2.2.

C. The heat flux is not imposed on the model as a boundary condition. The boundary condition is the film coefficient, which is computed as described above, with the ambient temperature of 1,475°F. This is applied as a step condition to the model. The heat flux transferred to the cask surface due to the fire is dependent on the cask surface temperature, which increases monotonically from the beginning of the fire condition. The peak heat flux, therefore, occurs at the beginning of the fire condition. The first solution time step is post processed to determine the peak flux. In post processing the solution, the quantity obtained from the program is the total flux passing through the surface of each element on the surface of the model. The convection coefficient used to generate the solution used the film coefficient as described above, which combined the convection and the radiation. Therefore, the total flux obtained from the solution has the radiation and convection flux combined. The averaged peak heat flux, resulting from both convection and radiation, is the ratio of the sum of all the heat flux from all surface elements divided by the total surface area. Therefore, the peak corresponds to the beginning of the fire and average is based on the area average. The details are contained in Appendix G of Calculation 71160-3015.

NAC INTERNATIONAL RESPONSE TO REQUEST FOR ADDITIONAL INFORMATION

THERMAL EVALUATION

3-8 Clarify the use of the half- and full-length models and correct the temperatures calculated for normal conditions of transport and hypothetical accident conditions, including Table 3.4-1, 3.5-1, and 3.5-2.

a. NAC's response to question 3-2 in letter dated January 13, 2015, compares results from half-length and full-length thermal models. It appears that the full-length model has approximately 15% more insolation than the half-length model but has lower component temperatures. This does not seem reasonable considering that the O-ring temperature for the half-length model was at a lower temperature of 184°F). (Note: Provide the higher temperature referred to in RAI 3-21 response.) Likewise, although item 2 on page 3.4-6 mentions that the top portion is 30% longer than the bottom portion, "which provides more surface area for heat rejection to the ambient," it does not address that the area covered by impact limiters is modeled as adiabatic (page 3.4-3), indicating there is no heat rejection.

b. Previously, a half-length model that did not include the lid and O-ring section was used to determine component temperatures. Section 3.4.1.1.1 in the SAR very briefly described a new full-length three-dimensional MAGNATRAN® ANSYS model. The full-length model resulted in an O-ring temperature during normal conditions of transport of 232°F, an increase from the half-length model value of 184°F. Except for the higher O-ring temperature, it appears that Table 3.4-1 lists temperatures from the half-length model. Explain the rationale for not relying on the full-length model results in the SAR that provided more accurate and bounding temperatures near the critical O-ring area and provide the component temperatures that use the full length model.

c. Explain whether the O-rings, which are part of the containment boundary, were explicitly modeled in the full length model; if not, explain how the O-ring temperatures were determined.

This information is needed to confirm compliance with 10 CFR 71.51, 10 CFR 71.71, and 10 CFR 71.73.

NAC International Response to Thermal Evaluation RAI 3-8:

A. As noted in NAC responses to questions 3-6 and 3-21 in letter dated January 13, 2015, the O-ring temperature in Table 3.4-1 of the SAR (Revision 14A) has been revised. The O-ring temperature of 184°F was an error and has been changed based on the analysis using the full-length cask model.

   Item 2 on SAR Page 3.4-6 includes the terms "surface area for heat rejection." This restricts the area for consideration to be that area which can reject heat, and it excludes the cask surface area corresponding to the overlap with the impact limiter.

B. The temperatures for the PWR configuration reported in SAR Table 3.4-1 are the bounding temperatures obtained from the half-length cask model, except the O-ring temperatures which were from the full-length model. A comparison of the maximum temperatures between the half-length model and full-length model was provided in NAC response to question 3-2 in letter dated January 13, 2015 (also see table below).

	PWR Half-length Model	PWR Full Model
Max. T of Fuel (°F)	726	722
Max. T of Basket (°F)	701	697
Max. T of NS4FR (°F)	264	263
Max. T of Canister Shell (°F)	364	362
Max. T of Lead (°F)	276	274
Max. T of Cask Inner Shell (°F)	297	294
Max. T of Cask Outer Shell (°F)	271	270

   The half-length cask model is an accurate representation of the basket, fuel assemblies, regions of contact, material properties, both effective and actual physical properties, and boundary conditions. The approach of using a simpler but conservative model has been applied in numerous previous transport applications. As shown in the table above, the maximum temperatures obtained from the half model are slightly conservative and, therefore, are reported in SAR Table 3.4-1.

C. The O-rings are not explicitly modeled in the full length model. The O-ring temperatures are determined based on the location of the O-rings in the full-length model. A contour plot for the full-length model is shown in Figure 3-8.1.

Figure 3-8.1 Temperature Contour for the Full-Length PWR Model

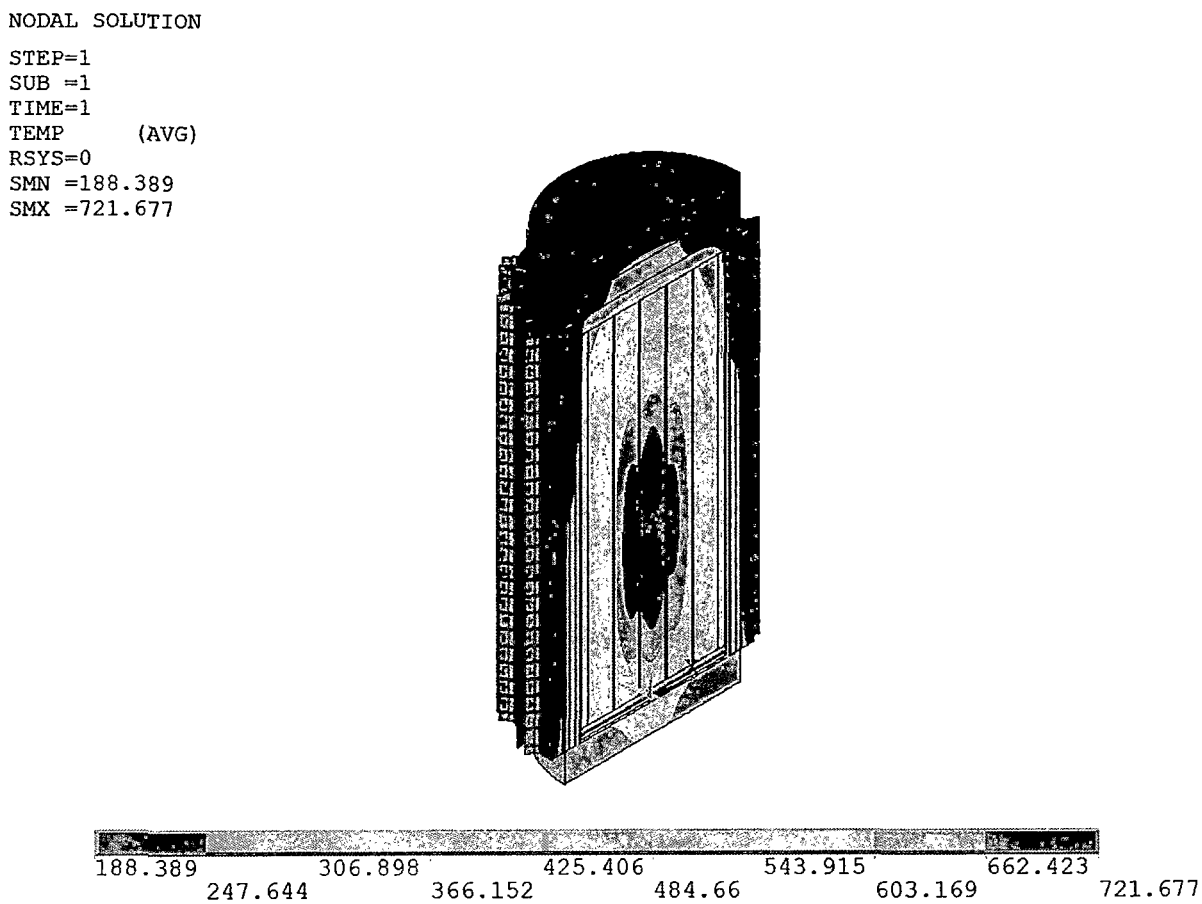

NAC INTERNATIONAL RESPONSE TO REQUEST FOR ADDITIONAL INFORMATION

THERMAL EVALUATION

3-9 Provide a grid sensitivity analysis as part of the normal conditions of transport and hypothetical accident conditions thermal analyses in the SAR.

NAC's response to question 3-18 in letter dated January 13, 2015, indicates that a grid sensitivity analysis for the ANSYS model is unnecessary for an FEA model. Grid sensitivity analyses are often performed for FEA models and, in fact, Appendix F of Calculation Package 71160-3020, Rev. 3, provides a grid sensitivity study for the MAGNASTOR® ANSYS FEA model, which indicated a temperature dependency on grid resolution. Grid sensitivity should be analyzed, considering the relatively small temperature margin of peak clad temperature (PCT) to the allowable value for normal conditions of transport. NRC confirmatory analysis indicates that the PCT may be above 752°F.

This information is needed to confirm compliance with 10 CFR 71.71 and 10 CFR 71.73.

NAC International Response to Thermal Evaluation RAI 3-9:

A finite element mesh sensitivity study is performed for the normal condition of transport for the PWR configuration. The three-dimensional full-length (360°) cask model (SAR Figure 3.4-13) described in Appendix K of NAC Calculation No. 71160-3014 is modified to perform a steady state analysis for the mesh sensitivity study for normal transport condition. The refinement was accomplished by increasing the element divisions in the axial direction. The number of the elements in the model was increased to 930,390 from 556,350, which is 67% more elements than the original mesh of the full-length cask model. Since the mesh divisions were changed, the constraint equations which connect the helium gap at canister shell surface and the cask inner shell were regenerated, resulting in a refined analytical connectivity. Consequently, the calculated maximum temperatures of the fuel cladding and cask/basket components from the refined model (see third temperature column in Table 3-9.1 below) are lower than those from the full length cask model with original mesh (see second temperature column in Table 3-9.1 below). Note that all temperatures calculated using the finer mesh model (in the third temperature column in Table 3-9.1) are also lower than the temperatures obtained from the original half-length cask model (first temperature column in Table 3-9.1), which are reported in SAR Table 3.4-1. Therefore, the finite element mesh used in the original half-length cask models in the SAR are conservative in determining the maximum temperatures of fuel cladding and basket/cask components. The details for this sensitivity study are contained in NAC Calculation No. 71160-3014, Appendix V.

A mesh sensitivity study is also performed for the model used in analysis of the fire accident condition for the PWR configuration. The three-dimensional sectional model described in SAR Section 3.5.1.1 is used for the sensitivity study for fire accident condition. The total number of

the elements in the model for the fire condition is increased to 55,564 from 25,164, which is 121% more elements than the original mesh. As shown in the Table 3-9.2 below, the analysis results for the key components using the refined mesh are identical to the temperatures using original model. The details for this study is contained in NAC Calculation No. 71160-3015, Appendix L.

Based on the studies described above, the finite element meshes used in the current analyses yield the same or conservative temperatures and, therefore, are adequate to identify the maximum fuel cladding and component temperatures for normal condition and fire accident condition. A discussion of the mesh sensitivity studies for the normal and fire accident conditions is added to SAR Section 3.4.1 and 3.5.1.1, respectively.

Table 3-9.1 Comparison of Maximum Temperatures for Normal Condition

	Maximum Temperature (°F)		
	Original Mesh Half-length Cask Model(1) (SAR Fig. 3.4-1)	Original Mesh Full-length Cask Model(2) (SAR Fig. 3.4-13)	Refined Mesh Based on Full-length Cask Model(3)
Fuel	726	722	693
Basket	701	697	666
NS4FR	264	263	261
Canister Shell	364	362	346
Lead	276	274	272
Cask Inner Shell	297	294	293
Cask Outer Shell	271	270	267

(1) See Main Body of NAC Calculation No. 71160-3014; Temperature Results presented in SAR Table 3.4-1
(2) See Appendix K of NAC Calculation No. 71160-3014
(3) See Appendix V of NAC Calculation No. 71160-3014

Table 3-9.2 Comparison of Maximum Component Temperatures for Fire Accident

	Maximum Temperature (°F)	
	Original Mesh	Refined Mesh
Lead	536	536
Inner Surface of the Inner Shell	460	460
Lid Inner O Ring	289	289

NAC INTERNATIONAL RESPONSE TO REQUEST FOR ADDITIONAL INFORMATION

THERMAL EVALUATION

3-10 Confirm that there are no adverse consequences (e.g., containment, shielding, thermal effects of changing gap sizes, etc.) due to temperature gradients/thermal stresses that may occur during hypothetical accident conditions.

Section 2.7.4.3 and Section 3.5.5 in the SAR indicates that thermal stresses were not calculated for hypothetical accident conditions. The potential effects of temperature gradients (e.g., gap size changes due to different thermal expansion coefficients of inner shell steel and lead gamma shield, etc.) and thermal stresses on packaging performance must be considered.

This information is needed to confirm compliance with 10 CFR 71.73.

NAC International Response to Thermal Evaluation RAI 3-10:

Section 2.1.2.2 identifies the accident condition stress criteria for the MAGNATRAN cask is the ASME Boiler & Pressure Vessel Code, Section III, Subsection NB, Appendix F. Sections such as F-1332 in Appendix F state that stresses resulting from thermal stresses are not to be considered. There is no requirement to calculate thermal stresses for accident conditions. Thermal stresses are considered to be secondary and as defined by the ASME Code, secondary stresses are self-limiting by definition.

The changes in the gap between the basket and canister shell and the gap between the canister shell and cask inner shell due to thermal expansion were reviewed at two time points of the transient fire condition. The two time points chosen were at the end of the fire when the outer surfaces reach maximum temperatures and the point where the inner surface of the transport cask reaches at maximum temperature. The results show minimal change in the gap between the basket and the canister and the gap between the canister and the cask inner shell. The canister and basket do not develop any additional stress due to contact with the adjacent component. The details of this gap clearance evaluation are contained in Appendix K of NAC Calculation No. 71160-3015.

Calculation of the volumetric expansion of the lead shielding and the cask cavity formed by the cask inner shell and the outer shell was performed for the point in the fire transient where the largest differential temperature exist between the inner shell and outer shell of the cask. This required the determination of the temperature differential for each time step solved in the thermal transient analysis. The thermal expansion calculation using the largest differential showed negligible difference (<0.01%) between the expanded volume of the lead versus the expanded volume of the cavity between the inner and outer shells. Therefore, there would be no significant change at the interface between the lead shielding and the interfaces with the inner shell or the outer shell of the cask. Since the lead has a much lower yield strength than either the inner shell

or the outer shell (approximately 0.3 ksi for the lead versus 20 ksi for the stainless steel), the lead will not exert any significant pressure on the cask due to radial expansion.

The change in bolt loads due to fire temperature increase was calculated for the point in the fire transient where the lid and bolt region reach a maximum temperature. Since the thermal expansion coefficient of the bolt is larger than the thermal expansion coefficient of the lid, the bolt load decreases from the preload at ambient conditions. Calculations of the minimum bolt load and the bolt load required to resist the accident pressure in the cask showed that the minimum bolt load was much greater than the bolt load needed to resist the accident pressure of 300 psi. Therefore, the integrity of the closure assembly would be maintained during the fire transient. The details of the bolt load evaluation is contained in Appendix L of NAC Calculation No. 71160-2108.

NAC INTERNATIONAL RESPONSE TO REQUEST FOR ADDITIONAL INFORMATION

THERMAL EVALUATION

3-11 Clarify and correct how gaps were modeled in the thermal ANSYS calculations (normal conditions of transport, hypothetical accident conditions, etc.) so that a review of the analyses can be performed. Include, in the ANSYS models, a more accurate, or bounding, representation for the contact area between the basket and canister shell, contact area between canister shell and the package, and the thermal conductivity between those gaps.

Gaps within a thermal model have an impact on thermal results. NAC's response to question 3-10 in letter dated January 13, 2015, did not adequately address the following, which would have an effect of component temperatures, including PCT:

a. Provide results that confirm the four "contact locations," and the area between them, shown in the Figure 3-10.1 (NAC response to question 3-10), pictorial actually represent physical contact between the separate components. It should be understood that an "arc of contact" does not necessarily represent a contact area.

b. NAC's response to question 3-10, page 10 of 37 of Calculation package 71160-3014, Rev. 0, indicates that applying the helium thermal conductivity to gaps within the package would be "overly conservative." However, SAR Section 3.2.2.3 states that the gas conductivity of the gap is used (which is not the 0.8 or 2 Btu/hr-in-°F imposed value). There is no basis for assuming a thermal conductivity of 0.8 Btu/hr-in-°F for gaps listed as 0.03 inch (or larger, some of which were listed as 0.28 inch). Gaps would more accurately be modeled using the thermal conductivity of the surrounding/backfill gas.

c. Provide the calculations that show how the thermal conductivities were determined. For example, there was no calculation showing the basis for choosing a contact thermal conductivity of 0.8 Btu/hr-in-F between the stainless steel components, considering that stainless steel can have a thermal conductivity of 0.867 Btu/hr-in-F and there would be some form of contact resistance between different components.

d. Provide further details associated with the calculation that showed a 1°F change in temperature when thermal conductivity changed from 2 Btu/hr-in-F to 0.8 Btu/hr-in-F.

e. There are many instances in Calculation Package 71160-3014, Rev. 0 (page 14, 15, etc.) in which gaps are modeled by "effective properties" that are "adjusted" by "factors" (0.2044, etc.). There is no clear discussion or calculation that

explains the rationale or procedure for modeling a gap with effective properties or applying an adjustment factor; the discussion in SAR Section 3.2.2.3 is very limited and there is nothing showing the relative contribution to conduction and radiation heat transfer in the presented results. Based on the limited description and presented results, it would appear that gaps should be modeled with the surrounding/backfill gas thermal conductivity, especially because the radiation heat transfer component would be small.

f. NAC's response to question 3-7(a.2) in letter dated January 13, 2015, indicates an assumed gap between the lead gamma shield and the steel body of the transportation package is conservative. This may be conservative for the cooldown phase of the fire test for hypothetical accident conditions, but it would not be conservative during normal conditions of transport because the higher temperature on the inner face and the small surface area would tend to over-estimate the heat transfer across the gap compared to putting the gap on the outer surface. This may have an effect on results; a sensitivity study should be performed considering the relatively small temperature margin of PCT during normal conditions of transport.

g. Include a calculation that describes the intent of Calculation Package 71160-3014, item 10 on page 15 of 37 (e.g., why 75% of helium thermal properties). Based on the limited description, it would appear that gaps should be modeled with the helium thermal conductivity.

h. NAC's response to question 3-10 in letter dated January 13, 2015, discusses the contact arc. However, it is the actual area of good contact (basket-to-shell and canister-to-shell) that affects heat transfer. It is difficult to understand how "contact" can be assumed for gaps that are 0.03 inch and larger. Provide information on the following contact areas that were used in the thermal analysis in the SAR:

1. The linear contact length in the thermal model at each location (as illustrated in Figure 3-10.1 and Figure 3-10.2) in the basket cross-section where it is assumed that there is perfect contact between the basket and the canister shell.

2. The axial length that the perfect contact between the basket and the canister shell is assumed to exist over in the thermal model.

3. The total contact area assumed at each location in the thermal model where it is assumed that there is perfect contact between the basket and the canister shell (Note: this is a redundant check on the information in (1) and (2) above; just for completeness.)

4. The linear contact length in the thermal model between the canister outer shell and the packaging inner liner for the package cross-section.

5. The axial length in the thermal model that contact between the canister shell and the packaging inner liner is assumed to exist over in the thermal model.

6. The value(s) of thermal conductivity used to represent contact conductance between elements assumed to be in contact, for the basket-to-shell contact region and the canister-to-shell package region.

i. The diagrams in Figure 3-10.1 and 3-10.2 are based on what appears to be an optimum orientation of the basket within the canister shell, relative to the assumed direction of the force of gravity. That is, this orientation appears to be one that would produce the maximum contact area. Is it expected that orientation of the canister within the package will be controlled to the degree that it can be ensured that this orientation will be maintained in all transport configurations? If not, a sensitivity study is needed to show the effect of canister orientation on contact area. The minimum contact area should be used in the thermal model, to ensure conservatism in the predicted canister component temperatures, including PCT.

This information is needed to confirm compliance with 10 CFR 71.71, and 10 CFR 71.73.

NAC International Response to Thermal Evaluation RAI 3-11:

a. The half-symmetry (180°) structural model for the PWR basket in Figure 3-10.1 (NAC response to question 3-10 of RAI-1) shows four locations of contact, which is equivalent to seven (7) locations for a full (360°) model. As shown in Figure 3.11-1, the PWR thermal model conservatively considers five (5) contact regions between the basket and the canister shell. At these contact regions, the basket is in contact with the canister shell and there is no physical gap between the basket and canister shell. However, there are gaps in the finite element model, as shown in the elements with color yellow/lime green in Figures 3-11.2 and 3-11.3. Note that Region 3 and Region 5 are similar to Region 2 and Region 4, respectively, and therefore, the close-up plots for Regions 3 and 5 are not provided. A thermal conductivity of 2.0 Btu/hr-in-°F (equivalent to the conductivity of carbon steel, which is the material of the basket), is assigned to the elements at the gap in the thermal model to simulate the contact (no gap) conditions.

The contact region between the canister shell and cask inner shell for the PWR thermal model is shown in Figure 3-11.4. Since there should be no gap between the canister shell and the cask inner shell in the contact region, the thin layer of elements between the canister shell and the cask inner shell (ranged from 0.03 to 0.09 inch thick) in the finite element model are assigned a thermal conductivity of 2.0 Btu/hr-in-°F to simulate the contact (no gap) conditions. Helium thermal

conductivity is used for the elements (between the canister shell and cask inner shell) outside the contact region.

Figure 3-11.5 shows the heat flux vectors from the basket to the canister shell. As shown in the plot the dominant heat flux vectors occur at the contact regions.

The half-symmetry (180°) structural model for the BWR basket in Figure 3-10.2 (NAC response to question 3-10 of RAI-1) shows four locations of contact, which is equivalent to four (4) locations for a full (360°) model. As shown in Figure 3.11-6, the BWR thermal model considers four (4) contact regions between the basket and the canister shell. The contact region between the canister and cask inner shell for the BWR thermal model is shown in Figure 3-11.7.

b. As noted in the response in 'a' above, a conductivity (2.0 Btu/hr-in-°F) was used for the elements in the contact regions of the model (between the basket and canister shell, and between the canister shell and cask inner shell) to simulate the contact (minimizing the temperature gradient through the thickness of these elements). The application for SAR Section 3.2.2.3 is used for modeling the combination of radiation and conduction for an actual/physical gap in a finite element model. This application is not used for the elements in the contact regions, where only conduction is considered.

c. The conductivity of 2.0 Btu/hr-in-°F (used in original models) or 0.8 Btu/hr-in-°F (for sensitivity study) were selected based on the thermal conductivity of carbon steel and stainless steel respectively. The intent was to allow the elements at the contact regions in the model to have a relatively small contact resistance (small ΔT through the thickness of the elements) since a gap does not exist at the regions where the components are in contact.

In order to demonstrate that the methodology described above is acceptable, a sensitivity analysis is performed using the PWR fine mesh thermal model corresponding to 0° basket orientation. Two Cases are considered:

<u>Case 1 (Base Case)</u>

The PWR fine mesh thermal model as described in the NAC response to Question No. 3-9 (45° basket orientation) is rotated to correspond to a 0° basket orientation, as shown in Figure 3-11.8. A total of four contact regions is considered between the basket and the canister shell (see NAC response to Question 3-11(i) for discussion on contact locations). The contact region between the canister shell and cask inner shell is shown in Figure 3-11.9. A thermal conductivity of 2.0 Btu/hr-in-°F is used for the elements in contact regions.

Case 2 (Study Case)

The thermal model for Case 2 is based on the model for Case 1 with the following changes:

- The entire basket (including the fuel regions) in the model is shifted down so that the minimum gap between the basket and the canister shell is 0.003 inch (See Figure 3-11.10).
- Thermal conductivity for the elements at contact regions between basket and canister shell is changed from 0.8 Btu/hr-in-°F to the thermal conductivities of helium (see Regions A and B in Figure 3-11.10).
- Thermal conductivity for the elements at contact regions between canister shell and cask inner shell is changed from 0.8 Btu/hr-in-°F to the thermal conductivities of helium (Figure 3-11.11).

The maximum fuel cladding temperature is calculated to be 697°F for Case 1 and 698°F for Case 2. The sensitivity study results indicate that the two different methods (as used in Case 1 and Case 2) of modeling the contact region would predict essentially identical temperature results for the fuel cladding as well as system components. It is concluded that the method of modeling the contact regions in the original models in the SAR (method for Case 1) is adequate. Note that, as shown in the NAC response to Question 3-9, the temperatures calculated using the original half-length cask models in the SAR are very conservative. Therefore, all the temperatures reported in the SAR remain bounding and no further change is required.

d. The sensitivity study was performed using the same thermal model with the conductivity changed from 2 Btu/hr-in-°F to 0.8 Btu/hr-in-°F for the elements between the basket and canister shell and elements between the canister shell and cask inner shell in the contact regions (See Figures 3-11.2 through Figure 3-11.4). See Appendix P of NAC Calculation No. 7116-3014 R3 for more details, which was previously submitted.

e. Adjusted conductivities are used for gaps in the model when the gap thickness in model is different from the actual/physical gap thickness. Thermal resistance is defined as L/(kA) for the conduction (where L is the length or gap thickness, k is the thermal conductivity and A is the cross sectional area). Since the thermal resistance is proportional to the length (gap thickness), the conductivity used in the elements at the gap in the model needs to be decreased by a factor (less than 1) if the modeled gap thickness is smaller than the actual gap thickness. Similarly, the conductivity used in the elements at the gap in the model needs to be increased by a factor (greater than 1) when the modeled gap is larger than actual gap.

For example, the physical gap between the canister bottom and the inner surface of the cask bottom plate is 5.625 inches based on design drawings while it is

modeled as 1.15 inches in the model. The gap is filled with helium. For the elements at this gap, orthotropic material properties (conductivities) are used: The conductivity in the direction across the gap is defined as helium conductivity with a factor of 0.2044 (1.15/5.625). For the other two directions (perpendicular to the gap), helium conductivities are used.

SAR Section 3.2.2.3 describes the calculation of the effective thermal conductivity (K_{eff}) for the combination of conduction and radiation. If the application of this Section is used for a gap in the model with a gap thickness different from the actual/physical gap thickness, the adjusted thermal conductivity will be used to for the 'K' (conduction term) in the expression of K_{eff}.

f. The cask inner shell, the gap, the lead and the outer shell form a cylindrical system. The effective thermal resistance of the following two configurations are compared to assess the effect of the gap location on the thermal performance of the cask for normal conditions of transport.

Configuration 1: The gap is located between the inner shell and the lead. The heat flows through the inner shell, the gap, the lead and then outer shell.

Configuration 2: The gap is located between the lead and the outer shell. The heat flows through the inner shell, the lead, the gap and then the outer shell.

The effective thermal resistance of a cylindrical system corresponding to the above configurations has been computed and documented in Appendix W of NAC Calculation No. 71160-3014, Rev. 4. The results of the derivation indicate that thermal resistance for Configuration 1 is 3% higher than that for Configuration 2. This confirms that the modeling of the gap at the inner shell/lead interface is bounding for the steady state analysis for normal condition of transport. The 3% difference of thermal resistance is considered to be insignificant for the evaluation of the fire accident condition, since the primary reason for the retardation of the heat leaving the cask after the fire is the mass of the shells and the lead.

g. Using 75% of the helium conductivity for the elements in the gap is to provide a slight conservatism of the thermal model for the evaluation of normal condition of transport. The gap thickness in the model is not uniform due to the method used to generate the solid model in ANSYS, from which the nodes and elements were generated. The thickness of the gap varies from 0.0089 inch to 0.015 inch. To account for the difference, a factor of 1.7 (=0.015/0.0089) was used to reduce the thermal conductivity assigned to the elements in the gap. Note that the conductivity used in the gap has an insignificant effect on the maximum temperature of the fuel cladding or cask components since the gap size is very small and the ΔT across the gap is minimal.

h. 1 – 5. As discussed in NAC response in 'a', the contact regions for the PWR thermal model are shown in Figures 3-11.2 and 3.11-3. The contact regions for the BWR thermal model are shown in Figures 3-11.6 and 3-11.7. The contact area information used in the thermal models for PWR and BWR configurations are provided below.

Contact Areas between PWR Basket and Canister Shell (Fig 3.11-2)

Contact Region	Circumferential Length (in.)	Axial Length (in.)	Contact Area (in^2)
1	0.466	72.0	33.55
2	0.793	72.0	57.10
3	0.793	72.0	57.10
4	2.562	72.0	184.46
5	2.562	72.0	184.46
		Area Sum =	516.67 in^2

Contact Areas between PWR Canister & Cask Inner Shell (Fig. 3-11.3)

Circumferential Length (in.)	Axial Length (in.)	Contact Area (in^2)
56.745	76.6	4,367.7

Contact Areas between BWR Basket and Canister Shell (Fig. 3-11.6)

Contact Region	Circumferential Length (in.)	Axial Length (in.)	Contact Area (in^2)
1	0.650	72.0	46.80
2	0.722	72.0	51.98
3	0.650	72.0	46.80
4	0.722	72.0	51.98
		Area Sum =	197.56 in^2

Contact Areas between BWR Canister and Cask Inner Shell (Fig. 3-11.7)

Circumferential Length (in.)	Axial Length (in.)	Contact Area (in^2)
41.269	83.6	3,450.1

6. A thermal conductivity of 2.0 Btu/hr-in-°F is used for elements for the basket-to-canister shell contact regions and the canister-to-cask inner shell contact region.

i. Using the same methodology described in the NAC response to NRC question 3-10 of RAI-1 (in Letter dated January 13, 2015), additional structural analyses were performed for 1g side load using the half-symmetry PWR basket model from Section 2.6.13 and the half-symmetry BWR basket model from SAR Section 2.6.15 to determine the contact regions with 0-degree basket orientation. Based on the analysis results, there are two contact locations between the basket and canister shell, as shown in Figure 3-11.12 and 3-11.13 for PWR and BWR basket respectively. Accordingly, four contact locations are to be considered for a full (360°) thermal model with 0° basket orientation.

To assess the effect of basket orientation (and different contact conditions) of the thermal models on maximum fuel cladding temperatures, a sensitivity analysis is performed as summarized in Table below. The full-length refined (fine mesh) PWR model (used in NAC responses to Question 3-9) is used for Case 1 (Base Case). Model for Case 2 is based on Model for Case 1 with the changes listed below (See Figures 3-11.8 and 3-11.9). Note that Case 2 Model is also used as in the sensitivity analysis in the response to question 3-11(c).

1. The basket is rotated to correspond a 0° basket orientation.
2. The basket is in contact with the canister shell at four locations
3. No. of elements simulating the contact between the basket and canister shell are reduced (e.g. two elements are used in Region 2 of Figure 3-11.3 and only one element is used in Region B of Figure 3-11.8)

Case	Basket Orientation	No. of Contact Regions between basket and canister shell	Figures Showing Contact Regions	Maximum Fuel Cladding Temperature	Model also used in NAC Responses to Question No.
1	45°	5	3-11.2 3-11.3 3-11.4	693°F	3-9
2	0°	4	3-11.8 3-11.9	697°F	3-11(c)

As shown in the table above, the difference in maximum temperatures of the fuel cladding is not significant (4°F). This comparison indicates that the system temperature is not sensitive to the basket orientation in the cask during transport condition. Note that the maximum fuel cladding temperatures for both cases are well below the maximum fuel cladding temperature of 726°F as determined by the original three-dimensional half-length PWR thermal model presented in the SAR Section 3.4.1.1.1. Based on the sensitivity studies performed for the PWR configuration (the comparison in the table above and in the responses to Question 3-9), it is concluded that the temperature results presented in the SAR for both the PWR and BWR configurations are bounding and conservative.

For clarification, a summary of thermal models and sensitivity analyses used in NAC responses to Thermal Questions are provided in the following tables.

Model ID	Description	Basket Orientation	Conductivity used in contact regions (Btu/hr-in-°F)	Max. Fuel Cladding Temperature	NAC Calculation 71160-3014
A	Original PWR Model in SAR Section 3.4.1.1.1, Fig. 3.4-1 (Half length)	45°	2.0	726°F	Main Body
B	Full Length PWR Model (SAR Fig. 3.4-13)	45°	2.0	722°F	Appendix K
C	Same as Model A with reduced conductivity at contact regions	45°	0.8	727°F	Appendix P
D	Refined Model (finer mesh) based on Model B	45°	2.0	693°F	Appendix V
E	Same as Model D with Basket rotated to correspond to 0°	0°	0.8	697°F	Appendix X
F	Same as Model E with basket shifted (gap≈0.003 inch at basket/canister and canister/cask contact regions)	0°	Helium	698°F	Appendix Y

Purpose of Sensitivity Study	Model Used (Max Fuel Temperature)	NAC Calculation 71160-3014	Response to NRC Question No.
Half-length vs Full-length Model	Model A vs Model B (726°F vs 722°F)	Appendix K	3-2 (RAI-1, NAC letter dated Jan 13, 2015)
Effect of Thermal Conductivity Used at Contact Regions (2.0 vs 0.8 Btu/hr-in-°F)	Model A vs Model C (726°F vs 727°F)	Appendix P	3-10 (RAI-1, NAC letter dated Jan 13, 2015)
Mesh Study: Original Mesh vs Finer Mesh	Model B vs Model D (722°F vs 693°F)	Appendix V	3-9
Basket Orientation (45° vs 0°) – different contact locations	Model D vs Model E (693°F vs 697°F)	Appendix X	3-11 (i)
Modeling Method of Contact Region (gaps with higher conductivity vs minimal gaps with helium conductivity)	Model E vs Model F (697°F vs 698°F)	Appendix Y	3-11 (c)

Figure 3-11.1 Contact Regions between PWR Basket and Canister Shell

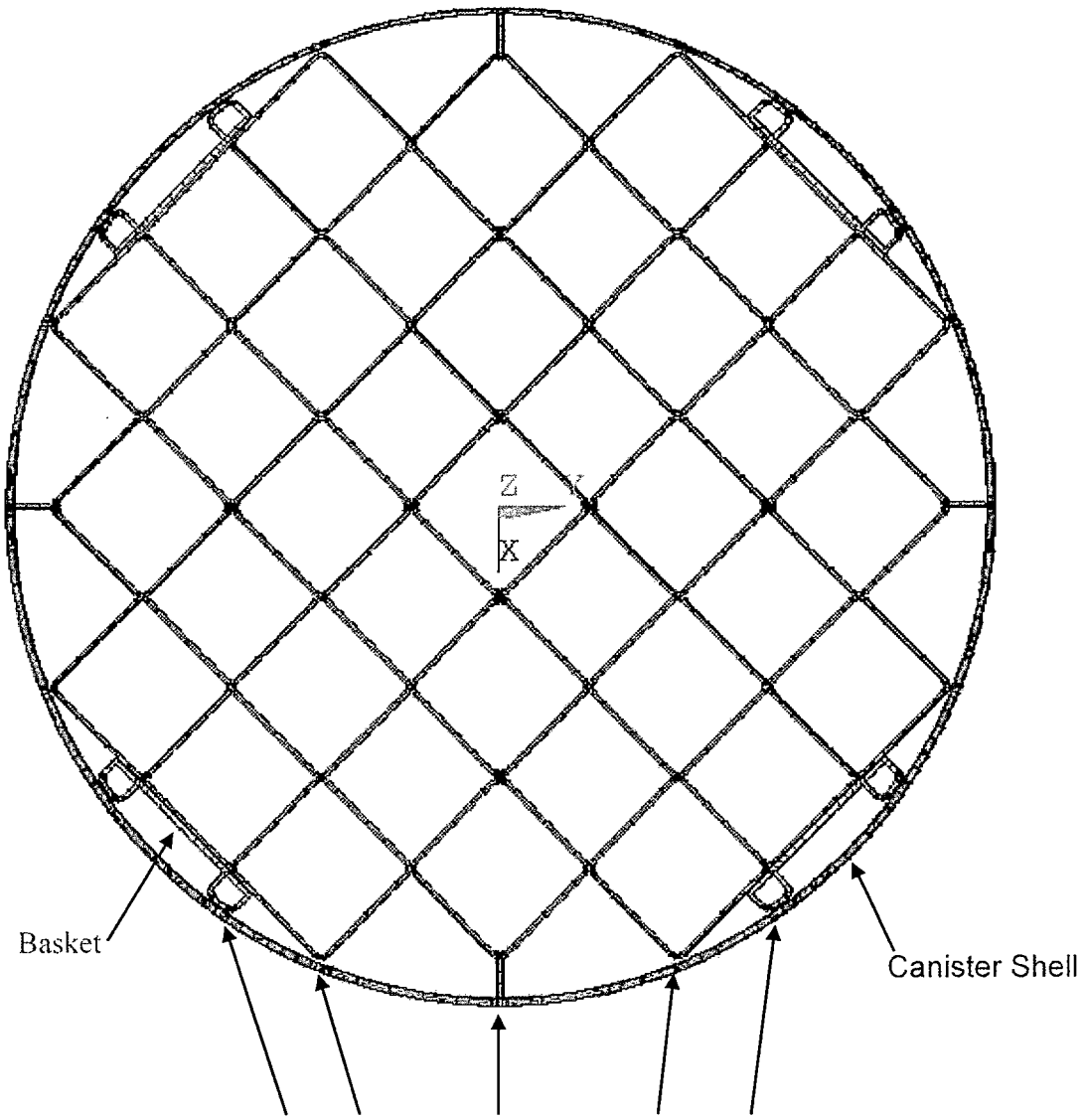

Basket is in contact with the canister shell in these locations. Physically there is no gap between the basket and canister shell in these locations.

Figure 3-11.2 Contact Regions between PWR Basket and Canister Shell in the Thermal Model

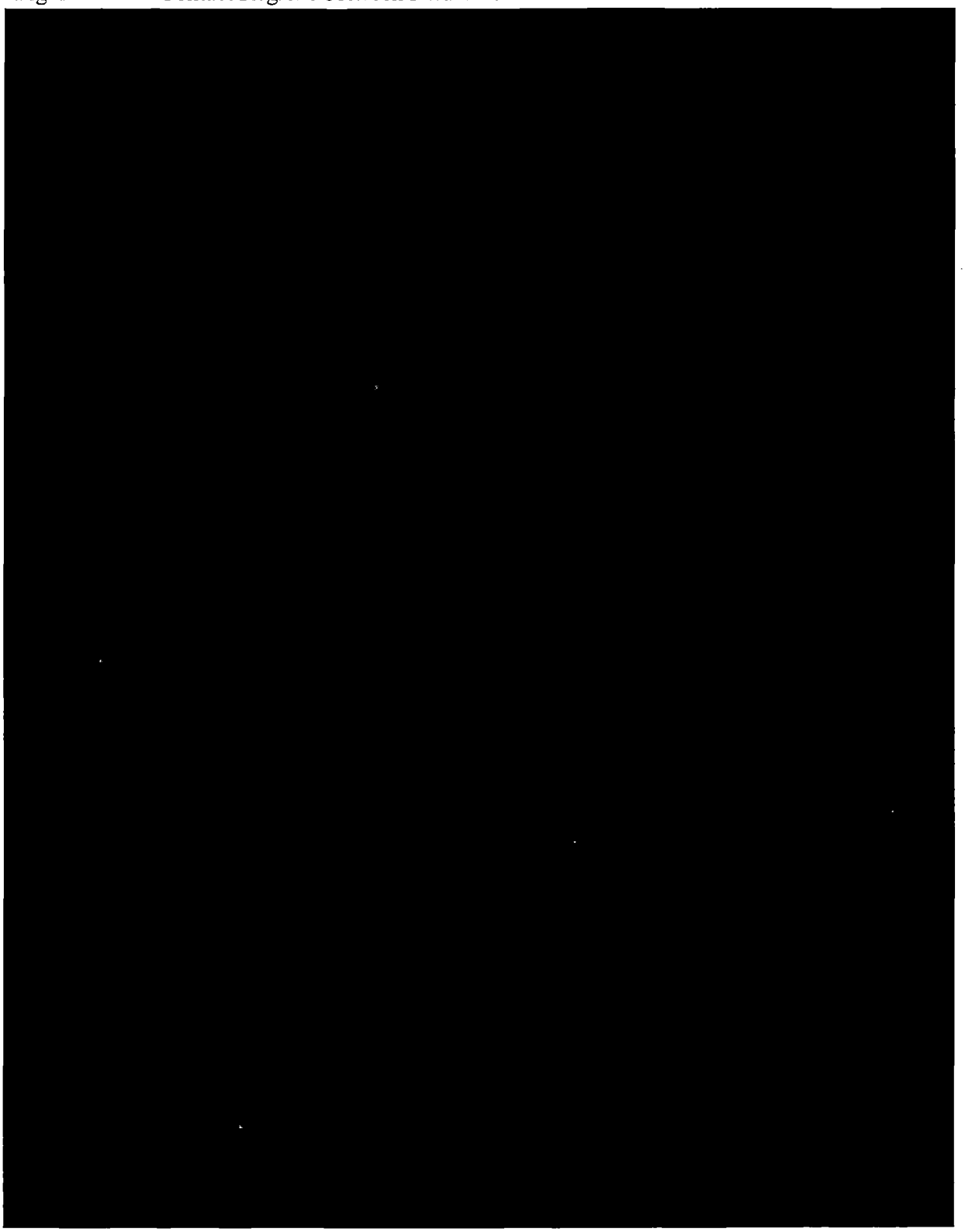

Figure 3-11.3 Contact between PWR Basket and Canister Shell (Close-up)

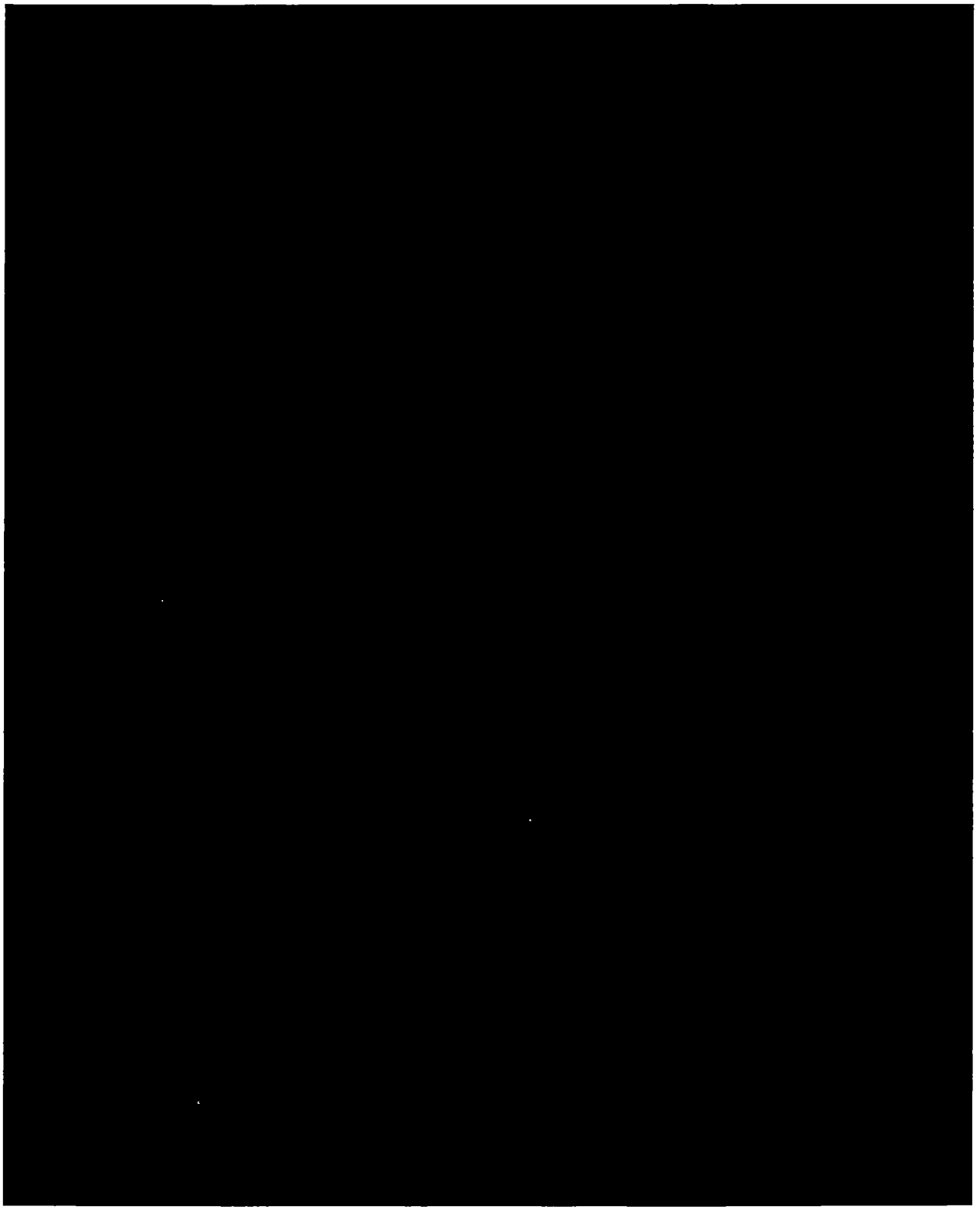

Figure 3-11.4 PWR Thermal Model - Contact Regions between the Canister and Cask Inner Shell

[redacted]

Figure 3-11.5 Heat Flux Plot for PWR Basket and Canister

[redacted]

Figure 3-11.6 Contact Regions between Basket and Canister Shell – BWR Model

[redacted]

Figure 3-11.7 Contact between Canister and Cask Inner Shell – BWR Model

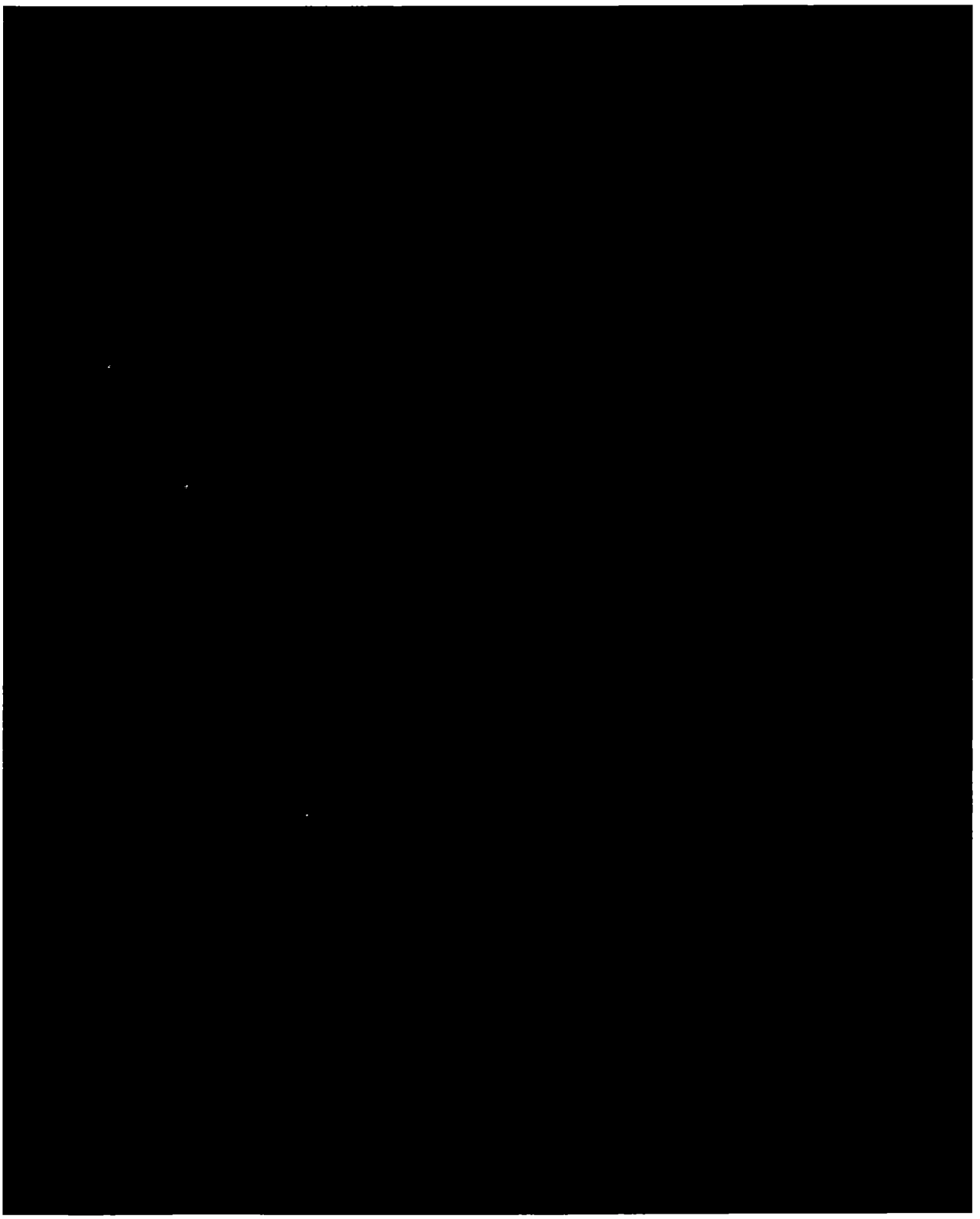

Figure 3-11.8 PWR Fine Mesh Thermal Model for Sensitivity Study (Case 1 for Question 3-11c and Case 2 for Question 3-11i) - 0° Basket Orientation – Contact between Basket and Canister Shell

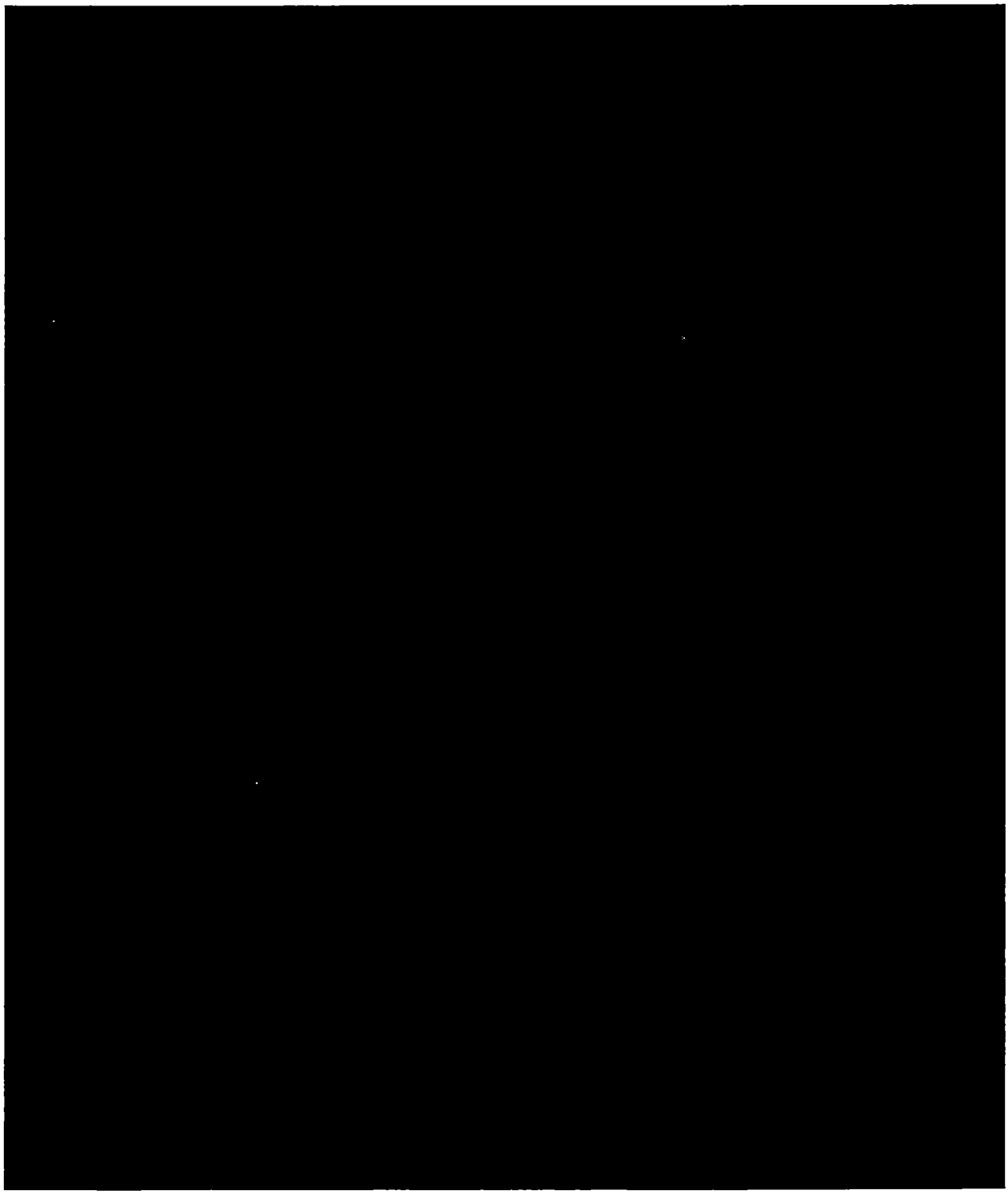

Figure 3-11.9 PWR Fine Mesh Thermal Model for Sensitivity Study (Case 1 for Question 3-11c and Case 2 for Question 3-11i) - 0° Basket Orientation – Contact Between Canister and Cask Inner Shell

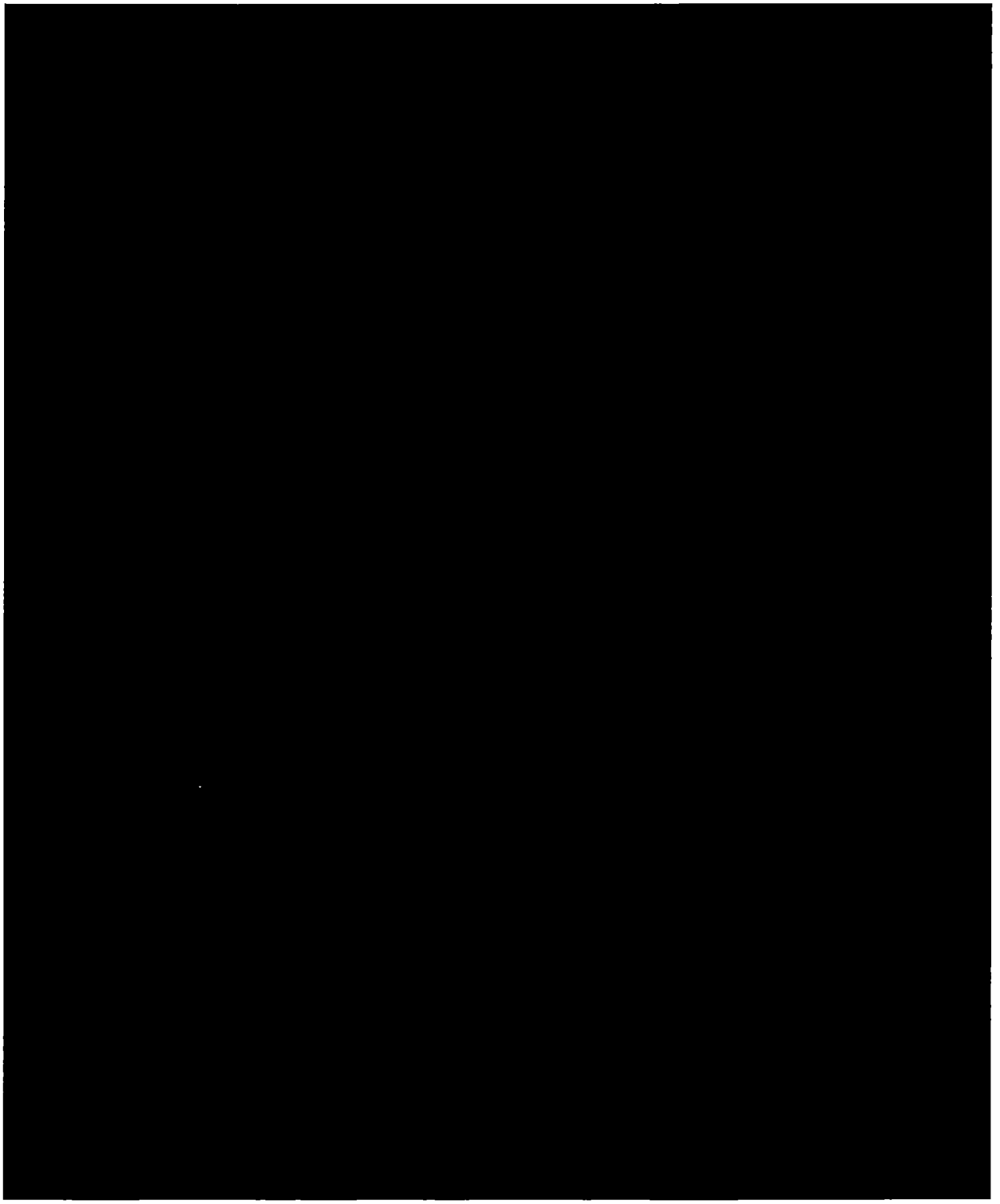

Figure 3-11.10 PWR Fine Mesh Model for Sensitivity Study Case 2 (Question 3-11c) – Contact between Basket and Canister Shell

[redacted]

Figure 3-11.11 PWR Fine Mesh Model for Sensitivity Study Case 2 (Question 3-11c) - Contact between Canister and Cask Inner Shell

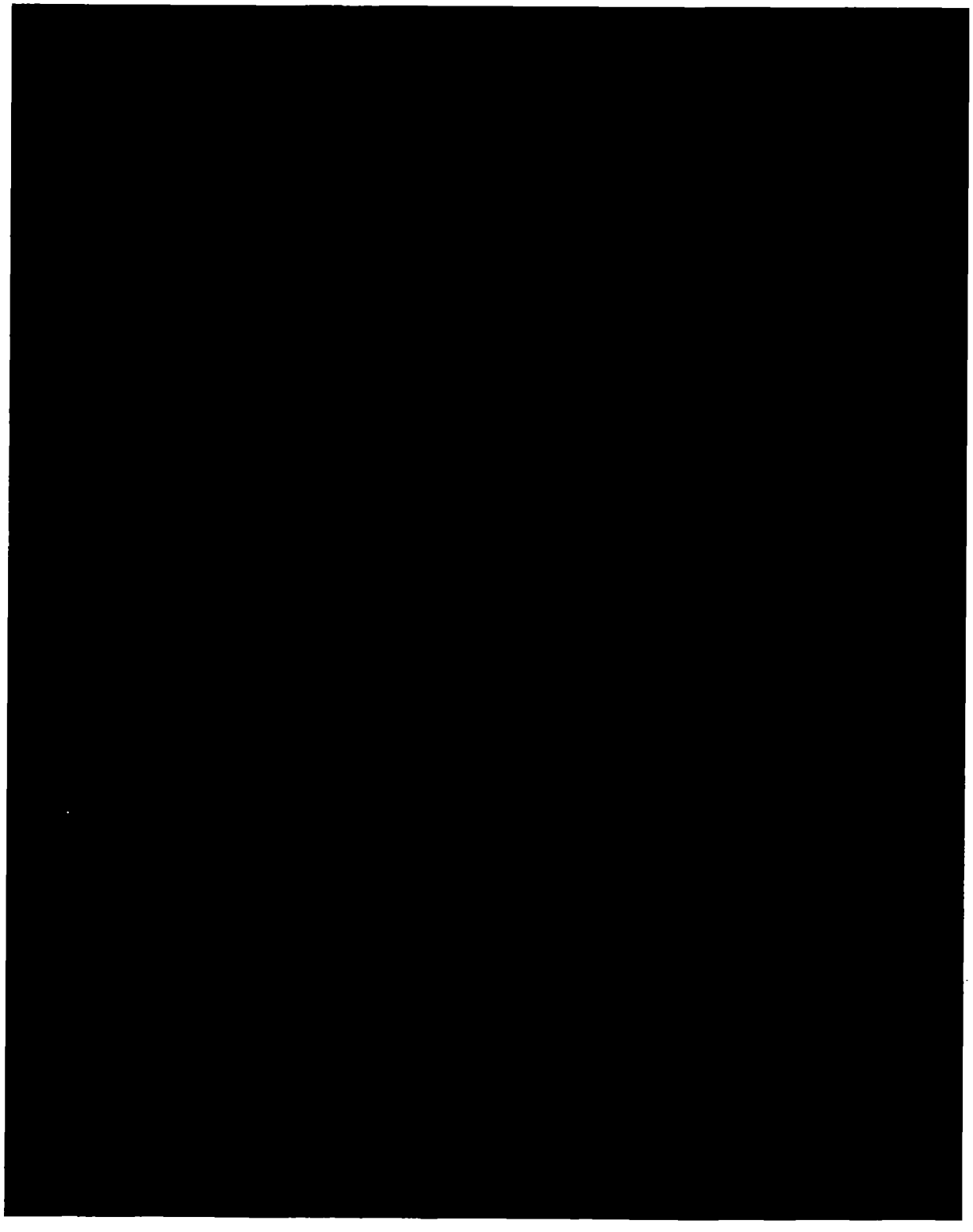

Figure 3-11.12 Location of Contact between PWR Basket and Canister Shell (0° Basket Orientation)

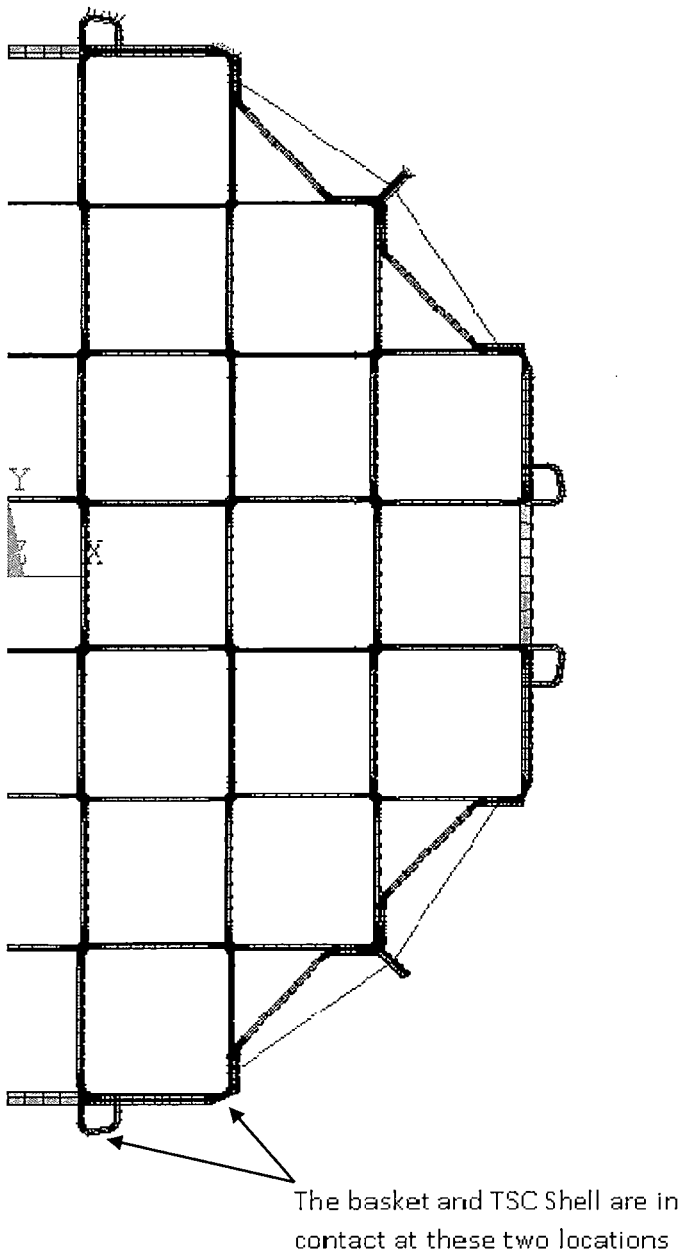

Figure 3-11.13 Location of Contact between BWR Basket and Canister Shell (0° Basket Orientation)

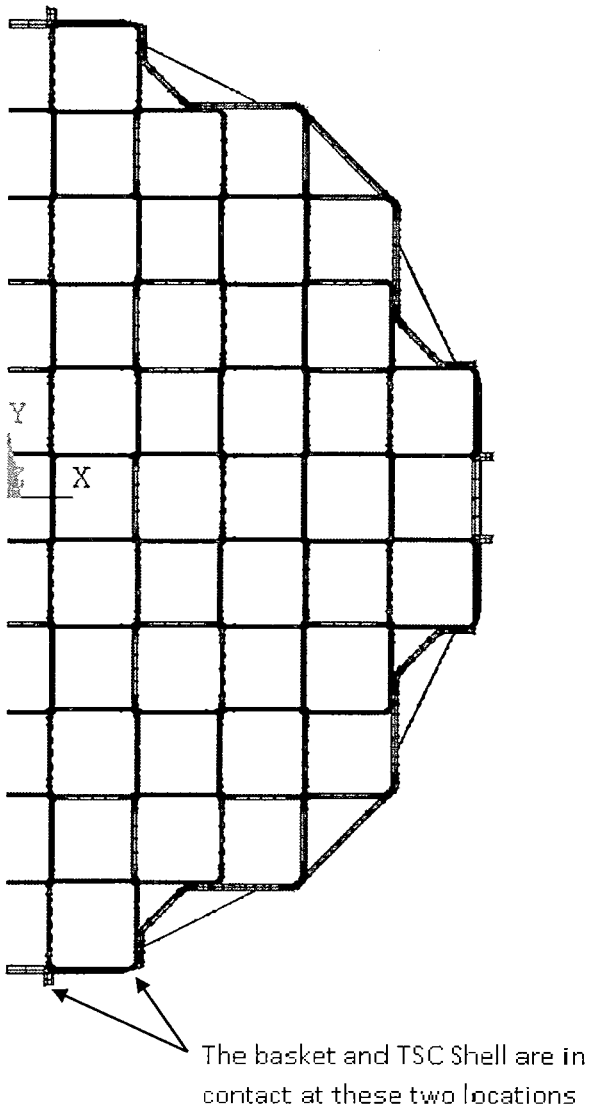

NAC INTERNATIONAL RESPONSE TO REQUEST FOR ADDITIONAL INFORMATION

THERMAL EVALUATION

3-12 Provide Calculation Packages 71160-3001, Rev. 3, and 71160-3002, Rev. 1, so that a review of the methodology and assumptions for the effective conductivity modeling can be performed.

NAC's response to question 3-3P in letter dated January 13, 2015, provided the effective thermal conductivity curves for the PWR and BWR fuel, which are different from expectations and require further review. In addition, specify whether the poison plates were homogenized with the fuel assemblies.

This information is needed to confirm compliance with 10 CFR 71.35.

NAC International Response to Thermal Evaluation RAI 3-12:

NAC Calculation Packages 71160-3001, Rev. 3, and 71160-3002, Rev. 1 are provided with the responses.

The poison plates were not homogenized with the fuel assemblies, but were modeled as being separate with appropriate effective material properties. The effective properties of the neutron absorber are determined using the model described in SAR Section 3.4.1.1.3 for PWR configuration and in Section 3.4.1.2.3 for BWR configuration. The effective conductivities of the neutron absorber are used in three dimensional cask models (Section 3.4.1.1.1 for PWR configuration and 3.4.1.2.1 for BWR configuration) as orthotropic conductivities.

NAC INTERNATIONAL RESPONSE TO REQUEST FOR ADDITIONAL INFORMATION

THERMAL EVALUATION

3-13 Justify the use of an average heat transfer coefficient correlation that is applied to the outer package surface during cooldown for both normal conditions of transport and hypothetical accident conditions thermal evaluations.

NAC's response to question 3-1 in letter dated January 13, 2015, and SAR Section 3.2.3, indicates that an average heat transfer coefficient correlation is applied as an outer package boundary condition. An average heat transfer correlation generally uses the average temperature over the particular geometry/length-scale of the correlation rather than the local temperature. The local heat transfer correlation would tend to be used when local temperature conditions are applied; the local correlation can be much less (e.g., 25% to over 30%) than the average heat transfer correlation. This reduction in heat transfer coefficient can be important considering the relatively small margin of the PCT to the allowable value for normal conditions of transport.

This information is needed to confirm compliance with 10 CFR 71.35, 10 CFR 71.71, and 10 CFR 71.73.

NAC International Response to Thermal Evaluation RAI 3-13:

As described in SAR Section 3.2.3, the film coefficient applied in analyses (ANSYS model) to the outer package surface for both normal and during cooldown for fire conditions is a function of the local surface temperature and the air temperature. This film coefficient is a local heat transfer coefficient that uses local surface temperature.

The purpose of RAI question 3-1 in the letter dated January 13, 2015, was to identify the fin effectiveness which utilized the flux by convection per unit length (W/m). The average film coefficient reported in the 3-1 response (January 2015) was not used to compute the effectiveness; it was simply listed for information only. It was not used in any models to obtain solutions.

NAC INTERNATIONAL RESPONSE TO REQUEST FOR ADDITIONAL INFORMATION

THERMAL EVALUATION

3-14 Clarify the areas associated with the 2D unfinned model and 3D finned model described in the NAC's response to question 3-1 in letter dated January 13, 2015, Appendix H Calculation Package 71160-3045 so that a review can be performed.

a. The model outer areas are listed in the second table of Appendix H of Calculation Package 71160-3045. Clarify whether the 2D half-symmetry, unfinned geometry models only one-half of the neutron shell. It is not clear how the listed area was determined.

b. The 3D finned model area (0.7132 m^2) in the table appears to be based on 360 degrees. However, the model is 180 degrees. It is not clear how the listed area was determined.

This information is needed to confirm compliance with 10 CFR 71.35 and 71.71.

NAC International Response to Thermal Evaluation RAI 3-14:

The planar 2D half-symmetry, un-finned geometry corresponds to only half of the cask body (not full 360° geometry). The surface area of 3.9443 m^2 is the total surface area of the half model, which corresponds to a unity length (1.0 m) for the 2D model defined by FLUENT. The effectiveness is computed based on total outer surface flux per unit length.

For the three dimensional model, the area of 0.7132 m^2 is the outer surface area of the half symmetry model (not full 360° geometry). This area of 0.7132 m^2 corresponds to a 3.5 inches (0.0889 m) in the cask axial direction.

NAC INTERNATIONAL RESPONSE TO REQUEST FOR ADDITIONAL INFORMATION

THERMAL EVALUATION

3-15 Provide the two experimental test reports (GA-A20770 and GA-A19897) discussed in NAC's response to question 3-9 and question 5-6P, in letter dated January 13, 2015.

NAC's responses refer to experiments performed on the NS-F-4 neutron absorber at high temperatures, but it was not certain whether the test conditions corresponded to those for the thermal test for hypothetical accident conditions (800°C for 30 minutes), and therefore, it is uncertain whether the results confirm the behavior of the neutron absorber during the 30 minute fire.

This information is needed to confirm compliance with 10 CFR 71.73.

NAC International Response to Thermal Evaluation RAI 3-15:

The two reports (GA-A20770 and GA-A19897) are provided as an enclosure to this submittal package. These two reports show that the NS-4-FR was exposed to temperatures from 800°C (1,472°F) to 1,000°C (1,832°F) for a period of 30 minutes. The report shows that the NS-4-FR developed a thin layer of char (1/16 inch) on the surface and remained intact during this period with a total weight loss of approximately 5%.

NAC INTERNATIONAL RESPONSE TO REQUEST FOR ADDITIONAL INFORMATION

THERMAL EVALUATION

3-16 Update the thermal models or demonstrate that the emissivity and absorptivity values used in the thermal models (SAR text and ANSYS input files) are realistic/bounding so as to provide accurate/conservative results.

According to NAC's response to question 3-18(d), the emissivity values listed on SAR pages 3.2-4 through 3.2-8 are also used as absorptivity values. Although this can be appropriate when dealing with spectral properties, it may not be valid when applying average emissivity and absorptivity values. For example, as noted in the response to question 3-18(d), a relatively low stainless steel emissivity would lessen the radiation heat transfer rate out of the package for normal conditions of transport. However, dust or surface coatings would tend to increase the absorptivity beyond a 0.36 value. A higher absorptivity would increase the insolation thermal input, which is a relatively large component, as noted in Table 3-2.1 and Table 3-2.2 (response to question 3-2).

This information is needed to confirm compliance with 10 CFR 71.71 and 71.73.

NAC International Response to Thermal Evaluation RAI 3-16:

The stainless steel/aluminum exposed to the environment do not have surface coatings. As per step 5, in SAR Section 7.3, the surface is to be decontaminated and cleaned prior to being used to transport. This would eliminate any significant level of dust from accumulating on the cask surface. Additionally, the cask will not be used without the personnel barrier. The personnel barrier would reduce the solar insolance impinging on the cask surface. The thermal evaluation applied the solar insolance to the cask body as though there was no personnel barrier. The current evaluations are considered to be bounding.

NAC INTERNATIONAL RESPONSE TO REQUEST FOR ADDITIONAL INFORMATION

CONTAINMENT EVALUATION

No questions.

NAC INTERNATIONAL RESPONSE TO REQUEST FOR ADDITIONAL INFORMATION

SHIELDING EVALUATION

5-1 Demonstrate the:

a. radial dose rates at the personnel barrier surface are less than the 200 mrem/hr limit, and

b. radial dose rates at the appropriate locations (i.e., package surface, personnel barrier surface, and 2 meters from the vehicle edge) meet their respective limits, accounting for the impacts of the alternating 2-inch and ¼-inch void gaps at the top of the neutron shield assemblies.

Maximum surface dose rates on the package radial surface above the neutron shield are significantly higher than 200 mrem/hr for both undamaged and damaged fuel contents. While these dose rates are lower than the limit for a package surface when the package is in an enclosure (i.e., personnel barrier), they cannot be relied on to show that the dose rates at the enclosure surface meet the dose rate limit of 200 mrem/hr.

Additionally, the mesh tally analysis in Section 5.8.12 of the application indicates that void areas in the neutron shield can result in significant radiation streaming. However, this analysis is limited to the thermal insulation and expansion foam areas near the neutron shield mid-plane area. Based on this analysis, the 2-inch tall void areas at the top of some of the neutron shield assemblies would also be areas of significant radiation streaming that, due to their size, could have a significant impact on package dose rates at the locations listed in b above. Since not all neutron shield assemblies have this size of void in their top end, this effect is not adequately captured by surface detectors that average the dose rate around the package circumference. Maximum radial dose rates for damaged fuel and undamaged fuel contents occur near this area of the package and so may be influenced by this azimuthal variation in the top ends of the neutron shield assemblies. Thus, the shielding analysis should be modified to address this effect using detectors of reasonable size both axially and azimuthally (e.g., 3 inches).

For both items a and b, above, the analyses should appropriately capture other azimuthal effects (e.g., spent fuel contents with specific characteristics being limited to specific basket locations) and include both spent fuel and non-fuel hardware contributions for both damaged fuel and undamaged fuel contents.

This information is needed to confirm compliance with 10 CFR 71.47.

NAC International Response to Shielding Evaluation RAI 5-1:

a. Per 71160-511, the personnel barrier has an outer radius of 62 inches, or 157.48 cm. Radial dose rates are calculated at 1 foot from the modeled cask surface (neutron shield assembly outer surface), which corresponds to a radius of 156.82 cm. The dose rates at the 1 foot detectors are used to demonstrate all personnel barrier dose rates are below the 200 mrem/hr limit. The maximum personnel barrier radial dose rates, including PWR, damaged PWR, and BWR, are all below 90 mrem/hr. Personnel barrier radial dose rates are added to applicable sections of the SAR for the PWR, damaged PWR, and BWR evaluations.

b. The maximum radial surface dose rates were taken from an azimuthal detector in the gap between the top of the neutron shield and bottom of the impact limiter.

   To evaluate the impact of the expansion foam at the top of the neutron shield assemblies additional cases are run with azimuthal detectors at the top two inches of the neutron shield assembly surface and one foot (personnel barrier) from the neutron shield surface. PWR and BWR loadings which produce bounding radial dose rates are evaluated. Results are added to Section 5.8.3.3 and 5.8.4.3 for PWR and BWR fuel, respectively. The results show peaking around the top of the neutron shield assembly at the surface but the peak remains below the maximum radial dose rates which occur at the gap above the neutron shield. The peaking flattens significantly at the one foot radial detector. Similarly, peak one foot azimuthal dose rates at the top of the neutron shield assemblies remain below the maximum radial one foot dose rates for each cask loading. As the peak is depreciated at 1 foot, no resolvable peak would be observed at 2 meters from the cask surface.

   At the personnel barrier the damaged fuel still has dose rate peaks due to the four damaged fuel locations. The additional azimuthal case shows the peak is 30% larger than the average. Maximum one foot radial dose rates for the damaged fuel remain under 90 mrem/hr even after a 30% increase. Results are added to Section 5.8.10.3.

NAC INTERNATIONAL RESPONSE TO REQUEST FOR ADDITIONAL INFORMATION

SHIELDING EVALUATION

5-2 Provide support for the statements regarding high burnup fuel and the analysis approach used for high burnup fuel described in Section 5.2 of the application, both in terms of radiation source and heat load.

Section 5.2 of the application cites NUREG/CR-6701, "Review of Technical Issues Related to Predicting Isotopic Compositions and Source Terms for High-Burnup LWR Fuel," specifically Appendices A and B. The information in those appendices and the nuclides considered there are important to criticality safety. Also, Appendix A states, in part in Section A.8, that the "sensitivity studies described [in Appendix A] only assess the influence of the underlying data parameters on the concentrations of the actinides and fission products as they [affect] the k of a spent fuel system." The same nuclides are not necessarily important to the radiation source term and the heat load, and the appendices' applicability as a basis for the proposed approach is unclear. It is also unclear that the appendices provide the discussions and conclusions described by the applicant.

It is also unclear that the applicant's approach results in any margin with respect to the shielding analysis and dose rates since the applicant changed its analysis method in response to the staff's previous request for information. Bounding dose rates are now calculated with high burnup fuel having the burnup, enrichment, and cooling time specifications in Table 5.8-16 that are at the reduced heat load limit for high burnup fuel.

This information is needed to confirm compliance with 10 CFR 71.47 and 71.51.

<u>NAC International Response to Shielding Evaluation RAI 5-2:</u>

NAC did not change this analysis method in the context of high burnup fuel dose rates. Table 5.8-16 represents the bounding cool times obtained by a 5% heat load reduction. Full heat load was used in the generation of dose rates. As a response to this RAI, Section 5.8.3.2, "Minimum Cool-time Specification," is revised to state that all dose rates, including high burnup fuel values, are generated using the maximum heat load of 23 kW per cask and that Table 5.8-16 contains the data, for the bounding reduced heat load evaluation, not the dose rate design basis set.

"PWR Cool Time Table Results" Section A.5 of proprietary calculation 71160-5508 provided with the previous set of RAI responses states the following "Two tables are shown for high burnup fuel (> 45 GWD/MTU), one for maximum dose rates evaluated at 23 kW/cask and another for minimum cool times at 21.85 kW/cask. Cool times for high burnup fuel are evaluated at 95% of the heat load limit (21.85 kW) while maximum dose rates are conservatively evaluated using a 23 kW cask heat load limit ensuring bounding dose rates." Note that the MAGNATRAN evaluations apply heat load and dose rate limits. Not all state points (burnup/enrichment/cool time) are heat load limited.

Section 5.2 acknowledges that the indicated reference cannot be solely relied on to determine acceptability of the source generation (in particular for high burnup fuel). All MAGNATRAN dose rate evaluations applied a reduced allowable dose rate limit at the critical 2 meter location. Applying a 9.5 mrem/hr limit (see Section 5.8.3.1 and Section 5.2) assures margin for analysis uncertainties for dose rate controlled state points. MAGNATRAN is primarily a heat load limited system with only a limited number of state points, all at non-typical high burnup and low enrichment, producing dose rate limited cool times. As stated in Section 5.2 further margin is produced by applying a fresh fuel composition (5wt% ^{235}U) in the shielding models which will significantly over predict subcritical multiplication for high burnup, i.e. largely depleted, spent fuel.

The SAR reference to NUREG/CR-6701 originates in NUREG/CR-6802 which in Section 3.3.34 (Source Validation Studies) states:

"Validation of the neutron and gamma sources is a difficult task. The approach generally taken is a validation of the concentrations of the important isotopes relative to neutron and gamma source terms. Measurements have been published for six of the seven isotopes discussed in Section 3.3.1. These isotopes (i.e., 60Co, 134Cs, 137Cs, 154Eu, 144Pr, 242Cm, and 244Cm) are the major contributors to both neutron and gamma-ray sources.

The above conclusions regarding isotopic importances are largely based on comparisons with measured data that contain maximum burnups of about 40 GWd/MTU. However, additional studies (NUREG/CR-6798) have recently become available that approach 50 GWd/MTU. Similar conclusions to those noted above are reached in this new study. Sensitivity studies have indicated that no significant change in the nature of the comparison is expected with burnups up to 75 GWd/MTU (NUREG/CR-6701)."

NUREG/CR-6701 in Appendix A and B includes discussion primarily on actinide generation/depletion. Discussion includes 244Cm and the precursor actinides. It is therefore applicable to the neutron source discussion. Trending in the actinide mix effects the fission product mix which provides the primary gamma source. No trending to bias in the actinide generation/depletion, in conjunction with assurance of an acceptable fission product mix and gamma source generation up to 45 GWd/MTU, will assure appropriate fission product generation at the higher burnup levels.

In the context of heat load generation it is appropriate to include NRUGE/CR-6972 as supporting documentation. This NUREG is specific to decay heat generation and does not contain any resolvable trending in heat load generation for PWR fuel up to 50 GWd/MTU.

All dose rates, including high burnup fuel dose rates, are calculated using full heat load (23 kW/cask). Cool times for high burnup fuel are calculated using 95% heat load (21.85 kW/cask). Also, the analysis includes a 5% margin to the 10 CFR 71.47 10 mrem/hr dose rate limit at 2 meters (applying a 9.5 mrem/hr limit). The 2 meter dose rate is the bounding dose rate for the MAGNATRAN system.

NAC INTERNATIONAL RESPONSE TO REQUEST FOR ADDITIONAL INFORMATION

SHIELDING EVALUATION

5-3 Revise the analysis to address the condition of short PWR assembly types being loaded into the long TSC.

The current analysis for PWR assemblies appears to be based on PWR assemblies being loaded into the short TSC, with the exception of the CE 16x16 assembly type. However, per Section 1.3.2 of the application all PWR assembly types can be loaded into the long TSC. The analysis does not appear to address this condition. A look at the input files provided with calculation package 71160-5508 shows that the PWR assemblies (excepting the CE 16x16 assemblies) were analyzed in the short TSC and not in the long TSC. Thus, it is not clear that the dose rates reported for PWR assemblies are bounding and meet the dose rate limits at the regulatory locations (package surface, personnel barrier surface and 2 meters from the vehicle edge). With short PWR assemblies in the long TSC, the upper hardware zones of these assemblies can now extend above the neutron shield and the lead shield since neither of these shields extends the whole length of the package cavity. Also, the fuel region can be closer to the top ends of the neutron shield and lead shield and so be less shielded versus when in the short TSC. The revised analysis should also account for the uncertainties in the method. The staff's evaluation of the uncertainties arising from the applicant's analysis method (e.g., due to assumptions and simplifications) indicates that dose rates for the currently analyzed configuration may have little margin to the personnel barrier surface and 2-meter dose rate limits.

This information is needed to confirm compliance with 10 CFR 71.47 and 71.51.

<u>NAC International Response to Shielding Evaluation RAI 5-3:</u>

Short PWR assemblies are restricted to loading into the short TSC. Text is revised in Section 1.3.2 to address this limitation.

"PWR fuel assemblies with the exception of fuel identified as type CE (16×16) in Table 1.3-6 must be loaded into a short TSC (i.e., be loaded into a transport configuration with a canister spacer). CE16 fuel may be loaded into either a short or long TSC. An exception to the PWR CE16 guideline is the System 80 16×16 fuel with an active fuel length of 150 inches whose overall length exceeds the short TSC cavity length and, therefore, must be loaded into the long TSC."

NAC INTERNATIONAL RESPONSE TO REQUEST FOR ADDITIONAL INFORMATION

SHIELDING EVALUATION

5-4 Justify how the assembly response functions can be used for estimating dose rates from BPRAs and TPDs if credit is taken for the masses of these non-fuel hardware (NFH) types, or modify the analysis appropriately.

The discussion of response functions for these NFH types remains unclear. The change to Section 5.8.5.1 of the application did not adequately address this issue. Differences in material properties in the models (NFH present vs. not present) result in different response functions. Thus, to take credit for the NFH mass, different response functions would need to be used. Otherwise, this implies that dose rates for assemblies without NFH are calculated with response functions that include the masses of the NFH, which would be incorrect.

This information is needed to confirm compliance with 10 CFR 71.47 and 71.51.

NAC International Response to Shielding Evaluation RAI 5-4:

Separate response functions are run for NFH. Fuel assembly hardware response functions are generated using only fuel assembly region masses, no NFH. The NFH evaluation adds the minimum mass of the BPRAs and thimble plugs into the respective analysis region and generates NFH specific responses. Section 5.8.5.1 is updated to more accurately describe the analysis.

Note that inclusion of NFH components produces bounding dose rates. The bounding configuration is a fuel assembly with NFH. Therefore, inclusion of the NFH mass into the fuel assembly response function would not be incorrect. The analysis presented in the SAR produces bounding dose rates as it conservatively neglects the NFH mass during fuel assembly response generation.

NAC INTERNATIONAL RESPONSE TO REQUEST FOR ADDITIONAL INFORMATION

SHIELDING EVALUATION

5-5 Modify the shielding analysis chapter to correct errors and inconsistencies within the chapter, as well as inconsistencies between the shielding chapter and the shielding calculation package and its associated files.

There are many inconsistencies and errors in the shielding chapter and between the shielding chapter and the calculation package. These items make it difficult to understand the application. They include differences in reported dose rates and bounding source term specifications, and incorrect model figures (e.g., the neutron shield assemblies figure has incorrect dimensions). These errors and inconsistencies are within the chapter (differences between text, figures, and tables) and between the chapter and the calculation package (text, figures, and tables). The GTCC sample input file should be updated to show the use of new surface detector divisions (for capturing axial lead slump, etc.). Also, revise the shielding analysis to change "doses" to "dose rates," as only dose rates are calculated.

This information is needed to confirm compliance with 10 CFR 71.33 and 71.35(a).

NAC International Response to Shielding Evaluation RAI 5-5:

All dose rates were re-checked against the calculation package along with the majority of figures and any inconsistencies were corrected. All occurrences of "dose" or "doses" without the clarifying term "rate" were corrected to include it. The GTCC sample input file refers to the normal conditions and therefore does not include the detector divisions capturing the axial lead slump from the accident conditions. Fuel evaluations did not show any significant dose rate changes as the result of the refined detector definitions. As GTCC evaluations have a large margin to dose rates limits, and fuel evaluations showed no significant dose rate increase, the GTCC evaluations were not revised for the refined detectors.

NAC INTERNATIONAL RESPONSE TO REQUEST FOR ADDITIONAL INFORMATION

CRITICALITY EVALUATION

6-1P See proprietary RAI responses.

NAC INTERNATIONAL RESPONSE TO REQUEST FOR ADDITIONAL INFORMATION

CRITICALITY EVALUATION

6-2P See proprietary RAI responses.

NAC INTERNATIONAL RESPONSE TO REQUEST FOR ADDITIONAL INFORMATION

CRITICALITY EVALUATION

6-3 Revise the application to ensure that absorbers in the SCALE/TRITON model are depleted by constant flux as opposed to constant power.

In the sample TRITON depletion input files provide for fuel (Figure 6.10.1-8) and for reactor control cluster assemblies (RCCAs) (Figure 6.10.1-20), it appears that Wet Annular Burnable Absorbers (WABA) and RCCA materials are depleted using constant power. Section 6.3 of NUREG/CR-7041 states:

> *"While depletion assuming a constant power is generally representative of a fuel element, this is not true for nonfuel elements. Targets, structural materials, and burnable poisons are generally "driven" by fluxes from neighboring fuel elements and do not contribute significantly to power production. Forcing a constant power in a burnable poison rod, for example, would result in a rapidly increasing flux due to depletion of the poison material, which is nonphysical. Allowing mixed-mode depletion within SCALE/TRITON better approximates the time-dependent flux behavior across an assembly."*

The application should ensure that absorber materials, including WABAs, RCCAs, and any other burnable absorbers or control elements, are modeled appropriately in all depletion models.

This information is needed to confirm compliance with 10 CFR 71.55 and 10 CFR 71.59.

<u>NAC International Response to Criticality Evaluation RAI 6-3:</u>

As stated in the RAI, nonfuel hardware power contribution is negligible to the system total power output. All TRITON depletion models apply a constant power to the fuel elements only as the depletion basis. Constant power within a fuel element is generally a good representation for commercial reactor operations. Constant power is not forced in the nonfuel hardware for the TRITON depletion calculations.

To address the RAI, additional depletion cases were run using the TRITON mixed-mode depletion feature. The cases from RAI 6-1P and 6-2P (additional depletion bands) were modified to include the mixed-mode depletion. There is a negligible impact on k_{eff} as a result of mixed-mode depletion. This includes depletion of the fuel with nonfuel hardware present, and depletion of the RCCA for reactivity control credit. Text is added to Sections 6.10.1.4.5 and 6.10.1.7.3 for the fuel depletion and RCCA depletion, respectively.

NAC INTERNATIONAL RESPONSE TO REQUEST FOR ADDITIONAL INFORMATION

CRITICALITY EVALUATION

6-4 Revise the application to clarify how the burnup uncertainty is incorporated into the determination of maximum initial enrichment for the PWR loading curves.

Burnup credit loading curves are typically constructed so that minimum burnup is a function of known initial enrichment, and the package user compares reactor burnup record values to the required minimum burnup. The burnup value to be used for loading acceptance is the reactor record value reduced by the uncertainty in that value (typically two times the in-core measurement uncertainty). For the MAGNATRAN® system, the applicant proposes PWR loading curves where the allowable initial enrichment is determined based on a known burnup value. It is not clear how burnup uncertainty is taken into account in this case.

This information is needed to confirm compliance with 10 CFR 71.55 and 10 CFR 71.59.

NAC International Response to Criticality Evaluation RAI 6-4:

The MAGNATRAN SAR, in the context of burnup credit, indicates the minimum burnup required for fuel assemblies to meet 10 CFR 71.55 and 71.59 requirements. When determining acceptability of the fuel assemblies for transport uncertainty in the burnup data (records or measurement) should be considered. Section 7.1.4 Item 4 is revised to address this requirement. Exact uncertainty values to be applied are subject to the detail/accuracy of information available at a particular site and are not specified within the MAGNATRAN SAR.

Section 7.1.4 note is added as follows:

"Fuel assemblies may use burnup credit to demonstrate criticality acceptability. When applying burnup credit the documented fuel assembly burnup must be adjusted downward (decreased) to account for reactor record or measurement uncertainty prior to comparison to CoC minimum requirements."

NAC INTERNATIONAL RESPONSE TO REQUEST FOR ADDITIONAL INFORMATION

CRITICALITY EVALUATION

6-5 Revise the application to include administrative loading procedures to prevent misloads in the PWR and PWR-DF canisters for contents evaluated with burnup credit.

A misload analysis should be coupled with additional administrative procedures to ensure that the transportation system will be loaded with fuel that is within the specifications of the approved contents. Procedures considered to protect against misloads in transportation packages that rely on burnup credit for criticality safety may include:

- Verification of the location of high reactivity fuel (i.e., fresh or severely underburned fuel) in the spent fuel pool both prior to and after loading,
- Qualitative verification that the assembly to be loaded is burned (visual or gross measurement),
- Verification, under a 10 CFR Part 71 quality assurance program, of the canister or package inventory and loading records prior to shipment for previously loaded systems,
- Quantitative measurement of any fuel assemblies without visible identification numbers,
- Independent, third-party verification of the loading process, including the fuel selection process and generation of the fuel move instructions, and
- Minimum soluble boron concentration in pool water, to offset potential misloads during loading and unloading.

This information is needed to confirm compliance with 10 CFR 71.55 and 10 CFR 71.59.

NAC International Response to Criticality Evaluation RAI 6-5:

Chapter 7, Section 7.1.4 has been revised to incorporate appropriate Notes to the TSC loading procedure to address the requirements of the first four bullets of the RAI.

Loading process and fuel movement instruction generation are performed according to industry standards under applicable QA programs. The NAC SAR for MAGNATRAN includes independent verification requirements within Section 7.1.2 and 7.1.4.

A soluble boron requirement would not "protect against misload". It may enhance defense-in-depth justification that a significant misload would not result in adverse radiological consequences. As transport requirements under 10 CFR 71.55 require the package to remain safe under fresh water introduction the addition of soluble boron requirements during loading and unloading are not considered to be appropriate by the applicant. In general terms Section 7 of the MAGNATRAN SAR contains the following text:

"TSCs containing spent nuclear fuel shall have been prepared for storage in accordance with the applicable 10 CFR 72 CoC No. 1031 (MAGNASTOR) and related Technical Specifications and Approved Contents."

The 10 CFR 72 CoC contains minimum soluble boron requirements for spent fuel loading.

NAC INTERNATIONAL RESPONSE TO REQUEST FOR ADDITIONAL INFORMATION

CRITICALITY EVALUATION

6-6 Revise the application to ensure that all calculated k_{eff} values for the MAGNATRAN® package are below the calculated Upper Safety Limit (USL).

Tables 6.10.3-1 and 6.10.3-2 appear to show $k_{eff} + 2\sigma$ values that are above the system USL of 0.9376 for some BWR fuel in the MAGNATRAN® system with the 0.027 g/cm^2 areal density neutron absorber plates. Revise the application to demonstrate that the maximum calculated $k_{eff} + 2\sigma$ values for all fuel and canister types are below the system USL.

This information is needed to confirm compliance with 10 CFR 71.55 and 10 CFR 71.59.

NAC International Response to Criticality Evaluation RAI 6-6:

Tables 6.10.3-1 and 6.10.3-2 are comparisons of calculated $k_{eff} + 2\sigma$ values for the transfer and transport overpacks. The comparisons are used to establish that utilizing the transfer overpack for fuel characterization and the most reactive basket physical configuration is acceptable. The comparisons are not used to establish maximum enrichment tables. Transport cask models are used to establish maximum enrichment tables. Maximum enrichment is established by demonstrating that maximum calculated $k_{eff} + 2\sigma$ values are less than the USL at the maximum enrichment. The comparisons of overpack models are explained in Section 6.10.3.2. Determination of maximum enrichments is described in Section 6.10.3.

NAC INTERNATIONAL RESPONSE TO REQUEST FOR ADDITIONAL INFORMATION

CRITICALITY EVALUATION

6-7 Revise the application to clarify the PWR fuel depletion assumptions regarding Control Element Assembly (CEA) insertion during irradiation."

Table 6.10.1-4 of the application lists several irradiation parameters assumed in the PWR depletion analysis, including assumptions regarding CEA insertion. For "CE Assembly Type CEA," the table gives the analyzed parameter as "Full Insertion," implying that CEAs were assumed to be fully inserted for the full burnup credited. However, this assumption is not discussed anywhere in the associated text of Section 6.10.1. The text of this section should be revised to clarify the CEA exposure assumption for CE fuel types.

Additionally, for "B&W and WE CEA," Table 6.10.1-4 gives the analyzed parameter as "≤ 20 cm insertion and/or ≤ 10 GWd/MTU Full Insertion at Power." While the 20 cm insertion parameter is discussed in the text of Section 6.10.1, the assumption of 10 GWd/MTU full insertion during irradiation is not. The application should be revised to clarify the assumptions regarding B&W and WE CEA insertion, and provide supporting analyses demonstrating that the 10 GWd/MTU CEA insertion assumption is appropriate.

This information is needed to confirm compliance with 10 CFR 71.55(b).

NAC International Response to Criticality Evaluation RAI 6-7:

CE fuel assemblies were depleted with full CEA insertion for the full burnup credited. B&W and WE assemblies were depleted with full BPRA insertion for the full burnup credited. Text is added to Section 6.10.1.4.5 to address the modeled inserts for fuel depletion calculations.

The 10 GWd/MTU CEA insertion assumption was based on data from NUREG-6759. NUREG-6759 shows negligible reactivity impact at burnups less than 10 GWd/MTU for enrichments greater than 4.0 wt% ^{235}U. After review of the reference data, it was decided to further reduce the considered burnup to 5 GWd/MTU for insertions greater than 20 cm. The reference data utilized a 5 GWd/MTU insertion assumption when considering insertion in later cycles. The reference data also demonstrates negligible effects on reactivity for enrichments down to 3.0 wt% ^{235}U. Insertion greater than 20 cm is limited to fuel assemblies in the control bank location during start-up or low power operations. The expected depletion during start-up is significantly less than 5 GWd/MTU, which is approximately equivalent to 5 months of insertion in an 18 month cycle. Extended low power operations are not typical in commercial power reactors.

To support the referenced NUREG with data for the MAGNATRAN system, Δk_{eff}'s are calculated for fuel assemblies with CEAs inserted for 5 GWd/MTU. The CEAs are replaced by

water following the 5 GWd/MTU depletion step. After one cycle, the Δk_{eff} is negligible. Fuel assemblies with low burnup (5 GWd/MTU) and low enrichment are not expected to be in spent fuel inventories. Therefore, the conclusions of NUREG-6759 are supported by the results. Full insertion of BPRAs for the full burnup is expected to bound any reasonable CEA insertion for fuel depletion calculations.

Text is added to Section 6.10.1.4.5 to address depletion with CEA insertion for WE and B&W fuel assemblies. The burnup restriction for full CEA insertion in Table 6.10.1-4 is replaced with "partial to full insertion allowed at low power or start-up operations."

NAC INTERNATIONAL RESPONSE TO REQUEST FOR ADDITIONAL INFORMATION

OPERATING PROCEDURES EVALUATION

7-1 Provide a verification in Chapter 7, "Package Operations," to ensure that accessible package surface temperatures will not exceed the limits specified in 10 CFR 71.43(g).

The thermal analyses indicate that surface temperatures are near the exclusive use shipment temperature limit; a test to determine surface temperature prior to shipment will help ensure that surface temperatures will remain below the allowable value.

This information is needed to confirm compliance with 10 CFR 71.43(g) and 71.87(k).

NAC International Response to Operating Procedures Evaluation RAI 7-1:

Chapter 7, Section 7.1.3, Step 16 has been incorporated to specify that a neutron shield shell surface temperature measurement of the MAGNATRAN package will be taken prior to final installation of the personnel barrier to confirm that the surface temperature does not exceed the maximum temperature limit of 85°C (185°F) for an exclusive use shipment as specified in 10 CFR 71.43(g).

NAC INTERNATIONAL RESPONSE TO REQUEST FOR ADDITIONAL INFORMATION

OPERATING PROCEDURES EVALUATION

7-2 Clarify and confirm that the allowable loading and unloading time periods presented in Chapter 7 accurately reflect the current MAGNATRAN® design:

Chapter 7 (including Sections 7.1.2, 7.1.4, 7.2.2, etc.) updated SAR pages include various loading and unloading time periods. For example, Section 7.1.2 lists a 44 hour time limit for loading into the MAGNATRAN® package. Page O17 of O18, Appendix O of Calculation Package 71160-3020, dated December 2010 lists a 44 hour time period, but it is based on a transfer cask with air transfer, according to Appendix L of Calculation Package 71160-3020. The applicability/relevance of certain Calculation Package 71160-3020 analyses to the MAGNATRAN® loading/unloading operations is uncertain. Confirm that the analyses presented in Calculation Package 71160-3020 were part of previously approved MAGNASTOR amendments, recognizing that the MAGNATRAN contents are not identical to the MAGNASTOR contents and to ensure that the MAGNASTOR thermal analyses are valid for the MAGNATRAN.

This information is needed to confirm compliance with 10 CFR 71.35 and 71.71.

NAC International Response to Operating Procedures Evaluation RAI 7-2:

NAC Calculation No. 71160-3020, Revision 15, Appendix O, presents the CFD transient analysis of the MAGNASTOR Transfer Cask (MTC) in the vertical orientation to move a loaded canister (TSC) having a maximum allowable decay heat load for transport (PWR – 23 kW; BWR – 22 kW) for three potential transfer conditions related to the loading and unloading of the MAGNATRAN transport cask. Condition 1) is the transfer of a loaded TSC from a concrete cask to the transport cask; Condition 2) is the transfer of a loaded TSC following fuel loading and closure operations to the transport cask; and Condition 3) is for the unloading of loaded TSC from the transport cask and placement in a safe condition in the MTC. The allowable transfer times for each of these conditions are summarized in Appendix O.7 and provided in the table below.

The MTC is designed to permit air flow between the annulus of the TSC and the inner shell of the MTC. However, for the transfer transient analysis in Appendix O no air flow was considered. The MTC has similar neutron shielding as contained in the MAGNATRAN cask and the MTC design does not have any copper thermal shunts through the neutron shielding or external fins as does the MAGNATRAN transport cask.

Therefore, when the air is not permitted to flow in the MTC, the transient analysis of the MTC in Appendix O provides bounding temperatures as compared to the transport cask.

For the transient condition of transferring a loaded TSC from a VCC to the transport cask and placement of the cask in a horizontal orientation, the maximum allowable transfer time is calculated as 41 hours.

For the transient condition of directly loaded TSC from the completion of external cooling of the TSC in the MTC through MAGNATRAN loading and placement in a horizontal position, the TSC temperature conditions correspond to the end of 24 hours of cooling and the initial temperatures for the TSC and contents are significantly lower than for a TSC directly removed from a concrete cask. This results in a maximum allowable transfer time of 65 hours reported in SAR 7.1.2, Step 9 for the period of time for the movement of the TSC from the end of the 24 hours of cooling to the transport cask and for the transport cask to be put into the horizontal position.

The time provided in Section 7.2.2 of < 6 hours to complete the removal of a loaded TSC from the MAGNATRAN cask and placement in a safe condition in a MTC is based on the time computed in Item 3 of Section O.7 in Appendix O of calculation 71160-3020.

The modeling methodology for the contents and the MTC has been approved in the FSAR for MAGNASTOR under Docket 72-1031 (CoC No. 1031). The spent fuel contents in terms of fuel types of the MAGNASTOR system are identical to the fuel types of the MAGNATRAN cask with respect to thermal performance. The capability of the TSC and internal basket to maintain confinement/containment, reject decay heat, and maintain the position of the fuel contents are the same for both MAGNASTOR (CoC No. 1031) and MAGNATRAN.

The applicable transfer times for the various transient conditions are summarized below and have been incorporated into the revised Chapter 7 procedures of the SAR.

Thermal Limits for Operation

Condition	Time Allowed (Hour)
1) Transfer from VCC to Transport Cask	≤ 41
2) Direct Loading of Transport Cask (i.e., Spent Fuel Pool in Transfer Cask direct to Transport Cask from termination of TSC external cooling)	≤ 65
3) Transfer from Transport Cask to Transfer Cask	≤ 6

NAC INTERNATIONAL RESPONSE TO REQUEST FOR ADDITIONAL INFORMATION

OPERATING PROCEDURES EVALUATION

7-3 Modify the package operations to address the following:

a. Section 7.1.5, steps 10 and 14 include options that are not supported as options in the technical drawings to be incorporated into the certificate of compliance.

b. Section 7.1.1, Step 5 note incorrectly refers to 71.87(i) and 71.47 for an empty package.

Section 7.1.5, step 10 includes a statement that the TSC closure ring is optional, and Drawing No. 71160-785, Rev. 2, includes a note stating the same thing. However, Drawing No. 71160-500, Rev. 4P, includes a note that states that GTCC TSCs without closure rings are not transportable.

Additionally, Section 7.1.5, Step 14 includes a statement that the outer vent and drain port covers are optional as well as an option to use both the inner and outer cover plates and only weld the outer cover plates. While the notes in Drawing No. 71160-785, Rev. 2, support the outer cover plates being optional, the notes in Drawing No. 71160-500, Rev. 4P, do not. Also, the notes in Drawing No. 71160-785, Rev. 2, do not appear to support the option for including both inner and outer cover plates with only the outer cover plates being welded.

Lastly, the appropriate reference for contamination and dose rate limits for an empty package is 49 CFR 173.428.

This information is needed to confirm compliance with 10 CFR 71.87.

NAC International Response to Operating Procedures Evaluation RAI 7-3:

a. The procedures in Section 7.1.5, Step 10 and Step 14 have been revised to require the installation and welding of the closure ring, and installation and welding of both the inner and outer port covers. It has been determined that as the options to not install and weld the redundant confinement closures are precluded on Drawing No. 71160-500, Rev. 4P, revision to Drawing No. 71160-785, Rev. 2 is not required as GTCC waste TSCs not meeting the requirements of Drawing No. 7160-500 are not authorized for transport.
b. Section 7.1.1, Step 5 was revised to correct the reference for contamination and dose rate limits of an empty packaging to 49 CFR 173.428.

NAC INTERNATIONAL RESPONSE TO REQUEST FOR ADDITIONAL INFORMATION

OPERATING PROCEDURES EVALUATION

7-4 Clarify or remove the statement on page 7.1-1 which states that the procedures for the loading, closure, and preparation for transport of a TSC are outside the scope of the application.

Page 7.1-1 states "*The procedures for the loading, closure and preparation for transport of a TSC, and for the removal of a loaded TSC from storage in a MAGNASTOR concrete cask (CC) at an ISFSI, are provided in the MAGNASTOR FSAR. Those procedures are outside the scope of these MAGNATRAN operating procedures.*" The procedures for loading a TSC and preparation for storage are outside the scope of the application, but procedures for loading a TSC and preparation for transport are within the scope of the application. Thus, the MAGNATRAN® operating procedures should ensure that the TSC is loaded, closed and prepared for transport in accordance with the MAGNATRAN® package design.

This information is needed to confirm compliance with 10 CFR 71.87.

NAC International Response to Operating Procedures Evaluation RAI 7-4:

The final two paragraphs of Section 7.1 have been revised as presented below to clarify the MAGNATRAN procedures that are provided in Chapter 7 will ensure that the TSC is loaded, closed and prepared for transport in accordance with the MAGNATRAN package design.

"The generic operating procedures for the loading, closure and dry transfer of a TSC into a MAGNATRAN transport cask and preparation of the package for transport are provided in the following sections.

The generic operating procedures for the loading, closure and preparation for storage of a TSC, and for the removal of a loaded TSC from storage in a MAGNASTOR concrete cask (CC) at an ISFSI, are provided in the MAGNASTOR FSAR. Those procedures are outside the scope of these MAGNATRAN operating procedures."

NAC INTERNATIONAL RESPONSE TO REQUEST FOR ADDITIONAL INFORMATION

OPERATING PROCEDURES EVALUATION

7-5 Revise page 7.1-5 to state that the maximum assembly average burnup for fuel assemblies to be transported off-site as undamaged is limited to ≤ 45,000 MWd/MTU.

Page 7.1-5 appears to contradict itself by saying that spent fuel assemblies to be transported must have a maximum assembly average burnup less than 45,000 MWd/MTU. The next sentence states that a fuel assembly for transportation that has a maximum assembly average burnup greater than 45,000 MWd/MTU but less than 60,000 MWd/MTU shall be transported as damaged fuel.

This information is needed to confirm compliance with 10 CFR 71.87.

NAC International Response to Operating Procedures Evaluation RAI 7-5:

Section 7.1.2 has been revised as follows to clarify the Note following Step 8:

"Maximum assembly average burnup for fuel assemblies to be transported off-site as undamaged is limited to ≤ 45,000 MWd/MTU. A fuel assembly to be transported off-site having a maximum assembly average burnup > 45,000 MWd/MTU but ≤ 60,000 MWd/MTU shall be loaded in a MAGNASTOR damaged fuel can (DFC)."

NAC INTERNATIONAL RESPONSE TO REQUEST FOR ADDITIONAL INFORMATION

OPERATING PROCEDURES EVALUATION

7-6 Revise Chapter 7, "Operating Procedures," to augment the canister decontamination procedures to include: 1) a description of how the decontamination will be conducted, 2) the criteria for salt and corrosive agent removal, and 3) the method for determining whether the salt had been remove from the crevices.

RAI 7-9 asked for a description in the operating procedures that the package exterior will be decontaminated of chloride-containing salts and other corrosive agents since the cask was made of 304 stainless steel and could be used in a marine atmosphere. "The operating procedures in Chapter 7 have been revised to include the decontamination/ cleaning of the package surfaces of chloride-containing salts and other corrosive agents..." The revision did not include: 1) description of how the decontamination was going to be conducted, 2) the criteria for salt and corrosive agent removal, or 3) method for determining if the salt had been remove from the crevices.

This information is needed to determine compliance with 10 CFR 71.43(d).

NAC International Response to Criticality Evaluation RAI 7-6:

The operating procedures of Chapter 7 have been revised to add detailed procedures for the proper cleaning of the MAGNATRAN exterior surfaces at receipt at a loading or unloading facility. The procedures include recommended cleaning methods and materials, and cautions regarding materials and methods that are not acceptable for use of the stainless steel surfaces. The procedures also include acceptance criteria and methods to confirm that the exterior MAGNATRAN stainless steel surfaces have been acceptably cleaned of salts and other corrosive agents.

NAC INTERNATIONAL RESPONSE TO REQUEST FOR ADDITIONAL INFORMATION

ACCEPTANCE AND MAINTENANCE EVALUATION

8-1 Modify the shielding acceptance test in Section 8.1.6.3 (and the equivalent maintenance test in Section 8.2.3) to compare the measured dose rates to estimated (i.e., calculated) dose rates for the specific contents loaded in the package for this test, with these estimated dose rates being the acceptance criteria.

The shielding effectiveness tests for both the acceptance tests and the maintenance program tests appear to use the regulatory dose rate limits for acceptance criteria. While meeting these limits demonstrates the particular shipment meets the regulations, it does not adequately demonstrate that the shielding performs as designed. The appropriate criteria for demonstrating the shielding performs as designed are estimated (i.e., calculated) dose rates that are representative of either a check source(s) that may be used for the test or for the loaded contents (e.g., assembly type, enrichment, burnup, cooling time), if the test is done with a loaded package.

This information is needed to confirm compliance with 10 CFR 71.85 and to ensure the package maintenance activities are performed in a way that assures continued compliance with the requirements in 10 CFR Part 71, Subparts E and F, during its service life.

NAC International Response to Acceptance and Maintenance Evaluation RAI 8-1:

Chapter 8, Sections 8.1.6.3 and 8.2.3 have been revised to specify that estimated (i.e., calculated) gamma and neutron dose rates based on the actual contents of the TSC loaded in the MAGNATRAN package will be developed for both the first use shielding effectiveness test after first loading and for future shielding effectiveness tests performed as part of the maintenance program.

Enclosure 2

List of SAR Changes

No. 71-9356 for the MAGNATRAN Cask

MAGNATRAN SAR, Revision 15A

List of Changes for the MAGNATRAN® SAR, RAI Responses

Chapter/Page/ Figure/Table	Description of Change
Note: The List of Effective Pages and the Chapter Table of Contents, List of Figures and List of Tables have been revised accordingly to reflect the list of changes detailed below.	
Chapter 1	
Page 1.3-7	Modified the depth on the next to last line of the page.
Page 1.3-21	Modified the fifth paragraph of Section 1.3.2, "Contents."
Page 1.3-22	Added text to the first paragraph on the page.
Pages 1.3-23 thru 1.3-25	Text flow changes.
Page 1.3-26	Modified limit item 11.i.
Page 1.3-27	Modified list items 11 m and 11.n.
Page 1.3-28	Text flow changes.
Page 1.3-29	Modified limit items 12.i and 12.l.
Page 1.3-30	Modified limit items 12.p and 12.q.
Page 1.3-31	Modified limit item 12.t.
Page 1.3-32	Modified limit item 13.m.
Pages 1.3-33 thru 1.3-34	Text flow changes.
Pages 1.3-35	Modified the note following Figure 1.3-6
Pages 1.3-36 thru 1.3-42	Text flow changes.
Page 1.3-43	Deleted the note following Table 1.3-11.
Pages 1.3-44 thru 1.3-45	Text flow changes.
Page 1.3-46	Modified Table 1.3-16.
Pages 1.3-47 thru 1.3-51	Text flow changes.
Page 1.4-3	Updated the revision to Drawing 71160-505 P (and NP).
Chapter 2	
Page 2.1.1-5	Added text to the end of the last paragraph in Section 2.1.1.3.
Page 2.1.1-6	Text flow changes.
Page 2.6.7.5-8	Modified the first paragraph on the page under heading, "Finite Element Model of the MAGNATRAN Transport Cask with Impact Limiters."
Page 2.6.7.5-19	Replaced Figure 2.6.7-3.
Page 2.6.12-1	Deleted text at the end of the third sentence in the first paragraph of Section 2.6.12.
Page 2.6.16.1-1	Deleted the first half of the second sentence in the first paragraph of Section 2.6.16.1.
Page 2.6.16.2-1	Added a sentence to the end of the first paragraph of Section 2.6.16.2.
Page 2.6.16-2-2	Deleted the second to last row of the embedded table at the top of the page.

Chapter/Page/ Figure/Table	Description of Change
Page 2.6.16.3-1	Modified the fourth column heading on the first embedded table following the first paragraph of Section 2.6.16.3.
Chapter 3	
Pages 3.4-6 thru 3.4-7	Added list item number "5" to the text in Section 3.4.1.1.1.
Pages 3.4-8 thru 3.4-14	Text flow changes.
Page 3.5-2	Added new paragraph to the end of Section 3.5.1.1.
Pages 3.5-3 thru 3.5-17	Text flow changes.
Chapter 4	
No Changes	
Chapter 5	
Pages 5.1-2 thru 5.1-4	Added the word "rates" to the text where indicated.
Page 5.1-6	Replaced Figure 5.1-1.
Pages 5.1-9 thru 5.1-11	Added the word "Rate" to column headings on Tables 5.1-3 thru 5.1-8, and modified the data contained in Tables 5.1-3, 5.1-5 and 5.1-6 where indicated.
Pages 5.2-2 thru 5.2-3	Added the word "rate" to the text where indicated.
Pages 5.2-10 thru 5.2-14	Added the word "Rate" to the titles of Tables 5.2-6 thru 5.2-9, and modified the last line of Table 5.2-8.
Page 5.3-1	Added the word "rate" on the last line of the page.
Page 5.5-4	Added the word "rate" to the middle of the first paragraph of Section 5.5.1.3.
Page 5.5-7	Replaced Figure 5.5-3.
Page 5.5-11	Added the word "rate" to the note following Table 5.5-1.
Pages 5.5-12 thru 5.5-13	Modified Tables 5.5-3 and 5.5-4.
Page 5.6-1	Added the word "rate" to the second paragraph of Section 5.6.1.1.
Pages 5.6-3 thru 5.6-4	Added the word "rate" or "rates" to Sections 5.6.3, 5.6.4 and 5.6.4.1 where indicated.
Page 5.8.2-2	Added the word "rate" to the second paragraph on the page.
Page 5.8.2-8	Added the word "Rate" to two column headings in Table 5.8-7.
Page 5.8.3-2	Added the word "rate" to the first paragraph of Section 5.8.3.2.
Page 5.8.3-3	Modified and added text throughout Section 5.8.3.3.
Pages 5.8.3-4 thru 5.8.3-12	Text flow changes.
Pages 5.8.3-13 thru 5.8.3-14	Added new Figures 5.8-16B and 5.8-16C.
Pages 5.8.3-15 thru 5.8.3-23	Text flow changes.
Pages 5.8.3-24 thru 5.8.3-25	Modified Tables 5.8-16 thru 5.8-18.
Page 5.8.4-1	Added the word "rate" to the first paragraph of Section 5.8.4.2.
Pages 5.8.4-2 thru 5.8.4-3	Modified and added text throughout Section 5.8.4.3.
Pages 5.8.4-12 thru 5.8.4-13	Added new Figures 5.8-29B and 5.8-29C.

Chapter/Page/ Figure/Table	Description of Change
Pages 5.8.4-14 thru 5.8.4-18	Text flow changes.
Page 5.8.4-19	Modified Table 5.8-21
Pages 5.8.4-20 thru 5.8.4-22	Text flow changes.
Page 5.8.4-23	Added the word "Rate" to the second column headings of Tables 5.8-25 and 5.8-26.
Pages 5.8.5-2 thru 5.8.5-3	Modified text in the paragraph that makes up Section 5.8.5.1.
Page 5.8.5-4	Added the word "rate" to the first sentence under heading, "Combination of Fuel, BPRA and Thimble Plug Dose Rates."
Page 5.8.5-5	Text flow changes.
Page 5.8.5-6	Modified text and split the last paragraph on the page.
Page 5.8.6-1	Added the word "rate" near the end of the first and second paragraphs of Section 5.8.6.
Page 5.8.6-5	Made and editorial change to Note "b.)" of Table 5.8.36; modified Table 5.8-37.
Pages 5.8.10-3 thru 5.8.10-4	Modified Sections 5.8.10-2 and 5.8.10-3 throughout, where indicated.
Pages 5.8.10-5 thru 5.8.10-12	Text flow changes.
Page 5.8.10-13	Added new Figure 5.8-60B.
Pages 5.8.10-14 thru 5.8.10-72	Text flow changes.
Pages 5.8.10-73 thru 5.8.10-75	Modified Tables 5.8-47, 5.8-49, 5.8-50 and 5.8-51.
Page 5.8.11-2	Added the word "rate" to the second line at the top of the page near the end of Section 5.8.11.2.
Page 5.8.11-17	Modified Table 5.8-53.
Page 5.8.11-18	Added the word "Rate" to the second column headings of Tables 5.8-54 and 5.8-55.
Page 5.8.12-1	Added the word "rates" to the second paragraph of Section 5.8.12.
Page 5.8.12-2	Added the word "rates" to the sixth paragraph of Section 5.8.12.1.
Pages 5.8.13-1 thru 5.8.13-2	Modified the first line of the fifth paragraph and added the word "rate" to the sixth and seventh paragraphs of Section 5.8.13.
Chapter 6	
Page 6.9-3	Added a new reference, number 42.
Page 6.10.1-8	Added a new paragraph in the middle of the page.
Pages 6.10.1-9 thru 6.10.1-10	Text flow changes.
Pages 6.10.1-11 thru 6.10.1-13	Added new Section 6.10.1.4.5, "The Effect of Inserts in the Fuel Depletion Calculation."
Pages 6.10.1-14 thru 6.10.1-20	Text flow changes.
Pages 6.10.1-21 thru 6.10.1-22	Added new text to the end of Section 6.10.1.7.3.
Pages 6.10.1-23 thru 6.10.1-80	Text flow changes.
Pages 6.10.1-81 thru 6.10.1-82	Added new Figures 6.10.1-32 and 6.10.1-33.

Chapter/Page/ Figure/Table	Description of Change
Pages 6.10.1-83 thru 6.10.1-85	Text flow changes
Page 6.10.1-86	Modified Table 6.10.1-4
Pages 6.10.1-87 thru 6.10.1-108	Text flow changes
Pages 6.10.1-109 thru 6.10.1-112	Added new Tables 6.10.1-39 thru 6.10.1-44.
Chapter 7	
Page 7.1-1	Modified the last two paragraphs of Section 7.1, "Package Loading."
Pages 7.1-2 thru 7.1-4	Modified the "Note" of Step 5; modified Step 7; added new Step 8, which required renumbering the remaining steps to 9 through 19.
Page 7.1-5	Text flow changes.
Pages 7.1-6 thru 7.1-7	Modified items 8 and 9 of Section 7.1.2, "Loading of Contents," where indicated.
Pages 7.1-8 thru 7.1-9	Text flow changes.
Page 7.1-10	Deleted the second sentence of Item 7 of Section 7.1.3, "Preparation for Transport."
Page 7.1-11	Added new Item 16 to Section 7.1.3; which required renumbering Items 17 thru 22.
Page 7.1-12	Added five new "Notes" following the first note of Item 4 of Section 7.1.4, "Loading the Transportable Storage Canister with Spent Fuel Contents."
Page 7.1-13	Text flow changes.
Page 7.1-14	Modified Item 17 of Section 7.1.4.
Page 7.1-15	Modified Items 10 and 14 of Section 7.1.5, "Loading the Transportable Storage Canister with GTCC Waste Contents."
Page 7.1-16	Text flow changes.
Page 7.2-1 thru 7.2-3	Modified Step 3 and added new Step 4 of Section 7.2.1, "Receipt of Package from Carrier," which required renumbering Steps 5 through 19.
Pages 7.2-4 thru 7.2-6	Text flow changes.
Page 7.3-1	Deleted the second sentence of Step 5 of Section 7.3, "Preparation of Empty Packaging for Transport."
Page 7.4-1	Added new reference numbers 8 and 9.
Chapter 8	
Page 8.1-25	Modified the last two paragraphs of Section 8.1.6.3, "Neutron and Gamma Shield Effectiveness Test."
Pages 8.1-26 thru 8.1-27	Text flow changes.
Pages 8.2-6 thru 8.2-7	Modified the sixth paragraph of Section 8.2.3, "Component and Material Tests."
Page 8.2-8	Text flow changes.

Enclosure 3

List of Drawing Changes

No. 71-9356 for the MAGNATRAN Cask

MAGNATRAN SAR, Revision 15A

List of Drawing Changes, MAGNATRAN SAR, Revision 15A

Drawing 71160-505, Lid Assembly Transport Cask, MAGNATRAN, Rev. 5P

[redacted]

Drawing 71160-505, Lid Assembly Transport Cask, MAGNATRAN, Rev. 5NP

Sheet 1:

1. Remove delta note 5.
2. Revise Delta note 4 to a general note.
3. Revise B.O.M. Item 2 description to state: "SEE NOTE 4".
4. Revise B.O.M. Item 9 to add a revcloud over the description.
5. Revise B.O.M. Items 14, 15 and 16 quantity to "A/R", was "12".

Enclosure 4

Supporting Calculations

No. 71-9356 for the MAGNATRAN Cask

MAGNATRAN SAR, Revision 15A

NOTE: Calculations are in separate binders, as Volumes 2 and 3 of 3 for the Proprietary Submittal

All Calculations Withheld In Their Entirety Per 10 CFR 2.390

Enclosure 4 Contents

Volume 2 of 3:

1. GA-A20770
2. GA-A19897
3. 71160-2101, Revision 7
4. 71160-2108, Revision 3
5. 71160-2121, Revision 0
6. 71160-3001, Revision 3
7. 71160-3002, Revision 1
8. 71160-3013, Revision 2
9. 71160-3014, Revision 4

Volume 3 of 3:

10. 71160-3015, Revision 4
11. 71160-3020, Revision 14
12. 71160-3045, Revision 2

Enclosure 5

MAGNATRAN SAR
LOEP and SAR Page Changes

No. 71-9356 for the MAGNATRAN Cask

MAGNATRAN SAR, Revision 15A

September 2015

Revision 15A

MAGNATRAN

(**M**odular **A**dvanced **G**eneration **N**uclear **A**ll-purpose **TRANsport**)

SAFETY ANALYSIS REPORT

NON-PROPRIETARY VERSION

Docket No. 71-9356

NAC INTERNATIONAL

Atlanta Corporate Headquarters: 3930 East Jones Bridge Road, Norcross, Georgia 30092 USA
Phone 770-447-1144, Fax 770-447-1797, www.nacintl.com

List of Effective Pages

Chapter 1
Page 1-i thru 1-iii ..... Revision 15A
Page 1-1 ..... Revision 12A
Page 1.1-1 thru 1.1-8 ..... Revision 12A
Page 1.2-1 thru 1.2-4 ..... Revision 12A
Page 1.2-5 ..... Revision 14A
Page 1.3-1 thru 1.3-6 ..... Revision 12A
Page 1.3-7 ..... Revision 15A
Page 1.3-8 thru 1.3-20 ..... Revision 12A
Page 1.3-21 thru 1.3-51 ..... Revision 15A
Page 1.4-1 thru 1.4-2 ..... Revision 12A
Page 1.4-3 ..... Revision 15A
Page 1.4-4 ..... Revision 14A

36 drawings (see Section 1.4.3)

Chapter 2
Page 2-i thru 2-iii ..... Revision 12A
Page 2-iv thru 2-xxiv ..... Revision 14A
Page 2-1 ..... Revision 12A
Page 2.1-1 ..... Revision 12A
Page 2.1.1-1 thru 2.1.1-4 ..... Revision 12A
Page 2.1.1-5 thru 2.1.1-6 ..... Revision 15A
Page 2.1.2-1 thru 2.1.2-5 ..... Revision 12A
Page 2.1.2-6 ..... Revision 14A
Page 2.1.2-7 ..... Revision 12A
Page 2.1.2-8 ..... Revision 14A
Page 2.1.2-9 thru 2.1.2-11 ..... Revision 12A
Page 2.1.3-1 thru 2.1.3-2 ..... Revision 12A
Page 2.1.4-1 thru 2.1.4-5 ..... Revision 12A
Page 2.2-1 ..... Revision 12A
Page 2.2.1-1 thru 2.2.1-17 ..... Revision 12A
Page 2.2.2-1 thru 2.2.2-3 ..... Revision 12A
Page 2.2.2-4 ..... Revision 14A
Page 2.2.2-5 thru 2.2.2-7 ..... Revision 12A
Page 2.2.2-8 thru 2.2.2-9 ..... Revision 14A
Page 2.2.3-1 ..... Revision 12A
Page 2.3-1 ..... Revision 12A
Page 2.3.1-1 ..... Revision 12A
Page 2.3.2-1 ..... Revision 12A
Page 2.4-1 thru 2.4-2 ..... Revision 12A
Page 2.5-1 ..... Revision 12A
Page 2.5.1-1 thru 2.5.1-12 ..... Revision 12A
Page 2.5.2-1 thru 2.5.2-2 ..... Revision 12A
Page 2.5.2-3 ..... Revision 14A
Page 2.5.2-4 thru 2.5.2-5 ..... Revision 12A
Page 2.5.2-6 ..... Revision 14A
Page 2.5.2-7 thru 2.5.2-19 ..... Revision 12A
Page 2.6-1 ..... Revision 12A
Page 2.6.1-1 thru 2.6.1-4 ..... Revision 12A
Page 2.6.1-5 ..... Revision 14A
Page 2.6.1-6 thru 2.6.1-8 ..... Revision 12A
Page 2.6.1-9 thru 2.6.1-15 ..... Revision 14A
Page 2.6.2-1 ..... Revision 14A
Page 2.6.2-2 thru 2.6.2-3 ..... Revision 12A
Page 2.6.2-4 thru 2.6.2-10 ..... Revision 14A
Page 2.6.3-1 ..... Revision 12A
Page 2.6.4-1 thru 2.6.4-2 ..... Revision 12A
Page 2.6.5-1 thru 2.6.5-3 ..... Revision 12A
Page 2.6.5-4 thru 2.6.5-5 ..... Revision 14A
Page 2.6.6-1 ..... Revision 12A
Page 2.6.7-1 ..... Revision 12A
Page 2.6.7.1-1 ..... Revision 12A
Page 2.6.7.1-2 thru 2.6.7.1-4 ..... Revision 14A
Page 2.6.7.1-5 ..... Revision 12A
Page 2.6.7.1-6 thru 2.6.7.1-8 ..... Revision 14A
Page 2.6.7.1-9 ..... Revision 12A
Page 2.6.7.2-1 ..... Revision 12A
Page 2.6.7.2-2 thru 2.6.7.2-4 ..... Revision 14A
Page 2.6.7.2-5 ..... Revision 12A
Page 2.6.7.3-1 ..... Revision 12A
Page 2.6.7.3-2 thru 2.6.7.3-4 ..... Revision 14A
Page 2.6.7.3-5 ..... Revision 12A
Page 2.6.7.3-6 thru 2.6.7.3-8 ..... Revision 14A
Page 2.6.7.4-1 ..... Revision 12A
Page 2.6.7.5-1 thru 2.6.7.5-7 ..... Revision 14A
Page 2.6.7.5-8 ..... Revision 15A
Page 2.6.7.5-9 thru 2.6.7.5-18 ..... Revision 14A
Page 2.6.7.5-19 ..... Revision 15A
Page 2.6.7.5-20 thru 2.6.7.5-34 ..... Revision 14A
Page 2.6.7.6-1 thru 2.6.7.6-5 ..... Revision 12A
Page 2.6.7.7-1 thru 2.6.7.7-15 ..... Revision 12A
Page 2.6.7.7-16 thru 2.6.7.7-17 ..... Revision 14A
Page 2.6.7.7-18 thru 2.6.7.7-19 ..... Revision 12A
Page 2.6.8-1 ..... Revision 12A
Page 2.6.9-1 ..... Revision 12A
Page 2.6.10-1 ..... Revision 12A
Page 2.6.11-1 thru 2.6.11-5 ..... Revision 12A
Page 2.6.12-1 ..... Revision 15A
Page 2.6.12-2 ..... Revision 12A
Page 2.6.12.1-1 ..... Revision 12A
Page 2.6.12.2-1 thru 2.6.12.2-7 ..... Revision 12A
Page 2.6.12-3-1 thru 2.6.12-3-4 ..... Revision 12A
Page 2.6.12.4-1 thru 2.6.12.4-12 ..... Revision 12A
Page 2.6.12.5-1 thru 2.6.12.5-6 ..... Revision 12A

List of Effective Pages (cont'd)

Page 2.6.12.6-1 thru 2.6.12.6-4.....Revision 12A
Page 2.6.12-7-1 thru 2.6.12-7-3.....Revision 12A
Page 2.6.12.8-1 thru 2.6.12.8-10....Revision 12A
Page 2.6.12.9-1 thru 2.6.12.9-6.....Revision 12A
Page 2.6.12.10-1 .....Revision 12A
Page 2.6.12.11-1 .....Revision 12A
Page 2.6.12.12-1 thru
2.6.12.12-2.....Revision 12A
Page 2.6.12.13-1 thru
2.6.12.13-3.....Revision 12A
Page 2.6.12-14-1 thru
2.6.12.14-2.....Revision 12A
Page 2.6.13-1 thru 2.6.13-2.....Revision 12A
Page 2.6.13.1-1 thru 2.6.13.1-2.....Revision 12A
Page 2.6.13.2-1 thru 2.6.13.2-13....Revision 12A
Page 2.6.13.3-1 thru 2.6.13.3-3.....Revision 12A
Page 2.6.13.4-1 thru 2.6.13.4-14....Revision 12A
Page 2.6.13.5-1 thru 2.6.13.5-2.....Revision 12A
Page 2.6.13.6-1 thru 2.6.13.6-5.....Revision 12A
Page 2.6.13.7-1 thru 2.6.13.7-4.....Revision 12A
Page 2.6.14-1 .....Revision 12A
Page 2.6.14.1-1 thru 2.6.14.1-8.....Revision 12A
Page 2.6.14.2-1 thru 2.6.14.2-2.....Revision 12A
Page 2.6.14.3-1 thru 2.6.14.3-14....Revision 12A
Page 2.6.14.4-1 thru 2.6.14.4-3.....Revision 12A
Page 2.6.15-1 thru 2.6.15-2.....Revision 12A
Page 2.6.15.1-1 thru 2.6.15.1-2.....Revision 12A
Page 2.6.15.2-1 thru 2.6.15.2-13....Revision 12A
Page 2.6.15.3-1 thru 2.6.15.3-2.....Revision 12A
Page 2.6.15.4-1 thru 2.6.15.4-15....Revision 12A
Page 2.6.15.5-1 .....Revision 12A
Page 2.6.15.6-1 thru 2.6.15.6-5.....Revision 12A
Page 2.6.15.7-1 thru 2.6.15.7-3.....Revision 12A
Page 2.6.16-1 .....Revision 12A
Page 2.6.16.1-1 .....Revision 15A
Page 2.6.16.2-1 thru 2.6.16.2-2.....Revision 15A
Page 2.6.16.2-3 thru 2.6.16.2-6.....Revision 12A
Page 2.6.16.3-1 .....Revision 15A
Page 2.6.16.3-2 thru 2.6.16.3-3.....Revision 12A
Page 2.6.16.4-1 thru 2.6.16.4-7.....Revision 12A
Page 2.6.16.5-1 thru 2.6.16.5-4.....Revision 12A
Page 2.6.16.6-1 thru 2.6.16.6-3.....Revision 12A
Page 2.6.16.7-1 thru 2.6.16.7-4.....Revision 12A
Page 2.6.16.8-1 thru 2.6.16.8-6.....Revision 12A
Page 2.6.16.9-1 thru 2.6.16.9-6.....Revision 12A
Page 2.6.16.10-1 .....Revision 12A
Page 2.6.16.11-1 .....Revision 12A
Page 2.6.16.12-1 .....Revision 12A
Page 2.6.16.13-1 thru 2.6.16.13-3 . Revision 12A
Page 2.6.17-1 .....Revision 12A
Page 2.6.17.1-1 .....Revision 12A
Page 2.6.17.2-1 thru 2.6.17.2-4 ..... Revision 12A
Page 2.6.17.3-1 thru 2.6.17.3-7 ..... Revision 12A
Page 2.7-1 .....Revision 12A
Page 2.7.1-1 thru 2.7.1-3 ..... Revision 12A
Page 2.7.1.1-1 thru 2.7.1.1-7 ..... Revision 14A
Page 2.7.1.2-1 .....Revision 12A
Page 2.7.1.2-2 thru 2.7.1.2-4 ..... Revision 14A
Page 2.7.1.3-1 .....Revision 12A
Page 2.7.1.3-2 thru 2.7.1.3-7 ..... Revision 14A
Page 2.7.1.4-1 .....Revision 14A
Page 2.7.1.5-1 .....Revision 14A
Page 2.7.1.5-2 .....Revision 12A
Page 2.7.1.5-3 .....Revision 14A
Page 2.7.1.6-1 .....Revision 12A
Page 2.7.1.7-1 thru 2.7.1.7-6 ..... Revision 12A
Page 2.7.1.8-1 .....Revision 14A
Page 2.7.1.8-2 .....Revision 12A
Page 2.7.1.8-3 .....Revision 14A
Page 2.7.1.8-4 thru 2.7.1.8-6 ..... Revision 12A
Page 2.7.2-1 .....Revision 12A
Page 2.7.3-1 thru 2.7.3-11 ..... Revision 12A
Page 2.7.4-1 thru 2.7.4-6 ..... Revision 12A
Page 2.7.5-1 .....Revision 12A
Page 2.7.6-1 .....Revision 12A
Page 2.7.7-1 .....Revision 12A
Page 2.7.7-2 thru 2.7.7-3 ..... Revision 14A
Page 2.7.8-1 thru 2.7.8-32 ..... Revision 12A
Page 2.7.9-1 thru 2.7.9-15 ..... Revision 12A
Page 2.7.10-1 thru 2.7.10-12 ..... Revision 12A
Page 2.7.11-1 thru 2.7.11-14 ..... Revision 12A
Page 2.7.12-1 thru 2.7.12-2 ..... Revision 12A
Page 2.7.12.1-1 thru 2.7.12.1-2 ..... Revision 12A
Page 2.7.12.2-1 thru 2.7.12.2-6 ..... Revision 12A
Page 2.7.12.3-1 thru 2.7.12.3-4 ..... Revision 12A
Page 2.7.12.4-1 thru 2.7.12.4-6 ..... Revision 12A
Page 2.7.12.5-1 .....Revision 12A
Page 2.7.12.6-1 thru 2.7.12.6-2 ..... Revision 12A
Page 2.7.13-1 .....Revision 12A
Page 2.7.13.1-1 thru 2.7.13.1-7 ..... Revision 14A
Page 2.7.13.2-1 thru 2.7.13.2-21 ... Revision 14A
Page 2.7.14-1 thru 2.7.14-8 ..... Revision 12A
Page 2.7.15-1 .....Revision 12A
Page 2.7.16-1 thru 2.7.16-2 ..... Revision 12A
Page 2.7.16-3 thru 2.7.16-4 ..... Revision 14A
Page 2.8-1 .....Revision 12A

List of Effective Pages (cont'd)

Page 2.9-1 ..... Revision 12A
Page 2.10-1 ..... Revision 12A
Page 2.11-1 ..... Revision 12A
Page 2.11.1-1 thru 2.11.1-12 ..... Revision 12A
Page 2.11.2-1 thru 2.11.2-4 ..... Revision 12A
Page 2.11.3-1 thru 2.11.3-6 ..... Revision 12A
Page 2.11.4-1 thru 2.11.4-3 ..... Revision 12A
Page 2.11.5-1 ..... Revision 12A
Page 2.12-1 ..... Revision 12A
Page 2.12.1-1 ..... Revision 14A
Page 2.12.1-2 ..... Revision 12A
Page 2.12.1-3 ..... Revision 14A
Page 2.12.1-4 ..... Revision 12A
Page 2.12.2-1 thru 2.12.2-4 ..... Revision 12A
Page 2.12.2-5 thru 2.12.2-82 ..... Revision 14A

Chapter 3
Page 3-i thru 3-iii ..... Revision 15A
Page 3-1 ..... Revision 12A
Page 3.1-1 ..... Revision 14A
Page 3.1-2 thru 3.1-3 ..... Revision 12A
Page 3.2-1 thru 3.2-7 ..... Revision 12A
Page 3.2-8 ..... Revision 14A
Page 3.3-1 ..... Revision 12A
Page 3.3-2 ..... Revision 14A
Page 3.4-1 thru 3.4-3 ..... Revision 12A
Page 3.4-4 ..... Revision 14A
Page 3.4-5 ..... Revision 12A
Page 3.4-6 thru 3.4-14 ..... Revision 15A
Page 3.4-15 thru 3.4-19 ..... Revision 14A
Page 3.4-20 thru 3.4-31 ..... Revision 12A
Page 3.4-32 thru 3.4-35 ..... Revision 14A
Page 3.5-1 ..... Revision 12A
Page 3.5-2 thru 3.5-17 ..... Revision 15A
Page 3.6-1 thru 3.6-2 ..... Revision 12A

Chapter 4
Page 4-i ..... Revision 14A
Page 4-ii ..... Revision 12A
Page 4-1 ..... Revision 12A
Page 4.1-1 ..... Revision 14A
Page 4.1-2 thru 4.1-6 ..... Revision 12A
Page 4.2-1 ..... Revision 14A
Page 4.2-2 ..... Revision 12A
Page 4.3-1 ..... Revision 14A
Page 4.3-2 ..... Revision 12A
Page 4.4-1 thru 4.4-3 ..... Revision 12A
Page 4.5-1 thru 4.5-9 ..... Revision 12A
Page 4.5-10 thru 4.5-19 ..... Revision 14A

Chapter 5
Page 5-i thru 5-ix ..... Revision 12A
Page 5-1 thru 5-3 ..... Revision 14A
Page 5.1-1 ..... Revision 14A
Page 5.1-2 thru 5.1-4 ..... Revision 15A
Page 5.1-5 ..... Revision 14A
Page 5.1-6 ..... Revision 15A
Page 5.1-7 thru 5.1-8 ..... Revision 14A
Page 5.1-9 thru 5.1-11 ..... Revision 15A
Page 5.1-12 ..... Revision 14A
Page 5.2-1 ..... Revision 12A
Page 5.2-2 thru 5.2-3 ..... Revision 15A
Page 5.2-4 ..... Revision 14A
Page 5.2-5 thru 5.2-7 ..... Revision 12A
Page 5.2-8 ..... Revision 14A
Page 5.2-9 ..... Revision 12A
Page 5.2-10 thru 5.2-13 ..... Revision 15A
Page 5.3-1 ..... Revision 15A
Page 5.3-2 ..... Revision 14A
Page 5.3-3 thru 5.3-6 ..... Revision 12A
Page 5.4-1 ..... Revision 12A
Page 5.4-2 ..... Revision 14A
Page 5.4-3 thru 5.4-5 ..... Revision 12A
Page 5.5-1 thru 5.5-3 ..... Revision 14A
Page 5.5-4 ..... Revision 15A
Page 5.5-5 ..... Revision 14A
Page 5.5-6 ..... Revision 12A
Page 5.5-7 ..... Revision 15A
Page 5.5-8 thru 5.5-10 ..... Revision 14A
Page 5.5-11 thru 5.5-13 ..... Revision 15A
Page 5.6-1 ..... Revision 15A
Page 5.6-2 ..... Revision 14A
Page 5.6-3 thru 5.6-4 ..... Revision 15A
Page 5.6-5 thru 5.6-27 ..... Revision 14A
Page 5.7-1 thru 5.7-3 ..... Revision 12A
Page 5.8-1 ..... Revision 12A
Page 5.8.1-1 ..... Revision 14A
Page 5.8.1-2 thru 5.8.1-4 ..... Revision 12A
Page 5.8.2-1 ..... Revision 12A
Page 5.8.2-2 ..... Revision 15A
Page 5.8.2-3 ..... Revision 14A
Page 5.8.2-4 thru 5.8.2-7 ..... Revision 12A
Page 5.8.2-8 ..... Revision 15A
Page 5.8.2-9 thru 5.8.2-11 ..... Revision 12A
Page 5.8.3-1 ..... Revision 14A
Page 5.8.3-2 thru 5.8.3-25 ..... Revision 15A

List of Effective Pages (cont'd)

Page 5.8.4-1 thru 5.8.4-3 ..... Revision 15A
Page 5.8.4-4 thru 5.8.4-11 ..... Revision 14A
Page 5.8.4-12 thru 5.8.4-23 ..... Revision 15A
Page 5.8.5-1 ..... Revision 14A
Page 5.8.5-2 thru 5.8.5-6 ..... Revision 15A
Page 5.8.5-7 thru 5.8.5-11 ..... Revision 14A
Page 5.8.6-1 ..... Revision 15A
Page 5.8.6-2 thru 5.8.6-4 ..... Revision 14A
Page 5.8.6-5 ..... Revision 15A
Page 5.8.6-6 thru 5.8.6-7 ..... Revision 14A
Page 5.8.7-1 thru 5.8.7-96 ..... Revision 14A
Page 5.8.8-1 ..... Revision 14A
Page 5.8.9-1 thru 5.8.9-5 ..... Revision 14A
Page 5.8.10-1 thru 5.8.10-2 ..... Revision 14A
Page 5.8.10-3 thru 5.8.10-75 ..... Revision 15A
Page 5.8.11-1 ..... Revision 14A
Page 5.8.11-2 ..... Revision 15A
Page 5.8.11-3 thru 5.8.11-16 ..... Revision 14A
Page 5.8.11-17 thru 5.8.11-18 ..... Revision 15A
Page 5.8.12-1 thru 5.8.12-2 ..... Revision 15A
Page 5.8.12-3 thru 5.8.12-20 ..... Revision 14A
Page 5.8.13-1 thru 5.8.13-2 ..... Revision 15A
Page 5.8.13-3 thru 5.8.13-5 ..... Revision 14A

Chapter 6
Page 6-i thru 6-ix ..... Revision 14A
Page 6-1 ..... Revision 14A
Page 6.1.1-1 thru 6.1.1-5 ..... Revision 14A
Page 6.1.2-1 thru 6.1.2-6 ..... Revision 14A
Page 6.1.3-1 ..... Revision 14A
Page 6.2.1-1 thru 6.2.1-5 ..... Revision 14A
Page 6.2.2-1 ..... Revision 14A
Page 6.2.3-1 ..... Revision 14A
Page 6.3.1-1 thru 6.3.1-7 ..... Revision 14A
Page 6.3.2-1 thru 6.3.2-3 ..... Revision 14A
Page 6.3.3-1 ..... Revision 14A
Page 6.3.4-1 ..... Revision 14A
Page 6.4-1 ..... Revision 14A
Page 6.4.1-1 thru 6.4.1-3 ..... Revision 14A
Page 6.4.2-1 thru 6.4.2-2 ..... Revision 14A
Page 6.5.1-1 ..... Revision 14A
Page 6.5.2-1 thru 6.5.2-2 ..... Revision 14A
Page 6.6.1-1 ..... Revision 14A
Page 6.6.2-1 thru 6.6.2-2 ..... Revision 14A
Page 6.6.3-1 thru 6.6.3-4 ..... Revision 14A
Page 6.7-1 ..... Revision 14A
Page 6.8.1-1 thru 6.8.1-69 ..... Revision 14A
Page 6.8.2-1 thru 6.8.2-3 ..... Revision 14A
Page 6.9-1 thru 6.9-2 ..... Revision 14A
Page 6.9-3 ..... Revision 15A
Page 6.10.1-1 thru 6.10.1-7 ..... Revision 14A
Page 6.10.1-8 thru 6.10.1-112 ..... Revision 15A
Page 6.10.2-1 thru 6.10.2-18 ..... Revision 14A
Page 6.10.3-1 thru 6.10.3-86 ..... Revision 14A

Chapter 7
Page 7-i ..... Revision 14A
Page 7-1 thru 7-2 ..... Revision 14A
Page 7.1-1 thru 7.1-16 ..... Revision 15A
Page 7.2-1 thru 7.2-6 ..... Revision 15A
Page 7.3-1 ..... Revision 15A
Page 7.4-1 ..... Revision 15A

Chapter 8
Page 8-i thru 8-ii ..... Revision 14A
Page 8-1 ..... Revision 12A
Page 8.1-1 ..... Revision 14A
Page 8.1-2 ..... Revision 12A
Page 8.1-3 ..... Revision 14A
Page 8.1-4 ..... Revision 12A
Page 8.1-5 thru 8.1-8 ..... Revision 14A
Page 8.1-9 thru 8.1-22 ..... Revision 12A
Page 8.1-23 thru 8.1-24 ..... Revision 14A
Page 8.1-25 thru 8.1-27 ..... Revision 15A
Page 8.1-28 thru 8.1-29 ..... Revision 14A
Page 8.2-1 thru 8.2-5 ..... Revision 14A
Page 8.2-6 thru 8.2-8 ..... Revision 15A
Page 8.3-1 thru 8.3-2 ..... Revision 12A

Chapter 1
General Description

Table of Contents

1 GENERAL INFORMATION 1-1

1.1 Terminology 1.1-1

1.2 Introduction 1.2-1
1.2.1 Cask System 1.2-1
1.2.2 Transport Cask Components 1.2-2

1.3 Package Description 1.3-1
1.3.1 Packaging 1.3-1
1.3.2 Contents 1.3-21
1.3.3 Special Requirements for Plutonium 1.3-51
1.3.4 Operational Features 1.3-51

1.4 Appendix 1.4-1
1.4.1 References 1.4-1
1.4.2 Quality Assurance 1.4-2
1.4.3 License Drawings 1.4-3

List of Figures

Figure 1.2-1 MAGNATRAN Transport Cask – Nominal Assembly Dimensions (inches) 1.2-4
Figure 1.2-2 Transport Configuration of the MAGNATRAN Transport Cask 1.2-5
Figure 1.3-1 MAGNASTOR TSC and Basket 1.3-13
Figure 1.3-2 MAGNATRAN Transport Cask Containment Boundary 1.3-14
Figure 1.3-3 MAGNASTOR Damaged Fuel Can 1.3-15
Figure 1.3-4 Schematic of DF Basket Assembly Configuration for PWR Fuel with Damaged Fuel Can Locations 1.3-33
Figure 1.3-5 Schematic of 82-Assembly BWR Basket Pattern 1.3-34
Figure 1.3-6 Schematic of 37-Assembly PWR Basket (33-, 35 and 36-Assembly Configuration Included) 1.3-35
Figure 1.3-7 Schematic of 87-Assembly BWR Basket 1.3-36
Figure 1.3-8 BWR Partial Length Fuel Rod Location Sketches 1.3-37

List of Tables

Table 1.3-1 Design Characteristics of the MAGNATRAN Transport Cask and Components 1.3-16
Table 1.3-2 Design Characteristics of the Transportable Storage Canister 1.3-18
Table 1.3-3 Design Characteristics of the Fuel Basket Assemblies 1.3-19
Table 1.3-4 Design Characteristics of the [redacted] Damaged Fuel Can 1.3-20
Table 1.3-5 Design Characteristics of the GTCC Waste Basket Liner and TSC 1.3-20
Table 1.3-6 PWR Fuel Assembly Characteristics 1.3-38
Table 1.3-7 Bounding PWR Fuel Assembly Geometry for Loading Criteria 1.3-39
Table 1.3-8 Maximum Initial Enrichment – 37-Assembly Undamaged Fuel Configuration – 0.036 g/cm^2 ^{10}B Absorber 1.3-40
Table 1.3-9 Maximum Initial enrichment – 37-Assembly Undamaged Fuel Configuration – 0.030 g/cm^2 ^{10}B Absorber 1.3-41
Table 1.3-10 Maximum Initial Enrichment – 37-Assembly Undamaged Fuel Configuration – 0.027 g/cm^2 ^{10}B Absorber 1.3-42
Table 1.3-11 Maximum Initial Enrichment – Undamaged Fuel Configuration WE15 – Optional Configurations 1.3-43
Table 1.3-12 Required Burnup – PWR Damaged Fuel Configuration – 0.036 g/cm^2 ^{10}B Absorber 1.3-44
Table 1.3-13 Maximum Initial Enrichment – PWR Damaged Fuel Configuration – 0.030 g/cm^2 ^{10}B Absorber 1.3-44
Table 1.3-14 Maximum Initial Enrichment – PWR Damaged Fuel Configuration – 0.027 g/cm^2 ^{10}B Absorber 1.3-45
Table 1.3-15 Maximum Initial Enrichment – Damaged Fuel Configuration WE15 – Optional Configurations 1.3-45
Table 1.3-16 Additional Fuel Assembly Cool Time Required to Load Nonfuel Hardware 1.3-46
Table 1.3-17 Allowed BPRA Burnup and Cool Time Combinations 1.3-46
Table 1.3-18 Allowed GTPD Burnup and Cool Time Combinations 1.3-46
Table 1.3-19 BWR Fuel Assembly Characteristics 1.3-47
Table 1.3-20 BWR Fuel Assembly Loading Criteria 1.3-48
Table 1.3-21 BWR Fuel Assembly Loading Criteria – Enrichment Limits for 87-Assembly and 82-Assembly Configurations with Axial Blanket 1.3-49
Table 1.3-22 Undamaged BWR Fuel Assembly Loading Criteria (Enrichment Limits for Fuel Without Axial Blanket) 1.3-50

Port and Coverplate

The MAGNATRAN has a lid port that is closed by a bolted Type 304/304L stainless steel coverplate with dual O-rings. The four coverplate bolts are SA-193, Grade B6, Type 410 stainless steel, socket head cap screws. The bolts are countersunk flush with the top of the coverplate. The basic configuration of the lid port and coverplate includes a 5.32-inch-diameter opening to recess the coverplate and for access to the port opening and the quick-disconnect installed there. Two concentric O-rings are located on the bottom face of the coverplate, an inner metal O-ring and an outer EPDM O-ring. The inner O-ring provides the containment boundary seal for the lid port. The outer O-ring and a test port located between the two O-rings provide the means to leak test the containment boundary seal. After the leak test is completed, the seal test port is closed by a threaded plug fitted with a metal boss seal.

Lifting Trunnions and Rotation Trunnions

The two lifting trunnions on the MAGNATRAN are Type 17-4 PH stainless steel, which are bolted into recesses in the top forging at diametrically opposite locations around the cask circumference. Each lifting trunnion is bolted to the top forging by nine SB637, GR N07718, nickel alloy bolts. The basic diameter of the lifting trunnions is 6.6 inches and the load-bearing width is 3.75 inches. A retainer, or flange, on the outer end of each lifting trunnion acts as a safety stop to ensure that proper engagement with the lift yoke is maintained. The MAGNATRAN lifting trunnions are designed and load tested in accordance with the requirements of ANSI N14.6 and 10 CFR 71.45(a).

Two rotation trunnions, located 17.65 inches above the bottom of the cask and circumferentially in line with the two lifting trunnions, are offset approximately 5 inches from the cask centerline to ensure that the cask rotates in the proper direction. The rotation trunnions also serve as the cask tiedown restraint in the aft longitudinal direction. Each rotation trunnion support is Type XM-19 stainless steel housing a 17-4 PH pin and is welded to the outer shell and bottom outer forging. The neutron shield assemblies are shaped to accommodate the location and operation of the rotation trunnions.

Transport Impact Limiters

The MAGNATRAN transport cask is equipped with removable impact limiters that are bolted over each end of the cask to ensure that the design impact loads for the cask are not exceeded for any of the normal conditions of transport and hypothetical accident conditions defined in 10 CFR 71. [redacted]

[redacted]

The lower impact limiter is bolted to the cask bottom plate by 16 equally spaced retaining rods and nuts. The upper impact limiter is similarly bolted to the cask lid.

Transportable Storage Canisters

The transportable storage canister (TSC) and the closure lid are dual-certified Type 304/304L stainless steel. The canister holds the fuel basket or GTCC waste basket liner assembly and contains the contents. A schematic of a typical TSC with a fuel basket is shown in Figure 1.3-1. There are two different length TSCs (short and long) to accommodate the various PWR and BWR fuel assembly lengths, damaged fuel (only short), and GTCC waste (only short). The TSC body (shell and bottom) and the closure lid provide confinement, shielding and lifting capability for the TSC. The loaded TSCs include a solid stainless steel closure lid or stainless steel/carbon steel closure lid assembly with a closure ring and dual port covers to provide a dual-welded closure system. The closure lid is positioned inside the TSC on the lifting lugs above the basket assembly following fuel loading, or on the top of the GTCC waste basket liner following GTCC waste loading. After the closure lid is placed on the TSC, the TSC is moved to a workstation and the closure lid is welded to the TSC. The vent and drain ports are penetrations through the lid, which provide access for auxiliary systems to drain, dry and helium backfill the TSC. Following completion of backfilling, the dual port covers are installed and welded in each port. Removable lifting fixtures installed in the closure lid are used to lift and lower the loaded TSC. The design characteristics of the TSCs are summarized in Table 1.3-2.

The fuel TSC is designed, fabricated, tested and inspected to the requirements of the ASME Boiler and Pressure Vessel Code (ASME Code), Section III, Division 1, Subsection NB, to the extent practical, except as noted in the Alternatives to the ASME Code provided in Table 2.1.4-1. The GTCC waste TSCs are fabricated using ASTM materials and are fabricated in accordance with ASME Code, Section III, Division 1, Subsection NF.

Fuel Baskets

Each TSC containing spent fuel includes a PWR, PWR-DF or BWR fuel basket that positions and supports the contents (fuel). Consistent with the TSC design, there are two different length fuel baskets (the two lengths are the same for both the PWR and the BWR fuel baskets). As

1.3.2 Contents

The MAGNASTOR fuel TSC or Greater Than Class C (GTCC) TSC can be transported in the MAGNATRAN.

The MAGNASTOR fuel TSC design capacity is up to 37 undamaged uranium PWR fuel assemblies in the 37 PWR basket assembly, or up to 87 undamaged uranium BWR fuel assemblies in the 87 BWR basket assembly. The fuel TSC with the DF basket assembly has a capacity of up to 37 undamaged uranium PWR fuel assemblies, including four DFC locations. DFCs may be placed in up to four of the DFC locations as shown in Figure 1.3-4.

Fuel assemblies are assigned to two groups of PWR and two groups of BWR fuel assemblies on the basis of fuel assembly length. Fuel assemblies are restricted to those with zirconium alloy-clad fuel rods; no steel-clad assemblies are considered. PWR fuel assemblies containing nonfuel hardware may be loaded in the TSC. BWR fuel assemblies containing channels may be loaded in the TSC.

The initial enrichment limits are shown in Table 1.3-6 and Table 1.3-19 for PWR and BWR fuel, respectively, and exclude the loading of fuel assemblies enriched to less than 1.3 wt % ^{235}U, including unenriched fuel assemblies. Fuel assemblies containing low enriched, unenriched, and/or annular axial end-blankets may be loaded into the TSC. The end blankets are typically regions of low enriched or natural uranium oxide. Unenriched (natural uranium oxide) end blankets are limited to a nominal length no greater than 6 inches (dimension applicable to top and bottom of the fuel rod, not cumulative).

BWR/2,3 fuel assemblies with a fuel assembly length of approximately 171 inches will be loaded into the short TSC (nominal length of 184.75 inches). BWR/4-6 fuel assemblies with a fuel assembly length of approximately 176 inches will be loaded into the long TSC (nominal length 191.75 inches). PWR fuel assemblies, with the exception of fuel identified as type CE 16×16, in Table 1.3-6 must be loaded into a short TSC (i.e., be loaded into a transport configuration with a canister spacer). CE16 fuel may be loaded into a either short or long TSC. An exception to the PWR CE16 guideline is the System 80 16×16 fuel with an active fuel length of 150 inches whose overall length exceeds the short TSC cavity length and, therefore, must be loaded into the long TSC.

Empty fuel rod positions are filled with a solid filler rod or a solid neutron absorber rod that displaces a volume not less than that of the original fuel rod.

A MAGNASTOR TSC may contain irradiated, nonfuel-bearing carbon and/or stainless steel material (e.g., loose nuts and bolts, etc.) provided that the bounding weight of the loaded TSC as shown in Table 2.1.3-1 is not exceeded.

Greater Than Class C (GTCC) waste is defined in 10 CFR 61.55(a)(3) and (4) by the concentration of long-lived radionuclides, i.e., ^{14}C, ^{59}Ni, and ^{94}NB, and/or short-lived radionuclides, i.e., ^{3}H, ^{60}Co, and ^{63}Ni. The disposal of GTCC waste is controlled by 10 CFR 61. GTCC waste consists of radiation activated and surface contaminated steel, and/or plasma cutting debris (dross). Stainless steel core baffle structure – baffle plates and angles, baffle formers, and lower core plates, located adjacent to the reactor vessel in a high neutron flux field, is the major component of GTCC waste.

The GTCC waste to be transported in the MAGNATRAN is placed in a GTCC waste basket liner, which is loaded into a GTCC TSC. The GTCC TSC and welded closure lid are geometrically identical to that of the fuel TSC.

PWR Fuel

The PWR fuel evaluations are based on bounding PWR fuel assembly parameters that maximize the source terms for the shielding evaluations, the reactivity for criticality evaluations, the decay heat load for the thermal evaluations, and the fuel weight for the structural evaluations. These bounding parameters are selected from the various spent fuel assemblies that are candidates for loading in the TSC. The bounding fuel assembly values are established based primarily on how the principal parameters are combined, and on the loading conditions (or restrictions) established for a group of fuel assemblies based on its parameters.

The limiting parameters of the PWR fuel assemblies authorized for loading in the TSC are shown in Table 1.3-6. The maximum initial enrichment authorized represents the peak fuel rod enrichment for variably enriched PWR fuel assemblies. The PWR fuel assembly characteristics are summarized by fuel assembly type in Chapter 6, with burnup credit loading curves correlating maximum initial enrichment for a given assembly average burnup at various absorber sheet loading, also listed in Chapter 6. Table 1.3-6 assembly physical information is limited to the analysis input of fuel mass, array configuration, and number of fuel rods. These analysis values are key inputs to the shielding and criticality evaluations in Chapters 5 and 6, respectively. Lattice parameters dictating system reactivity are detailed in Chapter 6. Enrichment limits are set for each fuel type to produce reactivities at the upper subcritical limit (USL).

The maximum TSC decay heat load for the transport of PWR fuel assemblies is 23.0 kW. The uniform loading pattern permitted limits assemblies to a maximum heat load of 0.622

kW/assembly. The bounding thermal evaluations are based on the Westinghouse 17×17 fuel assembly. The minimum cool times are determined based on the maximum decay heat load of the contents and meeting transport dose limits. The fuel assemblies and source terms that produce the maximum dose rates are summarized in Chapter 5.

The DF basket assembly configuration for PWR fuel with damaged fuel can locations is shown in Figure 1.3-4. Each DFC may contain an undamaged PWR fuel assembly, a damaged PWR fuel assembly, or PWR fuel debris equivalent to one PWR fuel assembly. Undamaged PWR fuel assemblies may be placed directly in the DFC locations of a DF Basket Assembly. PWR fuel assemblies loaded in a DFC shall not contain nonfuel hardware, with the exception of instrument tube tie components and steel inserts.

A PWR fuel assembly weight of 1,680 pounds based on a B&W 15×15 fuel assembly with control components inserted, has been structurally evaluated in each location of the PWR fuel basket, equaling a total contents weight of 62,160 lbs. A bounding weight of 1,814 pounds is evaluated for each loaded damaged fuel can in the damaged fuel configuration of the PWR DF fuel basket. A total contents weight of 61,184 lbs is specified for the PWR DF basket to limit the maximum loaded TSC weight to 104,500 lbs. The analyzed contents weight provides the most significant measure of the basket performance. Accordingly, a 5% increase in the maximum weight per undamaged fuel location of 1,765 lbs is permitted while maintaining a maximum contents weight consistent with the basket evaluation.

As noted in Table 1.3-6, PWR fuel assemblies may include nonfuel hardware placed into the fuel assembly guide tubes and/or instrument tube. Nonfuel hardware that is located in the active fuel region is referred to as inserts in this SAR. Nonfuel components, such as thimble plugs, may not reach into the active fuel region and do not have a significant effect on system reactivity.

Westinghouse 15×15 PWR fuel assemblies that have been enhanced to address top nozzle stress corrosion cracking may use nonfuel hardware to prevent the separation of the top nozzle.

BWR Fuel

The BWR fuel evaluations are based on bounding BWR fuel assembly parameters that maximize the source terms for the shielding evaluations, the reactivity for the criticality evaluations, the decay heat load for the thermal evaluations, and the fuel weight for the structural evaluations. These bounding parameters are selected from the various spent fuel assemblies that are candidates for loading in the TSC. The bounding fuel assembly values are established based primarily on how the principal parameters are combined, and on the loading conditions or restrictions established for a group of fuel assemblies based on its parameters. Each TSC may contain up to 87 undamaged BWR fuel assemblies. To increase allowed assembly enrichments

over those determined for the 87-assembly basket configuration, an optional 82-assembly loading pattern may be used. The required fuel assembly locations in the 82-assembly pattern are shown in Figure 1.3-5.

The limiting parameters of the BWR fuel assemblies authorized for loading in the TSC are shown in Table 1.3-19. The maximum initial enrichment represents the peak planar-average enrichment. The BWR fuel assembly characteristics are summarized by fuel type in Chapter 6. Table 1.3-19 assembly physical information is limited to the critical analysis input of fuel mass, array configuration, and number of fuel rods. These analysis values are key inputs to the shielding and criticality evaluations in Chapters 5 and 6. Lattice parameters dictating system reactivity are detailed in Chapter 6. Enrichment limits are set for each fuel type to produce reactivities at the USL. The maximum decay heat load per TSC for the transport of BWR fuel assemblies is 22.0 kW (0.253 kW/assembly). Only uniform loading is permitted for BWR fuel assemblies. The bounding thermal evaluations are based on the GE 10×10 fuel assembly. The minimum cooling times are determined based on the maximum decay heat load of the contents and meeting transport dose limits.

BWR fuel assemblies may contain partial-length fuel rods. Table 1.3-20 contains the type of BWR assemblies and the number of partial-length rods included in the analysis in this SAR. Locations for the partial-length rods within the lattice are illustrated in Figure 1.3-8.

A bounding BWR fuel assembly weight of 704 pounds based on the maximum weight of GE 7×7 and 8×8 assemblies with channels has been structurally evaluated in each storage location of the BWR basket as well as the two additional locations coinciding with the drain and vent ports, equaling a total contents weight of 62,656 lbs. The analyzed contents weight provides the most significant measure of the basket performance. Accordingly, a 5% increase in the maximum weight per fuel location of 739 lbs is permitted while maintaining a maximum contents weight consistent with the basket evaluation.

As noted in Table 1.3-19, the evaluation of BWR fuel envelops unchanneled assemblies and assemblies with channels up to 120 mils thick.

GTCC Waste

The GTCC waste to be transported in the MAGNATRAN transport cask consists of sections of core baffle plates and angles, baffle formers, lower core plates and miscellaneous related hardware associated with these components. The major components are cut into pieces of a size that are loaded into a GTCC waste basket liner. Small residual pieces of GTCC may be loaded into stainless steel strainer baskets for handling. The loaded strainer baskets are stacked in a stainless steel pipe cell that has been placed in the GTCC waste basket liner to retain spacing

prior to GTCC initial loading. Any dross material (fines and debris) generated by the cutting operations will be disposed of as low-level radioactive or GTCC waste.

Each GTCC waste basket liner may contain up to 55,000 pounds of GTCC waste including the weight of strainer baskets and pipe spacers. The GTCC waste basket liner is transported in a GTCC TSC with a welded closure lid. The GTCC waste basket liners have twelve 1.0-inch diameter holes in the bottom plate, and outer ring and middle supports under the bottom plate to facilitate free flow drainage from the liner. The GTCC TSC has a sump in the bottom plate, and the closure lid includes a drain tube assembly to enable draining and vacuum drying of the loaded TSC. Consequently, no hydrogen generation occurs as a result of residual water.

The radionuclide composition of the waste was determined based on radiochemical assay of samples and dose rate measurements. The isotope that primarily contributes to the radiological source term is ^{60}Co. The source terms applied in the evaluation of the GTCC waste are presented in Chapter 5 of this SAR.

Fuel and GTCC Content Limits

Spent fuel and GTCC waste shipments in the MAGNATRAN shall be subject to the following limits:

1. The maximum contents weight for the MAGNATRAN transport cask shall not exceed 106,000 pounds.
2. The design basis fuel characteristics shall be in accordance with Table 1.3-6 and Table 1.3-19.
3. The total decay heat of the cask cavity contents shall not exceed 23 kW for PWR fuel and 22 kW for BWR fuel. For GTCC waste content, the decay heat limit is 1.7 kW.
4. The total weight of the PWR fuel assemblies in the TSC, including standard nonfuel hardware and spacers (if used), shall not exceed 62,160 pounds.
5. The total weight of the PWR fuel assemblies in the DF PWR TSC, including standard nonfuel hardware and spacers (if used), shall not exceed 61,184 pounds.
6. The total weight of the BWR fuel assemblies in the TSC, including channels (if applicable), shall not exceed 62,656 pounds.
7. GTCC waste consists of solid, irradiated, and contaminated hardware provided the quantity of fissile material does not exceed a Type A quantity and does not exceed the mass limits of 10 CFR 71.15. The specific Curie content source of the GTCC shall be limited to a maximum of 2.7 Ci ^{60}Co/lb with a total ^{60}Co activity of 85,760 Ci at transport. The maximum allowed weight of this waste is 55,000 lbs.

8. Any number of MAGNATRAN casks may be shipped at one time by rail, ship, barge or heavy-haul vehicle with the exception of a PWR-DF basket with DFC which requires only one cask to be shipped at one time.
9. Radiation levels shall not exceed the requirements of 10 CFR 71.47 and 10 CFR 71.51 for a closed transport vehicle.
10. Surface contamination levels shall not exceed the requirements of 10 CFR 71.87(i)(1).
11. Cask contents transported in a TSC with a PWR fuel basket shall be uranium undamaged PWR fuel assemblies in accordance with the limiting values shown in Table 1.3-6 and Table 1.3-7 and shall meet the following specifications:
    a. Zirconium-based alloy cladding.
    b. Enrichment, post-irradiation cooling time and burnup credit load curves in accordance with Tables 1.3-6, 1.3-8 through 1.3-11, and Figure 1.3-6.
    c. Maximum assembly average burnup shall be ≤ 45,000 MWd/MTU. A fuel assembly with maximum assembly average burnup > 45,000 MWd/MTU shall be treated as damaged fuel and placed in a damaged fuel can for transport.
    d. Decay heat per fuel assembly: 622 watts (includes non-fuel hardware contribution)
    e. Nominal fresh fuel dimensions: assembly length (in.) ≤ 178.3
       assembly width (in.) ≤ 8.54
    f. Fuel assembly weight (lbs.): ≤ 1,765 (including nonfuel hardware and fuel spacers)
    g. Spent fuel contents shall be loaded in accordance with the loading tables in Chapter 5, Section 5.8.3, of this SAR.
    h. Quantity per TSC: up to 37 undamaged PWR fuel assemblies shown in Figure 1.3-6. Figure 1.3-6 indicates the fuel storage locations that shall be empty, at a minimum, when implementing the 36, 35 and 33 loading patterns for burnup credit purposes.
    i. Undamaged PWR fuel assemblies may contain nonfuel hardware (NFHW). Fuel assembly lattices not containing the nominal number of fuel rods specified in Table 1.3-7 must contain solid filler rods that displace a volume equal to, or greater than, that of the fuel rod that the filler rod replaces. Fuel assemblies may have stainless steel rods inserted to displace guide tube "dashpot" water. Nonfuel hardware cool times shall be in accordance with Tables 1.3-16 through 1.3-18. Alternatively, the ^{60}Co curie limits in Table 1.3-17 and Table 1.3-18 may be used to establish site-specific nonfuel hardware constraints. Note that fuel assemblies defined as CE14 and CE16 are not allowed to contain BPRA or TP type nonfuel hardware.
    j. Fuel spacers may be used in the TSCs to reduce axial gaps for the spent fuel assemblies and non-fuel hardware.

k. Unenriched and unirradiated (i.e., not inserted in-core) fuel assemblies are not authorized for loading. Unenriched axial blankets are permitted, provided that the nominal length of the blanket is not greater than six inches. An unenriched rod may be used as a replacement rod to return a fuel assembly to an undamaged condition.

l. Reactor control components (RCC) are restricted to fuel storage locations No. 11, 12, 13, 18, 19, 20, 25, 26 and 27 (Figure 1.3-6). Minimum RCC cool times are:

Minimum Cool Time (years)	Maximum Exposure (GWd/MTU)
10	180
14	270
20	360

Interpolation is not allowed between data points.

m. One Neutron Source or Neutron Source Assembly (NSA) is permitted to be loaded in a TSC in fuel storage locations No. 11, 12, 13, 18, 19, 20, 25, 26 or 27 (Figure 1.3-6). Neutron source assemblies may contain source rods attached to hardware similar in configuration to guide tube plug devices (thimble plugs) and burnable absorbers, in addition to containing burnable poison rodlets and/or thimble plug rodlets. For NSAs containing absorber rodlets, the BPRA cool time and burnup/exposure or hardware ^{60}Co curie limit listed in Table 1.3-17 are applied to the neutron sources. NSAs having only thimble plug rodlets require the thimble plug restriction in Table 1.3-18 to be applied. Combination NSAs, containing both thimble plug and burnable absorber rodlets must apply the more limiting of the two minimum cool time/curie limit. Fuel assemblies loaded with the NSAs must apply the additional cool times listed in Table 1.3-16. Fuel types indicated as CE14 and CE16 are not permitted to be loaded with NSAs.

n. Fuel assemblies may contain any number of unirradiated (i.e., not inserted in-core) nonfuel solid filler fuel replacement rods. Activated stainless steel rods are limited to five per assembly, one assembly per basket, at a maximum steel rod burnup/exposure of 32.5 GWd/MTU. Fuel assemblies with activated stainless steel rods must be cooled either a minimum of 21 years or the Section 5.3 loading table minimum cool time plus one year, whichever is greater.

o. Westinghouse fuel assemblies may contain a hafnium absorber assembly (HFRA) at a maximum burnup/exposure of 4.0 GWd/MTU and a minimum cool time of 16 years.

Fuel assemblies loaded with an HFRA must apply the additional cool times listed in Table 1.3-16.

p. Under-burned (assemblies with burnup less than that dictated by the burnup credit loading curve) Westinghouse 15×15 PWR fuel assemblies may be loaded provided that they include Ag-In-Cd full-length RCCAs and are loaded in the basket locations that RCCs are allowed (see item l for RCCA loading). Burnup must be greater than or equal to 12,000 MWd/MTU. Enrichment must be equal to or less than 4.05 wt. % ^{235}U. The basket must include absorber sheets with an effective ^{10}B areal density of 0.036 g/cm^2. For the loading of low burnup fuel, the RCCAs must be full length (i.e. spider component included). RCCA exposure must be equal to or less than 200,000 MWd/MTU. Any assemblies loaded without an RCCA inserted must meet the burnup credit loading curve for the applicable assembly loading profile.

12. Cask contents transported in a TSC with a DF Basket Assembly shall be uranium undamaged PWR fuel assemblies and damaged fuel (damaged PWR fuel assemblies or PWR fuel debris) in accordance with the limiting values shown in Table 1.3-6 and Table 1.3-7 and shall meet the following specifications:

a. Zirconium-based alloy cladding.

b. For the 33 non-DFC fuel locations in the DF Basket Assembly, enrichment, post-irradiation cooling time and burnup credit load curves in accordance with Tables 1.3-6, 1.3-12 through 1.3-15, and Figure 1.3-6 for a TSC with a DF Basket Assembly containing DFCs. For a TSC with a DF Basket Assembly that does not contain any DFCs, the enrichment, post-irradiation cooling time and burnup credit load curves in accordance with Tables 1.3-6, 1.3-8 through 1.3-11, and Figure 1.3-4 may be used for all fuel locations.

c. For the up to four DFC locations in a DF Basket Assembly containing damaged fuel, the damaged fuel shall have a minimum burnup of 5 GWd/MTU, a maximum enrichment of 4.05 wt % ^{235}U, and a minimum cool time of 15 years.

d. Maximum assembly average burnup shall be $\leq$ 45,000 MWd/MTU. A fuel assembly with maximum assembly average burnup > 45,000 MWd/MTU shall be treated as damaged fuel and placed in a damaged fuel can for transport.

e. Decay heat per fuel assembly: 622 watts (590.5 watts for burnup > 45,000 MWd/MTU includes non-fuel hardware contribution)

f. Nominal fresh fuel assembly: length (in.) $\leq$ 167.0

g. Nominal fresh fuel assembly: width (in.) $\leq$ 8.54

h. Fuel assembly weight (lbs.): $\leq$ 1,765 (including nonfuel hardware, DFCs and fuel spacers)

i. Spent fuel contents shall be loaded in accordance with the loading tables in Section 5.8.3 with additional cool time for damaged fuel found in Table 5.8-49 of this SAR. The additional cool time from Table 5.8-49 applies to all assemblies loaded in a damaged fuel TSC with damaged fuel. High burnup fuel is treated as damaged fuel and must apply the damaged fuel delta cool time as applicable.

j. Quantity per TSC: Up to a total of 37 undamaged PWR fuel assemblies, including up to four DFCs containing undamaged PWR fuel assemblies, damaged PWR fuel assemblies, and/or PWR fuel debris loaded in DFC location Nos. 4, 8, 30 and 34, as shown on Figure 1.3-4, for the DF Basket Assembly. Figure 1.3-6 indicates the fuel storage locations that shall be empty, at a minimum, when implementing the 36, 35 and 33 loading patterns for burnup credit purposes.

k. The contents of a DFC must be less than, or equivalent to, one undamaged PWR fuel assembly. PWR fuel assemblies loaded in a DFC shall not contain nonfuel hardware with the exception of instrument tube tie components, guide tube anchors or other similar devices, and steel inserts.

l. Undamaged PWR fuel assemblies not loaded in a DFC may contain nonfuel hardware consistent with Table 1.3-16. Fuel assembly lattices not containing the nominal number of fuel rods specified in Table 1.3-7 must contain solid filler rods that displace a volume equal to, or greater than, that of the fuel rod that the filler rod replaces. Fuel assemblies may have stainless steel rods inserted to displace guide tube "dashpot" water. Nonfuel hardware cool times shall be in accordance with Tables 1.3-16 through 1.3-18. Alternatively, the ^{60}Co curie limits in Tables 1.3-17 and 1.3-18 may be used to establish site-specific nonfuel hardware constraints. Note that fuel assemblies defined as CE14 and CE16 are not allowed to contain BPRA or TP type nonfuel hardware.

m. Fuel spacers may be used in the TSCs to reduce axial gaps for the spent fuel assemblies, non-fuel hardware or damaged fuel cans.

n. Unenriched and unirradiated (i.e., not inserted in-core) fuel assemblies are not authorized for loading. Unenriched axial blankets are permitted, provided that the nominal length of the blanket is not greater than six inches. An unenriched rod may be used as a replacement rod to return a fuel assembly to an undamaged condition.

o. Reactor control components (RCC) are restricted to fuel storage location Nos. 11, 12, 13, 18, 19, 20, 25, 26 and 27 (Figure 1.3-4). Minimum RCC cool times are:

Minimum Cool Time (years)	Maximum Exposure (GWd/MTU)
10	180
14	270
20	360

Interpolation is not allowed between data points.

p. One Neutron Source or Neutron Source Assembly (NSA) is permitted to be loaded in a TSC in fuel storage location Nos. 11, 12, 13, 18, 19, 20, 25, 26 or 27 (Figure 1.3-4). Neutron source assemblies may contain source rods attached to hardware similar in configuration to guide tube plug devices (thimble plugs) and burnable absorbers, in addition to containing burnable poison rodlets and/or thimble plug rodlets. For NSAs containing absorber rodlets, the BPRA cool time and burnup/exposure or hardware ^{60}Co curie limit listed in Table 1.3-17 are applied to the neutron sources. NSAs having only thimble plug rodlets require the thimble plug restriction in Table 1.3-18 to be applied. Combination NSAs, containing both thimble plug and burnable absorber rodlets must apply the more limiting of the two minimum cool time/curie limit. Fuel assemblies loaded with the NSAs must apply the additional cool times listed in Table 1.3-16. Fuel types indicated as CE14 and CE16 are not permitted to be loaded with NSAs.

q. Fuel assemblies may contain any number of unirradiated (i.e., not inserted in-core) nonfuel solid filler fuel replacement rods. Activated stainless steel rods are limited to five per assembly, one assembly per basket, at a maximum steel rod burnup/exposure of 32.5 GWd/MTU. Fuel assemblies with activated stainless steel rods must be cooled either a minimum of 21 years or the item 12.i indicated minimum cool time plus one year, whichever is greater.

r. Westinghouse fuel assemblies may contain a hafnium absorber assembly (HFRA) at a maximum burnup/exposure of 4.0 GWd/MTU and a minimum cool time of 16 years. Fuel assemblies loaded with an HFRA must apply the additional cool times listed in Table 1.3-16.

s. Under-burned (assemblies with burnup less than that dictated by the burnup credit loading curve) Westinghouse 15×15 PWR fuel assemblies may be loaded provided that they include Ag-In-Cd full-length RCCAs and are loaded in the basket locations that RCCs are allowed (see item o for RCCA loading). Burnup must be greater than or equal to 12,000 MWd/MTU. Enrichment must be equal to or less than 4.05 wt. % ^{235}U. The basket must include absorber sheets with an effective ^{10}B areal density of 0.036 g/cm^2.

For the loading of low burnup fuel, the RCCAs must be full length (i.e. spider component included). RCCA exposure must be equal to or less than 200,000 MWd/MTU. Any assemblies loaded without an RCCA inserted must meet the burnup credit loading curve for the applicable assembly loading profile.

t. Damaged CE 16×16 fuel assemblies are not to be loaded in the MAGNATRAN system.

13. Cask contents transported in a TSC with a BWR fuel basket shall be uranium undamaged BWR fuel assemblies in accordance with the limiting values shown in Table 1.3-19 and Table 1.3-20 and shall meet the following specifications:

a. Zirconium-based alloy cladding.

b. Enrichment, post-irradiation cooling time and average assembly burnup in accordance with Tables 1.3-19, 1.3-21, and 1.3.-22 and Figures 1.3-5, 1.3-7 and 1.3-8.

c. Decay heat per fuel assembly: uniform loading 253 watts

d. Nominal fresh fuel dimensions: assembly length (in.) $\leq$ 176.2

e. Assembly width (in.) $\leq$ 5.52

f. Fuel assembly weight (lbs.) $\leq$ 739 lbs (including channel and fuel spacers) with a maximum contents weight of 62,656 lbs.

g. Spent fuel contents shall be loaded in accordance with the loading tables in Chapter 5, Section 5.8.4, of this SAR.

h. Quantity per TSC: up to 87 undamaged BWR fuel assemblies as shown in Figure 1.3-7.

i. Allowable fuel assembly locations for the 82-assembly BWR fuel basket configurations are shown in Figure 1.3-5 (location numbering for the 82-assembly basket is the same as that shown for the 87-assembly basket in Figure 1.3-7).

j. Prior to use of the 82-assembly configuration, the center cell weldment and upper weldments with blocking strap must be in place to physically block the designated nonfuel locations (shown in Figure 1.3-5). Less than 82 assemblies may be loaded when implementing the 82-Assembly configuration provided the required fuel storage locations are empty, at a minimum.

k. BWR fuel assemblies may be unchanneled, or channeled with zirconium-based alloy channels.

l. BWR fuel assemblies with stainless steel channels are not authorized.

m. Fuel assembly lattices not containing the assembly type-specific nominal number of fuel rods specified in Table 1.3-20 must contain solid, unirradiated, filler rods that displace a volume equal to, or greater than, that of the fuel rod that the filler rod replaces

n. Spacers may be used in the TSCs to fill axial gaps and provide support for the spent fuel assemblies.

o. Unenriched and unirradiated (i.e., not inserted in-core) fuel assemblies are not authorized for loading. Unenriched axial blankets are permitted, provided that the nominal length of the blanket is not greater than six inches.

Figure 1.3-4 Schematic of DF Basket Assembly Configuration for PWR Fuel with Damaged Fuel Can Locations

[redacted]

Figure 1.3-5 Schematic of 82-Assembly BWR Basket Pattern

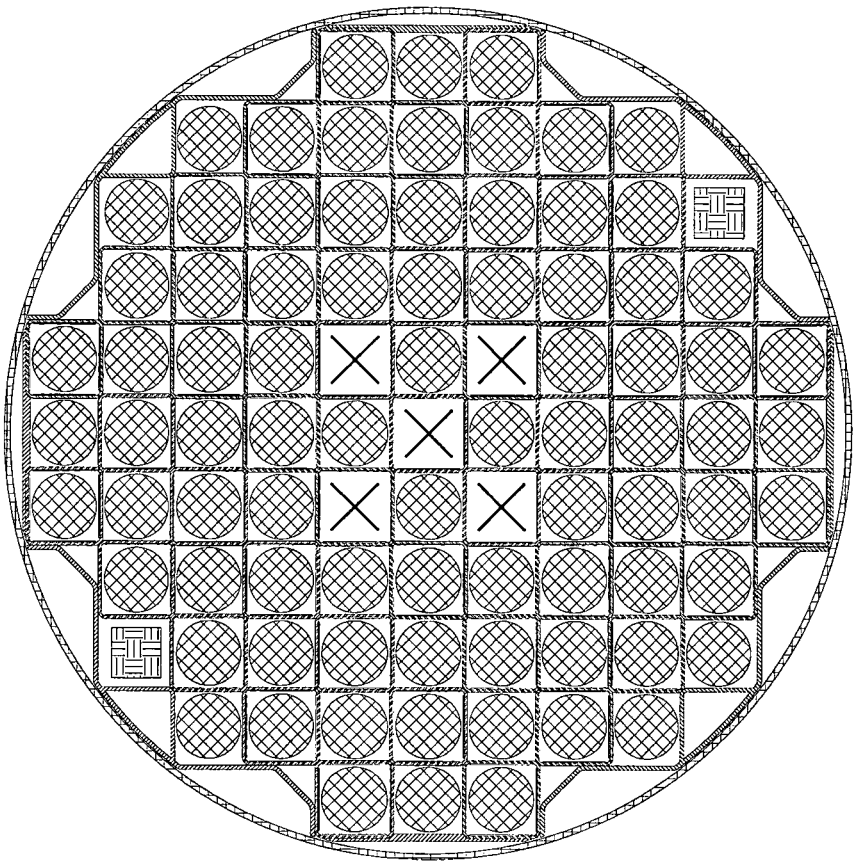

= Fuel Assembly Locations

= Vent/Drain Port Locations

= Designated Nonfuel Locations

Figure 1.3-6 Schematic of 37-Assembly PWR Basket (33-, 35 and 36-Assembly Configuration Included)

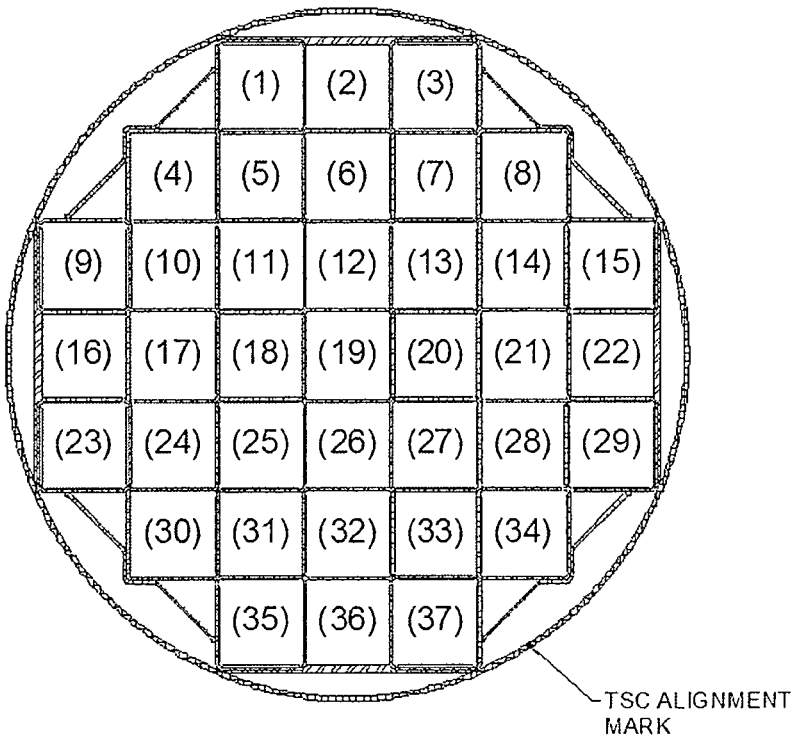

36 assembly loading: remove 19

35 assembly loading: remove 19, 18

33 assembly loading: remove 19, 18, 20, 12

Note: The 33 and 36-Assembly patterns also apply to the DF basket.

Figure 1.3-7 Schematic of 87-Assembly BWR Basket

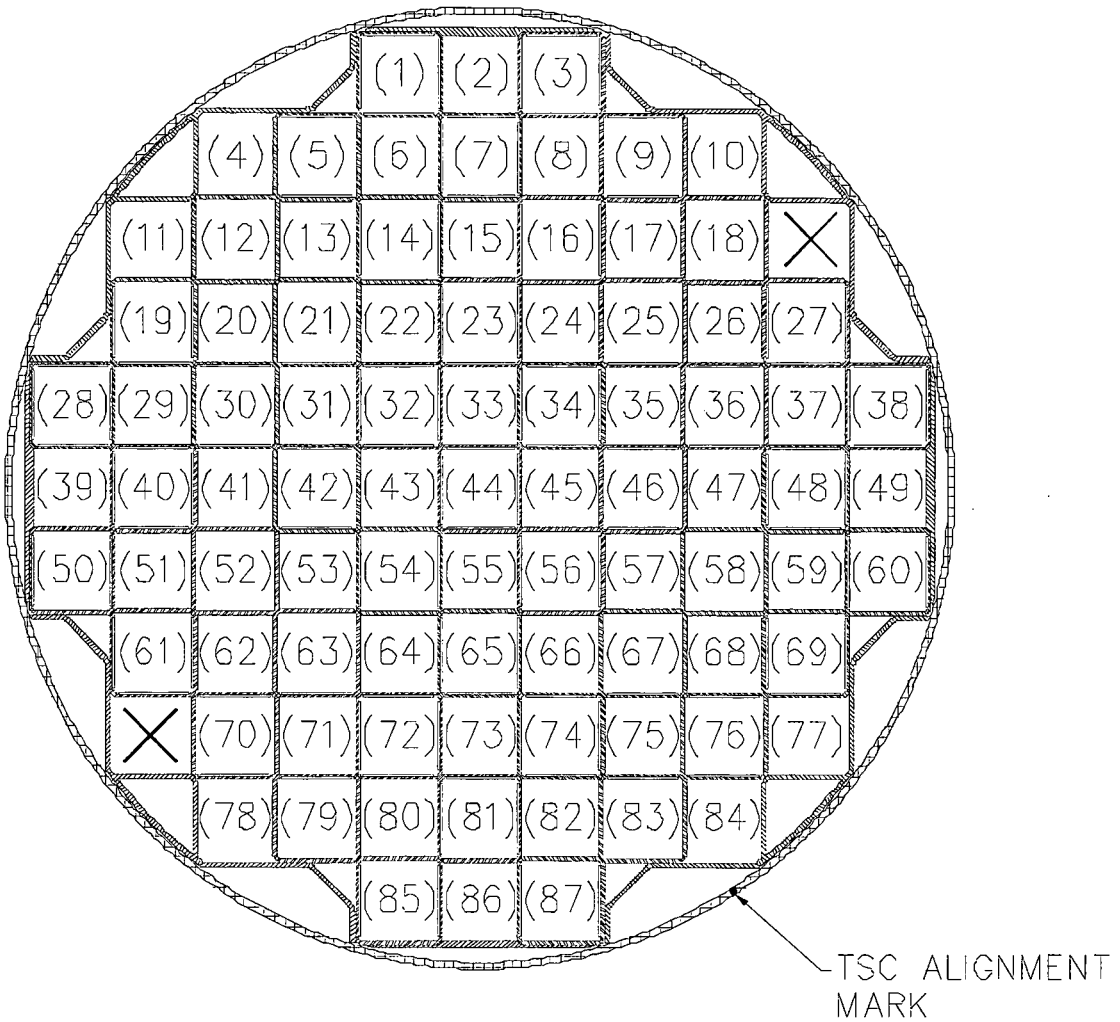

Note: Location numbering is identical for 82 and 87-Assembly Baskets.

Figure 1.3-8 BWR Partial Length Fuel Rod Location Sketches

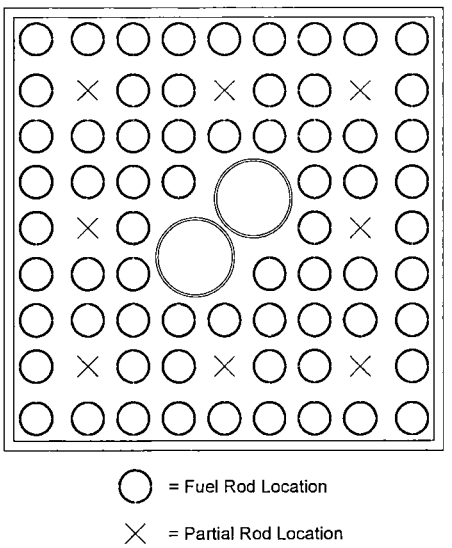

B9_74A 8 Partial Length Rods

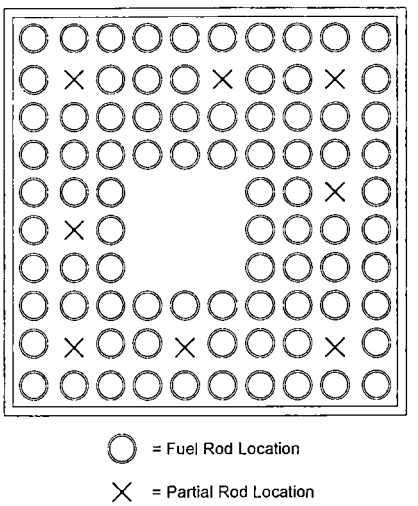

B10_91A 8 Partial Length Rods

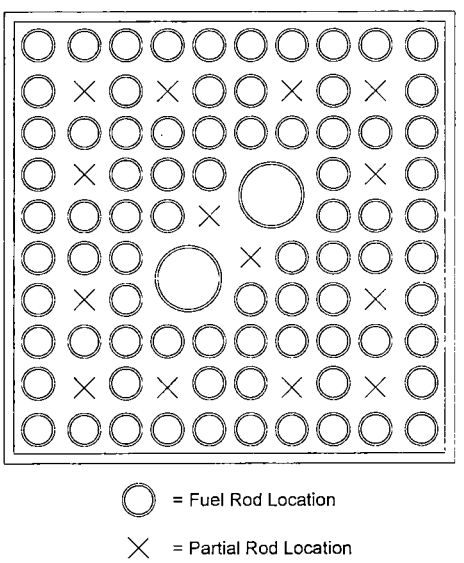

B10_92A 14 Partial Length Rods

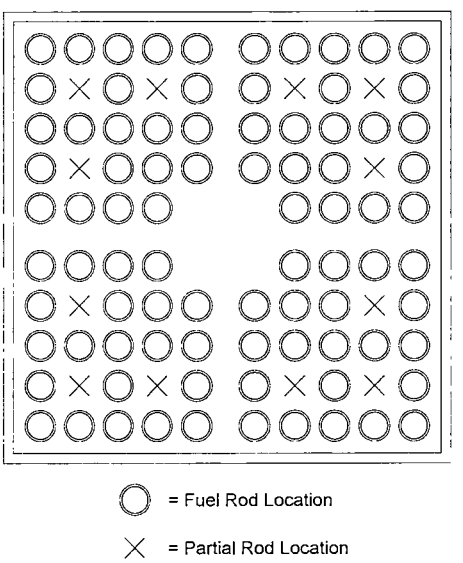

B10_96A 12 Partial Length Rods

Table 1.3-6 PWR Fuel Assembly Characteristics

Characteristic	Fuel Class					
	14×14	14×14	15×15	15×15	16×16	17×17
Base Fuel Type[a]	CE, SPC	W, SPC	W, SPC	BW, FCF	CE	BW, SPC, W, FCF
Max Initial Enrichment (wt% ^{235}U)	5.0	5.0	5.0	5.0	5.0	5.0
Min Initial Enrichment (wt% ^{235}U)	1.3	1.3	1.3	1.3	1.3	1.3
Number of Fuel Rods	176	179	204	208	236	264
Max Assembly Average Burnup (MWd/MTU)	60,000	60,000	60,000	60,000	60,000	60,000
Min Cool Time (years)	4	4	4	4	4	4
Max Weight (lb) per Storage Location	See Note 1	See Note 1	See Note 1	See Note 1	See Note 1	See Note 1
Max Decay Heat (Watts) per Fuel Location	622	622	622	622	622	622

- Fuel cladding is a zirconium-based alloy.
- All reported enrichment values are nominal preirradiation fabrication values.
- Weight includes the weight of nonfuel-bearing components.
- Assemblies may contain nonfuel hardware and/or fuel replacement rods (also referred to as filler rods). Filler rods are considered to be a component of spent nuclear fuel assemblies and not nonfuel hardware. Filler rods may be burnable absorber rods, stainless steel rods or zirconium alloy rods.
- PWR fuel is loaded using burnup credit. Maximum enrichment is as a function of minimum burnup as specified in Chapter 6. Maximum initial enrichment represents the peak fuel rod enrichment for variably-enriched fuel assemblies.
- Spacers may be used to axially position fuel assemblies to facilitate handling.
- Maximum uniform heat load is 622 watts per storage location.
- All fuel with burnup > 45,000 MWd/MTU is placed into Damaged Fuel Cans (DFC).

Notes:

1. Maximum weight per storage location is 1,765 lbs (including nonfuel hardware, DFCs and fuel spacers) with a maximum contents weight of 62,160 lbs for the PWR basket and 61,184 lbs for the DF basket.

[a] Indicates assembly and/or nuclear steam supply system (NSSS) vendor/type referenced for fuel input data. Fuel acceptability for loading is not restricted to the indicated vendor provided that the fuel assembly meets the load limits. Abbreviations are as follows: Westinghouse (W), Combustion Engineering (CE), Siemens Power Corporation (SPC), Babcock and Wilcox (BW), and Framatome Cogema Fuels (FCF).

Table 1.3-7 Bounding PWR Fuel Assembly Geometry for Loading Criteria

Assembly Type	No. of Fuel Rods	No. of Guide Tubes[1]	Geometry[2]					
			Max Pitch (inch)	Min Clad OD (inch)	Min Clad Thick. (inch)	Max Pellet OD (inch)	Max Active Length (inch)	Max Load (MTU)
BW15H1	208	17	0.568	0.43	0.0265	0.3686	144.0	0.4807
BW15H2	208	17	0.568	0.43	0.025	0.3735	144.0	0.4807
BW15H3	208	17	0.568	0.428	0.023	0.3742	144.0	0.4807
BW15H4	208	17	0.568	0.414	0.022	0.3622	144.0	0.4690
BW17H1	264	25	0.502	0.377	0.022	0.3252	144.0	0.4681
CE14H1	176	5	0.58	0.44	0.026	0.3805	137.0	0.4115
CE16H1	236	5	0.5063	0.382	0.025	0.325	150.0	0.4463
WE14H1	179	17	0.556	0.40	0.0162	0.3674	145.2	0.4144
WE15H1	204	21	0.563	0.422	0.0242	0.3669	144.0	0.4671
WE15H2	204	21	0.563	0.417	0.0265	0.357	144.0	0.4469
WE17H1	264	25	0.496	0.372	0.0205	0.3232	144.0	0.4671
WE17H2	264	25	0.496	0.36	0.0225	0.3088	144.0	0.4327

[1] Combined number of guide and instrument tubes.

[2] Assembly characteristics represent cold, unirradiated, nominal configurations.

Table 1.3-8 Maximum Initial Enrichment – 37-Assembly Undamaged Fuel Configuration – 0.036 g/cm^2 ^{10}B Absorber

Assembly ID	Zero (0) Burnup Max. Enr. (wt %)	Max Initial Enrichment (wt % ^{235}U) = C_4 × Burnup (GWd/MTU) + C_5					
		Burnup (GWd/MTU) < 18		18 ≤ Burnup (GWd/MTU) ≤ 30		Burnup (GWd/MTU) > 30	
		C_4	C_5	C_4	C_5	C_4	C_5
BW 15×15	1.9	0.0501	1.69	0.0693	1.65	0.0748	1.60
BW 17×17	1.9	0.0502	1.72	0.0687	1.70	0.0742	1.66
CE 14×14	2.1	0.0473	2.04	0.0675	2.03	0.0759	1.93
CE 16×16	2.1	0.0464	2.03	0.0657	2.06	0.0733	1.99
WE 14×14	2.2	0.0496	2.08	0.0672	2.21	0.0725	2.29
WE 15×15	1.9	0.0494	1.74	0.0683	1.72	0.0742	1.67
WE 17×17	1.9	0.0494	1.71	0.0685	1.68	0.0749	1.61

Table 1.3-9 Maximum Initial enrichment – 37-Assembly Undamaged Fuel Configuration – 0.030 g/cm^2 ^{10}B Absorber

Assembly ID	Zero (0) Burnup Max. Enr. (wt %)	Max Initial Enrichment (wt % ^{235}U) = C_4 × Burnup (GWd/MTU) + C_5					
		Burnup (GWd/MTU) < 18		18 ≤ Burnup (GWd/MTU) ≤ 30		Burnup (GWd/MTU) > 30	
		C_4	C_5	C_4	C_5	C_4	C_5
BW 15×15	1.8	0.0507	1.61	0.0687	1.59	0.0745	1.48
BW 17×17	1.9	0.0503	1.66	0.0683	1.63	0.0733	1.59
CE 14×14	2.1	0.0468	1.95	0.0664	1.97	0.0738	1.90
CE 16×16	2.1	0.0470	1.95	0.0649	1.99	0.0727	1.90
WE 14×14	2.1	0.0492	2.03	0.0680	2.10	0.0728	2.19
WE 15×15	1.9	0.0503	1.67	0.0675	1.66	0.0747	1.54
WE 17×17	1.9	0.0494	1.64	0.0685	1.58	0.0737	1.53

Table 1.3-10 Maximum Initial Enrichment – 37-Assembly Undamaged Fuel Configuration – 0.027 g/cm^2 ^{10}B Absorber

Assembly ID	Zero (0) Burnup Max. Enr. (wt %)	Max Initial Enrichment (wt % ^{235}U) = C_4 × Burnup (GWd/MTU) + C_5					
		Burnup (GWd/MTU) < 18		18 ≤ Burnup (GWd/MTU) ≤ 30		Burnup (GWd/MTU) > 30	
		C_4	C_5	C_4	C_5	C_4	C_5
BW 15×15	1.8	0.0508	1.58	0.0686	1.52	0.0754	1.41
BW 17×17	1.8	0.0503	1.62	0.0683	1.59	0.0748	1.47
CE 14×14	2.1	0.0471	1.92	0.0666	1.92	0.0729	1.87
CE 16×16	2.1	0.0462	1.93	0.0657	1.92	0.0747	1.75
WE 14×14	2.1	0.0499	1.98	0.0667	2.10	0.0743	2.07
WE 15×15	1.9	0.0503	1.63	0.0677	1.60	0.0749	1.46
WE 17×17	1.9	0.0497	1.60	0.0683	1.54	0.0749	1.41

Table 1.3-11 Maximum Initial Enrichment – Undamaged Fuel Configuration WE15 – Optional Configurations

# Assemblies	Zero (0) Burnup Maximum. Enrichment (wt % ^{235}U)	Max Initial Enrichment (wt % ^{235}U) = C_4 × Burnup (GWd/MTU) + C_5					
		Burnup (GWd/MTU) < 18		18 ≤ Burnup (GWd/MTU) ≤ 30		Burnup (GWd/MTU) > 30	
		C_4	C_5	C_4	C_5	C_4	C_5
0.036 g/cm² ^{10}B Absorber							
36	2.0	0.0497	1.93	0.0681	1.99	0.0747	2.00
35	2.1	0.0507	1.97	0.0673	2.08	0.0730	2.12
33	2.2	0.0504	2.12	0.0664	2.29	0.0745	2.32
0.030 g/cm² ^{10}B Absorber							
36	2.0	0.0494	1.87	0.0687	1.90	0.0737	1.93
35	2.0	0.0499	1.92	0.0688	1.97	0.0740	1.99
33	2.1	0.0497	2.06	0.0686	2.15	0.0724	2.29
0.027 g/cm² ^{10}B Absorber							
36	2.0	0.0501	1.83	0.0677	1.87	0.0741	1.84
35	2.0	0.0494	1.89	0.0675	1.94	0.0735	1.96
33	2.1	0.0492	2.03	0.0674	2.12	0.0730	2.21

Table 1.3-12 Required Burnup – PWR Damaged Fuel Configuration – 0.036 g/cm² ^{10}B Absorber

Assembly ID	Zero (0) Burnup Max. Enr. (wt %)	Max Initial Enrichment (wt % ^{235}U) = C_4 × Burnup (GWd/MTU) + C_5							
		Burnup (GWd/MTU) < 18		18 ≤ Burnup (GWd/MTU) ≤ 30		30 < Burnup (GWd/MTU) ≤ 50		50 < Burnup (GWd/MTU)	
		C_4	C_5	C_4	C_5	C_4	C_5	C_4	C_5
BW 15×15	1.6	0.0453	1.42	0.0681	1.29	0.0750	1.03	0.0750	0.736
BW 17×17	1.6	0.0476	1.45	0.0668	1.37	0.0712	1.17	0.0712	0.891
CE 14×14	1.9	0.0504	1.79	0.0696	1.75	0.0751	1.60	0.0751	1.60
CE 16×16	1.9	0.0484	1.79	0.0679	1.74	0.0758	1.52	0.0758	1.52
WE 14×14	1.9	0.0542	1.85	0.0729	1.85	0.0794	1.75	0.0794	1.75
WE 15×15	1.6	0.0482	1.43	0.0692	1.27	0.0738	1.08	0.0738	0.767
WE 17×17	1.6	0.0439	1.45	0.0657	1.35	0.0732	1.00	0.0732	0.700

Table 1.3-13 Maximum Initial Enrichment – PWR Damaged Fuel Configuration – 0.030 g/cm² ^{10}B Absorber

Assembly ID	Zero (0) Burnup Max. Enr. (wt %)	Max Initial Enrichment (wt % ^{235}U) = C_4 × Burnup (GWd/MTU) + C_5							
		Burnup (GWd/MTU) < 18		18 ≤ Burnup (GWd/MTU) ≤ 30		30 < Burnup (GWd/MTU) ≤ 50		50 < Burnup (GWd/MTU)	
		C_4	C_5	C_4	C_5	C_4	C_5	C_4	C_5
BW 15×15	1.5	0.0487	1.31	0.0660	1.26	0.0740	0.896	0.0740	0.614
BW 17×17	1.5	0.0470	1.37	0.0673	1.29	0.0745	0.937	0.0745	0.655
CE 14×14	1.8	0.0494	1.71	0.0705	1.64	0.0781	1.37	0.0781	1.37
CE 16×16	1.8	0.0489	1.71	0.0679	1.68	0.0724	1.52	0.0724	1.52
WE 14×14	1.9	0.0533	1.82	0.0725	1.76	0.0821	1.50	0.0821	1.50
WE 15×15	1.6	0.0475	1.35	0.0661	1.29	0.0746	0.859	0.0746	0.575
WE 17×17	1.6	0.0448	1.38	0.0646	1.26	0.0710	0.968	0.0710	0.691

Table 1.3-14 Maximum Initial Enrichment – PWR Damaged Fuel Configuration – 0.027 g/cm² ^{10}B Absorber

Assembly ID	Zero (0) Burnup Max. Enr. (wt %)	Max Initial Enrichment (wt % ^{235}U) = C_4 × Burnup (GWd/MTU) + C_5							
		Burnup (GWd/MTU) < 18		18 ≤ Burnup (GWd/MTU) ≤ 30		30 < Burnup (GWd/MTU) ≤ 50		50 < Burnup (GWd/MTU)	
		C_4	C_5	C_4	C_5	C_4	C_5	C_4	C_5
BW 15×15	1.5	0.0471	1.30	0.0666	1.19	0.0725	0.857	0.0725	0.581
BW 17×17	1.5	0.0474	1.36	0.0652	1.27	0.0724	0.918	0.0724	0.639
CE 14×14	1.8	0.0486	1.68	0.0696	1.61	0.0778	1.32	0.0778	1.32
CE 16×16	1.8	0.0493	1.66	0.0660	1.64	0.0761	1.33	0.0761	1.33
WE 14×14	1.8	0.0535	1.71	0.0694	1.75	0.0805	1.52	0.0805	1.52
WE 15×15	1.5	0.0465	1.33	0.0664	1.24	0.0710	0.968	0.0710	0.685
WE 17×17	1.5	0.0447	1.31	0.0647	1.25	0.0714	0.846	0.0714	0.564

Table 1.3-15 Maximum Initial Enrichment – Damaged Fuel Configuration WE15 – Optional Configurations

# of Assemblies	Zero (0) Burnup Max. Enr. (wt %)	Max Initial Enrichment (wt % ^{235}U) = C_4 × Burnup (GWd/MTU) + C_5							
		Burnup (GWd/MTU) < 18		18 ≤ Burnup (GWd/MTU) ≤ 30		30 < Burnup (GWd/MTU) ≤ 50		50 < Burnup (GWd/MTU)	
		C_4	C_5	C_4	C_5	C_4	C_5	C_4	C_5
0.036 g/cm² ^{10}B Absorber									
36	1.6	0.0483	1.53	0.0721	1.35	0.0750	1.17	0.0750	0.851
35	1.7	0.0532	1.51	0.0722	1.45	0.0778	1.14	0.0778	1.14
33	1.7	0.0524	1.60	0.0734	1.52	0.0791	1.22	0.0791	1.22
0.030 g/cm² ^{10}B Absorber									
36	1.6	0.0483	1.48	0.0707	1.32	0.0739	1.15	0.0739	0.811
35	1.6	0.0499	1.48	0.0722	1.34	0.0733	1.20	0.0733	0.847
33	1.7	0.0523	1.52	0.0728	1.40	0.0780	1.19	0.0780	1.19
0.027 g/cm² ^{10}B Absorber									
36	1.6	0.0473	1.42	0.0668	1.33	0.0731	1.02	0.0731	0.693
35	1.6	0.0477	1.46	0.0736	1.27	0.0738	1.13	0.0738	0.775
33	1.7	0.0491	1.51	0.0718	1.41	0.0784	1.09	0.0784	1.09

Table 1.3-16 Additional Fuel Assembly Cool Time Required to Load Nonfuel Hardware

Core (Assembly)	Additional Cool Time (years)			
	BPAA/HFRA	GTPD/NSA	RCC	NSA
CE 14×14	--	--	0.4	--
WE 14×14	1.1	0.1	0.3	1.1
WE 15×15	1.3	0.1	6.9	1.3
B&W 15×15	0.1	0.2	0.3	0.2
CE 16×16	--	--	0.4	--
WE 17×17	1.4	0.2	6.7	1.4
B&W 17×17	0.1	0.2	0.3	0.2

Note: Additional fuel assembly cooling time to be added to the minimum fuel assembly cool time based on fuel assembly initial enrichment and fuel assembly average burnup listed in the loading tables in Chapter 5.

Table 1.3-17 Allowed BPRA Burnup and Cool Time Combinations

Limiting Basis	Fuel Assembly				
	WE 14×14	WE 15×15	B&W 15×15	WE 17×17	B&W 17×17
Min. Cool Time (yr) for Exposure ≤ 70 GWd/MTU	8.0	8.0	8.0	8.0	8.0
Max ^{60}Co Activity (Ci)	704	901	26	894	27

Note: Specified minimum cool times for BPRAs are independent of the required minimum cool times for the fuel assembly containing the BPRA.

Table 1.3-18 Allowed GTPD Burnup and Cool Time Combinations

Limiting Basis	Fuel Assembly				
	WE 14×14	WE 15×15	B&W 15×15	WE 17×17	B&W 17×17
Min. Cool Time (yr) for Exposure ≤ 180 GWd/MTU	8.0	8.0	8.0	8.0	8.0
Max ^{60}Co Activity (Ci)	60.5	73.1	99.2	93.3	107.8

Note: Specified minimum cool times for thimble plugs are independent of the required minimum cool times for the fuel assembly containing the thimble plug.

Table 1.3-19 BWR Fuel Assembly Characteristics

Characteristic	Fuel Class			
	7×7	8×8	9×9	10×10
Base Fuel Type[a]	SPC, GE	SPC, GE	SPC, GE	SPC, GE, ABB
Max Initial Enrichment (wt% ^{235}U)	4.5	4.5	4.5	4.5
Number of Fuel Rods	48 49	59 60 61 62 63 64[b]	72 74[c] 76 79 80	91[c] 92[c] 96[c,d] 100[d]
Max Assembly Average Burnup (MWd/MTU)	45,000	45,000	45,000	45,000
Min Cool Time (years)	4	4	4	4
Min Average Enrichment (wt% ^{235}U)	1.3	1.3	1.3	1.3
Max Weight (lb) per Storage Location	See Note 1	See Note 1	See Note 1	See Note 1
Max Decay Heat (Watts) per Fuel Location	253	253	253	253

- Each BWR fuel assembly may have a zirconium-based alloy channel ≤ 120 mil thick.
- Assembly weight includes the weight of the channel.
- Maximum initial enrichment is the peak planar-average enrichment.
- Water rods may occupy more than one fuel lattice location. Fuel assembly to contain nominal number of water rods for the specific assembly design.
- All enrichment values are nominal pre-irradiation fabrication values.
- Spacers may be used to axially position fuel assemblies to facilitate handling.

Notes:

1. Maximum weight per storage location is 739 lbs (including fuel spacers) with a maximum contents weight of 62,656 lbs.

[a] Indicates assembly vendor/type referenced for fuel input data. Fuel acceptability for loading is not restricted to the indicated vendor/type provided that the fuel assembly meets the limits listed in Table 6..2.1-1. Table 6.2.1-2 contains vendor information by fuel rod array. Abbreviations are as follows: General Electric/Global Nuclear Fuels (GE), Exxon/Advanced Nuclear Fuels/Siemens Power Corporation (SPC).
[b] May be composed of four subchannel clusters.
[c] Assemblies may contain partial-length fuel rods.
[d] Composed of four subchannel clusters.

Table 1.3-20 BWR Fuel Assembly Loading Criteria

		Geometry[3,4]						
Assembly Type	Number of Fuel Rods	Number of Partial Length Rods[1]	Max Pitch (inch)	Min Clad OD (inch)	Min Clad Thick. (inch)	Max Pellet OD (inch)	Max Active Length (inch)	Max Loading (MTU)
B7_48A	48	N/A	0.7380	0.5700	0.03600	0.4900	144.0	0.1981
B7_49A	49	N/A	0.7380	0.5630	0.03200	0.4880	146.0	0.2034
B7_49B	49	N/A	0.7380	0.5630	0.03200	0.4910	150.0	0.2037
B8_59A	59	N/A	0.6400	0.4930	0.03400	0.4160	150.0	0.1828
B8_60A	60	N/A	0.6417	0.4840	0.03150	0.4110	150.0	0.1815
B8_60B	60	N/A	0.6400	0.4830	0.03000	0.4140	150.0	0.1841
B8_61B	61	N/A	0.6400	0.4830	0.03000	0.4140	150.0	0.1872
B8_62A	62	N/A	0.6417	0.4830	0.02900	0.4160	150.0	0.1921
B8_63A	63	N/A	0.6420	0.4840	0.02725	0.4195	150.0	0.1985
B8_64A	64	N/A	0.6420	0.4840	0.02725	0.4195	150.0	0.1996
B8_64B[5]	64	N/A	0.6090	0.4576	0.02900	0.3913	150.0	0.1755
B9_72A	72	N/A	0.5720	0.4330	0.02600	0.3740	150.0	0.1803
B9_74A	74[2]	8	0.5720	0.4240	0.02390	0.3760	150.0	0.1873
B9_76A	76	N/A	0.5720	0.4170	0.02090	0.3750	150.0	0.1914
B9_79A	79	N/A	0.5720	0.4240	0.02390	0.3760	150.0	0.1979
B9_80A	80	N/A	0.5720	0.4230	0.02950	0.3565	150.0	0.1821
B10_91A	91[2]	8	0.5100	0.3957	0.02385	0.3420	150.0	0.1906
B10_92A	92[2]	14	0.5100	0.4040	0.02600	0.3455	150.0	0.1946
B10_96A[5]	96[2]	12	0.4880	0.3780	0.02430	0.3224	150.0	0.1787
B10_100A[5]	100	N/A	0.4880	0.3780	0.02430	0.3224	150.0	0.1861

1 Location of the partial length rods is illustrated in Figure 1.3-8.
2 Assemblies may contain partial-length fuel rods.
3 Assembly characteristics represent cold, unirradiated, nominal configurations.
4 Maximum channel thickness allowed is 120 mils (nominal).
5 Composed of four subchannel clusters.

Table 1.3-21 BWR Fuel Assembly Loading Criteria – Enrichment Limits for 87-Assembly and 82-Assembly Configurations with Axial Blanket

	Max. Initial Enrichment[a] (wt % ^{235}U)					
	Absorber[b] 0.027 ^{10}B g/cm^2		Absorber[b] 0.0225 ^{10}B g/cm^2		Absorber[b] 0.02 ^{10}B g/cm^2	
	87-Assy Basket	82-Assy Basket	87-Assy Basket	82-Assy Basket	87-Assy Basket	82-Assy Basket
B7_48A	4.0%	4.5%	3.7%	4.5%	3.6%	4.4%
B7_49A	3.8%	4.5%	3.6%	4.4%	3.5%	4.3%
B7_49B	3.8%	4.5%	3.6%	4.4%	3.5%	4.2%
B8_59A	3.9%	4.5%	3.7%	4.5%	3.6%	4.3%
B8_60A	3.8%	4.5%	3.7%	4.4%	3.5%	4.2%
B8_60B	3.8%	4.5%	3.6%	4.3%	3.5%	4.2%
B8_61B	3.8%	4.5%	3.6%	4.3%	3.5%	4.2%
B8_62A	3.8%	4.5%	3.6%	4.3%	3.5%	4.1%
B8_63A	3.8%	4.5%	3.6%	4.3%	3.4%	4.2%
B8_64A	3.8%	4.5%	3.6%	4.3%	3.5%	4.2%
B8_64B	3.6%	4.3%	3.4%	4.1%	3.3%	4.0%
B9_72A	3.8%	4.5%	3.6%	4.3%	3.4%	4.1%
B9_74A	3.7%	4.3%	3.4%	4.1%	3.4%	4.0%
B9_76A	3.5%	4.2%	3.4%	4.0%	3.3%	3.9%
B9_79A	3.7%	4.4%	3.4%	4.2%	3.3%	4.0%
B9_80A	3.8%	4.5%	3.6%	4.3%	3.5%	4.2%
B10_91A	3.7%	4.5%	3.6%	4.3%	3.5%	4.1%
B10_92A	3.8%	4.5%	3.6%	4.3%	3.5%	4.1%
B10_96A	3.7%	4.3%	3.5%	4.1%	3.4%	4.0%
B10_100A	3.6%	4.4%	3.5%	4.1%	3.4%	4.0%

[a] Maximum planar average.
[b] Borated aluminum neutron absorber sheet effective areal ^{10}B density.

Table 1.3-22 Undamaged BWR Fuel Assembly Loading Criteria (Enrichment Limits for Fuel Without Axial Blanket)

	Max. Initial Enrichment[a] (wt % ^{235}U)					
	Absorber[b] 0.027 ^{10}B g/cm^2		Absorber[b] 0.0225 ^{10}B g/cm^2		Absorber[b] 0.02 ^{10}B g/cm^2	
Fuel Type	87-Assy Basket	82-Assy Basket	87-Assy Basket	82-Assy Basket	87-Assy Basket	82-Assy Basket
B7_48A	3.9%	4.5%	3.7%	4.5%	3.6%	4.3%
B7_49A	3.7%	4.5%	3.6%	4.3%	3.4%	4.1%
B7_49B	3.7%	4.5%	3.6%	4.3%	3.5%	4.2%
B8_59A	3.8%	4.5%	3.7%	4.4%	3.5%	4.3%
B8_60A	3.7%	4.5%	3.6%	4.3%	3.5%	4.1%
B8_60B	3.7%	4.4%	3.5%	4.2%	3.4%	4.1%
B8_61B	3.7%	4.5%	3.6%	4.3%	3.5%	4.1%
B8_62A	3.6%	4.4%	3.5%	4.2%	3.4%	4.1%
B8_63A	3.7%	4.4%	3.5%	4.2%	3.4%	4.1%
B8_64A	3.7%	4.5%	3.5%	4.3%	3.4%	4.1%
B8_64B	3.6%	4.2%	3.4%	4.1%	3.3%	4.0%
B9_72A	3.7%	4.4%	3.5%	4.2%	3.4%	4.1%
B9_74A	3.6%	4.2%	3.4%	4.1%	3.3%	4.0%
B9_76A	3.5%	4.1%	3.3%	4.0%	3.2%	3.8%
B9_79A	3.5%	4.2%	3.4%	4.1%	3.2%	3.9%
B9_80A	3.7%	4.5%	3.6%	4.3%	3.5%	4.1%
B10_91A	3.7%	4.4%	3.5%	4.2%	3.4%	4.1%
B10_92A	3.7%	4.4%	3.6%	4.2%	3.4%	4.1%
B10_96A	3.6%	4.2%	3.4%	4.1%	3.4%	4.0%
B10_100A	3.6%	4.3%	3.4%	4.0%	3.3%	3.9%

[a] Maximum planar average.
[b] Borated aluminum neutron absorber sheet effective areal ^{10}B density.

1.3.3 Special Requirements for Plutonium

All shipments containing plutonium must be made with the contents in solid form, if the contents contain greater than 0.74 TBq (20 Ci) of plutonium.

1.3.4 Operational Features

The MAGNATRAN is designed for easy loading, unloading and handling at a nuclear facility. Cask loading and unloading operations are accomplished dry using a transfer cask to handle the TSC containing the fuel or GTCC waste. Detailed operating procedures are presented in Chapter 7.

The cask lid and the port cover are one-piece components designed to reduce handling times and to maintain personnel dose rates at levels that are as low as is reasonably achievable (ALARA). For improved handling operations, a quick-disconnect fitting is used in the lid port. All operational features are shown on the License Drawings provided in Section 1.4-3.

1.4.3 License Drawings

This section presents the list of License Drawings for MAGNATRAN.

Drawing Number	Title	Revision No.
71160-500	Shipping Configuration, Transport Cask, MAGNATRAN	1NP
71160-501	Assembly, Transport Cask, MAGNATRAN	0
71160-502	Transport Cask Body, MAGNATRAN	3NP
71160-504	Misc. Details, Transport Cask, MAGNATRAN	1
71160-505	Lid Assembly, Transport Cask, MAGNATRAN	5NP
71160-506	Cask Cavity Spacer, MAGNATRAN	1
71160-511	Personnel Barrier, Shipping Configuration, Transport Cask, MAGNATRAN	1
71160-512	Nameplate, MAGNATRAN	1
71160-530	Misc. Details, Impact Limiter, MAGNATRAN	1
71160-531	Impact Limiter, Transport Cask, MAGNATRAN	2P*
71160-551	Fuel Tube Assembly, MAGNASTOR – 37 PWR	10NP
71160-559	Lifting Trunnion, Transport Cask, MAGNATRAN	0
71160-571	Details, Neutron Absorber, Retainer, MAGNASTOR – 37 PWR	8
71160-572	Details, Neutron Absorber, Retainer, MAGNASTOR – 87 BWR	8NP
71160-574	Basket Support Weldments, MAGNASTOR – 37 PWR	6
71160-575	Basket Assembly, MAGNASTOR – 37 PWR	11NP
71160-581	Shell Weldment, TSC, MAGNASTOR	4
71160-584	Details, TSC, MAGNASTOR	8
71160-585	TSC Assembly, MAGNASTOR	11
71160-591	Fuel Tube Assembly, MAGNASTOR – 87 BWR	8NP
71160-598	Basket Support Weldments, MAGNASTOR – 87 BWR	7NP
71160-599	Basket Assembly, MAGNASTOR – 87 BWR	8NP
71160-600	Basket Assembly, MAGNASTOR – 82 BWR	5NP
71160-601	Damaged Fuel Can (DFC), Assembly, MAGNASTOR	0
71160-602	Damaged Fuel Can (DFC), Details, MAGNASTOR	0

* License drawing is proprietary in its entirety and not included in the non-proprietary version of the SAR. It is included on the List of License Drawings for reference only.

1.4.3 License Drawings (cont'd)

Drawing Number	Title	Revision No.
71160-620	Top Fuel Spacer, MAGNASTOR	1P*
71160-671	Details, Neutron Absorber, Retainer, For DF Corner Weldment, MAGNASTOR – 37 PWR	0
71160-673	Damaged Fuel Can (DFC), Spacer, MAGNASTOR	1
71160-674	DF Corner Weldment, MAGNASTOR	3NP
71160-675	DF Basket Assembly, 37 Assembly PWR, MAGNASTOR	3NP
71160-681	DF, Shell Weldment, TSC, MAGNASTOR	0
71160-684	Details, DF Closure Lid, MAGNASTOR	2
71160-685	DF, TSC Assembly, MAGNASTOR	5
71160-711	GTCC Waste Basket Liner, MAGNASTOR	1
71160-781	Shell Weldment, GTCC TSC, MAGNASTOR	1
71160-785	GTCC TSC, Assembly, MAGNASTOR	3

1R-229575

REV	CHANGE
0NP	INITIAL ISSUE
1NP	INC. DCR. 0NPA
2NP	INC. DCR. 1NPA
3NP	INC. DCR. 2NPA
4NP	INC. DCR. 3NPA
5NP	INC. DCR. 4NPA

Security-Related Information
Figure Withheld Under CFR 2.390

: PROPRIETARY INFORMATION REMOVED

UNLESS OTHERWISE STATED	GROUP	NAME	DATE
DIMENSIONS AND TOLERANCES SHALL BE PER ASME Y14.5M-94	PREPARED	[illegible]	9-23-15
ALL FINISHED DEPTH CHAMFERS ARE TO BE CONSIDERED AS A MAX. DEPTH OF PERFECT THREADS	CHECKED	[illegible]	9-23-15
	STRESS ANALYSIS	[illegible]	9-23-15
	ENGINEERING	[illegible]	9-23-15
ALL DIMENSIONS ARE IN INCHES	APPROVED	[illegible]	9-23-15
MACHINED SURFACES TO BE 125 OR BETTER	RELEASED	[illegible]	9-24-15
NEXT ASSEMBLY 71160-501			
DRAWING TYPE: LICENSE			

NAC INTERNATIONAL

LID ASSEMBLY
TRANSPORT CASK,
MAGNATRAN

PROJECT 71160 | DRAWING 505 | REV. 5NP | SHT. 1 OF 4

Security-Related Information
Figure Withheld Under CFR 2.390

NAC INTERNATIONAL

LID ASSEMBLY
TRANSPORT CASK,
MAGNATRAN

PROJECT 71160 | DRAWING 505 | REV SNP | SH 2 OF 4

Security-Related Information
Figure Withheld Under CFR 2.390

NAC INTERNATIONAL

LID ASSEMBLY
TRANSPORT CASK,
MAGNATRAN

PROJECT 71160

DRAWING 505

REV SNP

SH 3 OF 4

Security-Related Information
Figure Withheld Under CFR 2.390

NAC INTERNATIONAL

LID ASSEMBLY
TRANSPORT CASK,
MAGNATRAN

71160 | 505

pool until a GTCC TSC in the transfer cask is moved into the pool. The loaded waste basket liner will be placed into the GTCC TSC and the closure lid lowered into the TSC to rest on the top of the waste basket liner. The remaining TSC transfer and closure operations proceed as described for the spent fuel TSCs. The remaining TSC transfer and closure operations proceed as described Chapter 7, Section 7.1.5 for GTCC TSCs. Note that the GTCC TSC does not require redundant closure so the installation and welding of the closure ring and the redundant vent and drain port covers is not required.

2.1.1.4 Fuel Basket Assembly

A fuel basket assembly is located inside the TSC. There are two different length fuel baskets. The fuel basket assembly and TSC are handled as one unit. The fuel basket assembly is designed with a capacity of up to 37 undamaged PWR fuel assemblies in the 37 PWR basket assembly or up to 87 undamaged BWR fuel assemblies in the 87 BWR basket assembly. The DF Basket Assembly is designed to transport up to four Damaged Fuel Cans (DFC). The DF Basket Assembly has a capacity of up to 37 undamaged PWR fuel assemblies, including four DFC locations. DFCs may be placed in up to four of the DFC locations. Each DFC may contain an undamaged PWR fuel assembly, a damaged PWR fuel assembly, or PWR fuel debris equivalent to one PWR fuel assembly. Undamaged PWR fuel assemblies may be placed directly in the DFC locations of a DF Basket Assembly.

The basket structure provides the fuel assemblies with lateral support, decay heat removal capability, and criticality control during all normal conditions of transport and hypothetical accident conditions. Both the PWR and BWR fuel baskets consist of an arrangement of square fuel tubes held in a right-circular cylinder configuration by side and corner support weldments that are bolted to the outer fuel tubes. Both designs minimize horizontal surfaces that could entrain water and provide an open path for water flow to the drain tube and sump in the bottom of the TSC. Detailed descriptions of the basket assemblies are provided in Section 1.3.1, with the geometry and materials of fabrication being described on the license drawings presented in Section 1.4.3.

The basket assemblies are evaluated for normal conditions of transport and hypothetical accident conditions for both PWR fuel and BWR fuel. These analyses show that the fuel baskets maintain their fuel assembly support, decay heat removal and criticality control functions for all of the evaluated conditions.

2.1.1.5 GTCC Waste Basket Liner

A GTCC waste basket liner is designed to hold GTCC waste (e.g., reactor baffle plates and angles, baffle formers, and lower core plates) and dimensionally fit in a TSC. The waste basket liner design includes a shell (structural and shield functions) and welded bottom plate, and lifting

lugs welded on the inside diameter of the shell so that the liner may be loaded with GTCC waste prior to being inserted into a TSC (Table 1.3-5). The liner design also includes an outer ring and a middle support under the bottom plate and drain holes in the bottom plate to facilitate free flow drainage from the liner. The GTCC TSC includes a sump location in the bottom plate, and the closure lid includes a drain tube assembly to enable draining and drying of the loaded TSC.

2.1.1.6 Damaged Fuel Can

The MAGNASTOR Damaged Fuel Can (DFC), shown in Figure 1.3-3, is provided to accommodate damaged PWR fuel assemblies. The primary function of the DFC is to confine the fuel material within the can to minimize the potential for dispersal of the fuel material into the TSC cavity. In normal operation, the DFC is in a vertical orientation. The DFC may also contain PWR fuel assemblies in an undamaged condition or fuel debris equivalent to one PWR fuel assembly. Up to four DFCs may be loaded, one into each outer corner, in the DF Basket Assembly. Figure 1.3-3 provides nominal dimensions for the DFC. Variations in DFC length and width are acceptable as long as the DFC fits into its associated TSC and has sufficient fuel assembly clearance.

If needed, a DFC spacer is used in the DF basket assembly to position the DFC for DFC lid retention and ease of handling. The DFC lid and bottom include screened drain holes.

2.1.1.7 Cask Cavity Spacer

A cask cavity spacer is used in the upper end of the MAGNATRAN cask cavity to limit the axial movement of the short TSCs. The spacer consists of six concentric rings welded to a flat plate (Drawing No. 71160-506). The depth of the rings, i.e., the length of the spacer, is approximately seven inches, which represents the difference in length between the short and long TSCs. The spacer is bolted through the flat plate to the underside of the cask lid.

above. At cold and hot temperature conditions, the strain rate effects exhibit the similar trend. In the CY quarter-scale model drop simulation, the instantaneous peak strain rate of an individual element is less than 300/s. The instantaneous peak average strain rate of the entire balsa wood block is less than 80/s.

In the full scale Magnatran drop simulation under HOT condition, the instantaneous peak strain rate of an individual element is less than 125/s. The instantaneous peak average strain rate of the entire balsa wood block is less than 10/s.

In the full scale Magnatran drop simulation under COLD condition, the instantaneous peak strain rate of an individual element is less than 130/s. The instantaneous peak average strain rate of the entire balsa wood block is less than 11/s.

The strain rate table is adequate to cover the strain rate range of interest. With the higher stress at high strain rate, the overall effect is that more energy is being dissipated for the same amount of crush of wood. In the macroscopic analyses of balsawood loaded parallel to the grain direction, the highest stress of the balsa wood occurs before the granular wood fiber starts to buckle under pressure at volumetric strain less the 30%. When the wood fiber buckles, it bends and forms a kink. When the wood fiber is being bended and twisted, the wood fiber undergoes the greatest length change but at the lowest stiffness value. At this transition stage, the strain rate is the greatest, but the stress is the lowest. This phenomenon can be observed on every stress strain curve of the balsa wood test result. Therefore, the stress increase at early stage of crush due to high strain-rate has no significant effect on the overall peak acceleration. Due to the increased energy absorption, the net effect on the drop simulation is to reduce the percentage of wood that reaches lock-up condition. The impact limiter stops at lesser crush and results in a smaller peak acceleration that occurs towards the final stage of the crush.

As can be seen in Figure 2.6.7.5-20 through Figure 2.6.7.5-23, all test data indicate that the slopes of the yield stress of balsawood decreases after the initial threshold of the sudden stress increase at the volumetric strain level of about 3%. The yield stress continues to decrease to about 60% volumetric strain, which is the effective useable deformation that the balsa wood can withstand. After the compressive volumetric strain exceeds 60%, the stress suddenly increases exponentially and reaches the lockup state. Since LSDYNA material model introduces numerical instability in the form of negative volume with negative stress-strain curve, the stress-strain curve is modified to show an ever-increasing slope (normalized), while preserving the total energy absorbed in the first 60% of the crushable volume. Therefore the final stress-strain curve reported in the table has slightly higher stress at 40% volumetric strain than at 10% volumetric strain.

Finite Element Model of the MAGNATRAN Transport Cask with Impact Limiters

The side drop, end drop, and corner drop analyses were performed using the LS-DYNA program. The model is constructed of eight-node brick and four-node shell elements. Using the symmetry plane that exists for the various drop orientations, two finite element models are developed to perform the required drop scenarios as shown in Figure 2.6.7-3. A half symmetry model is used to simulate the end drops and corner drops. The model used in the end drop and corner drop uses a single impact limiter in the model with the weight of upper impact limiter combined with the cask weight. The longitudinal axis of the cask aligns with the Z-axis. The plane of symmetry is about the X-Z plane. The side drop model is similar to the model used for the end and corner drops, but a quarter symmetry model is used as shown in Figure 2.6.7-3. The description of the side drop model is not repeated in this section. The cask body section of the model, consisting of a cylinder, the TSC, and the contents, is represented by a solid cylinder. The redwood and the balsa wood were modeled as solid brick elements as shown in Figure 2.6.7-4. The stainless steel shells enclosing the redwood and balsa wood were modeled as shell elements, as shown in Figure 2.6.7-5. Since a half symmetry model is used, only eight of the 16 threaded rods attaching the impact limiter to the cask are modeled. Each threaded rod is modeled as a series of beam elements with stainless steel elastic plastic properties. Each threaded rod is sufficiently subdivided with elements to allow each threaded rod to independently experience collapse. The model for the threaded rods is shown in Figure 2.6.7-5.

Boundary Conditions and Initial Conditions

The LS-DYNA "Automatic Single Surface" contact algorithm is employed between each part in the impact limiter, the cask body and the impact limiter shells. The package model impacts a rigid plane ("Rigidwall Geometric Flat"). Symmetry boundary conditions are imposed on the nodes in the X-Y plane for all drop conditions. For side drop cases, the initial velocity is in the X direction. For end drop cases, the initial velocity is in the –Y direction. For the corner drop and oblique drop cases, the initial velocity is defined by a vector consist of components in both X and Y directions. The weight of the finite element model bounds the loaded MAGNATRAN transport cask.

Because the flexibility of the items described above has no contribution to increasing the maximum accelerations of the overall cask body, the cask body of the loaded MAGNATRAN transport cask is modeled as a rigid body.

The wood impact limiters remain in position on the cask body during all impact events. Quarter-scale drop tests of an NAC-STC cask assembly (Section 2.12.2.4) have shown that the impact limiters stay in place. The discussion of the impact limiter attachments is addressed in Section

Figure 2.6.7-3 LS-DYNA Model of the MAGNATRAN Transport Cask with Impact Limiters

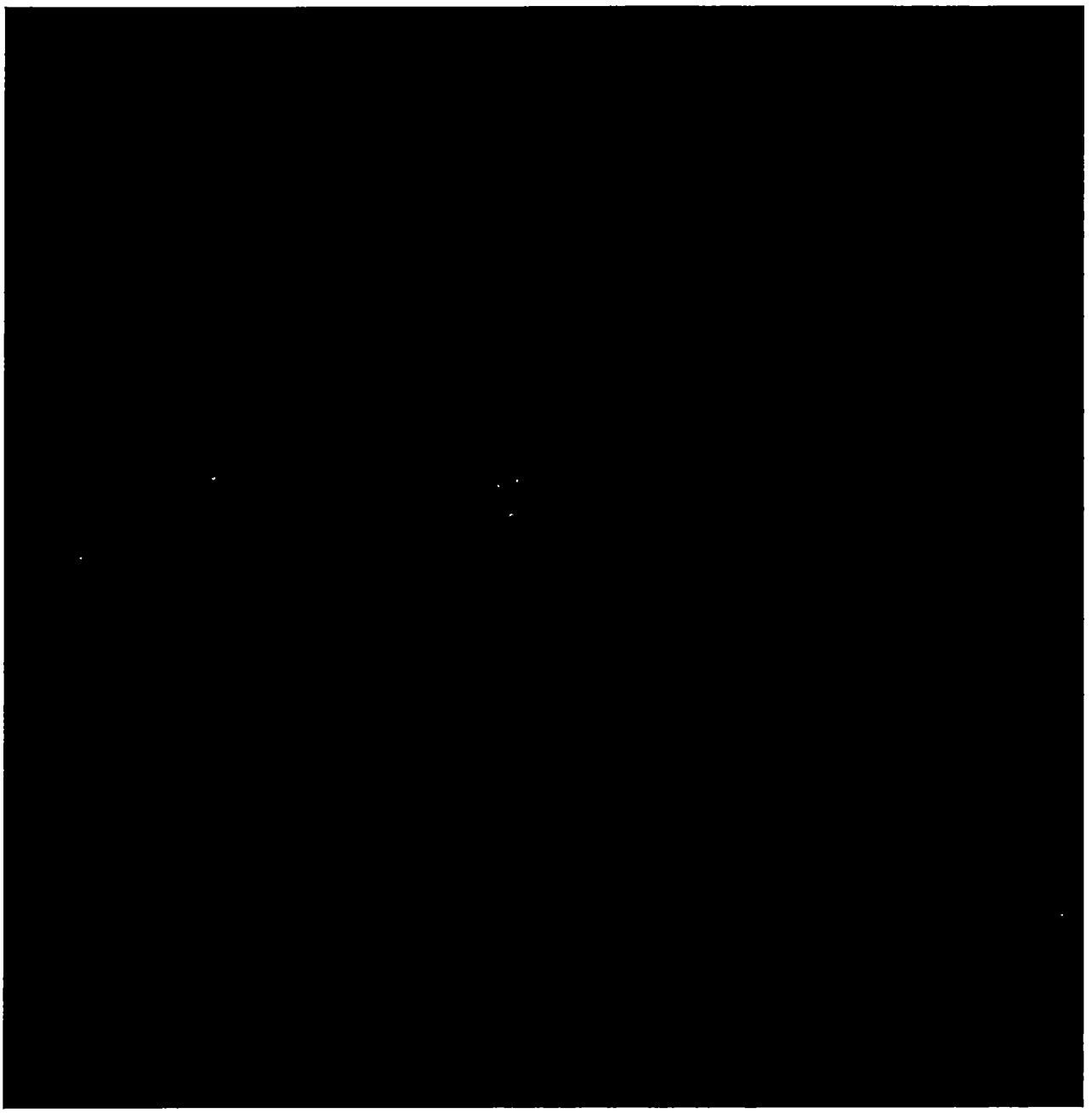

Figure 2.6.7-4 LS-DYNA Model of the Solid Elements of MAGNATRAN Impact Limiters

2.6.12 Transportable Storage Canister (TSC) Analysis – Normal Conditions of Transport

In this section, the Transportable Storage Canister (TSC) is evaluated for the normal conditions of transport. The TSC consists of a cylindrical stainless steel shell with a welded stainless steel bottom plate and a closure lid assembly at its top end. The TSC forms the confinement boundary for the basket assembly that contains the loaded PWR or BWR spent fuel basket. The TSC is designed to accommodate PWR and BWR classes of spent fuel. Figure 2.6.12-1 shows a TSC with a BWR fuel basket. TSCs are provided in four configurations designated TSC1 through TSC4. TSC1 and TSC2 include a 9-inch thick solid stainless steel closure lid assembly. TSC3 and TSC4 include a composite lid assembly consisting of a 4-inch thick stainless steel closure lid and a 5-inch thick A36 carbon steel shield plate that is coated using electroless nickel plating. The shield plate is attached to the closure lid by ten 1-½ inch diameter A193, Grade B6 bolts. The TSC closure lid is fabricated from Type 304 or 304L stainless steel, with material yield and ultimate strengths equal to, or greater than, those of SA240 Type 304. The stainless steel shell and bottom plate are dual-certified SA240 Type 304/304L. The TSC shell is a 0.5-inch thick plate formed into a 72-inch outer diameter cylinder and the bottom plate is 2.75-inch thick. The closure rings for all four TSC configurations are made from a ¾-inch square rolled bar. Alternatively, TSC3 and TSC4 closure rings may be made from a 1-½-inch × ¾-inch rolled bar. The closure rings are dual certified Type 304/304L stainless steel.

Two TSC lengths are designed to accommodate various lengths of fuel. A spacer is used to locate the short length TSCs in the cask cavity. The analysis of the cask cavity spacer is presented in Section 2.6.17. The geometries and materials of construction of the TSC, baskets, and spacers are described in Section 1.3.1.

Figure 2.6.12-1 TSC and Basket

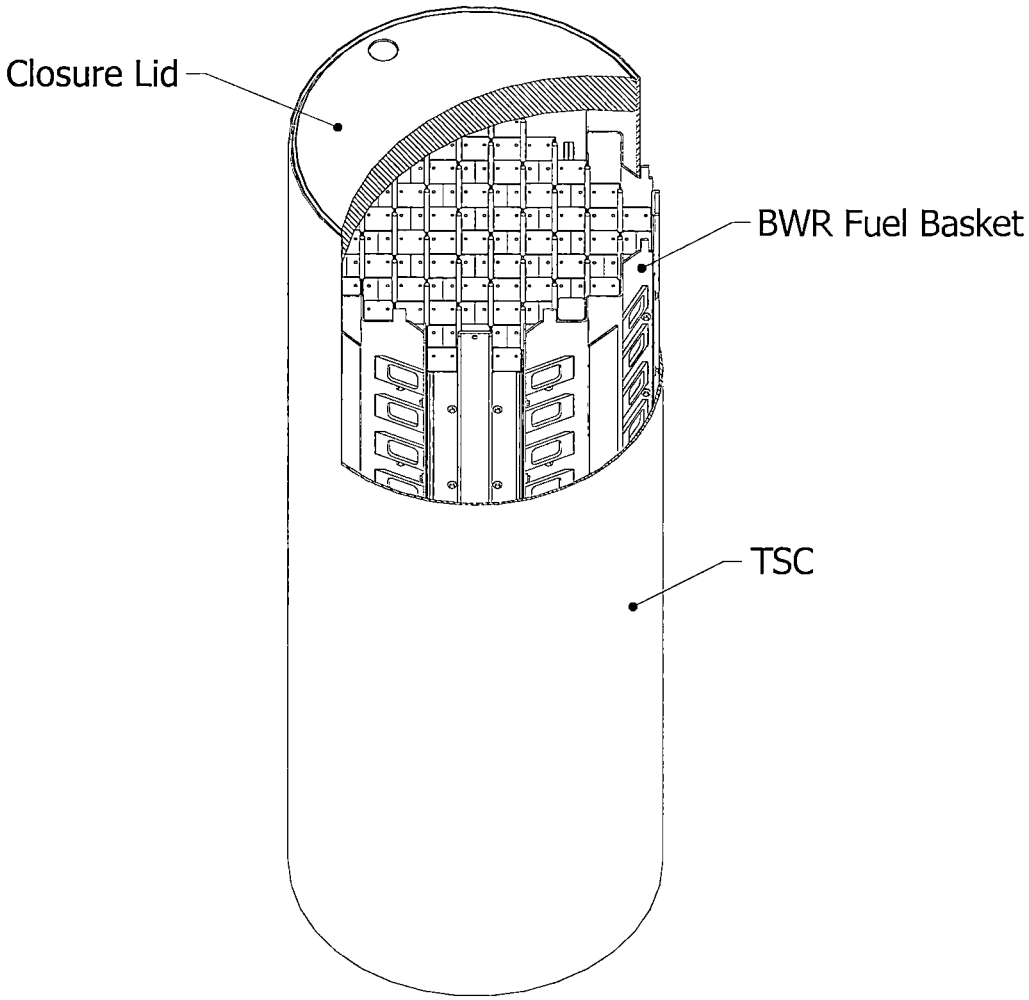

2.6.16.1 GTCC-TSC Analysis Description

The GTCC-TSC contains and confines the contents in the GTCC waste basket liner. The GTCC-TSC is not considered to provide containment during transport operation; the MAGNATRAN transport cask provides the containment boundary for transport. The GTCC-TSC in the transfer cask serves as the handling component for the waste basket liner and contents during loading and unloading from the transport cask.

The GTCC-TSC lid configuration is a composite lid design with a 4-inch stainless steel lid and a 5-inch thick carbon steel shield plate and a ¾-inch closure ring.

The structural design criteria for the GTCC-TSC are conservatively based on the ASME Code Section III, Subsection NB as compared to Subsection NF, which could be used to perform the structural evaluation. The GTCC-TSC will be fabricated using the Rules of ASME Code Section III, Subsection NF. Consistent with this criteria, the structural components of the GTCC-TSC are shown to satisfy the allowable stress limits presented in Table 2.1.2-2 and Table 2.1.2-3, as applicable.

The structural design criteria for the GTCC waste basket liner are based on the ASME Code Section III, Subsection NF. Consistent with this criteria, the structural components of the GTCC waste basket liner are shown to satisfy the allowable stress limits presented in Table 2.1.2-2 and Table 2.1.2-3, as applicable.

The GTCC-TSC and liner are analyzed by using the ANSYS finite element computer program for the 1-ft free drop condition in the top and bottom end, side, and top and bottom corner impact orientations. In addition, the effects of normal operating internal pressure and thermal stresses resulting from exposure of the cask to the hot (100°F ambient and solar insolance) and cold (-40°F ambient) normal conditions are evaluated.

2.6.16.2 GTCC-TSC Finite Element Model Description

The finite element model used to analyze the TSC portion of the GTCC-TSC assembly is Finite Element Model B, the model described in Section 2.6.12.2.2, including the relevant portions of the description in Section 2.6.12.2.1 (Finite Element Model A) that apply to both Model A and Model B. Model B is shown in Figure 2.6.12-3; its configuration includes the composite lid and the ¾-inch closure ring. However, for the GTCC-TSC the model has been modified to eliminate the 3/4-inch closure ring, and the redundant welded port cover.

A three-dimensional finite element model of the GTCC waste basket liner is also constructed using ANSYS. The waste basket liner shell, bottom plate and spacer rings are modeled with SOLID45 elements. By taking advantage of the symmetry of the waste basket liner and loadings, the model represents one-half (180° portion) of the waste basket liner including the liner shell, bottom plate and spacer rings. The three-dimensional finite element model of the waste basket liner is shown in Figure 2.6.16-1 and Figure 2.6.16-2. TARGE170 and CONTA174 surface-to-surface contact elements are modeled between the outer diameter of the liner shell and the inner diameter of the canister shell. These contact pairs are used between the top of the canister bottom plate and the bottom of the liner spacer rings, as well as between the top of the liner shell and the bottom of the shield plate.

The GTCC-TSC model uses a contents (payload) weight of 55,000 pounds.

The accelerations used in the GTCC-TSC 1-foot drop analyses are:

1-Foot Side Drop	15g
1-Foot End Drop	15g
1-Foot Corner Drop	8g

The internal pressure used in the GTCC-TSC 1-ft drop analyses is 5 psig.

The design parameters of the GTCC-TSC and GTCC-waste basket liner are:

GTCC-TSC Component	GTCC-TSC (inches)	GTCC - Waste Basket Liner (inches)
Length	184.8	173.03
Outside Diameter	72.0	70.5
Shell Thickness	0.5	2.0
Bottom Plate Thickness	2.75	1.0 (plus 1.0 thick ring segments)
Lid Type	Composite	-
Closure Lid Thickness	4.00	-
Shield Plate Thickness	5.00	-
Closure Lid Weld Size	0.5	-
Finite Element Model	B	

A pressure loading is applied to the inner surface of the liner to represent the weight of the GTCC waste basket contents. For end drops, a uniform pressure load is applied to either the canister lid or bottom plate. For the side drop, a uniform force is applied to the middle third of the inner shell surface and around a 90° sector of the liner circumference. For the bottom corner drop, a uniform load is applied to a 90° sector of the liner inner shell and a distributed pressure is applied to the bottom surface of the liner. For the top corner drop, a uniform load is applied to a 90° sector of the inner shell and a distributed pressure is applied to the bottom surface of the shield plate. To represent the internal pressure inside the canister during the transport conditions, bounding internal pressure for normal (5 psig) and accident (10 psig) conditions is modeled as a uniform pressure over the entire inner surface of the canister.

The inertial loads resulting from the weight of the liner and canister are considered by applying an appropriate deceleration factor (g-load) for either the 1-ft or 30-ft cask drops. Inertia loads from the GTCC liner contents are included by applying pressure on the inside of the liner. The canister is evaluated for the following drop orientations: top and bottom end drops, the side drop and top and bottom corner drops (20°).

A bounding temperature and thermal gradient for hot transport conditions (100°F ambient with solar insolance and maximum heat load) and cold transport conditions (-40°F without solar insolance) are used in a thermal analysis to compute temperatures throughout the canister. These temperatures are then used to calculate the thermal stresses in the canister and to determine the allowable stresses.

The thermal finite element model that was used for the PWR transport cask and internals (see Section 2.6.12.3) is used to compute the temperatures in the GTCC-TSC and waste basket liner,

2.6.16.3 Thermal Expansion and Thermal Stresses Evaluation of GTCC-TSC

A thermal stress evaluation is performed to determine the associated thermal stresses that result from the decay heat in the GTCC-TSC. Two ambient conditions are considered as shown in the following table.

Condition	Ambient Temperature	Solar Insolance Applied to Cask Surface	Content Decay Heat
Hot	100°F	Yes	Yes
Cold	-40°F	No	Yes

The thermal evaluation of the GTCC assembly is a three-step process. First the existing 3D thermal finite element model for the PWR transport cask and internals is used to predict the temperatures on the outer surface of the canister due to a heat load of 4 kW. The analysis is run for both the hot and cold ambient conditions. The surface temperatures for the canister from this 3D analysis are then applied to a 2D, axisymmetric thermal model of the GTCC waste assembly for both hot and cold cases, and these thermal analyses are run. The temperatures on all surfaces of the canister, shield plate, structural lid and the GTCC liner are then extracted and applied to a 3D thermal model of the GTCC assembly (canister plus liner) to obtain a 3D thermal solution, which is used to determine the thermally induced stresses in the GTCC assembly.

The GTCC component temperatures used in the analyses are:

Location	Hot	Cold
Closure Lid Center – Outer	184°F	35 °F
Shield Plate Center – Bottom	191 °F	48 °F
Shell Top (Closure Lid Outer Corner)	184 °F	35 °F
Shell Peak Temperature	184 °F	35 °F
Bottom Plate – Center	191°F	49 °F
Bottom Plate – Corner	190°F	35 °F
Shield Plate Edge – Inner	188 °F	43 °F
Shield Plate/ Closure Lid Junction – Center	191 °F	49 °F
Shield Plate/ Closure Lid Junction – Edge	188 °F	43 °F

The thermal stresses reported in Table 2.6.16-1 and Table 2.6.16-2 correspond to the maximum stresses for any circumferential section, for each of the locations shown in Figure 2.6.12-5. For Table 2.6.16-1 and Table 2.6.16-2, the angle of peak stress at each section is zero degrees.

The allowable stresses are evaluated at 250°F, which is higher than the maximum predicted temperature for the GTCC assembly of 227°F.

The differential thermal expansions of the GTCC-TSC and the cask inner shell in both the radial and axial directions are bounded by the results determined in Section 2.6.12.3 for the standard TSC because TSC materials and dimensions are the same, but the GTCC internal heat load is lower.

Chapter 3
Thermal Evaluation

Table of Contents

3 THERMAL EVALUATION 3-1

3.1 Discussion 3.1-1

3.2 Summary of Thermal Properties of Materials 3.2-1
3.2.1 Conductive Properties 3.2-1
3.2.2 Radiative Properties 3.2-1
3.2.3 Convective Properties 3.2-3

3.3 Technical Specifications for Components 3.3-1
3.3.1 Radiation Protection Components 3.3-1
3.3.2 Safe Operating Ranges 3.3-1

3.4 Thermal Evaluation for Normal Conditions of Transport 3.4-1
3.4.1 Thermal Models 3.4-2
3.4.2 Maximum Temperatures 3.4-15
3.4.3 Minimum Temperatures 3.4-16
3.4.4 Maximum Internal Pressures 3.4-16
3.4.5 Maximum Thermal Stresses 3.4-19
3.4.6 Evaluation of Package Performance for Normal Conditions of Transport 3.4-19

3.5 Thermal Evaluation for Hypothetical Accident Conditions 3.5-1
3.5.1 Thermal Models 3.5-1
3.5.2 Package Conditions and Environment 3.5-3
3.5.3 Package Temperatures 3.5-3
3.5.4 Maximum Internal Pressures 3.5-4
3.5.5 Maximum Thermal Stresses 3.5-4
3.5.6 Evaluation of Package Performance for Hypothetical Accident Conditions 3.5-5

3.6 References 3.6-1

List of Figures

Figure 3.4-1 Three-Dimensional PWR Cask Finite Element Model 3.4-20
Figure 3.4-2 Three-Dimensional Model of PWR Cask Loaded with DFC (Intact Fuel and Damaged Fuel Assemblies) 3.4-21
Figure 3.4-3 Design Basis PWR Fuel Assembly Axial Power Distribution 3.4-22
Figure 3.4-4 PWR 14×14 Fuel Assembly Two-Dimensional Finite Element Model 3.4-23
Figure 3.4-5 Two-Dimensional PWR Neutron Absorber Model 3.4-24
Figure 3.4-6 Three-Dimensional BWR Cask Finite Element Model 3.4-25
Figure 3.4-7 Design Basis BWR Fuel Assembly Axial Power Distribution 3.4-26
Figure 3.4-8 BWR 10×10 Fuel Assembly Two-Dimensional Finite Element Model 3.4-27
Figure 3.4-9 Two-Dimensional BWR Neutron Absorber Model 3.4-28
Figure 3.4-10 Two-Dimensional BWR Neutron Absorber Model with Fuel Channel Only 3.4-29
Figure 3.4-11 Three-Dimensional Periodic Cask CFD Model 3.4-30
Figure 3.4-12 Mesh of a Section of the Periodic Cask CFD Model 3.4-31
Figure 3.4-13 Three-Dimensional Full-Length (360°) PWR Cask Finite Element Model 3.4-32
Figure 3.5-1 Three-Dimensional Finite Element Cask Model (PWR and BWR) 3.5-6
Figure 3.5-2 Upper Region of Three-Dimensional Cask Finite Element Model 3.5-7
Figure 3.5-3 Cross-Section of Three-Dimensional Cask Finite Element Model 3.5-8
Figure 3.5-4 Hypothetical Accident Conditions Maximum Lead Temperature History 3.5-9
Figure 3.5-5 Hypothetical Accident Conditions Maximum Exterior Temperature History 3.5-10
Figure 3.5-6 Hypothetical Accident Conditions Maximum Cask Inner Shell Temperature History 3.5-11
Figure 3.5-7 Hypothetical Accident Conditions Maximum Cask Outer Shell Temperature History 3.5-12
Figure 3.5-8 Hypothetical Accident Conditions Maximum Lid Containment O-Ring Temperature History 3.5-13
Figure 3.5-9 Hypothetical Accident Conditions Maximum Temperature of Lid Coverplate Containment O-Ring 3.5-14

List of Tables

Table 3.1-1 Thermal Analysis Bounding Conditions – Normal Conditions of Transport 3.1-3
Table 3.2-1 Thermal Properties of Solid Neutron Shield (NS-4-FR) 3.2-4
Table 3.2-2 Thermal Properties of Stainless Steel 3.2-4
Table 3.2-3 Thermal Properties of Carbon Steel (A36, A588, A537) 3.2-5
Table 3.2-4 Thermal Properties of Nickel-Plated Steel 3.2-5
Table 3.2-5 Thermal Properties of Chemical Lead 3.2-5
Table 3.2-6 Thermal Properties of Type 1100 Aluminum Alloy 3.2-6
Table 3.2-7 Thermal Properties of Helium 3.2-6
Table 3.2-8 Thermal Properties of Dry Air 3.2-6
Table 3.2-9 Thermal Properties of Copper 3.2-7
Table 3.2-10 Thermal Properties of Zircaloy and Zircaloy-4 Cladding 3.2-7
Table 3.2-11 Thermal Properties of Fuel (UO_2) 3.2-7
Table 3.2-12 Neutron Absorber Material Minimum Effective Thermal Conductivity 3.2-8
Table 3.2-13 Gaps in the MAGNATRAN Transport Cask Model 3.2-8
Table 3.4-1 Maximum Component Temperatures – Normal Conditions of Transport, Maximum Decay Heat, Maximum Ambient Temperature 3.4-33
Table 3.4-2 Maximum Component Temperatures – Normal Conditions of Transport, Maximum Decay Heat, Minimum Ambient Temperature 3.4-34
Table 3.4-3 Maximum Internal Pressures for Transport Under Normal Conditions 3.4-34
Table 3.4-4 PWR Per Assembly Fuel Generated Gas Inventory 3.4-35
Table 3.4-5 PWR Canister Free Volume (No Fuel or Inserts) 3.4-35
Table 3.4-6 BWR Per Assembly Fuel Generated Gas Inventory 3.4-35
Table 3.4-7 BWR Canister Free Volume (No Fuel or Inserts) 3.4-35
Table 3.5-1 Maximum Component Temperatures – Hypothetical Accident Condition Fire Transient (PWR Cask) 3.5-15
Table 3.5-2 Maximum Component Temperatures – Hypothetical Accident Condition Fire Transient (BWR Cask) 3.5-16
Table 3.5-3 Maximum Internal Pressures for Hypothetical Accident Conditions 3.5-17

The contact is simulated by using a thermal conductivity of 2.0 BTU/hr-in-°F for the elements in the contact regions.

Solar insolance and ambient temperature conditions are applied to the cask surface including the surface of the cooling fins. Insolance is used at the exterior surface of the cask and the cooling fins and is based on the amount of insolation required by 10 CFR 71 to be applied over a 12-hr period evaluated in the steady state (applied over 24 hours simulating 12-hour period of solar exposure and 12-hour period of no solar exposure). The heat flux resulting from insolation on a curved surface is calculated as follows:

$$1475\frac{\text{Btu}}{12\text{ hr - ft}^2} \times \frac{12\text{ hr}}{24\text{ hr}} \times \frac{1\text{ ft}^2}{144\text{ in}^2} = 0.427\text{ Btu/hr-in}^2.$$

The heat flux resulting from insolance is factored by the emissivities of the materials on which the insolance is applied.

The model is analyzed for a steady-state condition to determine the maximum temperatures for the fuel, basket, TSC, cask shells, radial shielding and surface conditions under normal conditions of transport. All material thermal properties are shown in Table 3.2-1 through Table 3.2-12.

The fuel regions (inside tubes) are modeled as homogeneous regions with effective conductivities, determined by the two-dimensional fuel model as described in Section 3.4.1.1.2. The fuel tube and the neutron absorber plate, including gaps on both sides of the neutron absorber sheet and the gap between the stainless steel cladding for neutron absorber and disk, are modeled as one element thick with effective conductivities, as established by using the two-dimensional neutron absorber and tube model discussed in Section 3.4.1.1.3.

The neutron shield assembly of the MAGNATRAN Transport Cask is consisted of NS-4-FR, thermal insulator, and stainless steel shell. The orthotropic effective material properties are computed for the three layers as listed below.

1) 0.125-inch silicone foam
2) 0.125-inch thermal insulator
3) 0.12-inch stainless steel

In the model, radiation heat transfer is considered from the bottom of the fuel region to the top surface of the TSC bottom plate, and from the outer surfaces of the basket to the inner surface of the TSC shell. The radiation from the bottom of the fuel region to the top surface of the TSC bottom plate is modeled by using effective property as described in Section 3.2.2.1. The radiation from the exterior surfaces of the fuel tubes to the inner surface of the TSC shell is modeled by using ANSYS superelement, MATRIX50.

Radiation at the cask surface to ambient is combined with the convection effect by using the method described in Section 3.2.2.2. The convection heat transfer coefficient is calculated on the basis of the formula shown in Section 3.2.3. Effective emissivities are used for all radiation calculations, with the form factor taken to be unity. Effective emissivity is computed by using the following formula based on corresponding material emissivities:

$$\varepsilon_{eff} = 1/(1/\varepsilon_1 + 1/\varepsilon_2 - 1)$$

Solar insolance is applied to the cask surface for the "Hot" condition (ambient temperature = 100°F). A uniform heat flux is considered for the insolance.

Volumetric heat generation (Btu/hr-inch^3) is applied to the active fuel region on the basis of a total heat load of 23 kW, with an active fuel length of 144 inches, and an axial power distribution as shown in Figure 3.4-3.

There are a number of conservative conditions in this three-dimensional cask model:

1. The fuel assembly is conservatively considered to be located at the center of the basket slot. (The fuel assembly will be in contact with the fuel tube on its side since the cask is in the horizontal position during transport. The contact will reduce the maximum component temperature.)
2. The bottom portion of the loaded transport cask is modeled, while the top portion is not explicitly modeled. It is slightly conservative to model the bottom portion of the cask since the active fuel region is located closer to the cask bottom and the top portion is approximately 30% longer than the bottom portion, which provides more surface area for heat rejection to the ambient. Using the same modeling methodology used in the bottom model, a full-length (360°) three-dimensional finite element model, as shown in Figure 3.4-13, is generated for the PWR configuration. The model includes the canister lid and cask lid, with helium gap between the basket top and canister lid, and between canister lid and cask lid. A sensitivity analysis is performed using the full length model for the normal conditions of transport (maximum decay heat, 100°F ambient temperature) and the maximum fuel temperature is 4°F lower than that calculated by the bottom model, indicating that the bottom model is slightly conservative.
3. Convection heat transfer is conservatively ignored inside the cask and the TSC.
4. The gap between the lead and the cask inner shell is conservatively considered to be 360° around the shell. (A good portion of the lead will be in contact with the inner shell since the cask is in the horizontal position during transport. The contact will reduce the maximum component temperature.)
5. A finite element mesh sensitivity study is performed for the normal condition of transport for the PWR configuration. Instead of using the half-length (360°) cask model shown in Figure 3.4-1, the full-length (360^0) cask model discussed in Item 2 (Figure 3.4-13) is modified to perform a steady state analysis for the mesh sensitivity study for normal transport condition. The refined (finer mesh) full-length model contains 67% more elements compared to the original full-length model. Since the mesh divisions were

changed, the constraint equations which connect the helium gap at canister shell surface and the cask inner shell were regenerated, resulting in a refined analytical connectivity. Consequently, the calculated maximum temperatures of the fuel cladding and cask components from the refined model are lower than those from the original model. The mesh sensitivity study shows that using the half-length three-dimensional cask model (Figure 3.4-1) is conservative.

Damaged Fuel Configuration

The three-dimensional cask model loaded with PWR fuel assemblies described in this section is modified to simulate the configuration of the cask loaded with PWR fuel assemblies and damaged fuel cans (DFCs). Four damaged fuel cans are loaded in the PWR basket at the locations shown in Figure 3.4-2. The model described in this section is modified for the DFC geometry and the heat load applied to the DFC. A damaged fuel height of 107-inches is determined based on a 50% compaction of the damaged fuel. A damaged fuel length of 103 inches is conservatively used in this modified model. The damaged fuel is concentrated at the center, 51.5 inches, in the model (see Figure 3.4-2). The material properties of the center 51.5 inches in the DFC are conservatively modeled as the effective properties for the intact fuel assembly. It is conservative to neglect any contact among the fuel debris. The region below the damaged fuel region is conservatively modeled as helium without radiation. The conductance of the DFCs is conservatively not included in the model.

A computed heat generation rate based on the total heat load per canister (23kW), divided by 37 fuel assemblies and a volume corresponding to the 103 inches of damaged fuel, is applied to the damaged fuel regions at the four corner slots of the model.

The thermal evaluation of the MAGNATRAN transport cask loaded with PWR fuel assemblies and DFCs is performed for the normal transport condition (hot conditions, ambient temperature of 100°F). Due to the improved conduction performance of the damaged fuel basket configuration design, the maximum fuel temperature is 26°F lower for the basket loaded with DFCs than for the intact fuel basket configuration (Table 3.4-1). Therefore, the analysis results for the intact fuel configuration, shown in Table 3.4-1, bound the analysis results for the configuration of the basket loaded with DFCs.

GTCC Configuration

The MAGNATRAN cask system may contain a TSC with GTCC waste. The maximum heat load for the GTCC configuration is 1.7 kW, which is well below the design basis heat load of 23 kW for the PWR system. Therefore, the thermal analysis results obtained using the three-dimensional cask model with the 23 kW heat load for the PWR system, as described in this Section, bounds those for the GTCC configuration. No further evaluation is required.

3.4.1.1.2 Two-Dimensional Fuel Assembly Model: PWR Fuel

The effective conductivity of the fuel is determined by detailed two-dimensional finite element thermal models of the PWR fuel assembly. The model includes the fuel pellets, cladding, gas between the fuel rods, and gas occupying the gap between the fuel pellets and cladding. Modes of heat transfer modeled include conduction and radiation between individual fuel rods for the steady-state condition. Thermal analyses are performed for PWR 14×14, 15×15, 16×16 and 17×17 fuel assemblies. However, because the PWR 14×14 fuel assembly results in the lowest effective thermal conductivities, only the effective properties of that fuel assembly are used in the cask model presented in Section 3.4.1.1.1.

ANSYS PLANE55 conduction elements and MATRIX50 radiation elements are used to model conduction and radiation. Radiation elements are defined between fuel rods and between the fuel rods and the fuel tube. A typical PWR fuel assembly finite element model is shown in Figure 3.4-4, which corresponds to the 14×14 fuel assembly.

The effective conductivity for the fuel is determined by using an equation defined in the Sandia National Laboratory (SNL) Report SAND90-2406. Conservatively, 60% of the conductivities of fuel pellets (UO_2) are used in the models. The equation is used to determine the maximum temperature of a square cross-section of an isotropic homogeneous fuel with a uniform volumetric heat generation. At the boundary of the square cross-section, the temperature is constrained to be uniform. The expression for the temperature at the center of the fuel is given by:

$$T_c = T_e + 0.29468\ (Qa^2 / K_{eff})$$

where:

T_c = the temperature at the center of the fuel (°F)
T_e = the temperature applied to the exterior of the fuel (°F)
Q = volumetric heat generation rate (Btu/hr-in^3)
a = half-length of the square cross-section of the fuel (inch)
K_{eff} = effective thermal conductivity for the isotropic homogeneous fuel (Btu/hr-in-°F)

Volumetric heat generation (Btu/hr-in^3) based on the design heat load is applied to the pellets. The effective conductivity is determined based on the heat generated and the temperature difference from the center of the model to the edge of the model. Temperature-dependent effective properties are established by performing multiple analyses using different boundary temperatures. The effective conductivity in the axial direction and the effective density of the fuel assembly are calculated on the basis of the material area ratio. The effective specific heat is computed on the basis of a weighted mass average.

3.4.1.1.3 Two-Dimensional Neutron Absorber Model: PWR Fuel

The two-dimensional neutron absorber model is used to calculate the effective conductivities of the neutron absorber, and the neutron absorber retainer. These effective conductivities are used in the three-dimensional cask models (Section 3.4.1.1.1). As shown in Figure 3.4-5, the PWR neutron absorber model includes the neutron absorber, the stainless steel retainer, and the gaps between the neutron absorber and the stainless steel retainer and the surface of the fuel tube. Helium is considered in the gap.

ANSYS PLANE55 conduction elements and LINK31 radiation elements are used to construct the model. The model consists of four layers of conduction elements and two sets of radiation elements that are defined at the gaps (two for each gap). The thickness of the model (x-direction) is the distance measured from the outside surface of the stainless steel retainer to the inside surface of the fuel tube (assuming the neutron absorber is centered between the retainer and the fuel tube, and there is no contact for the length of the basket).

Heat flux is applied at the left side of the model, and the temperature at the right boundary of the model is specified. The heat flux is determined based on the design heat load. The maximum temperature of the model (at the left boundary) and the temperature difference (ΔT) across the model are calculated by the ANSYS model. The effective conductivity (K_{xx}) is determined using the following formula.

$$q = K_{xx} (A/L) \Delta T$$

or

$$K_{xx} = q \ L / (A \ \Delta T)$$

where:

K_{xx} = effective conductivity (Btu/hr-in-°F) in X direction (the X direction in Figure 3.4-5)
q = heat rate (Btu/hr)
A = area (in^2)
L = length (thickness) of model (in)
ΔT = temperature difference across the model (°F)

The temperature-dependent conductivity is determined by varying the temperature constraints at one boundary of the model and solving for the temperature difference. The effective conductivity for the parallel path (the Y direction in Figure 3.4-5) is calculated by the following:

$$K_{yy} = \frac{\sum K_i \, t_i}{L}$$

where:

K_i = thermal conductivity of each layer (Btu/hr-in-°F)
t_i = thickness of each layer (in)
L = total length (thickness) of the model (in)

3.4.1.2 Analytical Models: Cask with BWR Fuel

The finite element ANSYS models used in the thermal analysis of the cask transporting BWR fuel are similar to those used in the thermal analysis of the cask transporting PWR fuel discussed in previous sections. A three-dimensional model is employed to evaluate the cask in a horizontal position with the basket in contact with the TSC, which, in turn, is in contact with the cask inner shell. The fuel regions and the fuel tubes with neutron absorber plates are modeled by using effective conductivities. A detailed two-dimensional thermal model of the fuel assembly is used to determine the effective conductivity of the fuel. A two-dimensional thermal model of the fuel tube is used to calculate the effective conductivities of the fuel tube wall and neutron absorber plate. Another two-dimensional thermal model for the fuel tube is used to calculate the effective conductivity of the fuel tube wall with no neutron absorber plate present. These four ANSYS thermal models are described in the following sections.

3.4.1.2.1 Three-Dimensional Cask Model: Cask with BWR Fuel

The three dimensional MAGNATRAN transport cask model containing a BWR canister is a half-length finite element model (360°) constructed by using ANSYS Revision 10.0. The model considers the fuel assemblies, fuel tubes, basket plates, TSC shell and bottom plate, cask inner shell, lead, outer shell, neutron shield, copper and aluminum cooling fins, and neutron shield shell. The gaps between the individual components are also considered. The ANSYS model is shown in Figure 3.4-6. The internal cavity of the TSC contains the active fuel region, the bottom end fitting zone of the fuel assemblies, and fuel tubes enclosing the fuel assemblies.

The gas inside the TSC is modeled as helium. The gas inside the cask cavity is modeled as helium, because the cavity will be backfilled with helium following fuel loading prior to transport. The finite element model is constructed of ANSYS three-dimensional, solid brick, thermal conduction elements (SOLID70), as well as two-dimensional elements (SHELL57) to model heat conduction/combined conduction and thermal radiation and Superelement (MATRIX50) to model thermal radiation. The principal gaps applied to the model are described in Section 3.2.2.3.

Because the TSC is in the horizontal position during transport, the elements for the TSC shell are in contact with the inner shell of the cask. Similarly, the basket is in contact with the TSC shell.

A 65-degree contact arc is considered for the gaps between the TSC shell and the cask inner shell and a 64-degree arc (five small contact zones) is considered for the gaps between the basket and the TSC shell. The contact is simulated by turning the gap in the contact zones into carbon steel that has high thermal conductivities (in range of 2 Btu/hr-in-°F).

Solar insolance and ambient temperature conditions are applied to the cask surface including the heat fins. Insolance is used at the exterior surface of the cask and the heat fins and is based on the amount of insolation required by 10 CFR 71 to be applied over a 12-hour period evaluated in the steady state (applied over 24 hr simulating 12-hour period of solar exposure and 12-hour period of no solar exposure). The heat flux resulting from insolation on a curved surface is calculated as follows:

$$1475\frac{\text{Btu}}{12\text{ hr - ft}^2} \times \frac{12\text{ hr}}{24\text{ hr}} \times \frac{1\text{ ft}^2}{144\text{ in}^2} = 0.427\text{ Btu/hr-in}^2.$$

The heat flux resulting from solar insolance is factored by the emissivities of the materials on which the insolance is applied.

The model is analyzed to determine the maximum temperatures for the basket, TSC, cask shells, radial shielding, and surface conditions under normal conditions of transport. All material thermal properties are shown in Table 3.2-1 through Table 3.2-12.

The fuel regions (inside tubes) are modeled as homogeneous regions with effective conductivities, determined by the two-dimensional fuel model as described in Section 3.4.1.2.2. The fuel assembly tube and the neutron absorber plate, including gaps on both sides of the neutron absorber sheet and the gap between the stainless steel cladding for neutron absorber and disk, are modeled as one element thick with effective conductivities, as established by using the two-dimensional tube model discussed in Section 3.4.1.2.3.

The neutron shield assemblies of the MAGNATRAN transport cask consist of NS-4-FR, thermal insulator, and stainless steel shells. The orthotropic effective material properties are computed for the three layers as listed below.

1) 0.125-inch silicone foam
2) 0.125-inch thermal insulator
3) 0.12-inch stainless steel

In the model, radiation heat transfer is considered from the bottom of the fuel region to the top surface of the TSC bottom plate, and from the exterior surfaces of the fuel tubes to the inner surface of the TSC shell. The radiation from the bottom of the fuel region to the top surface of the TSC bottom plate is modeled by using effective properties. The radiation from the exterior surfaces of the fuel tubes to the inner surface of the TSC shell is modeled by using ANSYS Superelement, MATRIX50.

Radiation at the cask surface to ambient is combined with the convection effect by using the method described in Section 3.2.2.2. The convection heat transfer coefficient is calculated on the basis of the formula shown in Section 3.2.3. Effective emissivities are used for all radiation calculations, with the form factor taken to be unity. Effective emissivity is computed by using the following formula based on corresponding material emissivities:

$$\varepsilon_{eff} = 1/(1/\varepsilon_1 + 1/\varepsilon_2 - 1)$$

Solar insolance is applied to the cask surface for the "Hot" condition (ambient temperature = 100°F). A uniform heat flux is considered for the insolance.

Volumetric heat generation (Btu/hr-inch^3) is applied to the active fuel region of 87 assemblies on the basis of a total heat load of 22 kW, with an active fuel rod length of 144 inches, and an axial power distribution as shown in Figure 3.4-7.

The conservative conditions in this three-dimensional cask model are identical to those in the cask model for the PWR fuels.

3.4.1.2.2 Two-Dimensional Fuel Assembly Model: BWR Fuel

The two-dimensional fuel assembly models include the fuel pellets, cladding, fuel channel, and the helium occupying the space between fuel rods. The media is considered to be helium for transport conditions. The two-dimensional finite element models of the fuel assemblies are used to determine the effective conductivities for the BWR fuel assemblies. The effective conductivities are used in the three-dimensional fuel basket models described in Section 3.4.1.2.1. For the BWR fuel assemblies, four separate types are considered: 7×7, 8×8, 9×9 and 10×10. A fuel channel is considered since it may be present and it will result in bounding fuel cladding temperatures. The effective properties corresponding to the 10×10 BWR fuel assembly type (Table 3.2-11) are used in the cask model as presented in Section 3.4.1.2.1, since the 10×10 fuel has the lowest thermal conductivities.

Modes of heat transfer modeled include conduction and radiation between individual fuel rods for the steady-state condition. ANSYS PLANE55 conduction elements and MATRIX50 radiation elements are used to model conduction and radiation. Radiation elements are defined between fuel rods and between the fuel rods and the fuel channel. The BWR fuel assembly model only considers the region up to the inner surface of the channel, and a typical BWR fuel assembly is shown in Figure 3.4-8, which corresponds to the 10×10 fuel assembly.

The effective conductivity for the fuel is determined by using an equation defined in a Sandia National Laboratory (SNL) Report, as discussed in Section 3.4.1.1.2. Conservatively, 60% of the conductivities of fuel pellets (UO_2) are used in the models (Table 3.2-11).

Volumetric heat generation (Btu/hr-in^3) based on the design heat load is applied to the pellets. The effective conductivity is determined based on the heat generated and the temperature difference from the center of the model to the edge of the model. Temperature-dependent effective properties are established by performing multiple analyses using different boundary temperatures. The effective conductivity in the axial direction and the effective density of the fuel assembly are calculated on the basis of the material area ratio. The effective specific heat is computed on the basis of a weighted mass average.

3.4.1.2.3 Two-Dimensional Neutron Absorber Model: BWR Fuel

The two-dimensional neutron absorber model is used to calculate the effective conductivities of the neutron absorber, the neutron absorber retainer, and the fuel channel. These effective conductivities are used in the three-dimensional cask models (Section 3.4.1.2.1). Two neutron absorber models are required: one with the neutron absorber plate and channel, and one with the channel but without the neutron absorber plate, corresponding to the enveloping configurations of the 10×10 BWR fuel assembly.

ANSYS PLANE55 conduction elements and LINK31 radiation elements are used to construct the model. As shown in Figure 3.4-9, the first BWR neutron absorber model includes the fuel channel, the retainer, the neutron absorber and associated gaps. As shown in Figure 3.4-10, the second BWR neutron absorber model includes the fuel channel and the gap between the fuel channel and the fuel tube surface.

Heat flux is applied at the left side of the model (fuel channel for BWR model), and the temperature at the right boundary of the model is specified. The heat flux is determined based on the design heat load. The maximum temperature of the model (at the left boundary) and the temperature difference (ΔT) across the model are calculated by the ANSYS model. The effective conductivity (K_{xx}) is determined using the following formula.

$$q = K_{xx} (A/L) \Delta T$$

or

$$K_{xx} = q \ L / (A \ \Delta T)$$

where:

K_{xx} = effective conductivity (Btu/hr-in-°F) in X direction in Figure 3.4-9 and Figure 3.4-10
q = heat rate (Btu/hr)
A = area (in^2)
L = length (thickness) of model (in)
ΔT = temperature difference across the model (°F)

The temperature-dependent conductivity is determined by varying the temperature constraints at one boundary of the model and solving for the temperature difference. The effective conductivity for the parallel path (the Y direction in Figure 3.4-9 and Figure 3.4-10) is calculated by the following:

$$K_{yy} = \frac{\sum K_i t_i}{L}$$

where:

K_i = thermal conductivity of each layer (Btu/hr-in-°F)
t_i = thickness of each layer (in)
L = total length (thickness) of the model (in)

3.4.1.3 Analytical Models: Cask Periodic CFD Model

As shown in Figure 3.4-11, a three-dimensional periodic axial section of the cask is modeled using the Computational Fluid Dynamic (CFD) code, FLUENT. The model includes the cask outer shell, the neutron shield, the cooling fins and the surrounding air at ambient temperature of 100°F. In the cask axial direction, the model includes one-half the axial length of a fin. Half of the cask (180° in the circumferential direction) is modeled because of symmetry. A close-up section of the mesh is shown in Figure 3.4-12. The model contains 1,647,000 computational cells, with higher concentration of cells near the wall to capture the near-wall velocity and temperature gradients. Transitional k-ω turbulence model is used for the simulation. The mesh ensures that the average y+ is less than 1.0 on the cask surface wall. Natural convection of air surrounding the cask is simulated, and surface temperature and heat flux are determined from the simulation results to determine the convection film coefficients. The average convective film coefficients for eight divisions (180 degrees) of the cask outer surface in the circumferential direction are determined.

The personnel barrier is made from aluminum mesh with a large ratio of open area. Due to the small surface area of the aluminum mesh and the low emissivity of aluminum (0.22), the personnel barrier absorbs an insignificant amount of solar energy or radiant energy from the transport cask. The high percentage of open area allows free flow of the air through the aluminum mesh. The additional flow restriction by the mesh is insignificant; therefore, natural convection is not affected by the personnel barrier. The thermal effect of the personnel barrier on the transport thermal performance is insignificant; therefore, the personal barrier is not explicitly included in the CFD thermal model.

3.5 Thermal Evaluation for Hypothetical Accident Conditions

This section provides the thermal evaluation of the MAGNATRAN transport cask containing PWR or BWR fuel under hypothetical accident conditions. The objective of the thermal analysis of the cask under hypothetical accident conditions is to demonstrate that the cask containment boundary structural components are maintained within their safe operating temperature ranges.

Because the fire accident is considered to be of short duration, the limit for maximum cladding temperature may be higher than that for normal conditions of transport. A cladding temperature limit of 1,058°F, however, is conservatively applied. To determine their cumulative effect on the package, the tests specified in 10 CFR 71.73 are to be performed or analyzed in sequence. Thus, the MAGNATRAN transport cask is analyzed for the fire transient, specified in 10 CFR 71.73(c)(4), assuming that the package is in a form consistent with the damage sustained in the free-drop and puncture tests of 10 CFR 71.73.

3.5.1 Thermal Models

Finite element models are used in the thermal evaluation of the MAGNATRAN transport cask under hypothetical accident conditions. The same cask body model is used to evaluate the cask transporting the PWR fuel and the BWR fuel. Heat flux is applied differently for the PWR and BWR fuels to the inner shell of the cask model to simulate the decay heat of the fuel. The distribution of the heat flux corresponds to the power distribution shown in Figure 3.4-3 and Figure 3.4-7 for PWR and BWR fuel, respectively.

The environmental conditions and decay heat loads for the analysis are provided as discussed in Section 3.5.1.1. Convection during the fire accident has been considered. Results are given in the form of maximum component temperatures in Table 3.5-1 (PWR) and Table 3.5-2 (BWR).

3.5.1.1 Analytical Models

Taking advantage of the symmetry of geometry and thermal loads of the cask about its major axis, the finite element model of the cask (with PWR fuel and with BWR fuel) are three-dimensional one-fifteenth model representations of the cask. The finite element model is constructed by using ANSYS two-dimensional thermal shell (SHELL57) and three-dimensional thermal elements (SOLID70). The loaded TSCs are not explicitly modeled. The maximum temperatures of the basket components and fuel cladding are calculated by adding the maximum temperature difference between the cask inner shell and the component of interest from the normal condition results (Table 3.4-1) to the peak temperature of the inner shell from the fire accident condition. The inner shell peak temperatures for the hypothetical accident case are

provided in Table 3.5-1 and Table 3.5-2 for the PWR fuel and the BWR fuel, respectively. The cask model for PWR fuel and BWR fuel used in the accident condition evaluation is shown in Figures 3.5-1 through 3.5-3.

In the model, the cask body is modeled as three concentric shells (the inner stainless steel shell, the lead shielding, and the outer stainless steel shell), the layer of the neutron shield assemblies, and the cask fins. The gap between the cask and lead is considered.

The analyses of the finite element models are composed of three distinct phases:

1. Initial conditions (steady-state): Maximum decay heat of the fuel; ambient temperature = 100°F; solar insolance
2. 30-min fire (transient): Maximum decay heat of the fuel; fire temperature = 1,475°F (including convection and radiation); no solar insolance
3. Post-fire cool-down (transient): Maximum decay heat of the fuel; ambient temperature = 100°F; solar insolance

For the first two phases of the analyses, the neutron shield of NS-4-FR is considered to be functional. At the end of the 30-min fire transient, the neutron shield of NS-4-FR is considered to be voided. The air conductivity is then used for the voided NS-4-FR region.

The effect of impact limiters is included in the model for the fire analysis. The area covered by the impact limiter is assumed adiabatic. The fire transient models include natural convection and thermal radiation boundary conditions during all phases of the analyses and account for solar insolance effects in the pre- and post-fire transient phases. The natural convection during the fire is modeled with a convection coefficient of 0.01833 Btu/hr-in^2-°F that is 50% more than the value of 0.01222 Btu/hr-in^2-°F specified in the PATRAM '95 Proceedings. After the fire, the convection coefficient, as described in Section 3.2.3, is used. The natural convection and thermal radiation boundary conditions are applied to all external cask surfaces not covered by the impact limiters. The solar insolance boundary condition is also applied to all external cask surfaces not covered by the impact limiters. During all phases of the analyses, the areas of the cask covered by the impact limiters are modeled as adiabatic surfaces.

To confirm the adequacy of the finite element mesh, a sensitivity study for the mesh of finite element model for the PWR configuration of fire accident condition is performed. The three-dimensional model described in this section is used for the sensitivity study for the fire accident condition. The total number of the elements in the model for the fire condition is increased by a factor of 2.21 or 121% more elements than the original mesh. The mesh sensitivity study shows that using current mesh are conservative in determining the maximum component temperatures, and therefore, is adequate.

3.5.1.2 Test Model

The thermal analyses presented in Section 3.5-3 demonstrate that the MAGNATRAN transport cask is capable of meeting the design basis temperature requirements under hypothetical accident conditions. The methodology used in this analysis is conservative, consistent with those used in prior transport cask licensing, and sufficient to show that the cask meets the criteria set forth in Section 3.5. Therefore, no thermal test model is created.

3.5.2 Package Conditions and Environment

As demonstrated in Chapter 2, the MAGNATRAN transport cask body sustains no major damage as a result of the free drop and puncture events, and the impact limiters remain attached to the cask. Since the pin puncture only results in local damage to the neutron shield, the cask body is modeled in an undamaged configuration.

The emissivity of stainless steel is 0.36. The copper emissivity is 0.65. The aluminum emissivity of 0.22 is conservatively used for the aluminum plates on the cask surface. However, during the 30-min fire portion of the transient analysis, the emissivity is assumed to be 0.9. Also, the emissivity of the fire is assumed to be 1.0.

At the end of the fire, the NS-4-FR in the neutron shield is assumed to be destroyed. The result is a lower conductivity, and thus a greater resistance to heat leaving the cask. The emissivity of stainless steel of 0.36, the emissivity of aluminum of 0.22, and the emissivity of copper of 0.65 are again used, which also provides a greater resistance to heat leaving the cask. The cool-down is analyzed for a period of 64 hours after the end of the fire. At the end of the cool-down period, all cask components have already reached their maximum temperatures and have begun to cool down to their post-fire, steady-state temperatures.

3.5.3 Package Temperatures

The ANSYS computer code is used to evaluate the MAGNATRAN transport cask for the hypothetical accident fire. A steady-state initial temperature profile is calculated on the basis of a 100°F ambient temperature and solar insolance and used as initial condition for the 30-min fire transient, which considers exposure of the cask to a 1,475°F radiant environment. This exposure is followed by a 64-hour cool-down period, which considers exposure of the cask to a 100°F ambient temperature and solar insolance.

The safe operating temperature ranges of the components specified in Section 3.3.2 are also evaluated for the fire accident. These components include the metallic containment O-ring seals and lead gamma shielding. The radial neutron shield temperature is not considered to be

significant; therefore its loss is assumed in this accident. The shielding consequences of the fire accident on the radial neutron shield are provided in Chapter 5.

The maximum component temperatures during the hypothetical fire accident and cool-down period are provided in Table 3.5-1 (PWR) and Table 3.5-2 (BWR). The tables also show the maximum component temperatures for the fuel cladding, and the lead in the cask body. None of the safety-related components, with the exception of the radial neutron shield, as noted previously, exceeds its safe operating temperature as a result of the fire accident. The temperature histories of the major cask components are shown in Figures 3.5-4 through 3.5-9 for the PWR configuration. The temperature histories of the major cask components for the BWR configuration are not shown due to the similarity of the histories to those for the PWR configuration.

3.5.4 Maximum Internal Pressures

The internal pressure analysis requires the calculation of the free volume of the canister, calculation of the releasable quantity of fill and fission gas in the fuel assemblies, BPRA gases, and the subsequent calculation of the pressure in the canister and cask if these gases are added to the backfill helium pressure (initially at 1.36 atm) already present in the TSC and cask (Sections 3.4.1.1 and 3.4.1.2). TSC and cask pressures are determined for the accident condition of 100% fuel failure and maximum temperature. The method employed in the accident analyses is identical to that employed in the normal condition evaluation of Section 3.4.1.

For the accident condition, the gas quantities associated with 100% fuel rod failure are combined with the bounding fire accident average gas temperatures of 662°F, rounded to 670°F, to determine the system pressures. The maximum TSC pressure for the 100% fuel rod failure and maximum temperature accident (fire) condition is 276.6 psig (DF-PWR). The maximum transport cask pressure is 256.5 psig (DF-PWR), where the cask pressure assumes the loss of TSC confinement.

The maximum internal pressures for the hypothetical accident condition are summarized in Table 3.5-3.

3.5.5 Maximum Thermal Stresses

The maximum thermal stresses in the cask and the cask contents resulting from the hypothetical accident fire are not calculated. Thermal stresses are secondary stresses. Evaluation of secondary stresses is not required by the ASME code for accident conditions.

3.5.6 Evaluation of Package Performance for Hypothetical Accident Conditions

The MAGNATRAN transport cask thermal performance has been assessed for the hypothetical accident fire transient, as specified in 10 CFR 71. Except for the radial neutron shield, which is assumed to be lost, all cask components important to safety remain within their safe operating ranges. The ability of the cask to safely contain its radioactive contents is not compromised.

Figure 3.5-1 Three-Dimensional Finite Element Cask Model (PWR and BWR)

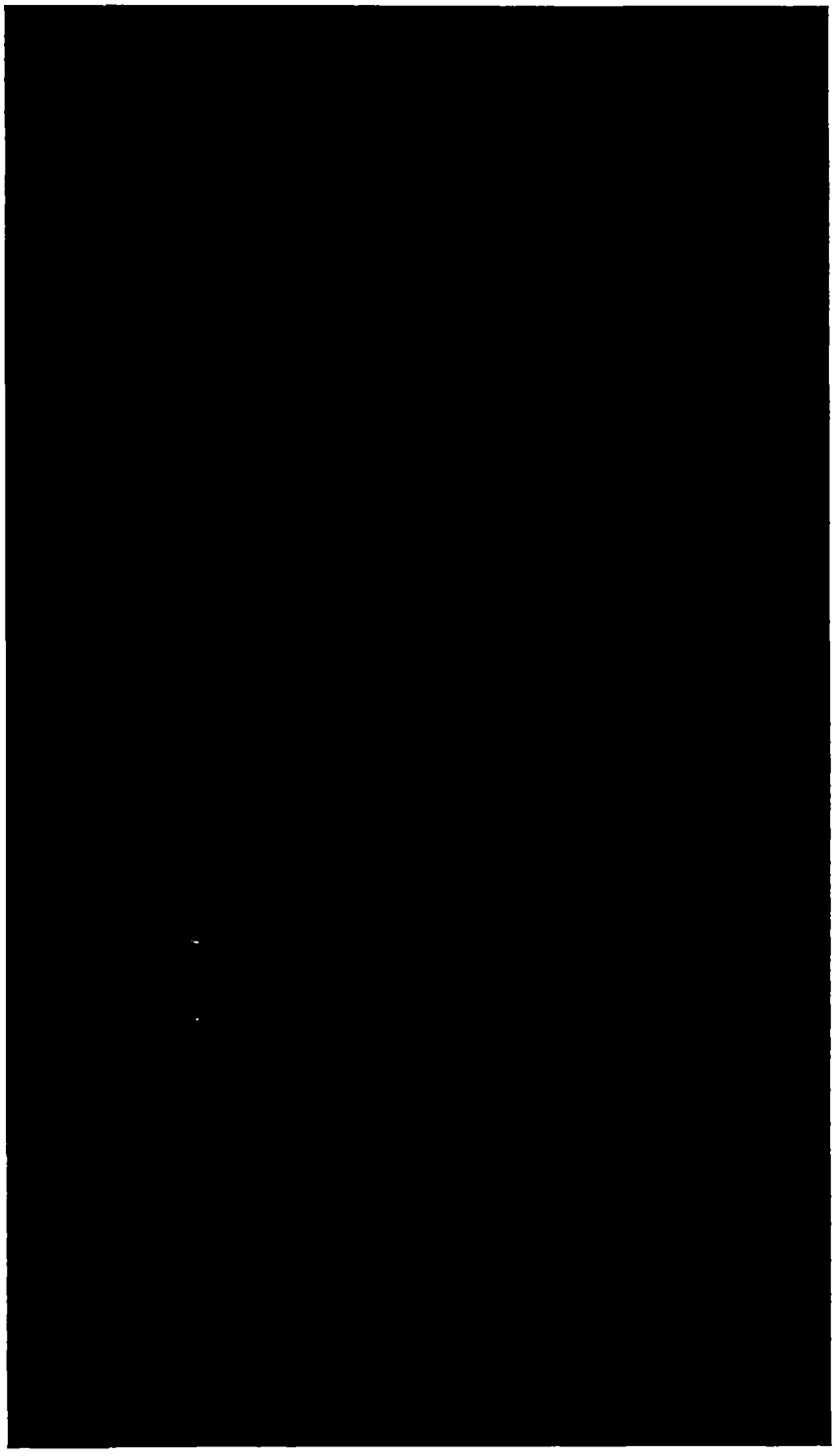

Figure 3.5-2 Upper Region of Three-Dimensional Cask Finite Element Model

[redacted]

Figure 3.5-3 Cross-Section of Three-Dimensional Cask Finite Element Model

[redacted]

Figure 3.5-4 Hypothetical Accident Conditions Maximum Lead Temperature History

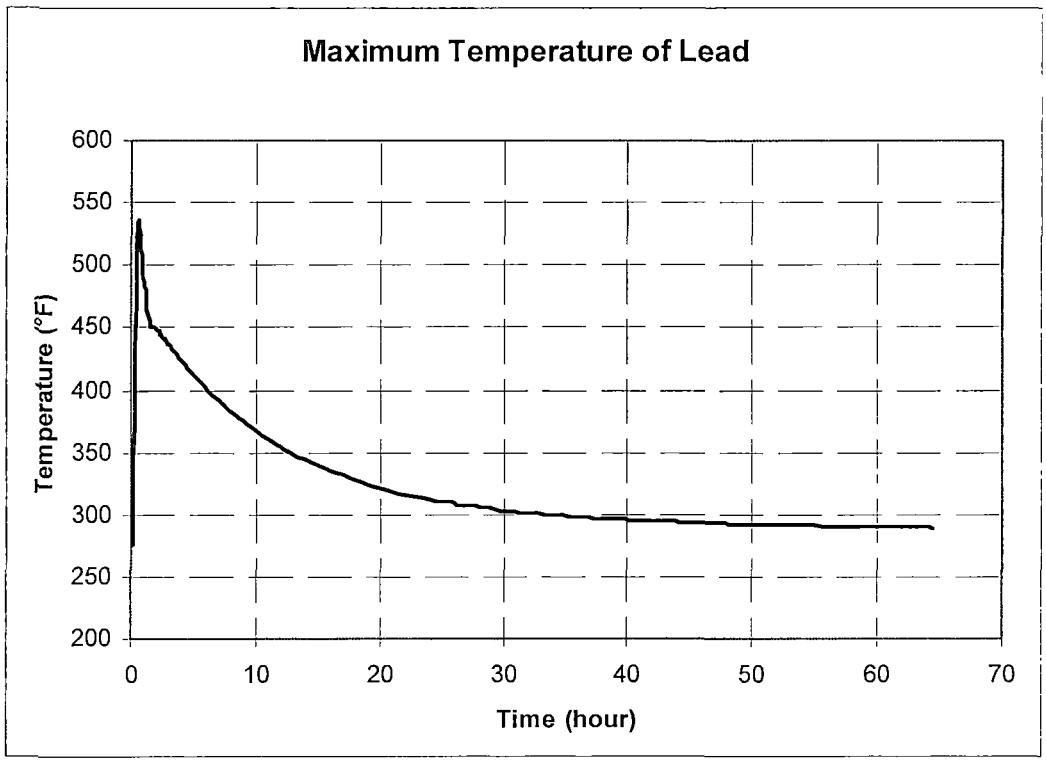

Figure 3.5-5 Hypothetical Accident Conditions Maximum Exterior Temperature History

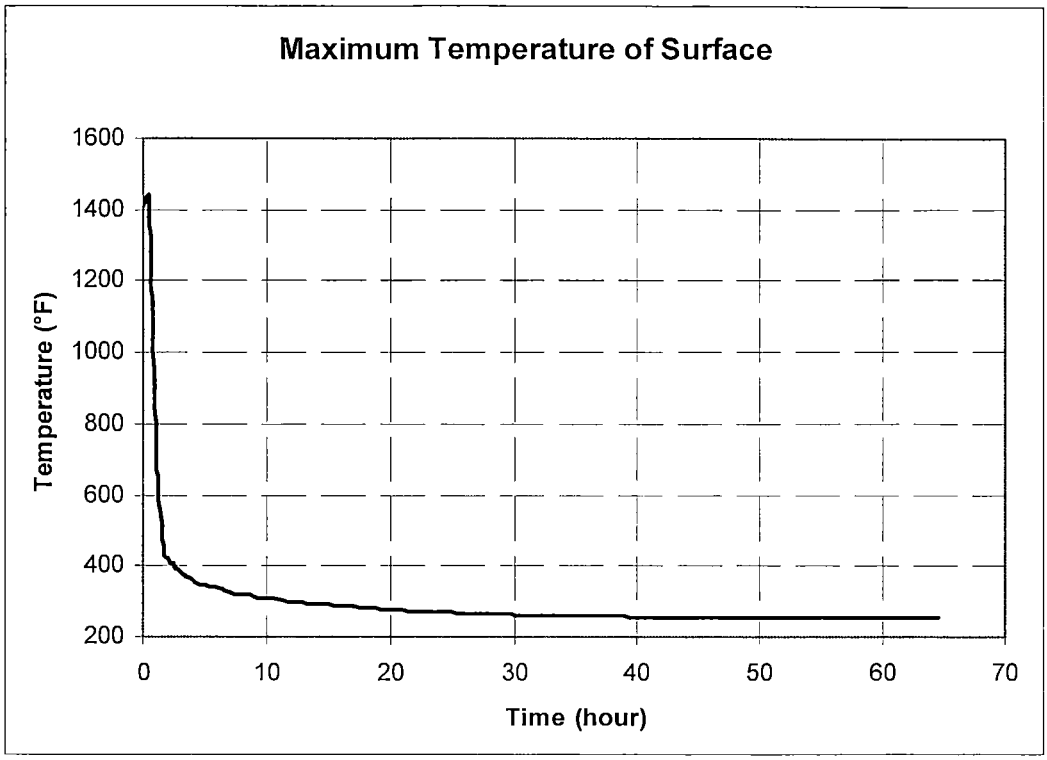

Figure 3.5-6 Hypothetical Accident Conditions Maximum Cask Inner Shell Temperature History

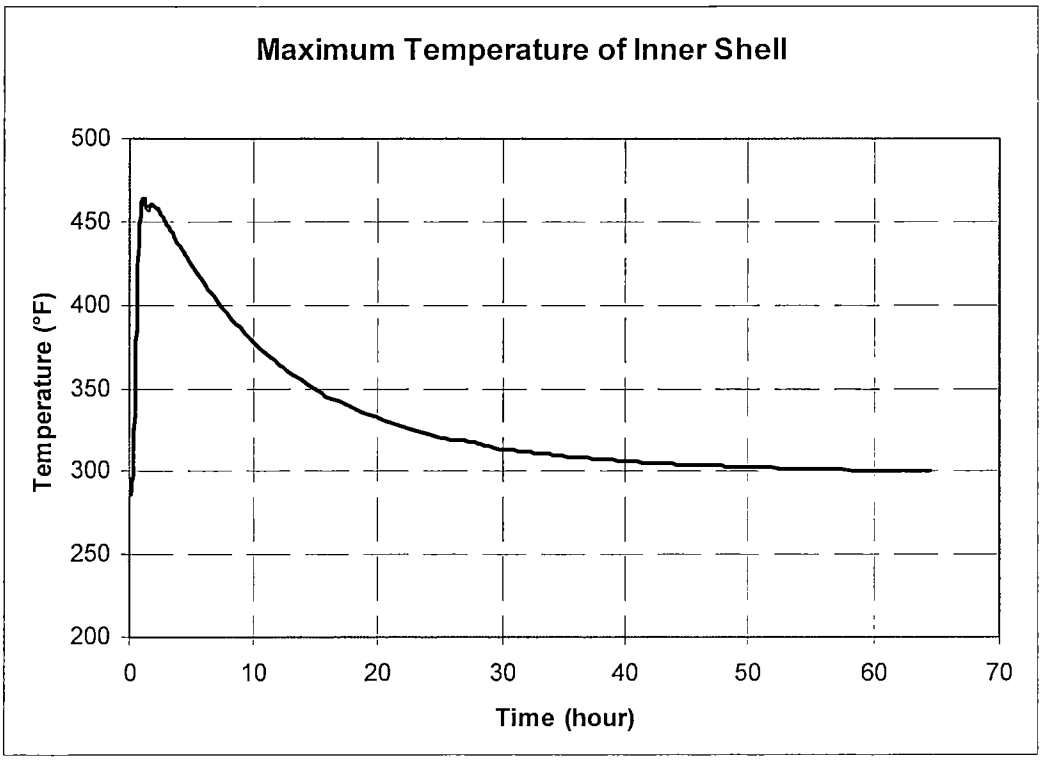

Figure 3.5-7 Hypothetical Accident Conditions Maximum Cask Outer Shell Temperature History

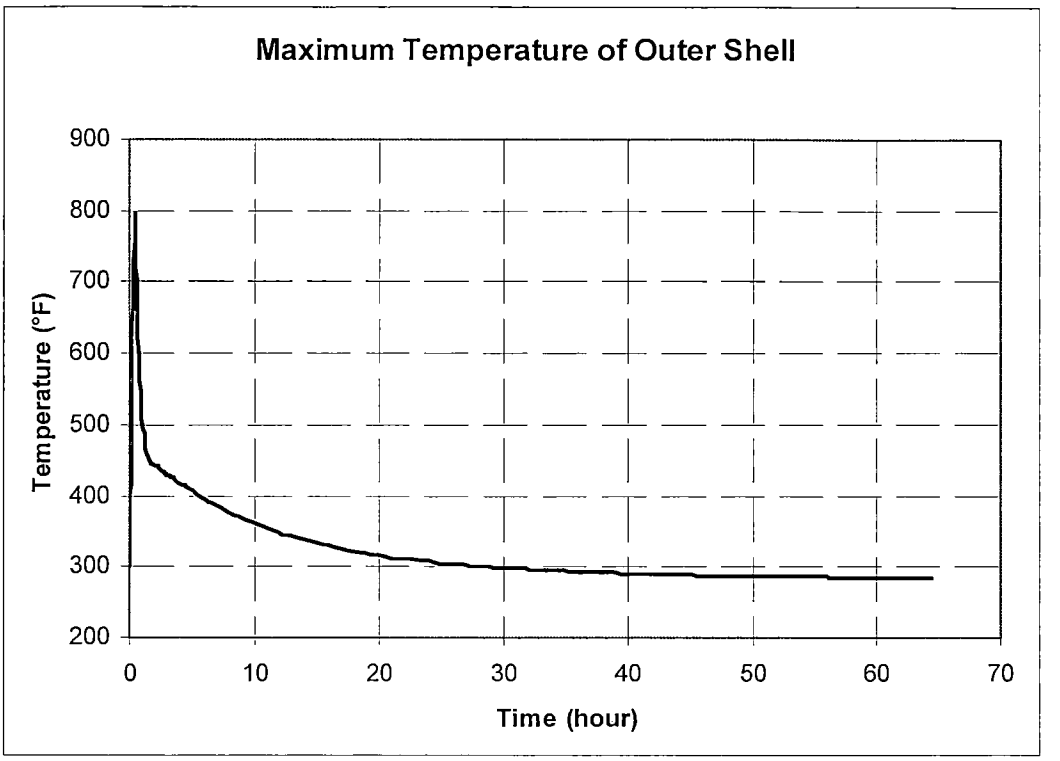

Figure 3.5-8 Hypothetical Accident Conditions Maximum Lid Containment O-Ring Temperature History

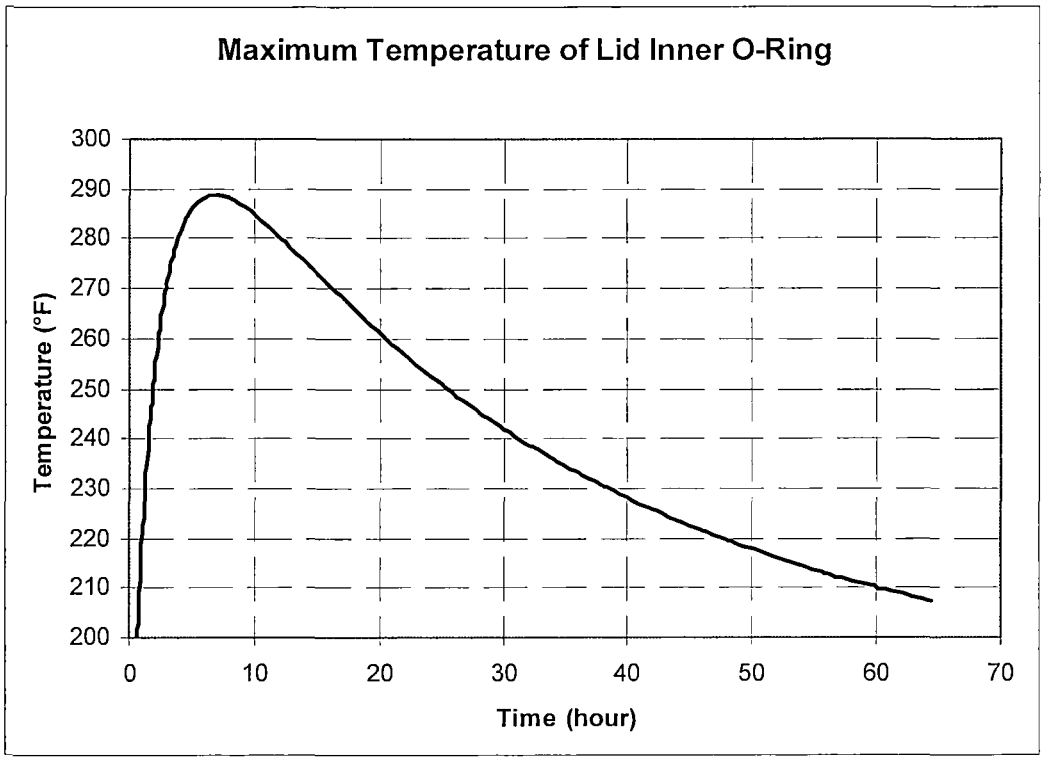

Figure 3.5-9 Hypothetical Accident Conditions Maximum Temperature of Lid Coverplate Containment O-Ring

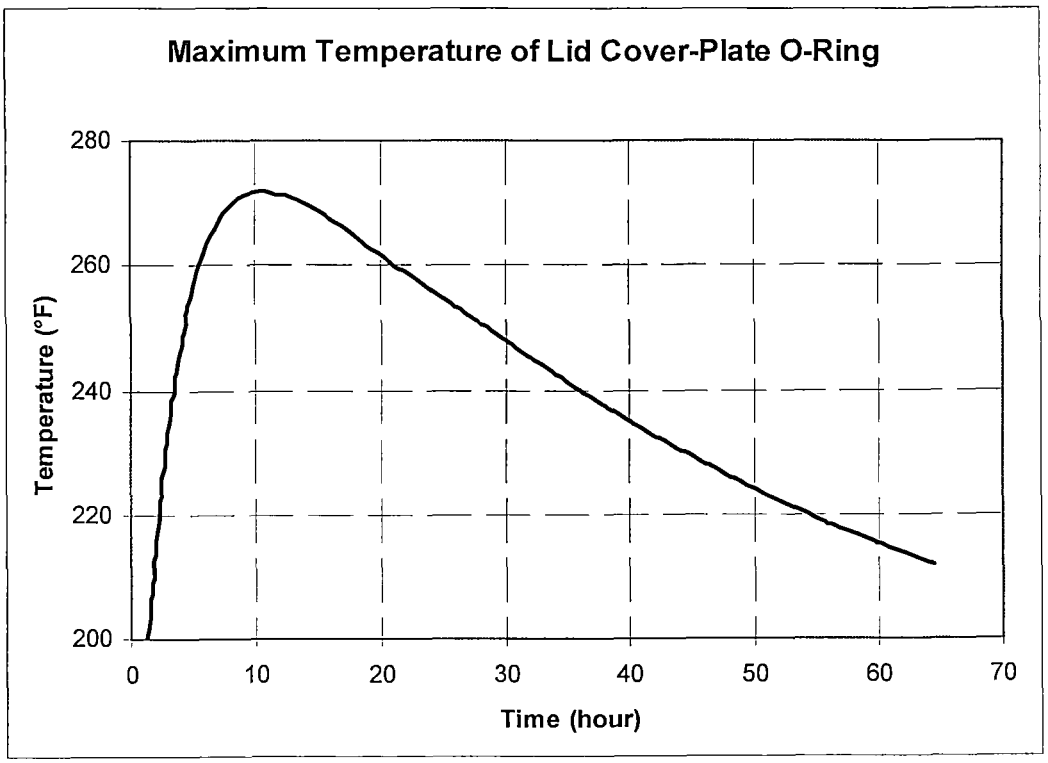

Table 3.5-1 Maximum Component Temperatures – Hypothetical Accident Condition Fire Transient (PWR Cask)

[redacted]

Table 3.5-2 Maximum Component Temperatures – Hypothetical Accident Condition Fire Transient (BWR Cask)

[redacted]

Table 3.5-3 Maximum Internal Pressures for Hypothetical Accident Conditions

[redacted]

List of Figures (cont'd)

Figure 5.6-10 Azimuthal Surface Dose Rate Profile by Source Type at Rotation Trunnion Elevation in Normal Conditions of Transport 5.6-15
Figure 5.6-11 [DELETED] 5.6-15
Figure 5.6-12 Bounding 1m Radial Dose Rate Profile for Accident Events of Transport 5.6-16
Figure 5.6-13 Bounding Top Axial Dose Rate Profiles for Accident Events of Transport 5.6-17
Figure 5.6-14 Bounding Bottom Axial Dose Rate Profiles for Accident Events of Transport 5.6-18
Figure 5.6-15 Bounding 2m from Transport Vehicle Dose Rate Profile for Normal Conditions of Transport – Damaged PWR Fuel 5.6-19
Figure 5.6-16 Bounding 2m from Top of Cask Dose Rate Profile for Normal Conditions of Transport – Damaged PWR Fuel 5.6-20
Figure 5.6-17 Bounding 2m from Bottom of Cask Dose Rate Profile for Normal Conditions of Transport – Damaged PWR Fuel 5.6-21
Figure 5.6-18 Bounding 1m from Side of Cask Dose Rate Profile for Accident Events of Transport – Damaged PWR Fuel 5.6-22
Figure 5.6-19 Bounding 1m from Top of Cask Dose Rate Profile for Accident Events of Transport – Damaged PWR Fuel 5.6-23
Figure 5.6-20 Bounding 1m from Bottom of Cask Dose Rate Profile for Accident Events of Transport – Damaged PWR Fuel 5.6-24
Figure 5.8-1 Comparison of Response Method to Direct Solution: Normal Condition Radial Surface – PWR Low Burnup/Low Enrichment 5.8.2-4
Figure 5.8-2 Comparison of Response Method to Direct Solution: Normal Condition Radial Surface – PWR Medium Burnup/Medium Enrichment 5.8.2-4
Figure 5.8-3 Comparison of Response Method to Direct Solution: Normal Condition Radial Surface – PWR High Burnup/High Enrichment 5.8.2-5
Figure 5.8-4 Comparison of Response Method to Direct Solution: Normal Condition Radial Surface – BWR Low Burnup/Low Enrichment 5.8.2-5
Figure 5.8-5 Comparison of Response Method to Direct Solution: Normal Condition Radial Surface – BWR Medium Burnup/Medium Enrichment 5.8.2-6
Figure 5.8-6 Comparison of Response Method to Direct Solution: Normal Condition Radial Surface 5.8.2-6
Figure 5.8-7 Normal Condition Radial Surface Dose Rates – Fresh Fuel versus Spent Fuel Isotopics – PWR – 60 GWd/MTU, 4.9 wt % ^{235}U 5.8.2-7
Figure 5.8-8 Accident Event Radial Surface Dose Rates– Fresh Fuel versus Spent Fuel Isotopics – PWR – 60 GWd/MTU, 4.9 wt % ^{235}U 5.8.2-7
Figure 5.8-9 PWR Basket, Top View 5.8.3-5
Figure 5.8-10 PWR Basket and TSC, Side View 5.8.3-6

List of Figures (cont'd)

Figure 5.8-11 PWR Bounding Radial Dose Rate Profiles for Normal Conditions of Transport 5.8.3-7
Figure 5.8-12 PWR Bounding Radial Surface Dose Rate Profile by Source Type for Normal Conditions of Transport 5.8.3-8
Figure 5.8-13 PWR Bounding 2m from Transport Vehicle Radial Dose Rate Profile by Source Type for Normal Conditions of Transport 5.8.3-9
Figure 5.8-14 PWR Bounding Top Axial Dose Rate Profiles for Normal Conditions of Transport 5.8.3-10
Figure 5.8-15 PWR Bounding Bottom Axial Dose Rate Profiles for Normal Conditions of Transport 5.8.3-11
Figure 5.8-16 PWR Azimuthal Radial Surface Dose Rate Profile by Source Type at Rotation Trunnion Elevation in Normal Conditions of Transport 5.8.3-12
Figure 5.8-16A PWR Azimuthal Radial Surface Dose Rate Profile by Source Type Neutron Shield Expansion Foam in Normal Conditions of Transport .. 5.8.3-13
Figure 5.8-16B PWR Azimuthal Radial 1-Foot Dose Rate Profile by Source Type Neutron Shield Expansion Foam in Normal Conditions of Transport .. 5.8.3-14
Figure 5.8-17 PWR Azimuthal Radial Surface Dose Rate Profile by Source Type over Neutron Shield Compartments in Normal Conditions of Transport 5.8.3-15
Figure 5.8-18 PWR Bounding Radial 1m Dose Rate Profile for Accident Events of Transport 5.8.3-16
Figure 5.8-19 PWR Bounding Top Axial Dose Rate Profiles for Accident Events of Transport 5.8.3-17
Figure 5.8-20 PWR Azimuthal Radial 1m Dose Rate Profile at Pin Puncture for Accident Events of Transport 5.8.3-18
Figure 5.8-21 PWR Bounding Bottom Axial Dose Rate Profiles for Accident Events of Transport 5.8.3-19
Figure 5.8-22 BWR Basket Top View 5.8.4-4
Figure 5.8-23 BWR Basket and TSC Side View 5.8.4-5
Figure 5.8-24 BWR Bounding Radial Dose Rate Profiles for Normal Conditions of Transport 5.8.4-6
Figure 5.8-25 BWR Bounding Radial Surface Dose Rate Profile by Source Type for Normal Conditions of Transport 5.8.4-7
Figure 5.8-26 BWR Bounding 2m from Transport Vehicle Radial Dose Rate Profile by Source Type for Normal Conditions of Transport 5.8.4-8
Figure 5.8-27 BWR Bounding Top Axial Dose Rate Profiles for Normal Conditions of Transport 5.8.4-9
Figure 5.8-28 BWR Bounding Bottom Axial Dose Rate Profiles for Normal Conditions of Transport 5.8.4-10
Figure 5.8-29 BWR Azimuthal Radial Surface Dose Rate Profile by Source Type at Rotation Trunnion Elevation in Normal Conditions of Transport 5.8.4-11

List of Figures (cont'd)

Figure 5.8-29B BWR Azimuthal Radial Surface Dose Rate Profile by Source Type at Neutron Shield Top Expansion Foam in Normal Conditions of Transport 5.8.4-12
Figure 5.8.29-C BWR Azimuthal Radial 1-Foot Dose Rate Profile by Source Type at Neutron Shield Top Expansion Foam in Normal Conditions of Transport 5.8.4-13
Figure 5.8-30 BWR Azimuthal Radial Surface Dose Rate Profile by Source Type above Neutron Shield Compartments in Normal Conditions of Transport 5.8.4-14
Figure 5.8-31 BWR Bounding Radial 1m Dose Rate Profile for Accident Events of Transport 5.8.4-15
Figure 5.8-32 BWR Bounding Top Axial Dose Rate Profiles for Accident Events of Transport 5.8.4-16
Figure 5.8-33 BWR Bounding Bottom Axial Dose Rate Profiles for Accident Events of Transport 5.8.4-17
Figure 5.8-34 PWR HFRA Source Term Sample Input File 5.8.5-7
Figure 5.8-35 [DELETED] – was Figure 5.8-34 in Revision 12A 5.8.5-7
Figure 5.8-36 [DELETED] – was Figure 5.8-35 in Revision 12A 5.8.5-7
Figure 5.8-37 [DELETED] – was Figure 5.8-36 in Revision 12A 5.8.5-7
Figure 5.8-38 CEA Stainless Steel/Inconel Spectrum Comparison 5.8.6-3
Figure 5.8-39 CEA Ag-In-Cd Spectrum Comparison 5.8.6-4
Figure 5.8-40 PWR Fuel Assembly Source Term Sample Input File 5.8.7-2
Figure 5.8-41 BWR Fuel Assembly Source Term Sample Input File 5.8.7-4
Figure 5.8-42 Normal Condition Transport Cask Sample Input File – PWR TSC 5.8.7-5
Figure 5.8-43 Normal Condition Transport Cask Sample Input File – BWR TSC 5.8.7-34
Figure 5.8-44 Accident Events Transport Cask Sample Input File – PWR TSC 5.8.7-51
Figure 5.8-45 Accident Events Transport Cask Sample Input File – BWR TSC 5.8.7-65
Figure 5.8-46 Millstone Sample Axial Burnup Profiles 5.8.9-3
Figure 5.8-47 [DELETED] – was Figure 5.8-46 in Revision 12A 5.8.10-5
Figure 5.8-48 [DELETED] – was Figure 5.8-47 in Revision 12A 5.8.10-5
Figure 5.8-49 [DELETED] – was Figure 5.8-48 in Revision 12A 5.8.10-5
Figure 5.8-50 [DELETED] – was Figure 5.8-49 in Revision 12A 5.8.10-5
Figure 5.8-51 [DELETED] – was Figure 5.8-50 in Revision 12A 5.8.10-5
Figure 5.8-52 [DELETED] – was Figure 5.8-51 in Revision 12A 5.8.10-5
Figure 5.8-53 Dose Rate Profile at 2m from Transport Vehicle of Normal Condition Cask – Damaged PWR Fuel 5.8.10-6
Figure 5.8-54 Dose Rate Profile at 2m from Top Surface of Normal Condition Cask – Damaged PWR Fuel 5.8.10-7
Figure 5.8-55 Dose Rate Profile at 2m from Bottom Surface of Normal Condition Cask – Damaged PWR Fue l 5.8.10-8
Figure 5.8-56 Dose Rate Profile at 1m from Radial Surface of Accident Event Cask – Damaged PWR Fuel 5.8.10-9

List of Figures (cont'd)

Figure 5.8-57 Dose Rate Profile at 1m from Top Surface of Accident Event Cask – Damaged PWR Fuel 5.8.10-10
Figure 5.8-58 Dose Rate Profile at 1m from Bottom Surface of Accident Event Cask – Damaged PWR Fuel 5.8.10-11
Figure 5.8-59 [DELETED] – was Figure 5.8-58 in Revision 12A 5.8.10-12
Figure 5.8-60 Damaged Fuel Azimuthal Dose Rate Profile at Transport Cask Radial 2-Meter Distance – Normal Conditions – Active Fuel Midplane 5.8.10-12
Figure 5.8-60B Damaged Fuel Azimuthal Dose Rate Profile at Transport Cask Radial 1-Foot Distance – Normal Conditions – Top of Neutron Shield 5.8-10-13
Figure 5.8-61 [DELETED] – was Figure 5.8-60 in Revision 12A 5.8.10-13
Figure 5.8-62 Normal Condition Cask Sample Input File – Damaged PWR Fuel TSC – Active Fuel Damaged Fuel 5.8.10-14
Figure 5.8-63 Accident Event Cask Sample Input File – Damaged PWR Fuel TSC – Nonfuel Hardware Region Damaged Fuel 5.8.10-44
Figure 5.8-64 ORIGEN-S Input File to Generate GTCC Waste Source Term 5.8.11-3
Figure 5.8-65 GTCC Model Sketch 5.8.11-4
Figure 5.8-66 VISED Image of GTCC Model Geometry 5.8.11-5
Figure 5.8-67 GTCC Sample Input File 5.8.11-6
Figure 5.8-68 Cooling Fin, Shield Bolt, and Expansion Foam Model Layout 5.8.12-5
Figure 5.8-69 Fuel Neutron, Surface Dose Rate (mRem/hr) Profile at Bolt Location . 5.8.12-6
Figure 5.8-70 Fuel Neutron, Surface Tally Dose Rate Comparison at Bolt Location .. 5.8.12-7
Figure 5.8-71 Fuel Gamma, Surface Dose Rate (mRem/hr) Profile at Bolt Location . 5.8.12-8
Figure 5.8-72 Fuel Gamma Surface Tally Dose Rate Comparison at Bolt Location ... 5.8.12-9
Figure 5.8-73 Fuel Neutron-Gamma, Surface Dose Rate (mRem/hr) Profile at Bolt Location 5.8.12-10
Figure 5.8-74 Fuel Neutron-Gamma Surface Tally Dose Rate Comparison at Bolt Location 5.8.12-11
Figure 5.8-75 Fuel Neutron, 2 Meter Dose Rate (mRem/hr) Profile at Bolt Location 5.8.12-12
Figure 5.8-76 Fuel Neutron, 2 Meter Tally Dose Rate Comparison at Bolt Location 5.8.12-13
Figure 5.8-77 Fuel Gamma, 2 Meter Dose Rate (mRem/hr) Profile at Bolt Location 5.8.12-14
Figure 5.8-78 Fuel Neutron-Gamma, 2 Meter Dose Rate (mRem/hr) Profile at Bolt Location 5.8.12-14
Figure 5.8-79 Bottom Rotation Trunnion Model Layout 5.8.12-15
Figure 5.8-80 Fuel Neutron, Surface Dose Rate (mRem/hr) Profile at Bottom Trunnion 5.8.12-16
Figure 5.8-81 Fuel Neutron, Surface Tally Dose Rate Comparison at Bottom Trunnion 5.8.12-17
Figure 5.8-82 Fuel Neutron, 2 Meter Dose Rate (mRem/hr) Profile at Bottom Trunnion 5.8.12-18
Figure 5.8-83 Fuel Neutron, 2 Meter Tally Dose Rate Comparison at Bottom Trunnion 5.8.12-19

List of Figures (cont'd)

Figure 5.8-84 Reconstituted Assembly Stainless Steel Rods Dose Rates [mrem/hr] – Normal Conditions Surface Azimuthal Detector 5.8.13-3
Figure 5.8-85 Reconstituted Assembly Stainless Steel Rods Dose Rates [mrem/hr] – Normal Conditions 2-meter Azimuthal Detector 5.8.13-4
Figure 5.8-86 Reconstituted Assembly Stainless Steel Rods Dose Rates [mrem/hr] – Accident Conditions 1-meter Azimuthal Detector 5.8.13-5

List of Tables

Table 5.1-1 Key Transport Cask Shielding Features 5.1-9
Table 5.1-2 Key TSC Shielding Features 5.1-9
Table 5.1-3 Normal Conditions Maximum Total Dose Rate Summary – Undamaged Fuel 5.1-9
Table 5.1-4 Maximum Hypothetical Accident Event Dose Rate Summary – Undamaged Fuel 5.1-10
Table 5.1-5 Normal Conditions Maximum Total Dose Rate Summary – Damaged PWR Fuel 5.1-10
Table 5.1-6 Maximum Hypothetical Accident Event Dose Rate Summary – Damaged PWR Fuel 5.1-10
Table 5.1-7 Normal Condition Maximum GTCC Waste Dose Rates 5.1-11
Table 5.1-8 Accident Condition Maximum GTCC Waste Dose Rates 5.1-11
Table 5.1-9 Bounding Source Type for Transport Cask Shielding – Undamaged Fuel 5.1-11
Table 5.1-10 Bounding Source Type for Transport Cask Shielding – Damaged PWR Fuel 5.1-12
Table 5.2-1 Key PWR Fuel Assembly Characteristics 5.2-6
Table 5.2-2 Key BWR Fuel Assembly Characteristics 5.2-6
Table 5.2-3 22-Group Gamma Energy Spectrum 5.2-7
Table 5.2-4 Bounding Regional Nonfuel Hardware Masses 5.2-8
Table 5.2-5 28-Group Neutron Energy Spectrum 5.2-9
Table 5.2-6 Gamma Source Spectrum – Maximum Radial Dose Configuration 5.2-10
Table 5.2-7 Neutron Source Spectrum – Maximum Radial Dose Configuration 5.2-11
Table 5.2-8 Gamma Source Spectrum – Maximum PWR Top Axial Dose Configuration 5.2-12
Table 5.2-9 Neutron Source Spectrum – Maximum PWR Top Axial Dose Configuration 5.2-13
Table 5.4-1 PWR Source Profile Integration 5.4-4
Table 5.4-2 BWR Source Profile Integration 5.4-5
Table 5.5-1 Typical Radial Surface Detector Division 5.5-11
Table 5.5-2 Typical Axial Surface Detector Division 5.5-11
Table 5.5-3 Fuel Basket, TSC, and Transport Cask Material Description 5.5-12
Table 5.5-4 Sample Fuel Region Homogenized Material Description (17a PWR Assembly) 5.5-13
Table 5.6-1 Sample Minimum Cool Time Calculation for WE 17 Fuel Assembly (Years) 5.6-25
Table 5.6-2 ANSI Standard Neutron Flux-To-Dose Rate Factors 5.6-25
Table 5.6-3 ANSI Standard Gamma Flux-To-Dose Rate Factors 5.6-26
Table 5.6-4 Bounding Source Type for Transport Cask Shielding – Undamaged Fuel 5.6-26
Table 5.6-5 Bounding Source Type for Transport Cask Shielding – Damaged PWR Fuel 5.6-27
Table 5.8-1 PWR Fuel Assembly Geometry Data 5.8.1-3

List of Tables (cont'd)

Table 5.8-2 PWR Fuel Assembly Nonzirconium Alloy-Based Hardware Mass 5.8.1-3
Table 5.8-3 PWR Sample In-Core Characteristics 5.8.1-3
Table 5.8-4 BWR Fuel Assembly Geometry Data 5.8.1-4
Table 5.8-5 BWR Fuel Assembly Nonzirconium Alloy-Based Hardware Quantities 5.8.1-4
Table 5.8-6 BWR Sample In-Core Characteristics 5.8.1-4
Table 5.8-7 Response Method to Direct Calculation Comparison – Transport Cask . 5.8.2-8
Table 5.8-8 Sample Gamma Response Calculation for Normal Condition Radial Surface-Fuel Centerline (35 GWd/MTU, 2.3 wt %, 7.6-Year Cooled 16a Hybrid) 5.8.2-9
Table 5.8-9 Sample Neutron Response Calculation for Normal Condition Radial Surface-Fuel Centerline (35 GWd/MTU, 2.3 wt %, 7.6-Year Cooled 16a Hybrid) 5.8.2-10
Table 5.8-10 Sample Hardware Gamma (Upper End-Fitting) Response Calculation for Normal Condition Radial Surface – Upper End-Fitting Elevation (35 GWd/MTU, 2.3 wt%, 7.6-Year Cooled 17a Hybrid) 5.8.2-11
Table 5.8-11 PWR Fuel Region Homogenization Sample Calculation 5.8.3-20
Table 5.8-12 PWR Nonfuel Hardware Homogenization Sample Calculation 5.8.3-20
Table 5.8-13 Key PWR Basket Geometry Features 5.8.3-20
Table 5.8-14 PWR Minimum Cool Time Solution 5.8.3-21
Table 5.8-14b Low Burnup PWR Fuel Loading Table 5.8.3-21
Table 5.8-15 Loading Table for PWR Fuel (23 kW/Cask) 5.8.3-22
Table 5.8-16 Loading Table for PWR Fuel (21.85 kW/Cask) 5.8.3-24
Table 5.8-17 PWR Normal Conditions Maximum Dose Rate Summary 5.8.3-25
Table 5.8-18 PWR Hypothetical Accident Event Maximum Dose Rate Summary ... 5.8.3-25
Table 5.8-19 BWR Fuel Region Homogenization Sample Calculation 5.8.4-18
Table 5.8-20 BWR Nonfuel Hardware Homogenization Sample Calculation 5.8.4-18
Table 5.8-21 BWR Fuel Region Homogenized Material Description 5.8.4-19
Table 5.8-22 Key BWR Basket Geometry Features 5.8.4-20
Table 5.8-23 BWR Minimum Cool Time Solution 5.8.4-20
Table 5.8-23b Low Burnup BWR Fuel Loading Table 5.8.4-20
Table 5.8-24 Loading Table for BWR Fuel (23 kW/Cask) 5.8.4-21
Table 5.8-25 BWR Normal Conditions Maximum Dose Rate Summary 5.8.4-23
Table 5.8-26 BWR Hypothetical Accident Event Maximum Dose Rate Summary .. 5.8.4-23
Table 5.8-27 Sample Core Type BPRA Hardware Summary – Westinghouse 15×15 Core 5.8.5-8
Table 5.8-28 Bounding Regional Nonfuel Hardware Masses 5.8.5-8
Table 5.8-29 Allowed BPRA Exposure and Cool Time Combinations 5.8.5-9
Table 5.8-30 BPRA Maximum Transport Detector Surface Dose Rates 5.8.5-9
Table 5.8-31 Allowed GTPD/NSA Exposure and Cool Time Combinations 5.8.5-9
Table 5.8-32 Thimble Plug Maximum Surface Dose Rates 5.8.5-10
Table 5.8-33 Westinghouse Fuel Reduced 2-Meter Dose Rates to Load NFHW 5.8.5-10

List of Tables (cont'd)

Table 5.8-34 Additional Fuel Assembly Cool Time Required to Load NFHW 5.8.5-10
Table 5.8-35 HFRA vs. BPRA Source Comparison 5.8.5-11
Table 5.8-36 Bounding CEA Mass Quantities Descriptions 5.8.6-5
Table 5.8-37 CEA Maximum Surface Dose Rates 5.8.6-5
Table 5.8-38 Gamma Source Comparison for CEA Primary Absorber Materials 5.8.6-6
Table 5.8-39 Dose Rates from Ag-In-Cd Based CEAs as a Function of Exposure and Cool Time 5.8.6-7
Table 5.8-40 CEA Maximum Exposure and Minimum Cool Time Summary 5.8.6-7
Table 5.8-41 [DELETED] – was Table 5.8-38 in Revision 12A 5.8.8-1
Table 5.8-42 [DELETED] – was Table 5.8-39 in Revision 12A 5.8.8-1
Table 5.8-43 [DELETED] – was Table 5.8-40 in Revision 12A 5.8.8-1
Table 5.8-44 [DELETED] – was Table 5.8-41 in Revision 12A 5.8.8-1
Table 5.8-45 Zoned Fuel and Profile Effects on Source Magnitudes 5.8.9-4
Table 5.8-46 Millstone Zoned Fuel Effects on Source Magnitudes 5.8.9-5
Table 5.8-47 Damaged Fuel Material Summary – 14a PWR Fuel 5.8.10-73
Table 5.8-48 PWR Damaged Fuel Comparison – Normal Conditions 2 Meter Radial Dose Rates 5.8.10-74
Table 5.8-49 Additional Cool Time Required for 23 kW Damaged PWR Fuel Contents 5.8.10-74
Table 5.8-50 Normal Condition Maximum Damaged PWR Fuel Dose Rates 5.8.10-75
Table 5.8-51 Accident Event Maximum Damaged PWR Fuel Dose Rates 5.8.10-75
Table 5.8-52 GTCC Source Spectrum 5.8.11-17
Table 5.8-53 GTCC Material Description 5.8.11-17
Table 5.8-54 Normal Condition Maximum GTCC Waste Dose Rates 5.8.11-18
Table 5.8-55 Accident Condition Maximum GTCC Waste Dose Rates 5.8.11-18
Table 5.8-56 Radial Surface Tally Detector Results for WE 14×14 Fuel Assembly 5.8.12-20
Table 5.8-57 Comparison of Surface Dose Rates with Localized Peaking 5.8.12-20

5.1 Description of Shielding Design

5.1.1 Design Features

The radiation protection provided by the package is in the form of solid multiwalled shielding materials that completely surround the fuel. These shielding materials include steel and lead for gamma shielding and a borated polymer (NS-4-FR) for neutron shielding. The multiwalled arrangement of steel and lead in the transport cask provides an optimal gamma shield. The NS-4-FR neutron shielding material, with a hydrogen density close to that of water, moderates neutrons and facilitates their capture in boron.

The configuration of the radial gamma shielding in the transport cask body is a thick stainless steel inner shell and outer shell with a lead-filled annulus between the two. The radial neutron shield assemblies surround the transport cask outer shell. The neutron shield assemblies are NS-4-FR wedges enclosed in stainless steel shells. Copper cooling fins are located below and between neutron shield assemblies. An aluminum cool fin is located on the exterior face of the neutron shield assemblies bolted to the cask body. Transport cask axial shielding is composed of steel plates and impact limiters. Impact limiters are composed of balsa wood and redwood surrounded by a thin steel shell. Only balsa wood is conservatively applied in the impact limiter model (lower density material). Key transport cask shielding dimensions are listed in Table 5.1-1. Details of the transport cask model are presented in Section 5.5.1, with materials defined in Section 5.5.2.

Further shielding is provided by the TSC and basket structure. The TSC is composed of a stainless steel shell capped by a bottom plate and closure lid. TSCs may be closed with either an all stainless steel closure lid or a composite carbon steel and stainless steel lid assembly. BWR and PWR evaluations are performed with the composite closure lid assembly. The composite lid assembly bounds the all stainless steel lid in shielding evaluations due to the lower density of carbon steel. Key TSC shielding characteristics are shown in Table 5.1-2. System-specific information on the basket structure is provided in Section 5.8.

5.1.2 Summary of Maximum Radiation Levels

The dose rate results are presented based on bounding heat loads and corresponding source terms based on a 23 kW PWR cask heat load and a 22 kW BWR cask heat load. Based on the code validation discussion in Section 5.2, a 5% uncertainty is applied to the heat loads for fuel assembly average burnups above 45 GWd/MTU. This results in an extension in minimum allowed cool time for those fuel assemblies, although bounding dose rates are conservatively reported from the higher heat load limit. For any fuel type, burnup, initial enrichment, and cool

time combination allowed, additional cool time and, therefore, reduced sources are associated with the lower cask heat load.

The calculated normal transport and hypothetical accident event dose rates are discussed in the following sections. The transport cask dose rates calculated include the following:

- neutrons and gamma-rays originating from the fuel
- neutrons resulting from subcritical multiplication
- secondary gamma-rays resulting from neutron capture in the neutron shield
- gamma-rays from activated materials in the grid spacers, end-fittings and plenum springs
- gamma-rays from activated nonfuel hardware (PWR only)

The results of the shielding analysis demonstrate that computed dose rates remain below 350 mrem/hr at all accessible locations on the surface of the package. The dose rates remain at or below 9.5 mrem/hr at locations 2 meters from the edge of the transport vehicle (any point 2 meters from the vertical planes projected from the outer edges of the conveyance), and 2 meters from the end surfaces of the impact limiters in the axial direction.

The MAGNATRAN cask requires rail or a heavy transport vehicle for movement. As shown in the dose rate summary tables, the maximum dose rates at 2 meters axially from the conservatively truncated impact limiter models were calculated at less than 4 mrem/hour. Occupied positions during transport are expected to be significantly further from the cask than 2 meters, and operator locations are expected to include shielding materials. Therefore, a transport configured MAGNATRAN system is expected to meet 2 mrem/hr at the "occupied location" limit of exclusive use vehicle.

In addition, the hypothetical accident events do not result in a dose rate that exceeds the accident event dose rate limit of 1 rem/hr at 1 meter from the transport cask surface. Therefore, the package satisfies the regulatory criteria of 10 CFR 71.47 under normal conditions of transport, and 10 CFR 71.51(a) for hypothetical accident events.

In the tabulated results, computed dose rates are reported along with the relative uncertainty associated with each computed value expressed as a percentage. The relative uncertainty corresponds to plus or minus one standard deviation in the quoted value.

Maximum dose rates are presented individually for damaged and undamaged fuel assembly payloads. Detailed PWR and BWR dose rate summaries for undamaged fuel are provided in Sections 5.8.3 and 5.8.4, respectively. The dose rate discussions in Sections 5.8.3 and 5.8.4 include plots detailing locations of maximum dose rates. The relevant data for damaged fuel is found in Section 5.8.10. Dose rates reported in this section are obtained from surface tally evaluations. Increases on the cask surface dose rates associated with radiation streaming through

paths not captured by the surface tallies are discussed in Section 5.8.12. Although some localized peaking occurs at areas over the neutron shield assemblies these locations do not produce maximum dose rates. At 2-meters from the transport package no resolvable peaking occurs.

GTCC dose rate discussions are documented in Section 5.8.11.

5.1.2.1 Undamaged Fuel

Normal Operating Conditions

The maximum radial and axial dose rates calculated for the package during normal conditions of transport are shown in Table 5.1-3. The locations of the maximum dose rates during normal conditions of transport relative to the transport cask body are shown in Figure 5.1-1. Table 5.1-3 presents the maximum computed dose rates and corresponding relative uncertainties on radial and axial surfaces outside the transport cask. In the radial case, dose rates indicated at the "2m position" correspond to a position 2 meters from the edge of a 124-inch-wide standard railcar. For axial results, this position corresponds to a dose rate location 2 meters from the modeled upper or lower impact limiter surface (as shown in the modeling section, impact limiters are conservatively truncated in height).

Dose rates shown in Table 5.1-3 and Figure 5.1-1 correspond to maximum values regardless of payload type and TSC length. Additional bounding dose rate information is provided in Section 5.6.4.

Hypothetical Accident Events

Table 5.1-4 provides accident dose rates. Dose rates are calculated based on the loss of the impact limiters, the loss of aluminum cooling fins (copper cooling fins are retained), pin puncture, the combustion of gaseous elements in the transport cask neutron shield, and both radial and axial lead slumps. The locations of the maximum hypothetical accident dose rates relative to the transport cask body are shown in Figure 5.1-2.

An accident involving the complete loss of the impact limiters is not credible. Axial and radial lead slumps resulting from postulated transport cask side-drop and end-drop accidents are modeled simultaneously in the analysis. In the event of a transport cask end drop, the lead gamma shielding could slump and fill the annular gap (if one exists) created by the cooling of the lead after fabrication. If the transport cask is subjected to a side drop, the lead gamma shielding could slump and create a void on the upper side of the transport cask. A combined accident event model clearly bounds any accident configuration postulated to occur during fuel transport.

The dose rates presented here, and further detailed in Section 5.6.4 and Section 5.8, show that neither the partial loss of the neutron shielding nor the lead slump conditions will result in dose rates that exceed the limit of 1 rem/hr at 1 meter from the surface of the transport cask.

The bounding fuel type, cool time, burnup and initial enrichment for each detector surface under normal conditions and accident events is given in Table 5.1-9. BWR results are bounding for radial detectors and PWR results are bounding for axial detectors.

5.1.2.2 Damaged Fuel

Damaged PWR fuel may be loaded in damaged fuel cans (DFCs) in the four corner assembly locations of the PWR damaged fuel basket (DF Basket Assembly). [redacted] model includes the neutron absorber sheets and reduces the ^{235}U enrichment to the maximum allowed fresh fuel enrichment from the criticality evaluation (2 wt% ^{235}U). Additional undamaged cases are run with the same model changes to enable a direct comparison in the damaged fuel evaluation. To ensure that the worst case configuration is considered, two damaged fuel scenarios are evaluated.

The first scenario assumes the damaged fuel collects over the active fuel length of the fuel assembly. This scenario is modeled by filling the fuel assembly interstitial volume with UO_2 and increasing the fuel neutron, gamma and n-gamma source consistent with this increase in mass. A comparison of dose rate profiles for the 37-assembly undamaged fuel results and the combination of 33 undamaged assemblies and four DFCs in Section 5.8.10 demonstrates that the damaged fuel over the active fuel region increases dose rates.

In the second scenario, damaged fuel is assumed to migrate from the active fuel into the nonfuel hardware (i.e., lower end fitting, upper plenum, and upper end fitting) regions of the fuel assembly, filling all the modeled void space. However, no credit is taken for the reduction in hardware dose rate due to the added UO_2 mass and self-shielding nor for the reduction in fuel mass migrated from the active fuel region. In this scenario, dose rates increase due to the addition of damaged fuel.

As both scenarios result in increased dose rates, damaged fuel maximum dose rates reported in this section are based on a combination (simple addition of dose rates) of the two scenarios.

Damaged fuel is limited to PWR contents placed into a short TSC (i.e., TSC requiring a top cask cavity spacer). As the top cask cavity spacer maintains the location of the source region away from the gap between the neutron shield and the upper impact limiter, the dose rate at the gap is lower and the undamaged fuel dose rates are bounding for radial 1m and 2m dose rate locations.

Normal Operating Conditions

The maximum radial and axial dose rates calculated for the package under normal conditions of transport for damaged PWR fuel are shown in Table 5.1-5. The locations of the maximum dose rates during normal conditions of transport relative to the transport cask body for damaged PWR fuel are shown in Figure 5.1-3. Additional bounding dose rate information is provided in Section 5.6.4.

Hypothetical Accident Events

Table 5.1-6 provides the calculated hypothetical accident condition dose rates. The locations of the maximum hypothetical accident dose rates relative to the transport cask body are shown in Figure 5.1-4. Additional bounding dose rate information is provided in Section 5.6.4.

The bounding PWR fuel type, cool time, burnup and initial enrichment for each detector under normal conditions and accident events are given in Table 5.1-10.

5.1.2.3 Greater than Class C (GTCC) Waste

GTCC waste may be transported in the MAGNATRAN canister. Only the "short" TSC is evaluated for GTCC contents. This configuration contains a top spacer in the transport cask cavity separating the GTCC source region from the impact limiter to neutron shield assembly gap where maximum dose rates occur. The shielding evaluation of GTCC waste is based on quantities of waste from the decommissioning of Zion Nuclear Power Station (ZNPS). Bounding source terms were generated based on the maximum GTCC weight loaded in the TSC, as defined by project-specific operational control (32,000 lbs). Maximum dose rates for the normal condition of transport for GTCC waste are presented in Table 5.1-7 and Figure 5.1-5. The maximum dose rates for the accident condition of transport for GTCC waste are presented in Table 5.1-8 and Figure 5.1-6. The Transport Index for GTCC waste shipments is 2.4 mrem/hr, while the maximum heat load is 1.7 kW.

Figure 5.1-1 Location of Maximum Dose Rates for Normal Conditions of Transport – Undamaged Fuel

[redacted]

Figure 5.1-2 Location of Maximum Dose Rates for Hypothetical Accident Events – Undamaged Fuel

[redacted]

Table 5.1-1 Key Transport Cask Shielding Features

[redacted]

Table 5.1-2 Key TSC Shielding Features

[redacted]

Table 5.1-3 Normal Conditions Maximum Total Dose Rate Summary – Undamaged Fuel

[redacted]

Table 5.1-4 Maximum Hypothetical Accident Event Dose Rate Summary – Undamaged Fuel

[redacted]

Table 5.1-5 Normal Conditions Maximum Total Dose Rate Summary – Damaged PWR Fuel

[redacted]

Table 5.1-6 Maximum Hypothetical Accident Event Dose Rate Summary – Damaged PWR Fuel

[redacted]

Table 5.1-7 Normal Condition Maximum GTCC Waste Dose Rates

[redacted]

Table 5.1-8 Accident Condition Maximum GTCC Waste Dose Rates

[redacted]

Table 5.1-9 Bounding Source Type for Transport Cask Shielding – Undamaged Fuel

Model	Detector Biasing	Fuel Type	Burnup [GWd/MTU]	Enrichment [wt % ^{235}U]	Cool Time [Years]
Normal Conditions	Radial	09b	30	4.3	7.7
	Top Axial	14b	60	3.3	37.6
	Bottom Axial	14a	60	3.3	32.5
Accident Events	Radial	07a	60	3.3	42.3
	Top Axial	14b	60	3.3	37.6
	Bottom Axial	14a	60	3.3	32.5

Table 5.1-10 Bounding Source Type for Transport Cask Shielding – Damaged PWR Fuel

Model	Detector Biasing	Fuel Type	Burnup [GWd/MTU]	Enrichment [wt % ^{235}U]	Cool Time [Years]
Normal Conditions	Radial	14a	55	3.3	24.2
	Top Axial	14b	60	3.3	37.6
	Bottom Axial	14a	60	3.3	32.5
Accident Events	Radial	14a	60	3.3	32.5
	Top Axial	14b	60	3.3	37.6
	Bottom Axial	14a	60	3.3	32.5

5.2 Source Specification

To generate radiation and thermal source terms, the PWR and BWR fuel assembly types are surveyed and grouped by primary characteristics critical to shielding and source term evaluations. Critical criteria are the basic reactor type in which the fuel assembly operated, fuel mass (MTU) and hardware mass. For each assembly group, a hybrid assembly is generated. The hybrid assembly contains the maximum fuel mass and hardware masses of any assembly within the group. This combination leads to a conservative source term in each TSC. The critical characteristics are listed in Table 5.2-1 for PWR assemblies and Table 5.2-2 for BWR assemblies. Fuel assembly hardware quantities for nonzirconium-based hardware are included in Section 5.8.1. This hardware may contribute significantly to transport cask surface dose rates as a result of ^{59}Co activation. Refer to Section 5.8.1 for the geometry aspects and hardware quantities of the evaluated PWR and BWR fuel assembly hybrids.

The SAS2H code sequence of the SCALE 4.4 package with 44-group ENDF/B-V cross-section libraries is used to generate source terms for the shielding analysis. SAS2H includes an XSDRNPM neutronics model of the fuel assembly and the ORIGEN-S code for fuel depletion and source term calculations. Source terms are generated for both UO_2 fuel and fuel assembly hardware.

The 44-group library (44GROUPNDF5) is composed primarily of ENDF/B-V cross-sections with ENDF/B-VI data for a limited number of isotopes (e.g., ^{154}Eu and ^{155}Eu). The cross-section set is collapsed using an LWR spectrum. References 25 through 29 contain extensive SAS2H validation for PWR burnups up to 47 GWd/MTU and BWR burnups up to 57 GWd/MTU. As indicated in the reference documentation, the combination of the SCALE 4.4 SAS2H sequence and the 44 GROUPNDF5 cross-section library is applicable to LWR fuel assembly source term generation for high burnup fuel.

Open literature validations of the SCALE SAS2H/44 group library versus experimental data do not extend to the system allowable assembly average burnup of 60 GWd/MTU peak average rod. Studies performed in NUREG/CR-6701 (Appendix A and Appendix B) indicate no analysis trends in system sensitivity for LWR SAS2H/44GROUPNDF5 evaluations up to a burnup of 75 GWd/MTU. As such, the SAS2H/44GROUPNDF5 sequence is applicable to the high burnup fuel evaluated.

Source terms are generated on an assembly average burnup basis using SAS2H and are adjusted to reflect the burnup profile as discussed in Section 5.3 and Section 5.6. Peak average rod burnup limitations are the result of limited available data on the material properties of high burnup fuel cladding and its behavior during storage conditions. The peak average rod burnup is only listed in this section to demonstrate that available validation data on SAS2H of burnups up

to 57 GWd/MTU, and trending in NUREG/CR-6701 up to 75 GWd/MTU, are applicable to the assemblies evaluated.

Due to the limited experimental PWR and BWR data available for the SAS2H sequence as applied to higher burnup (> 45 GWd/MTU) fuel assemblies, a 5% decrement in heat load is applied at the higher burnup fuel levels. The heat load decrement implies an extension in minimum cool time required for higher burnup fuel and provides additional margin to account for any uncertainties in the source generation method. Note that this reduction will also reduce neutron and gamma source terms below those previously discussed in Section 5.1.

Measured to calculated isotope ratios in the code validation, while near 1, do not eliminate the potential for under prediction of neutron and gamma source term. Source generation methods are designed to compensate for this by applying conservative inputs, such as constant power versus reduced power at end of life and constant boron content in the PWR moderator rather than sloped boron content going from high to low. To provide additional margin, and to provide reasonable assurance that dose rate limits will be met on the system, dose rate limits at 2-meter from conveyance, the limiting dose rate location, is reduced to 9.5 mrem/hr in all analysis. A further conservatism, a very conservative subcritical multiplication, is discussed in the neutron source section (Section 5.2.2).

The hardware activation is calculated by light element transmutation using the in-core neutron flux spectrum produced by the SAS2H neutronics model. The effects of axial flux spectrum and magnitude variation on hardware activation are estimated by flux ratios determined from empirical data. Refer to Section 5.8.1 for the in-core reactor primary system properties required for burnup calculations for the PWR and BWR systems. Refer to Section 5.8.7 for sample PWR and BWR SAS2H input files.

Rather than determining a single cool time, burnup and initial enrichment combination acceptable for all payloads, source terms are produced in the following range:

- Assembly average burnup from 30,000 MWd/MTU to 60,000 MWd/MTU
- Assembly average initial enrichment 2.1 wt% ^{235}U to 4.9 wt% ^{235}U
- Cool time from 4 years to 60 years

5.2.1 Gamma Source

The gamma source term of the spent fuel assembly is composed of fuel gamma source (i.e., fission product and actinide sources) and a light element activation source primarily associated with fuel hardware. Spectra are initially produced in the default 18-group energy spectrum of ORIGEN-S at reactor shutdown. The source is then decayed and rebinned into the 22-energy

group gamma structure shown in Table 5.2-3. The 22-group structure shown is the default MCBEND structure and provides improved binning at the ^{60}Co energy lines. Source generation and rebin are accomplished in the same computer run using the SCALE 4.4 stacked input file structure.

The light element gamma spectra contain contributions primarily from ^{60}Co due to the activation of stainless steel or inconel hardware components. Hardware activation is based on an assembly average nonzirconium alloy structural material ^{59}Co level of 0.8 g/kg. Minor dose rate contributions result from the hardware ^{59}Ni and ^{58}Fe activation and activation of the zirconium alloy clad impurities. The nonzirconium alloy hardware gamma spectral distribution is determined by the irradiation of 1 kg of material (modeled as stainless steel) in the in-core flux spectrum produced by the SAS2H neutronics calculation. Activated fuel assembly hardware source term magnitudes are determined by multiplying the source strength from the 1 kg SAS2H run by the total mass of nonzirconium in the active fuel, plenum and end-fitting regions, and then multiplying this result by a regional flux activation ratio. This regional flux ratio accounts for the effects of both magnitude and spectrum variation on hardware activation. The following list provides the flux ratios for the various source regions.

Region	Generic PWR	CE16×16 PWR	B&W PWR	Generic BWR
Upper-End Fitting	0.10	0.05	0.10	0.10
Upper Plenum	0.20	0.20	0.20	0.20
Fuel	1.00	1.00	1.00	1.00
Lower Plenum	N/A	N/A	0.20	N/A
Lower-End Fitting	0.20	0.20	0.10	0.15

Additional gamma source is produced by nonfuel hardware included in the PWR system evaluation. Included nonfuel hardware components are control element assemblies (CEAs), reactor control cluster assemblies (RCCAs), burnable poison rod assemblies (BPRAs), thimble plugs (also referred to as guide tube plugs or flow mixers), reconstituted fuel assemblies with stainless steel fuel replacement rods, and hafnium flux reduction assemblies (HFRAs). Table 5.2-4 contains the activated nonfuel hardware mass by core type for BPRAs, thimble plugs, stainless steel rods, and HFRAs. Combustion Engineering (CE) cores employ integral absorber rods that replace some fuel rods. Assuming all lattice locations are filled with fuel rods bounds the in-lattice absorber rods. Refer to Section 5.8.5, Section 5.8.6 and Section 5.8.13 for more information on the nonfuel components.

Source term calculations are based on an exposure equivalent to 70 GWd/MTU for BPRAs (modeled as a three-cycle exposure, but may be any number of cycles), and an exposure equivalent to 180 GWd/MTU burnup for thimble plugs and 360 GWd/MTU burnup for CEAs. Exposure of the stainless steel fuel replacement rods is limited to 32.5 GWd/MTU, as the rods

were inserted after at least one cycle assembly depletion has occurred. The steel rods are designed to replace fuel rods that were removed for examination or due to failure. The number of replacement rods is limited to five per assembly and one assembly per cask. Up to 37 HFRAs may be loaded in the basket at a maximum exposure of 4.0 GWd/MTU per HFRA, and up to 20 Hf rods may be placed in one assembly. Activation of the nonfuel hardware is treated identical to that of the fuel assembly hardware, including the use of flux factors to account for the location of the activated material in relation to the full (100%) in-core flux employed in the SAS2H depletion calculations.

5.2.2 Neutron Source

Light water reactor spent fuel neutron sources result from actinide spontaneous fission and from (α,n) reactions. The isotopes ^{242}Cm and ^{244}Cm characteristically produce all but a few percent of the spontaneous fission neutrons and (α,n) source. Similar to the gamma spectrum, the neutron energy spectrum is decayed and rebinned into the MCBEND default neutron structure using ORIGEN-S. The MCBEND neutron spectrum is listed in Table 5.2-5.

Neutron shielding evaluations for fissile material must account for subcritical multiplication (neutron production) inside the system being evaluated. This subcritical multiplication is taken into account by MCNP. For PWR and BWR undamaged fuel evaluations the subcritical multiplication contains significant conservatism as the fuel material included in the model is fresh fuel at 5wt % ^{235}U and neutron absorbers are not modeled. Combining the high fissile material content and no neutron absorber significantly overpredicts the subcritical multiplication in the system and will therefore overpredict neutron and n-γ dose rates. Damaged fuel analysis applied fissile material content representative of the maximum material quantity allowed by Chapter 6 limitations and modeled neutron absorbers. The magnitude of this conservatism is addressed within the damaged fuel basket analysis (Section 5.8.10). Damaged fuel analysis contain their own subcritical multiplication conservatism as the fuel mass within the DFC modeled is significantly higher than that allowed for loading (see Section 5.8.10 for additional discussion).

Additional neutron source is produced by primary and secondary neutron source assemblies (NSAs) included in the PWR system. Primary and secondary sources have a neutron source magnitude similar to that of an irradiated fuel assembly. Neutron sources may be loaded in one of the center nine basket locations, provided the number of NSAs is limited to one per cask.

Table 5.2-5 28-Group Neutron Energy Spectrum

Group	E Lower [MeV]	E Upper [MeV]	E Average [MeV]
1	1.360E+01	1.460E+01	1.410E+01
2	1.250E+01	1.360E+01	1.305E+01
3	1.125E+01	1.250E+01	1.188E+01
4	1.000E+01	1.125E+01	1.063E+01
5	8.250E+00	1.000E+01	9.125E+00
6	7.000E+00	8.250E+00	7.625E+00
7	6.070E+00	7.000E+00	6.535E+00
8	4.720E+00	6.070E+00	5.395E+00
9	3.680E+00	4.720E+00	4.200E+00
10	2.870E+00	3.680E+00	3.275E+00
11	1.740E+00	2.870E+00	2.305E+00
12	6.400E-01	1.740E+00	1.190E+00
13	3.900E-01	6.400E-01	5.150E-01
14	1.100E-01	3.900E-01	2.500E-01
15	6.740E-02	1.100E-01	8.870E-02
16	2.480E-02	6.740E-02	4.610E-02
17	9.120E-03	2.480E-02	1.696E-02
18	2.950E-03	9.120E-03	6.035E-03
19	9.610E-04	2.950E-03	1.956E-03
20	3.540E-04	9.610E-04	6.575E-04
21	1.660E-04	3.540E-04	2.600E-04
22	4.810E-05	1.660E-04	1.071E-04
23	1.600E-05	4.810E-05	3.205E-05
24	4.000E-06	1.600E-05	1.000E-05
25	1.500E-06	4.000E-06	2.750E-06
26	5.500E-07	1.500E-06	1.025E-06
27	7.090E-08	5.500E-07	3.105E-07
28	1.000E-11	7.090E-08	3.546E-08

Table 5.2-6 Gamma Source Spectrum – Maximum Radial Dose Rate Configuration

Fuel Type Burnup Cool Time Initial Enrichment	PWR 60,000 MWd/MTU 34.6 yrs 3.3 wt % ^{235}U		BWR 30,000 MWd/MTU 7.7 yrs 4.3 wt % ^{235}U	
Group	[γ/sec/assy]	[γ/sec/kg]	[γ/sec/assy]	[γ/sec/kg]
1	0.0000E+00	0.0000E+00	0.0000E+00	0.0000E+00
2	1.2808E+04	2.5561E+01	4.3032E+02	1.9168E+00
3	2.4772E+05	4.9439E+02	8.3245E+03	3.7080E+01
4	1.1667E+06	2.3284E+03	3.9220E+04	1.7470E+02
5	5.9479E+06	1.1870E+04	2.0002E+05	8.9095E+02
6	1.4821E+07	2.9579E+04	4.9867E+05	2.2212E+03
7	4.3907E+07	8.7627E+04	3.4438E+08	1.5340E+06
8	2.9904E+08	5.9681E+05	2.7670E+09	1.2325E+07
9	2.8128E+09	5.6136E+06	7.6462E+10	3.4059E+08
10	5.4023E+10	1.0782E+08	6.4716E+10	2.8827E+08
11	4.4105E+11	8.8022E+08	5.7562E+11	2.5640E+09
12	4.6388E+12	9.2579E+09	8.0171E+12	3.5711E+10
13	2.9913E+12	5.9699E+09	4.9802E+12	2.2183E+10
14	6.2430E+12	1.2459E+10	2.9088E+13	1.2957E+11
15	1.1531E+15	2.3013E+12	5.4217E+14	2.4150E+12
16	1.5121E+13	3.0177E+10	6.2720E+13	2.7938E+11
17	2.1213E+13	4.2336E+10	1.3367E+13	5.9542E+10
18	3.1257E+13	6.2381E+10	1.9613E+13	8.7362E+10
19	1.0033E+14	2.0023E+11	6.5710E+13	2.9269E+11
20	1.6653E+14	3.3235E+11	9.0954E+13	4.0514E+11
21	3.6386E+14	7.2618E+11	2.0986E+14	9.3479E+11
22	2.8489E+14	5.6857E+11	1.5222E+14	6.7805E+11
Total	2.1507E+15	4.2923E+12	1.1994E+15	5.3427E+12

Table 5.2-7 Neutron Source Spectrum – Maximum Radial Dose Rate Configuration

Fuel Type Burnup Cool Time Initial Enrichment	PWR 60,000 MWd/MTU 34.6 yrs 3.3 wt % ^{235}U	BWR 30,000 MWd/MTU 7.7 yrs 4.3 wt % ^{235}U
Group	[n/sec/assy]	[n/sec/assy]
1	0.000E+00	0.000E+00
2	2.847E+04	9.458E+02
3	1.186E+05	3.941E+03
4	3.940E+05	1.309E+04
5	1.236E+06	4.107E+04
6	3.319E+06	1.103E+05
7	5.729E+06	1.903E+05
8	1.917E+07	6.368E+05
9	3.258E+07	1.098E+06
10	4.416E+07	1.558E+06
11	1.050E+08	3.713E+06
12	1.633E+08	5.509E+06
13	4.249E+07	1.415E+06
14	1.474E+07	4.912E+05
15	4.394E+02	4.074E+01
16	0.000E+00	0.000E+00
17	0.000E+00	0.000E+00
18	0.000E+00	0.000E+00
19	0.000E+00	0.000E+00
20	0.000E+00	0.000E+00
21	0.000E+00	0.000E+00
22	0.000E+00	0.000E+00
23	0.000E+00	0.000E+00
24	0.000E+00	0.000E+00
25	0.000E+00	0.000E+00
26	0.000E+00	0.000E+00
27	0.000E+00	0.000E+00
28	0.000E+00	0.000E+00
Total	4.323E+08	1.478E+07

Table 5.2-8 Gamma Source Spectrum – Maximum PWR Top Axial Dose Rate Configuration

Fuel Type Burnup Cool Time Initial Enrichment	PWR 60,000 MWd/MTU 37.6 yrs 3.3 wt % ^{235}U	
Group	[γ/sec/assy]	[γ/sec/kg]
1	0.0000E+00	0.0000E+00
2	1.1059E+04	2.3523E+01
3	2.1389E+05	4.5495E+02
4	1.0075E+06	2.1430E+03
5	5.1360E+06	1.0925E+04
6	1.2798E+07	2.7222E+04
7	3.7916E+07	8.0649E+04
8	3.0058E+08	6.3935E+05
9	2.3952E+09	5.0947E+06
10	4.5961E+10	9.7761E+07
11	3.6216E+11	7.7033E+08
12	3.7564E+12	7.9900E+09
13	2.4727E+12	5.2595E+09
14	5.1422E+12	1.0938E+10
15	9.9100E+14	2.1079E+12
16	1.2785E+13	2.7194E+10
17	1.8060E+13	3.8415E+10
18	2.6630E+13	5.6643E+10
19	8.5315E+13	1.8147E+11
20	1.4606E+14	3.1068E+11
21	3.1082E+14	6.6113E+11
22	2.4702E+14	5.2542E+11
Total	1.8495E+150.0000E+00	3.9340E+120.0000E+00

Table 5.2-9 Neutron Source Spectrum – Maximum PWR Top Axial Dose Rate Configuration

Fuel Type Burnup Cool Time Initial Enrichment	PWR 60,000 MWd/MTU 37.6 yrs 3.3 wt % ^{235}U
Group	[n/sec/assy]
1	0.000E+00
2	2.459E+04
3	1.024E+05
4	3.403E+05
5	1.068E+06
6	2.866E+06
7	4.948E+06
8	1.655E+07
9	2.816E+07
10	3.829E+07
11	9.106E+07
12	1.412E+08
13	3.670E+07
14	1.273E+07
15	4.225E+02
16	0.000E+00
17	0.000E+00
18	0.000E+00
19	0.000E+00
20	0.000E+00
21	0.000E+00
22	0.000E+00
23	0.000E+00
24	0.000E+00
25	0.000E+00
26	0.000E+00
27	0.000E+00
28	0.000E+00
Total	3.740E+08

5.3 Axial Burnup Profile

Fuel burned at least 30 GWd/MTU produces the maximum dose rates as shown in Section 5.1.2.

For PWR fuel, an enveloping axial burnup profile with a 1.08 uniform peaking factor is justified on the basis of calculated PWR data from Seabrook Station and Maine Yankee and measured Turkey Point gamma data. This normalized enveloping shape is shown in Figure 5.3-1. A uniform burnup peaking factor of 1.08 is applied between 15% and 85% of core height. Above and below these elevations, the relative burnup/decay heat decreases linearly to 0.547 at the top and bottom of the active fuel region.

For BWR fuel, an enveloping burnup profile with a 1.22 maximum peaking factor can be justified on the basis of calculated BWR burnup profile data from Columbia (formerly Washington Public Power) BWR/4-6 data. This normalized enveloping shape is shown in Figure 5.3-2.

Uniform peaking factors of 1.22 and 1.18 are applied from 15% to 55% and from 55% to 80% of core height, respectively. Above and below these elevations, the burnup profile decreases linearly to 0.043 at the top and bottom of the active fuel region. This profile bounds the burnup peaks listed in Vermont Yankee and Takoi-2 BWR nuclear power station burnup curves, demonstrating that the detailed information from Columbia represents typical BWR operational data and may be used as the generic licensing basis.

The axial burnup profile changes as fuel burnup progresses from initial in-core loading (0 GWd/MTU) to the maximum burnup requested (60 GWd/MTU). For PWR fuel assemblies, maximum burnup peaking occurs in the range of 10 to 15 GWd/MTU with a peak of approximately 1.25. The burnup profile peak then decreases as burnup increases to the 30 GWd/MTU range, after which the peak remains relatively constant. For BWR fuel assemblies, similar peaking occurs early during depletion with a bottom peak near 1.35 in the range of 10-20 GWd/MTU. The BWR peak burnup ratio then decreases to the 1.22 peak discussed above. Dose rate calculations summarized in Section 5.1 demonstrate that, at a fixed burnup profile, fuel assemblies burned in excess of 30 GWd/MTU produce maximum dose rates. For a fixed burnup profile, Figure 5.3-3 (normal conditions) and Figure 5.3-4 (accident events) illustrate the dose rate increase as a function of burnup that offsets any potential increase in burnup peak at lower burnup levels.

Figure 5.3-5 contains YAEC compiled PWR burnup profiles at 5 GWd/MTU increments showing low burnup fuel having a higher peak. Peaking is less than 10% higher for the low burnup material, which is a smaller increase than the dose rate decreases plotted in Figure 5.3-3 and

Figure 5.3-4 for the lower burnup fuels. The 30 GWd/MTU derived profile is applied in the shielding evaluations summarized in Sections 5.1 and 5.6 and detailed in Section 5.8.

PWR and BWR fuel assemblies may contain axial unenriched end regions (blankets). In particular, BWR/4-6 type reactor assemblies are typically designed with 6-inch unenriched axial blankets at the top and bottom of the fuel region. The BWR dataset employed in the calculation of the bounding burnup profile includes axial end-blankets and is, therefore, directly applicable to the MAGNATRAN contents. PWR information that constructed the PWR curve did not contain blanketed fuel. To demonstrate acceptability of the PWR profile to blanketed fuel, NAC compared the profile in Figure 5.3-1 to the YAEC-1937 profile for assemblies in the range of 30 to 35 GWd/MTU. The YAEC profile includes both blanketed and non-blanketed fuel assemblies. As seen in Figure 5.3-5, the profiles match well, demonstrating acceptability of the chosen profile across the range of PWR fuel assembly types.

The use of axial blankets in the fuel assembly has the potential for affecting overall source magnitudes, as sources vary as a function of enrichment at a fixed burnup (thus leading to higher sources at lower enrichment). Axial blankets may also shift the burnup profile and indirectly modify source magnitudes. End blanket effects on source magnitudes, in particular unenriched blankets, are discussed in Section 5.8.9 and demonstrated to be not significant to system performance.

than higher density redwood that is part of the limiter design. Impact limiter steel shell is not included in the model.

The normal condition (NCT) 10 CFR 71.71 specified temperature, pressure, vibration and water spray conditions have no effect on the geometry of the cask per structural analysis presented in Chapter 2. Chapter 2 documents the steel cylinder penetration test to result in a localized crush of the impact limiter, with no penetration. There is no effect on the cask body or neutron shield from the penetration condition. As there is no decrease in the amount of impact limiter shield material associated with the cylinder drop – only crush – and the model removed a significant amount of radial and axial material from the limiters, the as-modeled cask bounds the post-cylinder drop normal conditions of transport (NCT) cask configuration. Cask free and corner drops similarly may deform the impact limiters, but do not remove shield material from the system. No lead slump occurs as a result of the normal condition drops. Deformation of the impact limiters during NCT documented in Chapter 2 of the MAGNATRAN SAR results in a configuration bounded by the truncated limiters shown in Figure 5.5-1. Cask internals, including the canister spacers, are designed to retain positive safety margins through all transport conditions, including 10 CFR 71.71 NCT evaluations, and remain in their as-evaluated configuration.

The hypothetical accident event is modeled by removing the aluminum cooling fins (copper cooling fins are retained) and deleting gaseous elements (i.e., hydrogen, nitrogen and oxygen) from the NS-4-FR material description of the base case normal conditions model. Testing of the NS-4-FR material exposed to 10 CFR 71.73 fire conditions, summarized in General Atomics report GA-A20770 titled "Thermal Testing of Solid Neutron Shielding Materials," demonstrates only surface material changes (1/8- to 3/16-inch thick) with a material loss of 6 percent. This compares to a 50% material loss considered in the analysis. In addition to the NS-4-FR shield reduction, simultaneous axial and radial lead slumps are assumed to occur. Note that the 1-meter axial surface detectors are located with respect to the accident geometry of the transport cask (i.e., from the end of the cask and not the impact limiters for axial detectors). Normal condition shielding models include a 0.015-inch void between the lead and transport cask shell to account for the potential gap produced by differential thermal contraction between the lead gamma shield and the stainless steel transport cask inner and outer shells. For the lead slump conditions, voids are introduced in the lead gamma shielding on the basis of the redistribution of lead. As a result of the simultaneous application of radial and axial lead slumps in the accident event model, the total modeled lead volume is conservatively less than that actually present in the transport cask. The axial lead slump produces a gamma shield gap 0.87-inch high, while the radial slump reduces the radial gamma shield 0.47 inch. 10 CFR 71.73 also requires a puncture drop considering the cask drop on a vertical 6-inch diameter pin. The pin puncture on the neutron shield compartment, while not evaluated in the structural analysis section whose primary concern

is the cask shell, may result in localized loss of neutron shielding material. As the evaluated accident model includes a 50% material loss over the entire cask surface (including all gaseous materials that served as the primary neutron shielding component), and accident dose rates are limited at 1 meter from the package where any localized peak would be significantly dispersed, the pin puncture condition is considered bounded by the evaluated accident configuration.

Model sketches for accident event analysis are shown in Figure 5.5-4 and Figure 5.5-5.

5.5.1.3 MCNP Detector Mesh Definition

MCNP surface detectors are used to calculate dose rates at various distances from the transport cask. The surface tallies are subdivided using the FS tally segmentation card. A graphical illustration of the detector overlay on a transport cask is shown in Figure 5.5-6. Depicted are 1 meter and 2 meter detectors. For clarity, the transport cask surface detector and azimuthal (angular) divisions are not shown. Typical detector grids for the normal transport condition and accident events analyses are shown in Table 5.5-1 and Table 5.5-2. The dose rate maps produced by this method completely enclose the accessible transport cask surfaces. The 2 meters from transport cask vehicle boundary is based on a typical railcar width of 124 inches. As this dimension is smaller than the cask with limiters installed, and cask transport is expected with a conveyance vehicle of a width equal to, or greater than, the cask diameter, the value of 124 inches is conservative.

To assess the effect of radiation streaming, which may not be captured by the surface tallies evaluated, additional evaluations are performed in Section 5.8.12 with detailed mesh tallies. Cask features addressed in the mesh tallies are streaming paths associated with the cooling fins, neutron shield assembly voids and attachment bolts, and lower rotation trunnions.

5.5.2 Material Properties

Density and material compositions for structural components are primarily obtained from the standard composition library included with SCALE 4.4. The only exception to this rule is the density and composition of the neutron shielding material (NS-4-FR). The NS-4-FR composition is based on the material specification after curing. The neutron shield material description is modified to remove gaseous elements for the accident event evaluation. Note that the basket neutron absorber sheets are not included in the shielding model, except for the damaged fuel evaluation. Basket, TSC and transport cask material densities and compositions are shown in Table 5.5-3. Fuel region densities are calculated quantities dependent on the hardware and fuel masses in the assembly. A sample homogenized fuel assembly material description is shown in Table 5.5-4.

Figure 5.5-3 Normal Condition 3-D Model – Radial Detail – Neutron Shield Assemblies

[redacted]

Figure 5.5-4 Accident Event 3-D Model – Axial Detail

[redacted]

Table 5.5-1 Typical Radial Surface Detector Division

Location	Inner Radius [cm]	Axial			Azimuthal
		Lower [cm]	Upper [cm]	Div	Div
TopShellAzi	109.8650	451.5850	478.4995	1	36
Surface	126.1160	-89.2540	563.4720	100	1
HeatFinAzi	126.2160	176.0144	206.4944	1	60
TrunAzi	126.3160	-0.5080	34.4170	1	60
1ft	156.5960	-119.7340	593.9520	100	1
1mTopShellAzi	209.8650	451.5850	478.4995	1	36
1m	226.1160	-189.2540	663.4720	100	1
PunctureAzi	226.2160	246.3800	261.6200	1	60
2m+Railcar	357.4800	-289.2540	763.4720	100	1
4m	526.1160	-489.2540	963.4720	100	1

Note: GTCC waste is evaluated with a less refined mesh spacing. GTCC payload demonstrated significant margin to 10 CFR 71 dose rate limits. As demonstrated in Section 5.8.12, using a refined mesh tally, at the critical 2-meter distance no streaming related peaking can be resolved.

Table 5.5-2 Typical Axial Surface Detector Division

Location	Axial [cm]	Radial			Azimuthal
		Inner [cm]	Outer [cm]	Div	Div
Surface	563.4720	0.0000	126.1160	25	1
1ft	593.9520	0.0000	156.5960	25	1
1m	663.4720	0.0000	226.1160	25	1
2m	763.4720	0.0000	326.1160	25	1
4m	963.4720	0.0000	526.1160	25	1

Table 5.5-3 Fuel Basket, TSC, and Transport Cask Material Description

Material	Density [g/cm³]	Nuclide / Element	Density [atom/barn-cm]
Carbon and Low-Alloy Steel	7.8212	CARBON	3.9250E-03
		IRON	8.3494E-02
Stainless Steel	7.94	CHROMIUM	1.7472E-02
		MANGANESE	1.7407E-03
		IRON	5.9505E-02
		NICKEL	7.7392E-03
Lead	11.344	LEAD	3.2967E-02
NS-4-FR	1.6316	HYDROGEN	5.849E-02
		BORON-10	8.227E-05
		BORON-11	3.375E-04
		CARBON	2.277E-02
		NITROGEN	1.403E-03
		OXYGEN	2.606E-02
		ALUMINUM	7.751E-03
NS-4-FR (Fire Accident)	0.8089	BORON-10	8.227E-05
		BORON-11	3.375E-04
		CARBON	2.279E-02
		ALUMINUM	7.751E-03
Aluminum	2.702	ALUMINUM	6.0306E-02
Copper	8.92	COPPER-63	5.8471E-02
		COPPER-65	2.6062E-02
Balsa	0.1250	CARBON	2.7871E-03
		HYDROGEN	4.6451E-03
		OXYGEN	2.3226E-03

Table 5.5-4 Sample Fuel Region Homogenized Material Description (17a PWR Assembly)

Material	Density [g/cm³]	Nuclide / Element	Density [atom/barn-cm]
Lower End-Fitting	1.8782	CHROMIUM	4.1330E-03
		MANGANESE	4.1176E-04
		IRON	1.4076E-02
		NICKEL	1.8307E-03
Lower Plenum[a]	2.6798	CHROMIUM	3.1036E-05
		TIN	2.0391E-04
		IRON	3.6120E-05
		NITROGEN	5.7622E-05
		ZIRCONIUM	1.7376E-02
Active Fuel[a]	3.8195	URANIUM-235	3.5714E-04
		URANIUM-238	6.6999E-03
		ZIRCONIUM	4.2594E-03
		CHROMIUM	7.6082E-06
		TIN	4.9986E-05
		NITROGEN	1.4125E-05
		OXYGEN	1.4110E-02
		IRON	8.8542E-06
Upper Plenum[a]	0.7412	CHROMIUM	1.1717E-03
		TIN	1.5972E-05
		MANGANESE	1.1648E-04
		IRON	3.9848E-03
		NITROGEN	4.5135E-06
		NICKEL	5.1791E-04
		ZIRCONIUM	1.3611E-03
Upper End-Fitting	1.8385	CHROMIUM	4.0456E-03
		MANGANESE	4.0305E-04
		IRON	1.3778E-02
		NICKEL	1.7920E-03

[a] Zirconium alloy composition homogenized in this region is based on SCALE 4.3 material composition.

5.6 Shielding Evaluation

This section evaluates the shielding design of the MAGNATRAN package. The calculation methods, computer codes used and bounding results are described. Dose rate profiles are reported as a function of distance from the sides, top and bottom of the transport cask/package under normal conditions and accident events.

5.6.1 Methods

5.6.1.1 MCNP Dose Rate Evaluation

The shielding evaluations of the package are performed with MCNP6. Source terms include fuel neutron, fuel gamma and gamma contributions from activated hardware. As described in Section 5.2, these evaluations include the effect of fuel burnup peaking on fuel neutron and gamma source terms.

The MCNP shielding models described in Section 5.5.1 are used with the source terms described in Section 5.2 to estimate the dose rate profiles at the transport cask surface and at distances of 1 foot, 1 meter and 2 meters from the transport cask. The method of solution is continuous energy Monte Carlo, with a Monte Carlo-based weight window generator to accelerate code convergence. Radial or axial biasing is performed, depending on the desired dose rate location. Primary cross-section libraries employed are MCPLIB04 for gamma transport calculations and ENDF/B-VI continuous energy data libraries for neutron transport.

Significant validation literature is available for MCNP, as it is an industry standard tool for spent fuel cask evaluations. Available literature covers a range of shielding penetration problems ranging from slab geometry to spent fuel cask geometries. Confirmatory calculations against other validated shielding codes (SCALE and MCBEND) on NAC casks have further validated the use of MCNP for shielding evaluations.

MCNP calculations are performed using a response function approach for each source type present in each source region. There are eight source types: fuel neutron, fuel gamma, fuel n-gamma (secondary gammas arising from neutron interaction in the package), fuel region hardware, upper and lower plenum, and upper and lower end-fitting gamma sources.

In the response function method, each of the assemblies, and source regions within an assembly, is analyzed with a unit source in each relevant energy group. These sources are analyzed in a finite number of energy groups with a unit source in each group. The scalar product of source term and response function allows for the creation of large arrays of dose rate results, whether they are for a single detector, or the maximum or average over a detector surface. Further detail on the response function approach to generating dose rates is included in Section 5.8.2.

5.6.1.2 Loading Table Method/Minimum Cool Time Determination

The strategy used to determine limiting cooling times for each combination of fuel type, initial enrichment and burnup is listed as follows.

- Determine decay heat and dose rate values at each cool time step.
- Interpolate in the resulting collection of data to find minimum cooling time required to meet each limiting value: decay heat, transport cask normal condition surface and 2 meter dose rates, and transport cask accident event 1 meter dose rate.
- Select the maximum of this collection of minimum required cooling times, rounded up to the next tenth of a year, as the minimum required cooling time for this combination of burnup, enrichment and cool time.

While BWR dose rate calculations are straightforward, the addition of nonfuel hardware has the potential to complicate the PWR evaluations, because nonfuel hardware contributes to both transport cask heat load and radiation source. The heat load contribution is addressed by requiring additional fuel assembly cool time when loading nonfuel hardware. The dose rate effect of nonfuel hardware is determined by adding fuel assembly and nonfuel hardware dose rate profiles, and where applicable reducing the maximum dose rate for bare PWR fuel to allow loading nonfuel hardware and remaining under dose rate limits .

A sample calculation for the minimum cool time is shown in Table 5.6-1 for the Westinghouse 17×17 hybrid at a burnup of 45 GWd/MTU. Transport cask surface dose rates are not invoked in the sample minimum cool time calculation, as dose rates are substantially lower than limits.

5.6.2 Input and Output Data

Key package model parameters are translated into MCNP input files for exposure (dose rate) evaluations. Displayed in Figure 5.6-1 through Figure 5.6-4 are VISED-generated normal and accident event graphic representations of the transport cask models discussed in Section 5.3. Shown is the long TSC that does not require a top spacer. Short TSCs are spaced from the transport cask lid by a cask cavity spacer. No credit for spacer material is taken in the analysis, but the TSC is located at the "spaced" elevation during normal and accident analysis (see Figure 5.6-5). As shown in Figure 5.6-5, fuel assemblies are shifted to the top of the TSC cavity for evaluation of top and radial dose rates to maximize exposure to the reduced neutron shielding near the top of the transport cask cavity. All bottom dose rates are evaluated with the fuel, basket and TSC shifted down. Radial dose rate peaking associated with the rotation trunnions are addressed in Section 5.8.10 with the TSC at the bottom of the cask cavity and fuel shifted to the bottom of the TSC cavity.

VISED is an auxiliary graphics module supplied with the MCNP6 code package. Axial and radial normal and accident event images are included to show assembly source regions in relation to shield geometry. Corresponding MCNP input files are included in Section 5.8.7. Outputs are reviewed for general convergence and MCNP built-in statistical checks.

5.6.3 Flux-to-Dose Rate Conversion

The ANSI/ANS 6.1.1-1977 flux-to-dose rate conversion factors are used in all shielding evaluations. Neutron and gamma dose rate conversion factors are listed in Table 5.6-2 and Table 5.6-3, respectively.

5.6.4 External Radiation Levels

This section provides bounding dose rate profiles for the package based on the source terms presented in Section 5.2. Fuel source terms include contributions from fuel neutron, fuel gamma, and activated fuel and nonfuel hardware gamma components. The fuel assembly activated hardware gamma source terms include steel and inconel in the upper and lower fuel assembly end fittings, upper and lower fuel rod plenum hardware, and activated nonfuel material in the active fuel region. Nonfuel hardware evaluated includes PWR burnable poisons, thimble plugs, CEAs (RCCAs), HFRAs, steel replacement rods, and primary and secondary sources. The three-dimensional model dose rates include the effects of axial profiles.

Separate dose rate results are provided for undamaged and damaged fuel. Undamaged fuel represents the bounding dose rates from PWR or BWR contents, while damaged fuel is limited to PWR contents.

Multiple fuel types and depletion parameter sets (i.e., burnup, initial enrichment and cool time) combinations produce similar (bounding) dose rates at the 2-meter position, as the analysis is designed to calculate the minimum required cool time to produce 9.5 mrem/hr at the 2-meter position at a given burnup and initial enrichment (under the condition that heat load limit is met). The 2-meter position is controlling as cask surface dose rates are well below limit. The fuel type, burnup, enrichment and cool time reported as bounding in the following sections are, therefore, based on cask surface dose rates.

Plots of dose rate as a function of distance in this section rely on the "surface" being a cylindrical surface at the radius of the modeled neutron shield assembly. Tallies are taken at the outer shell surface between the impact and neutron shield assembly and at 1 meter from the outer shell surface at this elevation. Results for these locations are included in Section 5.8. The surface used for 1 meter tallies is illustrated in Figure 5.6-1.

5.6.4.1 Undamaged Fuel Assembly Baskets

The bounding fuel type, cool time, burnup and initial enrichment for each detector surface under normal conditions and accident events is given in Table 5.6-4. BWR results are bounding for radial detectors and PWR results are bounding for axial detectors.

Normal condition radial and axial dose rate profiles are shown in Figure 5.6-6, Figure 5.6-8, and Figure 5.6-9. Figure 5.6-7 includes a source type breakdown of the 2 meter dose rate profile. In the profile plots, each datum represents the circumferentially averaged dose rate at the corresponding elevation. Figure 5.6-6 indicates significant surface dose rate peaking near the top of the transport cask cavity. Hardware peaking near the top of the cavity is associated with the gap in complete leak coverage in the region above the neutron shield and the top of the cask cavity (Figure 5.6-1 illustrates the shield material distribution). The upper transport cask structure is symmetric and, therefore, does not require an azimuthal dose rate breakdown. Figure 5.6-10 contains an azimuthal breakdown of the transport cask surface; azimuthal average 2 meter dose rates at the rotation trunnion elevation are well below the NAC applied 9.5 mrem/hr limit (results shown are from surface tally, mesh tally results are shown in Section 5.8.12). The effect of radiation streaming through the neutron shield assembly voids and attachment bolts walls at the critical 2-meter distance was determined to insignificant in Section 5.8.12. Surface effects of the streaming not captured by the surface tally evaluations are also addressed in Section 5.8.12.

Maximum dose rates are summarized in Table 5.1-3. Refer to Sections 5.8.3 and 5.8.4 for further detail, such as content specific dose rates, and a detailed distance dependent breakdown in dose rate by source type.

Bounding accident event dose rates as a function of distance from the transport cask are shown in Figure 5.6-12 through Figure 5.6-14. As noted in the modeling section, accident event evaluations remove the impact limiters, assume combustion of gaseous elements from the NS-4-FR material description, remove the aluminum cooling fins (copper cooling fins are retained), and model a 6-inch diameter pin puncture through the neutron shield coincident to the radial lead slump, in addition to simultaneously applying both top and bottom axial lead slump and a radial lead slump. The latter conservatively removes significant quantities of lead. Maximum accident event dose rates are summarized in Table 5.1-4.

5.6.4.2 Damaged Fuel Assembly Baskets

Dose rates are calculated for fuel material reconfiguration, compaction, into either the active fuel region (elevation associated with active fuel in undamaged assemblies) or into regions associated with nonfuel hardware (plenum and end-fittings). Maximum dose rates for the combination of the two scenarios are reported in this section. Note that maximum radial dose rates reported are lower for damaged fuel as the undamaged fuel radial dose rates are obtained from BWR and

5.8.2 Response Function Method

In general, the response method for dose rates is based on the decomposition of the respective quantity into a weighted sum over energy. A dose rate response function, $R_{tpg}(\vec{r})$, gives the response at a point $\vec{r}$ to source particles arising from energy group g from a fuel assembly placed in basket position p. In practice, the spatial parameter, $\vec{r}$, is represented as discrete subsurface detectors on the cask surface. In addition, responses for detector average and maximum values may also be represented using this notation. In the case of a dose rate response, the response $R_{tpg}(\vec{r})$ is a scalar quantity.

For a given TSC loading, the total response to radiation of type t with source spectrum f_{tp} is given by:

$$C_t(\vec{r}) = \sum_p \sum_{g'} R_{tpg'}(\vec{r}) f_{tpg'} w_{tp}$$

where:

- $C_t(\vec{r})$ is the dose rate response to radiation of type t at location $\vec{r}$.
- $R_{tpg'}(\vec{r})$ is the response to radiation of type t with energy g' emanating from basket position p at location $\vec{r}$.
- $f_{tpg'}$ is the source strength for radiation of type t in group g' emanating from basket position p.
- w_{tp} is a weight factor applied to radiation of type t in basket position p and is used to scale hardware source spectra that are provided on a per-unit mass basis by the effective mass of activated material present in the source region.

The source type t refers to fuel gamma (Fg), fuel neutron (Fn), fuel n-gamma (Ng), fuel hardware (Hw), upper plenum (Up), upper fitting (Uf), lower plenum (Lp), or lower fitting (Lf) source regions.

Response functions (generated using MCNP) solve the particle transport equations at each relevant energy spectrum line using Monte Carlo techniques. The results of the individual energy spectrum lines are then statistically summed. As the basket is loaded uniformly, the dose rate response can be calculated for a source located in multiple fuel assembly locations using Monte Carlo sampling within MCNP. For the uniform loading, the basket position variable is, therefore, not required within the summation. Note that the term is still accounted for directly within the MCNP run.

Source terms are generated in a 28-group neutron and 22-group gamma structure. Dose rate responses are adequately modeled by evaluating only a subset of the source spectrum energy groups. In the fuel neutron case, no fuel neutron source spectra have nonzero values outside energy groups 2 through 15; and groups 2, 3 and 15 do not contribute significantly to the result. The fuel gamma response is accurately calculated by considering energy groups 7 through 15. Energy lines relevant to the analysis of activated zirconium, steel and inconel hardware are limited to groups 12 and 13. The remaining energy lines either contain no significant source magnitudes or are too low in energy to penetrate the cask shields.

A comparison of the results of the direct calculation (i.e., a calculation based on use of the complete gamma, neutron or hardware gamma source spectrum in an MCNP run) and dose rate response method (summation of dose rate calculation at each energy group) is documented to validate the dose rate response method, including the reduction in energy lines evaluated. A nominal dimension cask model is used for this comparison. Surface tally division coarser than those employed when calculating licensing dose rates are used in these comparison. Subcritical neutron multiplication in the comparisons are accounted for by using a source multiplier of 1.67 (based on a k_{eff}=0.4) rather than having MCNP calculate the multiplication within the code. As the comparison establishes that response function can be used to determine licensing dose rates, but does not itself calculate maximum dose rates, these modeling choices are acceptable.

Graphical comparisons of the two solution methods are generated for PWR and BWR normal condition radial biasing models at three burnup/enrichment combinations. The combinations evaluated are low burnup/low enrichment of 30 GWd/MTU and 2.5 wt % ^{235}U, medium burnup/medium enrichment of 45 GWd/MTU and 4.1 wt % ^{235}U, and a high burnup/high enrichment of 60 GWd/MTU and 4.9 wt % ^{235}U (PWR only). All cases are at system bounding minimum cool times (based on 24 kW PWR cases and 23 kW BWR cases). The comparison plots are included in Figure 5.8-1 through Figure 5.8-5. These comparison plots document the accuracy of the dose rate response method.

Direct calculation and dose rate response method results are also compared for the normal condition radial surface of the transport cask using the 16a hybrid at 35 GWd/MTU burnup, 2.3 wt % ^{235}U initial enrichment, and 8 years cool time. The cumulative results are plotted in Figure 5.8-6. A tabular comparison is presented in Table 5.8-7, along with a "% Diff" column that shows the percentage difference between the results of the direct solution of the problem and those of the dose rate response method solution. Sample response functions for a similar source term as that used in the generation of Figure 5.8-6 (i.e., 7.6 years cool time rather than 8) are included in Table 5.8-8 through Table 5.8-10. The tables demonstrate the implementation of the dose rate summation function, while simultaneously justifying the reduction in the number of

Figure 5.8-7 Normal Condition Radial Surface Dose Rates – Fresh Fuel versus Spent Fuel Isotopics – PWR – 60 GWd/MTU, 4.9 wt % ^{235}U

[redacted]

Figure 5.8-8 Accident Event Radial Surface Dose Rates– Fresh Fuel versus Spent Fuel Isotopics – PWR – 60 GWd/MTU, 4.9 wt % ^{235}U

[redacted]

Table 5.8-7 Response Method to Direct Calculation Comparison – Transport Cask

[redacted]

* Relative standard deviation.

5.8.3 37-Assembly PWR System

This section presents the detailed cool time and dose rate evaluations of the transport cask loaded with undamaged PWR fuel assemblies. Damaged PWR fuel dose rates are addressed in Section 5.8.10. PWR nonfuel hardware contributions to dose rate are included in Section 5.8.5 and Section 5.8.6. Irradiated stainless steel rods are addressed in Section 5.8.13.

Minimum cool times documented in this section are applicable to undamaged and damaged fuel with the following exceptions;

- Section 5.8.10 contains additional cool time required for a subset of fuel type / burnup / enrichment when employing the damaged fuel TSC.
- Sections 5.8.5 and 5.8.6 contain the additional cool time required for a fuel assembly to be loaded with non-fuel hardware (either DF basket or non-DF basket; non-fuel hardware is not permitted in a DFC).
- Section 5.8.13 specifies an additional year cool time be applied to fuel assemblies having irradiated stainless steel rods.

Additional cool times specified are cumulative (e.g., for a fuel assembly containing stainless steel replacement rods and loaded with non-fuel hardware the cool time deltas specified are to be added together).

5.8.3.1 PWR Fuel and Basket Models

The three-dimensional shielding evaluation includes a homogenized fuel assembly model and a detailed three-dimensional basket model.

Fuel Assembly Model

Based on the fuel assembly physical parameters provided in Table 5.8-1 and the hardware masses in Table 5.8-2, homogenized treatments of fuel assembly source regions are developed. The homogenized fuel assembly is represented in the model as a stack of boxes with width equal to the fuel assembly width. The height of each box corresponds to the modeled height of the corresponding assembly region.

Sample fuel and nonfuel hardware homogenizations for the source regions for the 17a assembly are shown in Table 5.8-11 and Table 5.8-12. Similar composition sets are generated for the remaining fuel assembly hybrids.

Basket Model

The basket is composed of coated carbon steel tubes, pinned together at the corners, and held together by side and corner weldments. Twenty-one fuel tubes, in combination with the weldments, form 37 fuel openings. Key PWR basket geometry features are summarized in Table 5.8-13. The corner weldments provide structural support, but do not serve as a physical restraint to the fuel assemblies. Pin spacers or tube extensions maintain the tube axial spacing within the TSC cavity. The neutron absorber sheets are not modeled. Radial and axial sketches of the basket within the TSC are shown in Figure 5.8-9 and Figure 5.8-10, respectively.

5.8.3.2 Minimum Cool-time Specification

SAS2H generates heat loads for all PWR fuel types listed in Section 5.8.1.1. Based on a 23 kW per cask (621.6 W per assembly) heat load and transport dose rate limits*, minimum allowed cool times for each fuel type are calculated. Calculated heat loads and radiation sources account for fuel material (actinide and fission product) and hardware (light element) generated sources. Minimum cool times are conservatively rounded up to the nearest one-tenth of a year. A sample minimum cool time calculation for a PWR assembly is shown in Table 5.8-14. The resulting minimum cool times are listed in assembly-specific loading tables (see Table 5.8-15 and Table 5.8-16).

Allowed low burnup (up to 30,000 MWd/MTU) fuel loadings are shown in Table 5.8.14b. Note that the listed minimum cool times at each burnup step are bounding for all PWR fuel types and initial enrichments above the minimum enrichment specified. Collapsing the fuel type and initial enrichment-dependent minimum cool time matrix to a single value may result in a minimum cool time longer than individual values presented for higher burnups in the detailed tables that follow.

The loading table removes combinations of high burnup and low enrichment (e.g., 60 GWd/MTU and 1.9 wt % ^{235}U) from the contents definition. Source term data covering these combinations produces unrealistic source terms due to the complete consumption of fissile uranium early in the burnup cycle and the SAS2H input of a fixed power density. To maintain power density, ORIGEN-S (SAS2H) will substantially increase flux levels, which would not occur during core operation of the assembly, to produce fissile material and to produce power by nonthermal fission. The increased flux level "breeds" higher actinides, which in turn increases source significantly. Because a high burnup and low enrichment combination would require repeated reinsertion of a burned assembly, the combination is excluded.

---

* The only relevant dose rate limit is the normal condition 9.5 mrem/hr limit at 2 meters from the transport cask conveyance, as cask surface dose rates are substantially below regulatory limits.

5.8.3.3 Transport Cask Dose Rates

Using the dose rate response method, transport cask dose rates are tabulated for all allowed cool time, burnup, and initial enrichment combinations for each of the assembly types. Minimum cool times are based on the shortest cool time meeting both heat load and dose rate limits (rounded up to the nearest tenth of a year). Resulting normal conditions of operation maximum dose rates as a function of distance from the transport cask surface are shown in Figure 5.8-11 for the cask radial surface, Figure 5.8-14 for the cask top, and Figure 5.8-15 for the cask bottom. The radial 1 foot results correspond to the personnel barrier. Breakdowns of the cask surface radial and two-meter dose rates into the source components are shown in Figure 5.8-12 and Figure 5.8-13.

The azimuthal dose rate distribution over the potential streaming paths of the lower trunnion rotation pockets is illustrated in Figure 5.8-16. Simiarly, dose rates from azimuthal detectors at the height of the expansion foam at the top of the neutron shields are shown in Figure 5.8-16B and Figure 5.8-16C for cask surface and 1 foot, respectively. At the surface of the neutron shield there is resolvable peaking due to the expansion foam gap but the peak flattens significantly by the 1 foot detector location corresponding to the personnel barrier. Maximum surface and 1 foot dose rates are found higher up the cask at the gap between the top impact limiter and the neutron shield assemblies.

The dose rate profile at the surface of the cask shell exposed between the top impact limiter and the neutron shield assemblies is shown in Figure 5.8-17 and is the location of maximum surface dose rates. Cask accident event dose rates are plotted in Figure 5.8-18 for the cask radial surface at one meter and Figure 5.8-19 and Figure 5.8-21 for the cask top and bottom axial surfaces, respectively. Figure 5.8-20 shows a 1-meter radial azimuthal plot at the same height as the pin puncture. The figure shows no resolvable dose rate peaking or streaming at the location of the pin puncture at a distance of 1 meter. Assembly maximum dose rate summaries for normal conditions and accident events are listed in Table 5.8-17 and Table 5.8-18, respectively. Note that the listed dose rates account for fuel assembly source terms only with nonfuel hardware considered in Sections 5.8.5 and 5.8.6. Presence of irradiated stainless steel rods is considered in Section 5.8.13.

The bounding payload types for each detector surface are as follows.

Model	Direction	Fuel Type	Burnup (GWd/MTU)	Initial Enrichment (wt % ^{235}U)	Cool Time (yrs)
Normal	Radial	16a	40	2.5	11.6
	Top	14b	60	3.3	37.6
	Bottom	14a	60	3.3	32.5
Accident	Radial	14a	60	3.3	32.5
	Top	14b	60	3.3	37.6
	Bottom	14a	60	3.3	32.5

Note that the limiting fuel type, cool time, burnup, and initial enrichment for normal conditions radial dose rates is based on the limiting surface dose rate because the 9.5 mrem/hr normal conditions 2 meter radial dose rate limit occurs for numerous fuel assembly/source term combinations.

Figure 5.8-9 PWR Basket, Top View

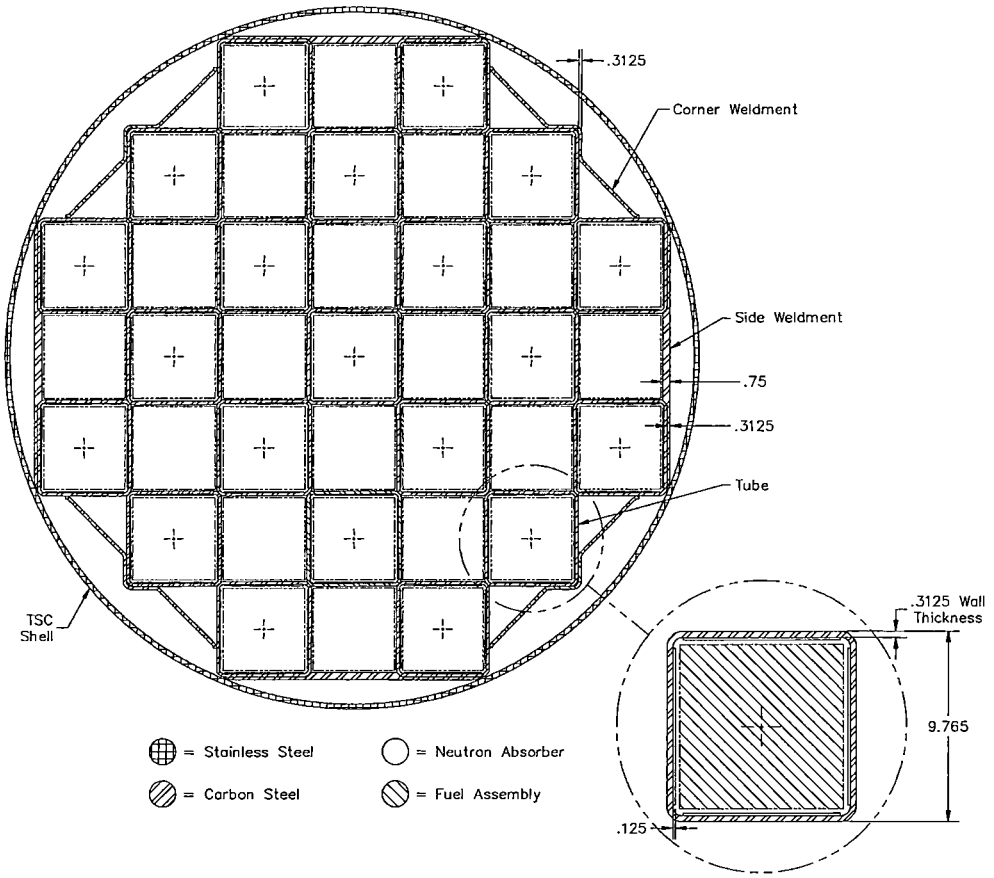

(Dimensions in inches)

Note: Neutron absorber sheets are not modeled in the undamaged PWR shielding evaluation.

Figure 5.8-10 PWR Basket and TSC, Side View

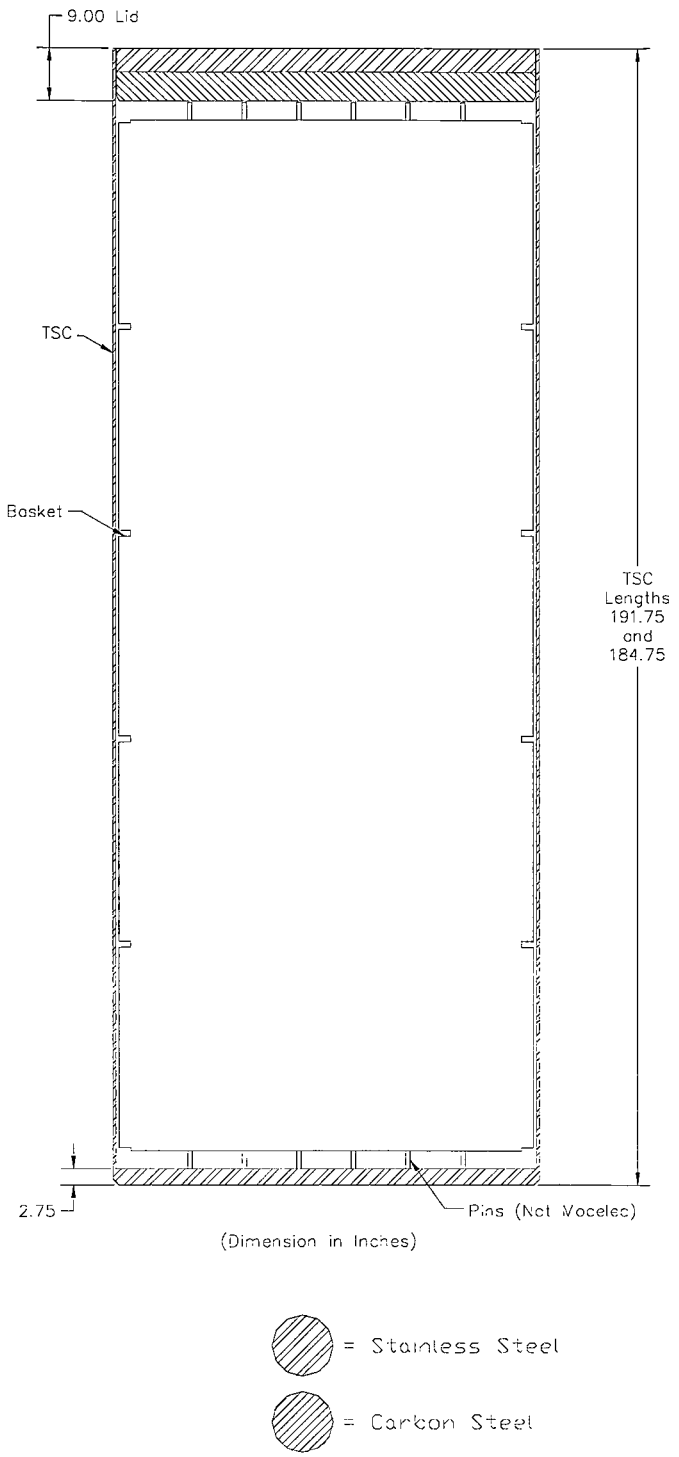

Figure 5.8-11 PWR Bounding Radial Dose Rate Profiles for Normal Conditions of Transport

Figure 5.8-12 PWR Bounding Radial Surface Dose Rate Profile by Source Type for Normal Conditions of Transport

[redacted]

Figure 5.8-13 PWR Bounding 2m from Transport Vehicle Radial Dose Rate Profile by Source Type for Normal Conditions of Transport

[redacted]

Figure 5.8-14 PWR Bounding Top Axial Dose Rate Profiles for Normal Conditions of Transport

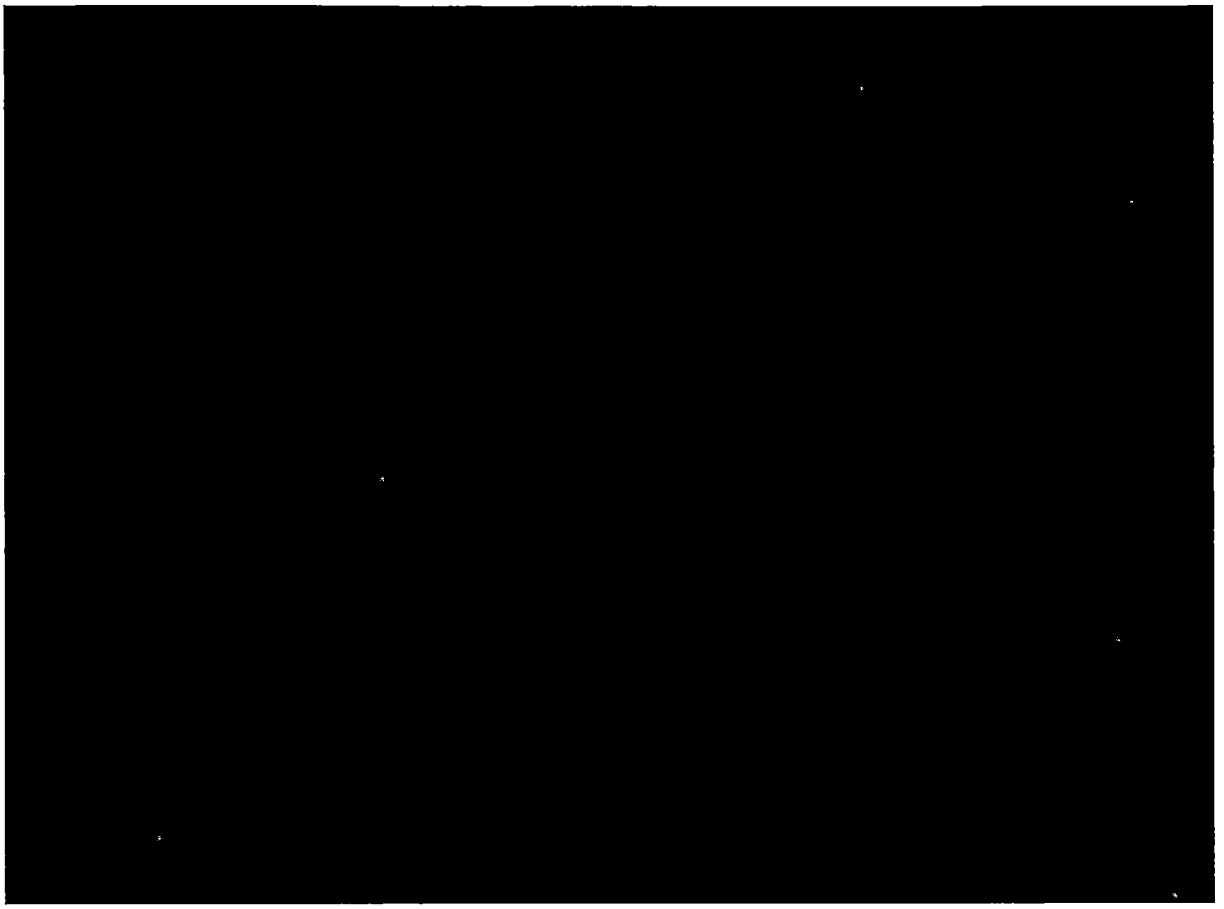

Figure 5.8-15 PWR Bounding Bottom Axial Dose Rate Profiles for Normal Conditions of Transport

[redacted]

Figure 5.8-16 PWR Azimuthal Radial Surface Dose Rate Profile by Source Type at Rotation Trunnion Elevation in Normal Conditions of Transport

[redacted]

Figure 5.8-16B PWR Azimuthal Radial Surface Dose Rate Profile by Source Type Neutron Shield Expansion Foam in Normal Conditions of Transport

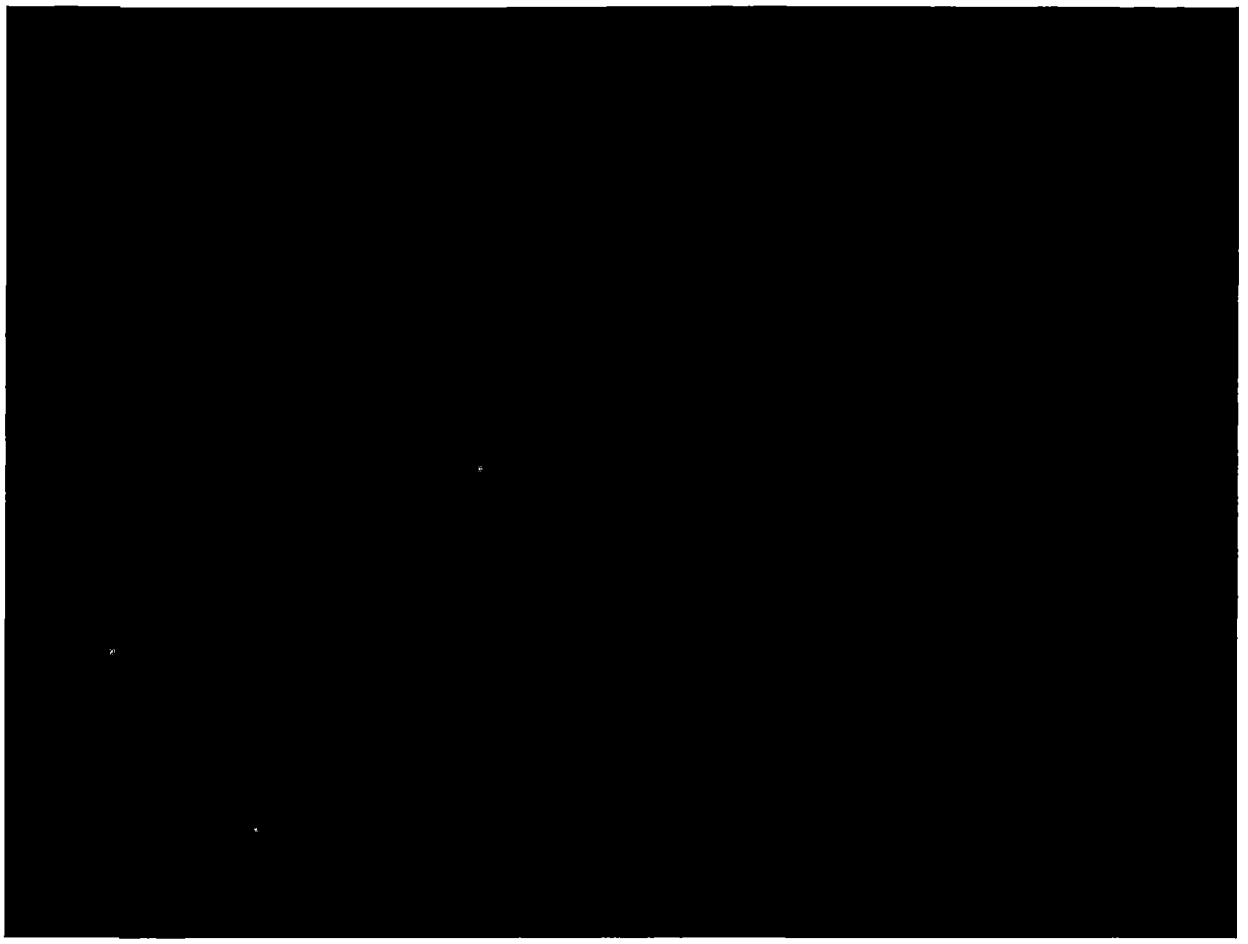

Figure 5.8-16C PWR Azimuthal Radial 1-Foot Dose Rate Profile by Source Type Neutron Shield Expansion Foam in Normal Conditions of Transport

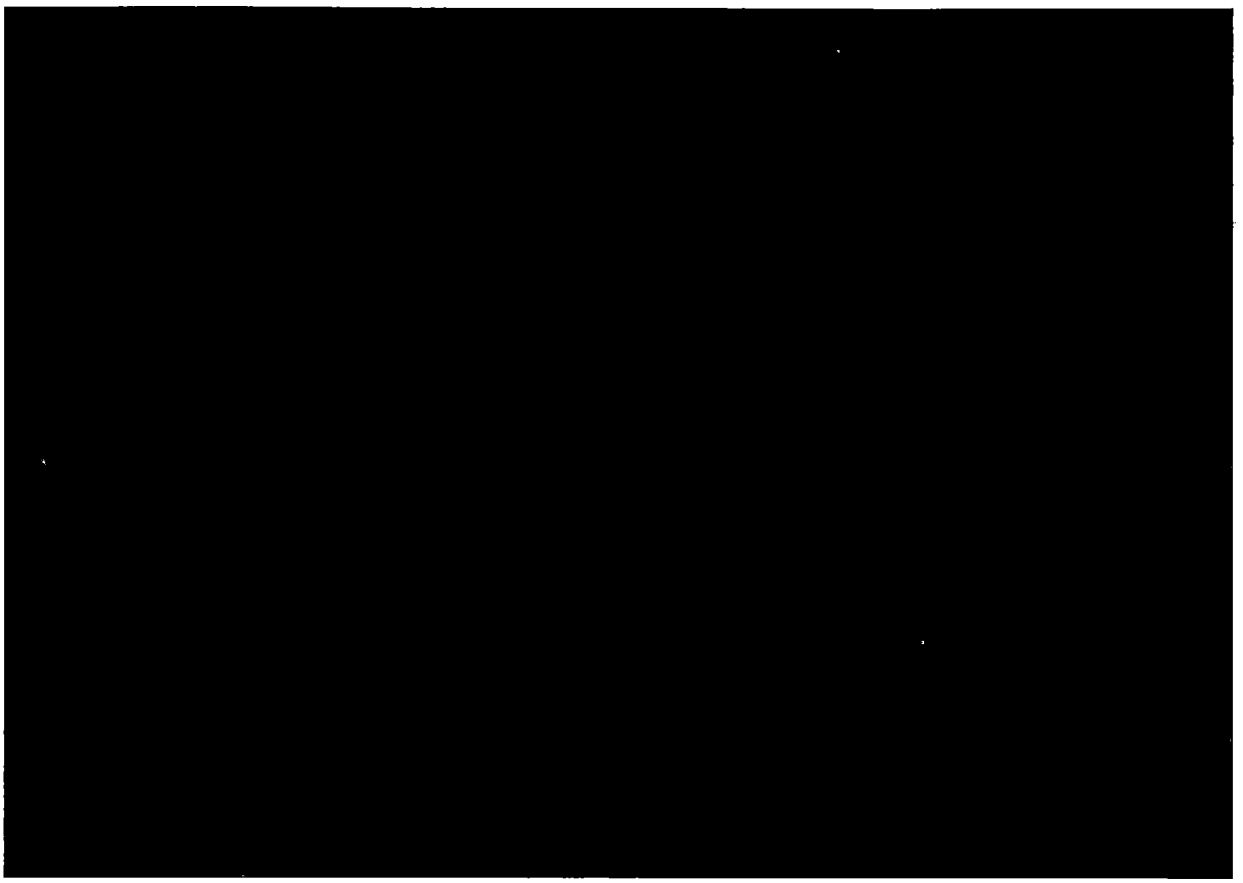

Figure 5.8-17 PWR Azimuthal Radial Surface Dose Rate Profile by Source Type over Neutron Shield Compartments in Normal Conditions of Transport

[redacted]

Figure 5.8-18 PWR Bounding Radial 1m Dose Rate Profile for Accident Events of Transport

[redacted]

Figure 5.8-19 PWR Bounding Top Axial Dose Rate Profiles for Accident Events of Transport

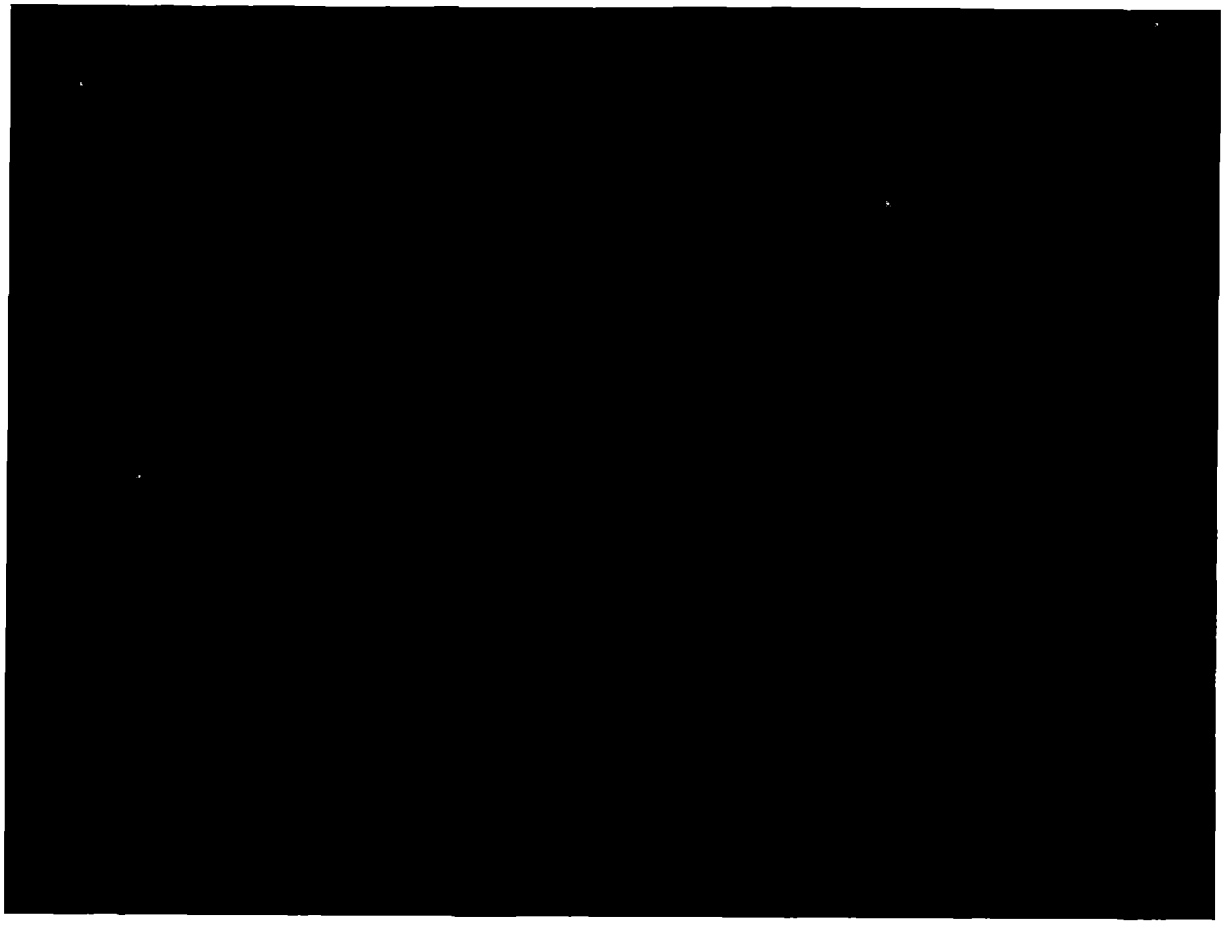

Figure 5.8-20 PWR Azimuthal Radial 1m Dose Rate Profile at Pin Puncture for Accident Events of Transport

[redacted]

Figure 5.8-21 PWR Bounding Bottom Axial Dose Rate Profiles for Accident Events of Transport

[redacted]

Table 5.8-11 PWR Fuel Region Homogenization Sample Calculation

Component	Area [cm²]	Area Fraction	Volume Fraction of Components		
			UO_2	Void	Clad
Fuel	1.3913E+02	3.0375E-01	3.0375E-01		
Gap	5.6649E+00	1.2367E-02		1.2367E-02	
Clad	4.2318E+01	9.2389E-02			9.2389E-02
Guide Tube	3.4075E+00	7.4392E-03			7.4392E-03
Instrument Tube	1.4198E-01	3.0997E-04			3.0997E-04
Inside Tubes	2.5881E+01	5.6502E-02		5.6502E-02	
Interstitial*	2.4150E+02	5.2725E-01		5.2725E-01	
Total	458.0473162	1.0000E+00	3.0375E-01	5.9612E-01	1.0014E-01

Table 5.8-12 PWR Nonfuel Hardware Homogenization Sample Calculation

Region	Assy Mass SS [kg/assy]	SS Volume [cm³/assy]	Modeled Dimensions		Volume Fraction
			Height [cm]	Volume [cm³/assy]	
Lower Nozzle	5.90	7.4307E+02	6.8580	3.1413E+03	2.3655E-01
Lower Plenum†	0.00	0.0000E+00	1.7399	7.9696E+02	0.0000E+00
Fuel Hardware	5.44	6.8514E+02	365.7600	1.6754E+05	4.0895E-03
Upper Plenum	5.41	6.8086E+02	22.2123	1.0174E+04	6.6919E-02
Upper Nozzle	7.85	9.8866E+02	9.3218	4.2698E+03	2.3155E-01

Table 5.8-13 Key PWR Basket Geometry Features

Feature	Material	Dimension
Tube	Carbon Steel	9.76-in outer width, 5/16-in thick
Side Weldment	Carbon Steel	0.75-in thick
Corner Weldment	Carbon Steel	5/16-in thick
Top Spacer Pin	--	3.0-in long
Bottom Spacer Pin	--	3.0-in long

* Space in fuel assembly width envelope outside fuel rods, guide tubes, and instrument tube.
† Represents the fuel rod end-cap.

Table 5.8-14 PWR Minimum Cool Time Solution

Minimum Enrichment [wt % ^{235}U]	Minimum Cool Time (years)			Active Constraint
	Decay Heat (23 kW/cask)	Normal 2m+Railcar (8.5 mrem/hr)*	Limiting	
2.7	19.9	19.7	20.0	Decay Heat
2.9	19.5	17.4	19.6	Decay Heat
3.1	19.4	15.3	19.4	Decay Heat
3.3	19.1	13.3	19.1	Decay Heat
3.5	18.8	11.5	18.8	Decay Heat
3.7	18.6	9.9	18.7	Decay Heat
3.9	18.4	8.7	18.4	Decay Heat
4.1	18.2	7.8	18.3	Decay Heat
4.3	18.1	7.1	18.1	Decay Heat
4.5	17.9	6.6	18.0	Decay Heat
4.7	17.7	6.2	17.7	Decay Heat
4.9	17.6	5.9	17.6	Decay Heat

Note: Sample calculation for the 17a fuel type at 45 GWd/MTU. Cask surface (normal), 1m (accident), and axial (normal and accident) dose rates are significantly below limits at all cool-times meeting assembly heat load limits and are therefore not listed.

Table 5.8-14b Low Burnup PWR Fuel Loading Table

Max. Assembly Avg. Burnup [MWd/MTU]	Min. Assembly Avg. Initial Enrichment [wt% 235U]	Minimum Cool Time [Years]
10,000	1.3	4.0
15,000	1.5	4.0
20,000	1.7	4.4
25,000	1.9	5.5
30,000	2.1	6.9

* 10 CFR 71 dose rate limit is 10 mrem/hr at 2 meters. NAC conservatively reduces the limit to 9.5 mrem/hr. The limit for WE 17x17 bare fuel is reduced further to 8.5 mrem/hr to allow loading any nonfuel hardware while remaining under 9.5 mrem/hr at 2 meters.

Table 5.8-15 Loading Table for PWR Fuel (23 kW/Cask)

Minimum Initial Assembly Avg. Enrichment wt % ^{235}U (E)	Assembly Average Burnup ≤ 30 GWd/MTU Minimum Cooling Time (years)						
	CE 14×14	WE 14×14	WE 15×15	B&W 15×15	CE 16×16	WE 17×17	B&W 17×17
2.1 ≤ E < 2.3	5.7	5.8	6.7	6.9	6.3	6.8	6.8
2.3 ≤ E < 2.5	5.7	5.8	6.6	6.9	6.2	6.7	6.7
2.5 ≤ E < 2.7	5.6	5.7	6.6	6.8	6.1	6.6	6.6
2.7 ≤ E < 2.9	5.5	5.6	6.5	6.7	6.0	6.6	6.6
2.9 ≤ E < 3.1	5.6	5.6	6.4	6.7	6.0	6.5	6.5
3.1 ≤ E < 3.3	5.4	5.6	6.4	6.6	6.0	6.5	6.5
3.3 ≤ E < 3.5	5.4	5.5	6.3	6.6	5.9	6.4	6.4
3.5 ≤ E < 3.7	5.3	5.5	6.3	6.5	5.9	6.4	6.4
3.7 ≤ E < 3.9	5.3	5.4	6.2	6.5	5.9	6.3	6.3
3.9 ≤ E < 4.1	5.3	5.4	6.2	6.5	5.8	6.3	6.3
4.1 ≤ E < 4.3	5.2	5.4	6.1	6.4	5.8	6.3	6.3
4.3 ≤ E < 4.5	5.2	5.3	6.1	6.4	5.8	6.2	6.2
4.5 ≤ E < 4.7	5.2	5.3	6.1	6.4	5.8	6.2	6.2
4.7 ≤ E < 4.9	5.1	5.3	6.0	6.3	5.7	6.1	6.1
E ≥ 4.9	5.1	5.2	6.0	6.3	5.7	6.1	6.1
Minimum Initial Assembly Avg. Enrichment wt % ^{235}U (E)	30 < Assembly Average Burnup ≤ 35 GWd/MTU Minimum Cooling Time (years)						
	CE 14×14	WE 14×14	WE 15×15	B&W 15×15	CE 16×16	WE 17×17	B&W 17×17
2.1 ≤ E < 2.3	-	-	9.2	-	-	-	-
2.3 ≤ E < 2.5	7.1	7.4	9.0	9.6	8.1	9.1	9.1
2.5 ≤ E < 2.7	7.0	7.2	8.9	9.5	8.0	9.0	9.0
2.7 ≤ E < 2.9	6.9	7.1	8.8	9.3	7.9	8.9	8.8
2.9 ≤ E < 3.1	6.8	7.0	8.7	9.2	7.8	8.8	8.7
3.1 ≤ E < 3.3	6.8	7.0	8.6	9.0	7.7	8.6	8.6
3.3 ≤ E < 3.5	6.7	6.9	8.5	9.0	7.7	8.6	8.6
3.5 ≤ E < 3.7	6.7	6.9	8.4	8.9	7.6	8.5	8.5
3.7 ≤ E < 3.9	6.6	6.8	8.3	8.9	7.5	8.4	8.4
3.9 ≤ E < 4.1	6.5	6.7	8.2	8.8	7.5	8.4	8.4
4.1 ≤ E < 4.3	6.5	6.7	8.2	8.7	7.4	8.3	8.3
4.3 ≤ E < 4.5	6.4	6.6	8.1	8.7	7.4	8.2	8.2
4.5 ≤ E < 4.7	6.4	6.6	8.1	8.6	7.3	8.2	8.2
4.7 ≤ E < 4.9	6.4	6.6	8.0	8.6	7.3	8.1	8.1
E ≥ 4.9	6.3	6.5	8.0	8.5	7.2	8.1	8.1

Table 5.8-15 Loading Table for PWR Fuel (23 kW/Cask) (cont'd)

Minimum Initial Assembly Avg. Enrichment wt % ^{235}U (E)	35 < Assembly Average Burnup ≤ 40 GWd/MTU Minimum Cooling Time (years)						
	CE 14×14	WE 14×14	WE 15×15	B&W 15×15	CE 16×16	WE 17×17	B&W 17×17
2.1 ≤ E < 2.3	-	-	-	-	-	-	-
2.3 ≤ E < 2.5	-	-	-	-	-	-	-
2.5 ≤ E < 2.7	9.7	11.9	13.5	14.7	11.6	13.7	13.7
2.7 ≤ E < 2.9	9.5	10.1	13.3	14.4	11.5	13.4	13.4
2.9 ≤ E < 3.1	9.3	9.8	13.1	14.1	11.3	13.2	13.2
3.1 ≤ E < 3.3	9.1	9.7	12.8	14.0	11.1	13.0	13.0
3.3 ≤ E < 3.5	9.0	9.5	12.6	13.8	10.9	12.8	12.8
3.5 ≤ E < 3.7	8.9	9.4	12.5	13.6	10.8	12.7	12.6
3.7 ≤ E < 3.9	8.8	9.3	12.3	13.5	10.7	12.5	12.5
3.9 ≤ E < 4.1	8.7	9.1	12.1	13.3	10.5	12.3	12.3
4.1 ≤ E < 4.3	8.6	9.0	12.0	13.2	10.4	12.2	12.2
4.3 ≤ E < 4.5	8.5	9.0	11.9	13.1	10.3	12.1	12.1
4.5 ≤ E < 4.7	8.4	8.9	11.8	13.0	10.2	12.0	12.0
4.7 ≤ E < 4.9	8.4	8.8	11.7	12.8	10.2	12.0	11.9
E ≥ 4.9	8.3	8.8	11.7	12.8	10.1	11.9	11.9

Minimum Initial Assembly Avg. Enrichment wt % ^{235}U (E)	40 < Assembly Average Burnup ≤ 45 GWd/MTU Minimum Cooling Time (years)						
	CE 14×14	WE 14×14	WE 15×15	B&W 15×15	CE 16×16	WE 17×17	B&W 17×17
2.1 ≤ E < 2.3	-	-	-	-	-	-	-
2.3 ≤ E < 2.5	-	-	-	-	-	-	-
2.5 ≤ E < 2.7	-	-	-	-	-	-	-
2.7 ≤ E < 2.9	14.5	19.0	20.0	21.3	17.2	20.0	20.0
2.9 ≤ E < 3.1	13.6	16.7	19.3	21.0	16.8	19.6	19.6
3.1 ≤ E < 3.3	13.4	14.6	19.0	20.7	16.5	19.4	19.3
3.3 ≤ E < 3.5	13.1	14.1	18.7	20.4	16.3	19.1	19.1
3.5 ≤ E < 3.7	12.9	13.8	18.6	20.2	16.0	18.8	18.8
3.7 ≤ E < 3.9	12.7	13.7	18.3	19.9	15.8	18.7	18.6
3.9 ≤ E < 4.1	12.5	13.5	18.1	19.7	15.6	18.4	18.4
4.1 ≤ E < 4.3	12.3	13.3	17.9	19.6	15.4	18.3	18.3
4.3 ≤ E < 4.5	12.1	13.1	17.7	19.4	15.3	18.1	18.0
4.5 ≤ E < 4.7	12.0	13.0	17.6	19.2	15.2	18.0	17.9
4.7 ≤ E < 4.9	11.9	12.8	17.4	19.0	15.0	17.7	17.8
E ≥ 4.9	11.8	12.7	17.3	19.0	14.9	17.6	17.6

Table 5.8-16 Loading Table for PWR Fuel (21.85 kW/Cask)

Minimum Initial Assembly Avg. Enrichment wt % ^{235}U (E)	45 < Assembly Average Burnup ≤ 50 GWd/MTU Minimum Cooling Time (years)						
	CE 14×14	WE 14×14	WE 15×15	B&W 15×15	CE 16×16	WE 17×17	B&W 17×17
2.1 ≤ E < 2.3	-	-	-	-	-	-	-
2.3 ≤ E < 2.5	-	-	-	-	-	-	-
2.5 ≤ E < 2.7	-	-	-	-	-	-	-
2.7 ≤ E < 2.9	-	-	29.5	-	-	-	-
2.9 ≤ E < 3.1	21.7	25.2	28.4	30.3	25.7	28.9	28.8
3.1 ≤ E < 3.3	21.3	22.9	28.2	30.1	25.4	28.7	28.6
3.3 ≤ E < 3.5	21.1	22.2	28.0	29.8	25.1	28.4	28.4
3.5 ≤ E < 3.7	20.7	21.9	27.7	29.7	24.9	28.1	28.1
3.7 ≤ E < 3.9	20.5	21.7	27.5	29.4	24.7	28.0	28.0
3.9 ≤ E < 4.1	20.2	21.4	27.3	29.2	24.4	27.8	27.7
4.1 ≤ E < 4.3	20.0	21.2	27.1	29.0	24.2	27.6	27.5
4.3 ≤ E < 4.5	19.7	21.0	26.9	28.8	24.0	27.4	27.4
4.5 ≤ E < 4.7	19.6	20.7	26.7	28.7	23.9	27.3	27.2
4.7 ≤ E < 4.9	19.4	20.5	26.5	28.5	23.7	27.1	27.0
E ≥ 4.9	19.2	20.4	26.3	28.3	23.5	27.0	26.9

Minimum Initial Assembly Avg. Enrichment wt % ^{235}U (E)	50 < Assembly Average Burnup ≤ 55 GWd/MTU Minimum Cooling Time (years)						
	CE 14×14	WE 14×14	WE 15×15	B&W 15×15	CE 16×16	WE 17×17	B&W 17×17
2.1 ≤ E < 2.3	-	-	-	-	-	-	-
2.3 ≤ E < 2.5	-	-	-	-	-	-	-
2.5 ≤ E < 2.7	-	-	-	-	-	-	-
2.7 ≤ E < 2.9	-	-	-	-	-	-	-
2.9 ≤ E < 3.1	-	-	-	-	-	-	-
3.1 ≤ E < 3.3	26.8	31.7	33.8	35.8	31.6	34.9	34.9
3.3 ≤ E < 3.5	26.4	29.4	33.5	35.5	31.3	34.7	34.6
3.5 ≤ E < 3.7	26.2	28.1	33.3	35.3	31.1	34.5	34.4
3.7 ≤ E < 3.9	25.9	27.9	33.1	35.1	30.9	34.4	34.2
3.9 ≤ E < 4.1	25.7	27.6	32.9	34.9	30.6	34.1	34.1
4.1 ≤ E < 4.3	25.4	27.4	32.8	34.8	30.5	34.0	33.9
4.3 ≤ E < 4.5	25.1	27.2	32.5	34.6	30.1	33.9	33.8
4.5 ≤ E < 4.7	25.0	26.9	32.4	34.5	30.0	33.7	33.7
4.7 ≤ E < 4.9	24.7	26.7	32.3	34.3	29.8	33.5	33.4
E ≥ 4.9	24.5	26.6	32.0	34.2	29.7	33.4	33.3

Table 5.8-16 Loading Table for PWR Fuel (21.85 kW/Cask) (cont'd)

Minimum Initial Assembly Avg. Enrichment wt % ^{235}U (E)	55 < Assembly Average Burnup ≤ 60 GWd/MTU Minimum Cooling Time (years)						
	CE 14×14	WE 14×14	WE 15×15	B&W 15×15	CE 16×16	WE 17×17	B&W 17×17
2.1 ≤ E < 2.3	-	-	-	-	-	-	-
2.3 ≤ E < 2.5	-	-	-	-	-	-	-
2.5 ≤ E < 2.7	-	-	-	-	-	-	-
2.7 ≤ E < 2.9	-	-	-	-	-	-	-
2.9 ≤ E < 3.1	-	-	-	-	-	-	-
3.1 ≤ E < 3.3	-	-	41.3	-	-	-	-
3.3 ≤ E < 3.5	32.5	37.6	39.1	41.2	36.2	39.8	39.7
3.5 ≤ E < 3.7	31.7	35.4	38.9	41.0	35.9	39.6	39.5
3.7 ≤ E < 3.9	31.4	33.6	38.7	41.0	35.8	39.4	39.3
3.9 ≤ E < 4.1	31.1	33.4	38.6	40.8	35.6	39.3	39.1
4.1 ≤ E < 4.3	30.9	33.2	38.4	40.6	35.4	39.1	39.0
4.3 ≤ E < 4.5	30.7	33.0	38.3	40.4	35.2	38.9	38.9
4.5 ≤ E < 4.7	30.5	32.8	38.1	40.3	35.0	38.8	38.7
4.7 ≤ E < 4.9	30.3	32.6	38.0	40.1	34.8	38.7	38.6
E ≥ 4.9	30.0	32.4	37.9	40.1	34.8	38.6	38.5

Table 5.8-17 PWR Normal Conditions Maximum Dose Rate Summary

[redacted]

Table 5.8-18 PWR Hypothetical Accident Event Maximum Dose Rate Summary

[redacted]

5.8.4 87-Assembly BWR System

This section presents the detailed evaluation of the transport cask loaded with BWR fuel assemblies.

5.8.4.1 BWR Fuel and Basket Models

The three-dimensional shielding evaluation includes a homogenized fuel assembly model and a detailed three-dimensional basket model.

Fuel Assembly Model

Based on the fuel assembly physical parameters provided in Table 5.8-4 and the hardware masses in Table 5.8-5, homogenized treatments of fuel assembly source regions are developed. The homogenized fuel assembly is represented in the model as a stack of boxes with width equal to the fuel assembly width. The height of each box corresponds to the modeled height of the corresponding assembly region.

Sample homogenizations for the source regions for the 09b assembly are shown in Table 5.8-19 and Table 5.8-20. The resulting fuel compositions on an atom/barn-cm basis are shown in Table 5.8-21. Similar compositions sets are generated for the remaining fuel assembly hybrids. Note that the zirconium fuel assembly channel is not included in the model.

Basket Model

The basket is composed of coated carbon steel tubes, pinned together at the corners, and held together by side and corner weldments. Forty-five fuel tubes, in combination with the weldments, form 89 fuel openings. Two openings are located below the TSC port covers. To minimize exposure and meet ALARA constraints, the basket capacity is reduced to 87 assemblies by prohibiting fuel assembly loading into the openings beneath the ports. Pin spacers or tube extensions maintain the tube axial spacing within the TSC cavity. The neutron absorber sheets are not modeled. In dry transport, the presence of the neutron absorber sheets provides minimal shielding and could, therefore, be removed without a significant increase in exposure. Key basket characteristics are shown in Table 5.8-22. Radial and axial sketches of the BWR basket within the TSC are shown in Figure 5.8-22 and Figure 5.8-23, respectively.

5.8.4.2 Minimum Cool-time Specification

SAS2H generates heat loads for all BWR fuel types listed in Section 5.8.1.2. Based on a 22 kW per cask (252.8 W per assembly) heat load and transport dose rate limits, minimum allowed cool times for each fuel type are calculated. Calculated heat loads and radiation sources account for fuel material (actinide and fission product) and hardware (light element) generated sources.

Minimum cool times are conservatively rounded up to the nearest one-tenth of a year. A sample minimum cool-time calculation for a BWR assembly is shown in Table 5.8-23. Allowed low burnup (up to 30,000 MWd/MTU) fuel loadings are shown in Table 5.8-23b. Note that the listed minimum cool times at each burnup step are bounding for all BWR fuel types and initial enrichments above the minimum enrichment specified. Collapsing the fuel type and initial enrichment-dependent minimum cool time matrix to a single value may result in a minimum cool time longer than individual values presented for higher burnups in the detailed tables that follow. The resulting minimum cool times are listed in an assembly specific loading table (see Table 5.8-24).

Note that the loading table removes combinations of high burnup and low enrichment (e.g., 45 GWd/MTU and 1.9 wt% 235U) from the payload definition. Source term data covering these combinations is generated, but produces unrealistic source terms due to the complete consumption of fissile uranium early in the burnup cycle and the SAS2H input of a fixed power density. To maintain power density, ORIGEN-S (SAS2H) will substantially increase flux levels, which would not occur during core operation of the assembly, to produce fissile material and to produce power by nonthermal fission. The increased flux level "breeds" higher actinides, which in turn increase source significantly. Because a high burnup and low enrichment combination would require repeated reinsertion of a burned assembly, the combination is excluded.

5.8.4.3 Transport Cask Dose Rates

Using the dose rate response method, transport cask dose rates are tabulated for all allowed cool time, burnup, and initial enrichment combinations for each of the assembly types. Minimum cool times are based on the shortest cool time meeting both heat load and dose rate limits (rounded up to the nearest tenth of a year). Resulting normal conditions of operation maximum dose rates as a function of distance from the transport cask surface are shown in Figure 5.8-24 for the cask radial surface, Figure 5.8-27 for the cask top, and Figure 5.8-28 for the cask bottom. The radial 1 foot dose rate results correspond to the personnel barrier. Breakdowns of the cask radial surface and two-meter dose rates into the source components are shown in Figure 5.8-25and Figure 5.8-26, respectively.

The azimuthal dose distribution over the potential streaming paths of the lower trunnion rotation pockets and neutron shield compartment walls is illustrated in Figure 5.8-29. Surface and 1 foot azimuthal detectors at the axial height of the expansion foam in the neutron shield are shown in Figure 5.8-29B and Figure 5.8-29C, respectivley. There is discernable peaking at the cask surface due to the neutron shield top expansion foam, but the peak flattens by the 1 foot boundary corresponding to the personnel barrier. Maximum surface and 1 foot dose rates occur

higher along the cask at the gap between the top impact limiter and the neutron shield assemblies.

The dose rate profile at the exposed cask surface below the top impact limiter and above the neutron shield assemblies is shown in Figure 5.8-30 and is the location of maximum cask surface dose rates. Cask accident event dose rates are plotted in Figure 5.8-31 for the cask radial surface at one meter and Figure 5.8-32 and Figure 5.8-33 for the cask top and bottom axial surfaces, respectively. Assembly maximum dose rate summaries for normal and accident events are listed in Table 5.8-25 and Table 5.8-26, respectively.

The bounding payloads for each detector surface are listed as follows.

Model	Direction	Fuel Type	Burnup (GWd/MTU)	Initial Enrichment (wt % ^{235}U)	Cool Time (yrs)
Normal	Radial	09b	30	4.3	7.7
	Top	10a	45	2.7	21.5
	Bottom	09a	45	2.7	17.4
Accident	Radial	07a	45	2.7	22.3
	Top	10a	45	2.7	21.5
	Bottom	09a	45	2.7	17.4

Note that the limiting fuel type, cool time, burnup, and initial enrichment for normal conditions radial dose rates is based on the limiting surface dose rate because the 10 mrem/hr normal conditions 2 meter radial dose rate limit occurs for numerous fuel assembly/source term combinations.

Figure 5.8-22 BWR Basket Top View

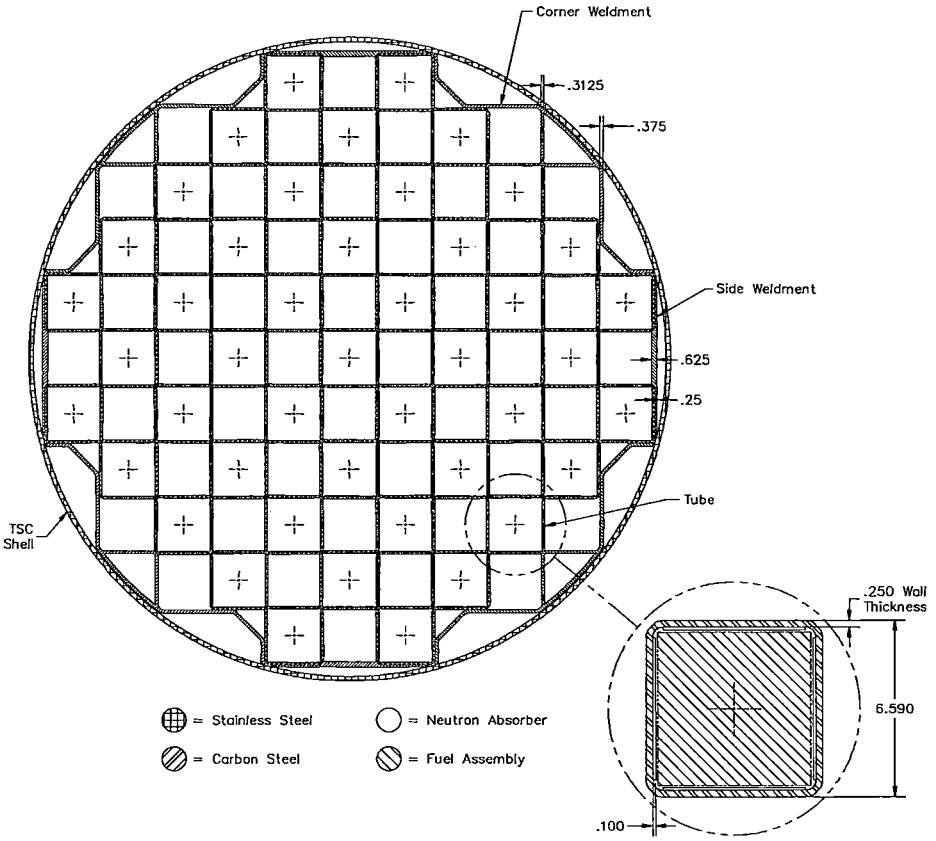

Note: Neutron absorber sheets are not modeled in the BWR shielding evaluation.

Figure 5.8-29 BWR Azimuthal Radial Surface Dose Rate Profile by Source Type at Rotation Trunnion Elevation in Normal Conditions of Transport

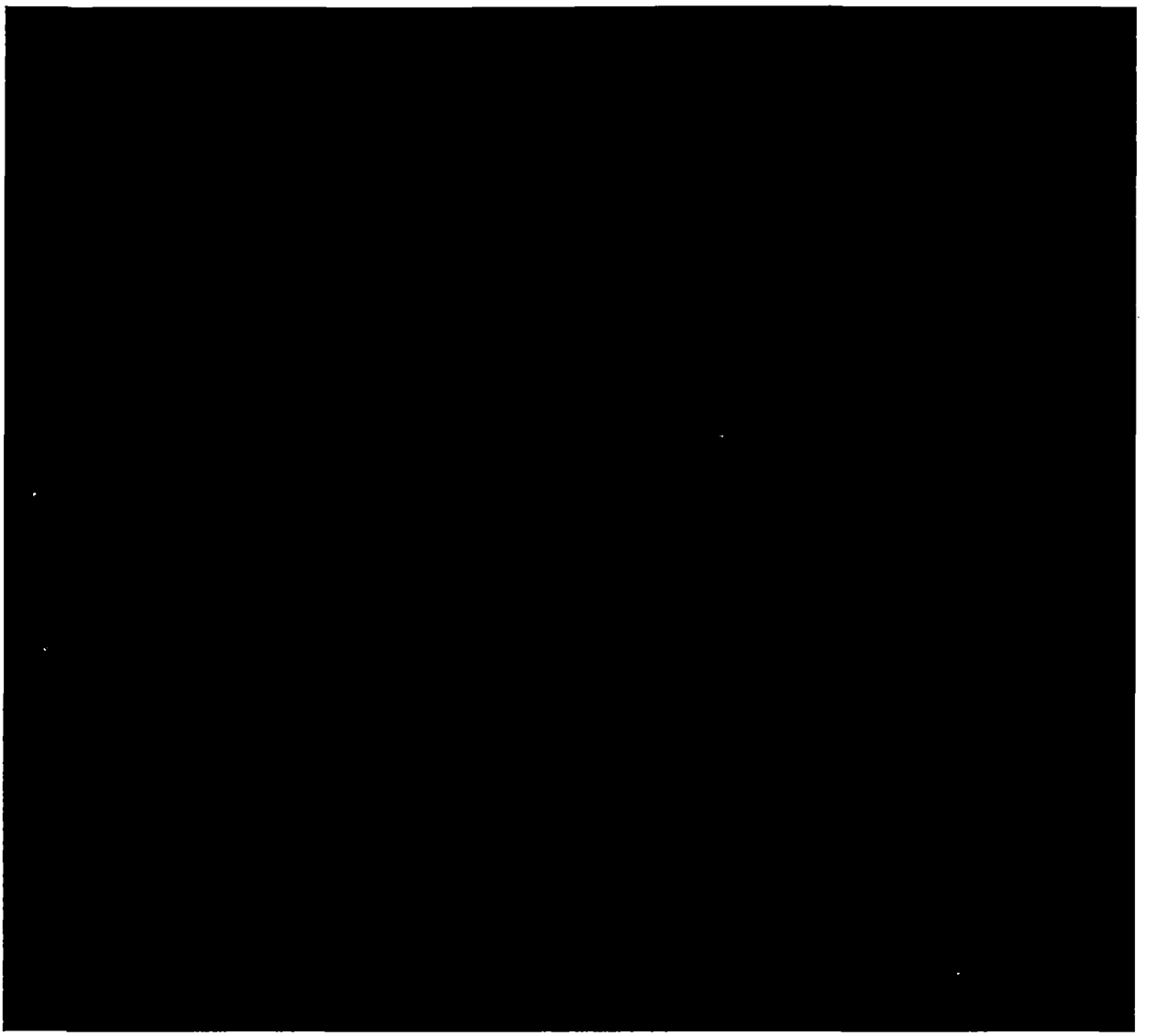

Figure 5.8-29B BWR Azimuthal Radial Surface Dose Rate Profile by Source Type at Neutron Shield Top Expansion Foam in Normal Conditions of Transport

[redacted]

Figure 5.8-29C BWR Azimuthal Radial 1-Foot Dose Rate Profile by Source Type at Neutron Shield Top Expansion Foam in Normal Conditions of Transport

[redacted]

Figure 5.8-30 BWR Azimuthal Radial Surface Dose Rate Profile by Source Type above Neutron Shield Compartments in Normal Conditions of Transport

[redacted]

Figure 5.8-31 BWR Bounding Radial 1m Dose Rate Profile for Accident Events of Transport

[redacted]

Figure 5.8-32 BWR Bounding Top Axial Dose Rate Profiles for Accident Events of Transport

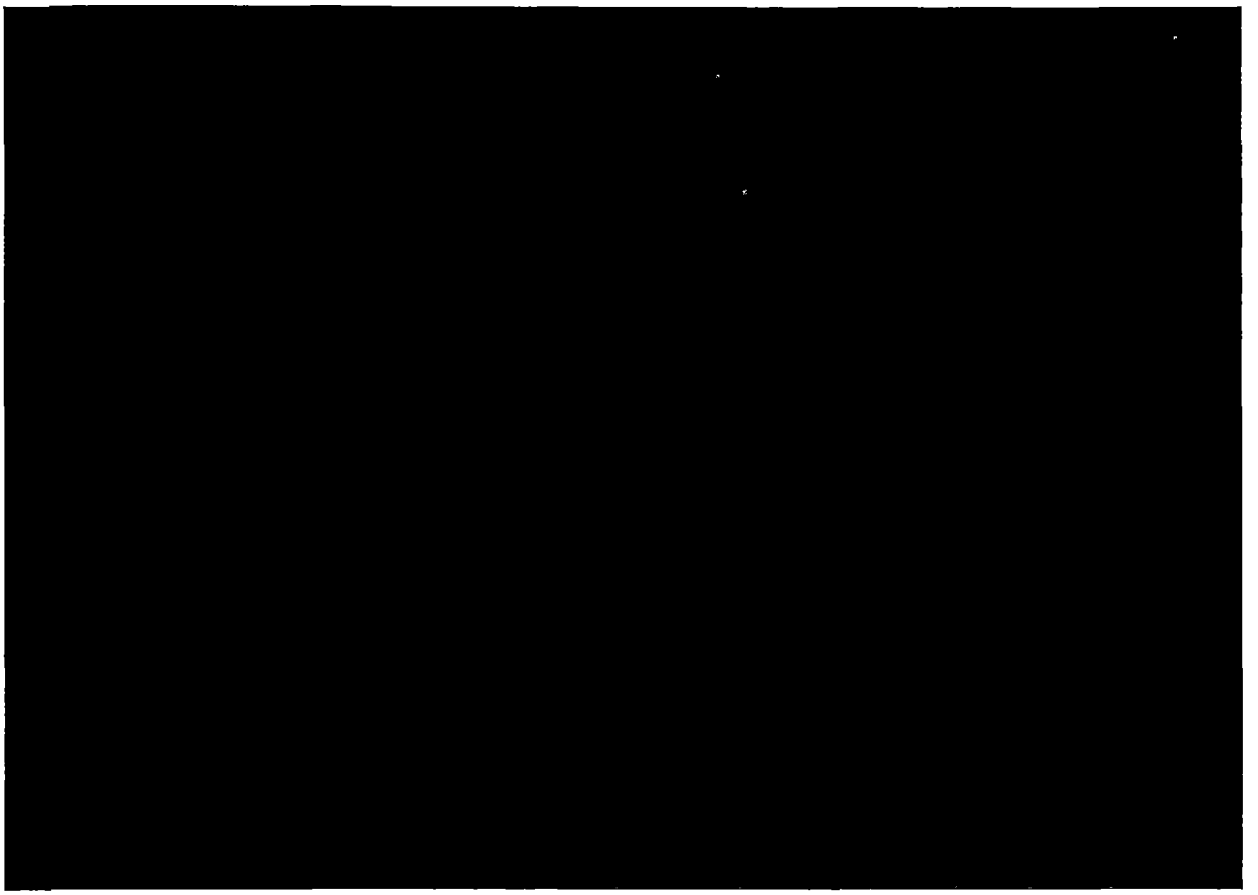

Figure 5.8-33 BWR Bounding Bottom Axial Dose Rate Profiles for Accident Events of Transport

[redacted]

Table 5.8-19 BWR Fuel Region Homogenization Sample Calculation

Component	Area [cm²]	Area Fraction	Volume Fraction of Components		
			UO_2	Void	Clad
Fuel	5.6593E+01	2.8809E-01	2.8809E-01		
Gap	2.8033E+00	1.4271E-02		1.4271E-02	
Clad	1.8455E+01	9.3945E-02			9.3945E-02
Water Rods	4.6792E-01	2.3820E-03			2.3820E-03
Inside Water Rods	1.5024E+00	7.6484E-03		7.6484E-03	
Interstitial*	1.1662E+02	5.9366E-01		5.9366E-01	
Total	1.9644E+02	1.0000E+00	2.8809E-01	6.1558E-01	9.6327E-02

Table 5.8-20 BWR Nonfuel Hardware Homogenization Sample Calculation

Region	Assy Mass SS [kg/assy]	SS Volume [cm³/assy]	Modeled Dimensions		Volume Fraction
			Height [cm]	Volume [cm³/assy]	
Lower Nozzle	4.74	5.9698E+02	17.1704	3.3730E+03	1.7699E-01
Lower Plenum †	0.00	0.0000E+00	1.5875	3.1185E+02	0.0000E+00
Fuel Hardware	0.25	3.1033E+01	381.0000	7.4844E+04	4.1463E-04
Upper Plenum	1.71	2.1480E+02	28.6421	5.6265E+03	3.8177E-02
Upper Nozzle	2.08	2.6196E+02	19.0500	3.7422E+03	7.0003E-02

* Space in fuel assembly width envelope outside fuel rods and water rod(s).
† Represents fuel rod end-cap.

Table 5.8-21 BWR Fuel Region Homogenized Material Description

Material	Density [g/cm³]	Nuclide/Element	Density [atoms/b-cm]
Lower End-Fitting	1.4053	CHROMIUM	3.0924E-03
		MANGANESE	3.0808E-04
		IRON	1.0532E-02
		NICKEL	1.3698E-03
Lower Plenum	2.5998	CHROMIUM	3.0110E-05
		TIN	1.9782E-04
		IRON	3.5042E-05
		NITROGEN	5.5902E-05
		ZIRCONIUM	1.6857E-02
Active Fuel	3.6315	URANIUM-235	3.3873E-04
		URANIUM-238	6.3545E-03
		ZIRCONIUM	4.0975E-03
		CHROMIUM	7.3187E-06
		TIN	4.8083E-05
		NITROGEN	1.3587E-05
		OXYGEN	1.3383E-02
		IRON	8.5174E-06
Upper Plenum*	0.3830	CHROMIUM	6.6797E-04
		TIN	6.0773E-06
		MANGANESE	6.6453E-05
		IRON	2.2728E-03
		NITROGEN	1.7174E-06
		NICKEL	2.9546E-04
		ZIRCONIUM	5.1787E-04
Upper End-Fitting	0.5558	CHROMIUM	1.2231E-03
		MANGANESE	1.2185E-04
		IRON	4.1655E-03
		NICKEL	5.4177 E-04

* Contains a zirconium alloy component due to the addition of the fuel rod end-plug material in the homogenization.

Table 5.8-22 Key BWR Basket Geometry Features

[redacted]

Table 5.8-23 BWR Minimum Cool Time Solution

Minimum Enrichment [wt % ^{235}U]	Minimum Cool Time (years)			Active Constraint
	Decay Heat (23 kW/cask)	Normal 2m+Railcar (10 mrem/hr)	Limiting	
2.7	19.3	22.7	22.7	Dose Rate
2.9	19.0	20.0	20.0	Dose Rate
3.1	18.7	17.8	18.8	Decay Heat
3.3	18.5	16.9	18.6	Decay Heat
3.5	18.3	16.0	18.3	Decay Heat
3.7	18.0	15.2	18.0	Decay Heat
3.9	17.9	14.5	17.9	Decay Heat
4.1	17.7	13.8	17.7	Decay Heat
4.3	17.6	13.2	17.7	Decay Heat
4.5	17.4	12.6	17.5	Decay Heat
4.7	17.3	12.1	17.4	Decay Heat
4.9	17.2	11.6	17.3	Decay Heat

Note: Sample calculation for the 09b fuel type at 45 GWd/MTU. Cask surface (normal), 1m (accident), and axial (normal and accident) dose rates are significantly below limits at all cool-times meeting assembly heat load limits and are therefore not listed.

Table 5.8-23b Low Burnup BWR Fuel Loading Table

Max. Assembly Avg. Burnup [MWd/MTU]	Min. Assembly Avg. Initial Enrichment [wt% 235U]	Minimum Cool Time [Years]
10,000	1.3	6.3
15,000	1.5	8.6
20,000	1.7	10.3
25,000	1.9	11.9
30,000	2.1	13.7

Table 5.8-24 Loading Table for BWR Fuel (23 kW/Cask)

Minimum Initial Assembly Avg. Enrichment wt % ^{235}U (E)	Assembly Average Burnup ≤ 30 GWd/MTU Minimum Cooling Time (years)						
	BWR/2-3 7×7	BWR/4-6 7×7	BWR/2-3 8×8	BWR/4-6 8×8	BWR/2-3 9×9	BWR/4-6 9×9	BWR/4-6 10×10
2.1 ≤ E < 2.3	6.5	12.3	5.8	13.7	5.3	13.0	13.5
2.3 ≤ E < 2.5	6.3	11.6	5.7	13.0	5.2	12.3	12.8
2.5 ≤ E < 2.7	6.3	11.0	5.7	12.3	5.1	11.7	12.2
2.7 ≤ E < 2.9	6.2	10.3	5.6	11.8	5.1	11.1	11.6
2.9 ≤ E < 3.1	6.1	9.8	5.6	11.2	5.0	10.5	11.1
3.1 ≤ E < 3.3	6.0	9.3	5.5	10.7	5.0	10.0	10.6
3.3 ≤ E < 3.5	6.0	8.8	5.5	10.2	4.9	9.6	10.0
3.5 ≤ E < 3.7	6.0	8.4	5.4	9.8	4.9	9.1	9.6
3.7 ≤ E < 3.9	5.9	8.0	5.4	9.4	4.9	8.8	9.2
3.9 ≤ E < 4.1	5.9	7.7	5.3	9.0	4.8	8.4	8.9
4.1 ≤ E < 4.3	5.9	7.4	5.3	8.7	4.8	8.0	8.5
4.3 ≤ E < 4.5	5.8	7.0	5.3	8.4	4.8	7.7	8.2
4.5 ≤ E < 4.7	5.8	6.8	5.2	8.1	4.7	7.5	7.9
4.7 ≤ E < 4.9	5.8	6.5	5.2	7.8	4.7	7.2	7.6
E ≥ 4.9	5.7	6.3	5.2	7.6	4.7	6.9	7.4
Minimum Initial Assembly Avg. Enrichment wt % ^{235}U (E)	**30 < Assembly Average Burnup ≤ 35 GWd/MTU Minimum Cooling Time (years)**						
	BWR/2-3 7×7	BWR/4-6 7×7	BWR/2-3 8×8	BWR/4-6 8×8	BWR/2-3 9×9	BWR/4-6 9×9	BWR/4-6 10×10
2.1 ≤ E < 2.3	-	-	-	-	-	-	-
2.3 ≤ E < 2.5	8.9	14.3	7.6	15.6	6.6	15.0	15.5
2.5 ≤ E < 2.7	8.8	13.5	7.5	14.8	6.5	14.1	14.6
2.7 ≤ E < 2.9	8.6	12.7	7.3	14.0	6.4	13.4	13.9
2.9 ≤ E < 3.1	8.5	12.0	7.2	13.4	6.3	12.7	13.2
3.1 ≤ E < 3.3	8.4	11.4	7.2	12.8	6.3	12.1	12.6
3.3 ≤ E < 3.5	8.3	10.8	7.1	12.2	6.2	11.5	12.0
3.5 ≤ E < 3.7	8.2	10.3	7.0	11.7	6.1	11.0	11.5
3.7 ≤ E < 3.9	8.1	9.8	6.9	11.2	6.0	10.6	11.0
3.9 ≤ E < 4.1	8.0	9.3	6.9	10.8	6.0	10.1	10.6
4.1 ≤ E < 4.3	8.0	8.9	6.9	10.4	6.0	9.7	10.1
4.3 ≤ E < 4.5	8.0	8.7	6.8	10.0	6.0	9.3	9.8
4.5 ≤ E < 4.7	7.9	8.6	6.8	9.6	5.9	8.9	9.4
4.7 ≤ E < 4.9	7.8	8.6	6.7	9.3	5.9	8.6	9.1
E ≥ 4.9	7.8	8.6	6.7	9.0	5.9	8.3	8.8

Table 5.8-24 Loading Table for BWR Fuel (23 kW/Cask) (cont'd)

Minimum Initial Assembly Avg. Enrichment wt % ^{235}U (E)	35 < Assembly Average Burnup ≤ 40 GWd/MTU Minimum Cooling Time (years)						
	BWR/2-3 7×7	BWR/4-6 7×7	BWR/2-3 8×8	BWR/4-6 8×8	BWR/2-3 9×9	BWR/4-6 9×9	BWR/4-6 10×10
2.1 ≤ E < 2.3	-	-	-	-	-	-	-
2.3 ≤ E < 2.5	-	-	-	-	-	-	-
2.5 ≤ E < 2.7	14.6	16.9	12.2	18.0	10.0	17.3	17.7
2.7 ≤ E < 2.9	13.3	15.8	10.7	17.0	8.7	16.3	16.7
2.9 ≤ E < 3.1	13.1	14.9	10.5	16.0	8.5	15.4	15.8
3.1 ≤ E < 3.3	12.9	14.1	10.3	15.2	8.4	14.6	15.0
3.3 ≤ E < 3.5	12.6	13.9	10.1	14.5	8.3	13.8	14.3
3.5 ≤ E < 3.7	12.5	13.7	10.0	13.8	8.2	13.2	13.6
3.7 ≤ E < 3.9	12.4	13.6	9.9	13.3	8.0	12.6	13.0
3.9 ≤ E < 4.1	12.2	13.5	9.8	12.7	8.0	12.1	12.5
4.1 ≤ E < 4.3	12.0	13.4	9.7	12.3	7.9	12.0	11.9
4.3 ≤ E < 4.5	11.9	13.3	9.6	12.2	7.9	12.0	11.5
4.5 ≤ E < 4.7	11.9	13.1	9.6	12.1	7.8	11.9	11.2
4.7 ≤ E < 4.9	11.8	13.0	9.5	12.0	7.8	11.8	11.2
E ≥ 4.9	11.8	13.0	9.4	12.0	7.7	11.8	11.1

Minimum Initial Assembly Avg. Enrichment wt % ^{235}U (E)	40 < Assembly Average Burnup ≤ 45 GWd/MTU Minimum Cooling Time (years)						
	BWR/2-3 7×7	BWR/4-6 7×7	BWR/2-3 8×8	BWR/4-6 8×8	BWR/2-3 9×9	BWR/4-6 9×9	BWR/4-6 10×10
2.1 ≤ E < 2.3	-	-	-	-	-	-	-
2.3 ≤ E < 2.5	-	-	-	-	-	-	-
2.5 ≤ E < 2.7	-	-	-	-	-	-	-
2.7 ≤ E < 2.9	22.3	24.0	19.9	22.9	17.4	22.7	21.5
2.9 ≤ E < 3.1	19.7	21.4	17.2	20.3	14.8	20.0	19.4
3.1 ≤ E < 3.3	18.9	20.5	15.4	19.1	12.3	18.8	18.2
3.3 ≤ E < 3.5	18.7	20.2	15.2	18.8	11.9	18.6	17.4
3.5 ≤ E < 3.7	18.5	20.0	15.0	18.7	11.7	18.3	17.2
3.7 ≤ E < 3.9	18.2	19.9	14.7	18.5	11.5	18.0	17.1
3.9 ≤ E < 4.1	18.1	19.6	14.6	18.2	11.4	17.9	16.9
4.1 ≤ E < 4.3	17.8	19.5	14.3	18.1	11.3	17.7	16.7
4.3 ≤ E < 4.5	17.8	19.4	14.3	18.0	11.2	17.7	16.5
4.5 ≤ E < 4.7	17.6	19.2	14.1	17.8	11.1	17.5	16.5
4.7 ≤ E < 4.9	17.4	19.0	14.0	17.8	11.0	17.4	16.3
E ≥ 4.9	17.3	18.9	13.8	17.7	10.9	17.3	16.2

Table 5.8-25 BWR Normal Conditions Maximum Dose Rate Summary

[redacted]

Table 5.8-26 BWR Hypothetical Accident Event Maximum Dose Rate Summary

[redacted]

5.8.5 Nonfuel Hardware Components (Non RCCA/CEA)

The PWR fuel assembly basket is designed to store nonfuel components inside the fuel assembly. Only nonfuel hardware components from the same nonfuel hardware assembly may be loaded into the same basket location.

Component pieces of the nonfuel hardware are permitted to be loaded. Permitting the loading of partial components allows for the condition in which non-fuel hardware was damaged during movement, in particular the condition in which non-fuel hardware rods are stuck in the guide tubes. Rod/rodlets may be stuck in the guide tube and detach when attempting the removal of nonfuel hardware from the assembly. This type of damage would result in a hub component with some rods attached and a limited number of rods remaining in the original assembly. Rods that are no longer firmly attached to the top structure may be individually loaded into guide tubes. Provided the non-fuel hardware top structure is loaded with rods attached the non-fuel hardware will be at its evaluated configuration with reduced source (due to removal of the some of the rod/rodlets). Rod/rodlets "stuck" in their guide tube locations are also bounded as the source region is at or near its evaluated location with reduced overall source due to removal the hub along with potentially still attached rods. The only potentially significant condition arises when considering loose rods in the guide tube and no hub structure. Of highest significance to shielding analysis is movement of activated material from fuel to plenum and plenum to top nozzle region as the cask top region produces maximum dose rates. Removal of the hub structure removes a significant quantity of source from the system for this condition. While potentially replacing hub source with rod/rodlet source the amount of material moving into this region is smaller than the material removed compensating for higher source in the higher activated "lower" regions. Overall this type of shift will not significantly affect system dose rates (in particular at the limiting 2-meter location).

Nonfuel components, except reactor control elements (see Section 5.8.6), that may be stored include the following.

- **BPRAs (Burnable Poison Rod Assemblies)**

  Burnable poison rods are employed in the majority of PWR cores as either replacement rods for fuel rods, typical of CE cores, or as BPRAs in Westinghouse and B&W cores. Common types of BPRAs are Westinghouse Pyrex BPRAs, Westinghouse WABA, and B&W/Framatome Al_2O_3-B_4C zirconium alloy rods. BPRAs are composed of a set of rods made from an absorber material suspended from a spider structure located on the top-end fitting of the assembly. BPRAs are designed to reduce reactivity in fresh fuel, but may remain in a fuel assembly for more than one cycle. Potential BPRA source regions are the top-end fitting, top plenum, and active fuel regions. The amount of activated material

depends on the number of absorber (poison) rods attached to the BPRA and the material of the BPRA. Guide tube locations not occupied by absorber rods are typically occupied by short plug rods extending into the upper plenum region of the assembly. BPRA rods may be composed of activated material such as steel or a relatively inert material such as zirconium alloy. Table 5.8-27 provides a summary of Westinghouse 15×15 core BPRA types and the maximum regional masses chosen for the analysis. BPRAs for the remaining Westinghouse and B&W cores are treated similarly. A summary of BPRA characteristics for fuel placed into the transport system is listed in Table 5.8-28. Poison rods replacing fuel rods are enveloped in the shielding analysis because they are typically constructed with a zirconium alloy clad and do not contain a significant amount of activated material, in particular compared to the fuel rod that they replace.

- **Thimble Plugs**

Thimble plugs are similar to BPRAs in that they are attached to a spider resting on the end-fitting tie plate. Thimble plugs extend into the upper plenum region of the fuel assembly and block flow through the guide tubes during in-core operations. Thimble plug components do not extend into the active fuel region. They may be reused in multiple cycles and can experience significantly higher exposure than BPRAs. Thimble plug masses evaluated for each core are shown in Table 5.8-28.

- **Hafnium Flux Reduction Assembly (HFRA)**

Hafnium flux reduction assemblies (HFRAs) are used to reduce neutron flux, typically at peripheral core locations where reactor vessel damage due to neutron fluence is a concern. Hafnium rods are inserted into guide tube locations and their maximum number is governed by the number of guide tubes.

- **Primary and Secondary Sources**

Nuclear reactors use neutron sources for startup. Primary sources, typically californium or an alpha emitter (e.g., americium, plutonium, polonium) and beryllium, and secondary sources (e.g., antimony-beryllium) are inserted into a guide/instrument tube of a fuel assembly to produce neutron source assemblies (NSAs).

Activation of the nonfuel hardware assemblies are quantified by the exposure which is defined for the purposes of this evaluation by the assembly average burnup in which the nonfuel hardware component was placed.

5.8.5.1 Modeling Detail

Dose rates for BPRA and thimble plug components are evaluated using response functions for the hardware source regions of interest. The response calculations for the NFH components do

not apply the fuel assembly hardware response functions. Each NFH region, for each fuel type, was evaluated using a separate response function set. Credit is taken for the increased region masses and the associated increase in self-shielding. The BPRA and thimble plug activated hardware is primarily composed of stainless steel. A 0.8 g/kg ^{59}Co impurity is applied against this material.

5.8.5.2 Dose Rate and Heat Load Impact

To simplify loading limits for BPRAs and thimble plugs, a uniform minimum cool time of eight years is applied to these components. BPRAs are evaluated to a maximum exposure of 70 GWd/MTU, with thimble plugs being limited to a maximum exposure of 180 GWd/MTU. The BPRAs and thimble plugs for each core configuration are independently evaluated.

In-core instrumentation thimbles are not specifically addressed in these calculations. Mass, and sources associated with this component are typically small and are bounded by those evaluated for the remaining non-fuel hardware components. The added fuel assembly cool time associated with this component should be obtained from the bounding BPRA/TP definition for Westinghouse and B&W type fuels and the RCCA/CEA data for CE type fuels.

BPRAs

Table 5.8-29 lists the allowed BPRA loading configurations expressed in curie limits. The radiation source for the BPRAs is dominated by ^{60}Co gammas. Therefore, the spectrum of the activated BPRAs is not decay time sensitive. System users may choose to directly implement the eight-year minimum cool time on a generic fuel type basis or to determine site-specific minimum BPRA cool times based on the ^{60}Co curie limit in Table 5.8-29.

Maximum dose rates from BPRAs on the transport detector surfaces are listed in Table 5.8-30. As the addition of BPRAs may increase the reported fuel-only dose rates above limits, some fuel assemblies have additional requirements to allow loading NFHW. The combination of fuel, BPRA, and thimble plug dose rates is discussed further, later in this section.

Thimble Plugs

Table 5.8-31 lists the allowed thimble plug loading configurations expressed in curie limits. The radiation source for the thimble plugs is dominated by ^{60}Co gammas. Therefore, the spectrum of the activated thimble plugs is not decay time sensitive. System users may choose to directly implement the eight year minimum cool time on a generic fuel type basis or to determine site-specific minimum thimble plug cool times based on the ^{60}Co curie limit in Table 5.8-31.

Maximum dose rates from thimble plugs on the transport detector surfaces are listed in Table 5.8-32. As the addition of thimble plugs may increase the reported fuel-only dose rates

above limits, some fuel assemblies have additional requirements to allow loading NFHW. The combination of fuel, BPRA and thimble plug dose rates is discussed below.

Combination of Fuel, BPRA and Thimble Plug Dose Rates

For each assembly type, the maximum nonfuel hardware subdetector response is individually added to the corresponding fuel assemblies maximum response to produce a combined dose rate profile and maximum dose rates. As BPRAs and thimble plugs occupy the same location in the fuel assembly, the maximum dose rate from either the BPRAs or thimble plugs is choosen and added to the dose rate from the fuel without nonfuel hardware. Dose rates remain under limits (including the 9.5 mrem/hr limit at 2 meters) with the addition of nonfuel hardware to B&W fuel, which are heat load limited. Adding the hardware to Westinghouse fuel may push dose rates over the 9.5 mrem/hr limit. To allow loading of nonfuel hardware in Westinghouse fuel, the required fuel assembly minimum cool times are extended by restricting the normal condition radial 2 meter dose rates for fuel assembly without nonfuel hardware to those in Table 5.8-33.

The additional heat from the nonfuel hardware requires an extended fuel assembly cool time to compensate for the additional heat from the hardware. The additional fuel assembly cool time needed to load non-fuel hardware is shown in Table 5.8-34.

Hafnium Flux Reduction Assembly (HFRA)

Due to the effectiveness of the hafnium rods in reducing neutron flux, coupled with the HFRA in-core location at the core periphery (high neutron leakage, low power), the exposure of the hafnium rods is limited to 4,000 MWd/MTU with a cool time of 16 years. The SAS2H input for this exposure is shown in Figure 5.8-34. The input file models an initial enrichment of 1.1 wt % ^{235}U, consistent with the insertion of hafnium rods after two cycles of exposure.

The source from 20 hafnium rods (full-length modeled mass of 70.45 kg) is compared to the active fuel region BPRA source for Westinghouse 15×15 (15a) fuel (55 GWd/MTU exposure, 3.1 wt % ^{235}U, and 8 years cool time) in Table 5.8-35. The only energy group where HFRAs have considerable gamma source, at a considerable strength, when compared to BPRAs is group 11. The HFRA has about 116 times more gamma/sec in group 11 but the magnitude of the contribution from group 11 is insignificant when compared to surrounding groups. The HFRA group 11 is on the order of 10^4 which is nine orders of magnitude smaller than the BPRA group 12 (10^{13}) and four orders of magnitude smaller than the BPRA higher energy group 9 (10^8). Neither BPRAs nor HFRAs have a significant source in group 10 with 10^{-1} and 10^{-4}, respectively. Therefore, HFRAs are bounded by BPRAs and placement in any basket location is acceptable.

Fuel assemblies loaded with an HFRA should apply the additional cool time required for loading a BPRA which is provided in Table 5.8-35. The loading of HFRAs is limited to Westinghouse fuel assemblies. This is based on the reasonable expectation that Westinghouse 14×14 and Westinghouse 17×17 BPRAs and HFRAs are similar in design to the Westinghouse 15×15 hardware evaluated.

Primary and Secondary Sources

Primary neutron source strengths are on the order of 5×10^8 neutrons/second when they are initially put into the reactor. Even without considering in-core parasitic neutron absorption and subsequent decay of the source isotopes, the source strength diminishes as the source isotopes decay over time. A majority of the isotopes have half-lives on the order of days or a few years, and the source strength will be significantly diminished before the neutron source is loaded into transport. The ^{238}Pu and ^{241}Am isotopes have half-lives of 87 and 433 years, respectively, and their source strength would not have diminished significantly since initial use. Due to neutron absorption in-core primary neutron sources are typically depleted and have a significantly lower source strength (typically requiring replacement with secondary neutron sources as a result of the depletion).

Secondary neutrons sources become active after activation by thermal neutrons in the reactor core. The most common secondary source, SbBe, relies on the gamma decay of ^{124}Sb to produce a γ,n reaction in Be. As ^{124}Sb has a half-life of 2.7 years, the strength of the source significantly diminishes once removed from the reactor core as the production of ^{124}Sb ends. As maximum source strength occurs at core shutdown, and is typically designed to produce a source no higher than the primary source due to source decay, the secondary sources are not bounding for system performance.

As the initial source strength of neutron sources has about the same order of magnitude of a fuel assembly, the loading of a single neutron source in a system with 37 fuel assemblies would have less than a 3% effect on the neutron source in the system. The loading of neutron sources is restricted to one assembly, regardless of neutron source type, in one of the nine interior locations. Due to shielding provided by the outer assemblies, the dose rate effect of the already small source increase in the system is further mitigated. Therefore, there is no significant dose rate effect of loading a primary or secondary neutron source.

Neutron source assemblies (NSA) may contain source rods attached to hardware similar in configuration to guide tube plug devices (thimble plugs) and burnable absorbers, in addition to containing burnable poison rodlets and/or thimble plug rodlets. For NSAs containing absorber rodlets, the BPRA cool time and burnup/exposure or hardware ^{60}Co curie limit are applied to the neutron sources. NSAs having only thimble plug rodlets require the thimble plug restriction to

be applied. Combination NSAs, containing both thimble plug and burnable absorber rodlets, must apply the more limiting of the two minimum cool time/curie limits. Fuel assemblies loaded with NSAs will apply the limiting additional cool time for BPRAs or TPs.

CE 14×14 and 16×16 assembly types were not evaluated with BPRA/TP non-fuel hardware. Only RCCAs were considered for these fuel types. NSAs are not permitted for loading for CE 14×14 and 16×16 fuel types.

Based on location of the NSA in one of the center 9 basket opening, which are shielded by the exterior fuel assemblies, there is no significant dose associated with the NSA source.

5.8.6 Nonfuel Hardware Component – Reactor Control Elements

Reactor control element (e.g., CEAs and RCCAs) material quantities and the core region in which the material was exposed to the neutron activation flux were obtained from the DOE characteristics database. Bounding mass quantities activated in the assembly top and gas plenum regions are listed in Table 5.8-36 for the seven analyzed assembly configurations. Similar to the fuel assembly hardware evaluation, the plenum material is activated at a 0.2 flux factor, with top material activation at a 0.1 flux factor (0.05 for the CE 16×16 fuel). Material above the top is not considered to be activated to a significant extent and is, therefore, not modeled. In the shielding evaluation, the source material activated in the plenum region of the fuel assembly is located at the bottom of the active fuel region. This is the result of the full insertion of the CEA into the assembly under storage conditions. The CEA material classified as that in the top assembly region is modeled directly above the active fuel region. To minimize the increased dose rate due to loading of CEAs, only the center nine basket locations are allowed to contain the added source.

CEA response functions are evaluated in groups 11 through 15 based on the significant energy lines of the Ag-In-Cd, inconel, and stainless steel light element spectra. CEAs may also contain hafnium as the primary absorber nuclide. As seen in Table 5.8-38, the source for hafnium components of the absorber is not significant when compared to the source of steel/inconel or Ag-In-Cd based absorbers. The minimum cool time for CEAs is initially set uniformly at 10 years, with a maximum exposure of 180 GWd/MTU to assess dose rate effects on the system.

Maximum CEA dose rates are calculated for the Westinghouse 17×17 bounding CEA description due to the significant amount of Ag-In-Cd and steel/inconel activated in the assembly upper plenum region. Results are shown in Table 5.8-37.

Due to the CEA source being modeled in MCNP at the bottom of the active fuel, the limiting radial dose rates calculated for PWR fuel are not increased by the loading of CEAs. At the bottom of the cask, slight dose rate increases are calculated, but are negligible when compared to the limiting fuel dose rates.

The additional fuel assembly cool time required to load CEAs is shown in Table 5.8-34 per fuel type. As an increase in cool time will also decrease the fuel source term, the strict application of increased cool time without a recalculation of fuel dose rates is conservative.

The cask system is evaluated for higher CEA burnup/exposure than the 180,000 MWd/MTU, 10-year-cooled case used to establish baseline dose rate effects. The effects of higher burnup/exposure on steel/inconel absorber and the steel hardware of other absorbers is evaluated by reviewing the source spectrum in Table 5.8-38 that demonstrates that the overwhelming majority of the source is in energy groups 12 and 13, which correspond to the ^{60}Co energy lines.

Figure 5.8-38 is then used to compare the source strength in groups 12 and 13 with higher exposures at a cool time of 12 years. The figure demonstrates that the increase in cool time is enough to reduce the source to less than the 180 GWd/MTU and 10-year-cooled source. A similar comparison is made in Figure 5.8-39 for group 15 of the Ag-In-Cd absorber. Group 15 was chosen for the comparison as it represents the group producing maximum energy and source magnitude. As shown in Figure 5.8-39, due to the longer half-life of the isotopes producing these gamma rays, additional cool time is required. The complete source spectrum is, therefore, used to determine dose rate effects on the system with minimum cool times of 14 and 20 years for maximum exposures of 270 and 360 GWd/MTU, respectively. As shown in Table 5.8-39, these exposure/cool time combinations are bounded by the baseline 180,000 MWd/MTU, 10-year cool time state point. Table 5.8-40 lists the exposure cool time combinations applicable to all CEA types.

Table 5.8-36 Bounding CEA Mass Quantities Descriptions

		Mass Quantities (kg)						
Material	Neutron Zone*	CE 14x14	WE 14x14	WE 15x15	B&W 15x15	CE 16x16	WE 17x17	B&W 17x17
Steel/Inconel	Top	2.495	0.17	0.88	0.488	2.857	14.87	0.488
Ag-In-Cd	Top	0	0.86	0	1.581	1.089	0	1.581
Steel/Inconel	Gas Plenum	2.495	0.59	16.30	0.488	2.857	23.60	0.488
Ag-In-Cd	Gas Plenum	2.767	1.82	58.70	1.581	2.812	51.80	1.581

Note: a.) Units in kg.

b.) WE15 and WE17 CEA masses are total CEA mass not activated mass in the corresponding assembly region. When fully inserted, assemblies do not generate a significant neutron flux for activation of the CEAs. The weight data and therefore calculated heat load and source are very conservative.

Table 5.8-37 CEA Maximum Surface Dose Rates

[redacted]

* Neutron zone is the assembly region flux factor applied in the activation analysis. Zones are obtained from DOE/RW-0184, Volume 5 of 6.

Table 5.8-38 Gamma Source Comparison for CEA Primary Absorber Materials

Group	Steel/Inconel 180 GWd/MTU 10-yr cooled (gamma/sec/kg)	Ag-In-Cd 180 GWd/MTU 10-yr cooled (gamma/sec/kg)	Hafnium 360 GWd/MTU 10-yr cooled (gamma/sec/kg)
1	0.000E+00	0.000E+00	0.000E+00
2	0.000E+00	0.000E+00	0.000E+00
3	0.000E+00	0.000E+00	0.000E+00
4	0.000E+00	0.000E+00	0.000E+00
5	0.000E+00	0.000E+00	0.000E+00
6	0.000E+00	0.000E+00	0.000E+00
7	6.508E-16	1.351E-09	0.000E+00
8	7.212E+04	7.637E+02	0.000E+00
9	4.651E+07	2.810E+05	1.739E-17
10	6.989E-06	1.370E+07	3.596E-05
11	1.236E+01	7.785E+09	3.438E+03
12	4.406E+12	1.120E+10	2.294E+06
13	4.644E+12	7.394E+08	5.918E+06
14	1.126E+09	5.100E+10	1.873E+05
15	8.200E+06	3.525E+13	2.442E+01
16	2.361E+07	1.589E+13	9.747E+01
17	3.736E+08	2.023E+10	1.976E+03
18	2.847E+08	3.069E+10	1.216E+06
19	5.734E+09	1.013E+11	2.178E+06
20	2.377E+10	1.607E+12	7.323E+06
21	6.830E+10	8.541E+12	3.077E+05
22	8.206E+10	2.695E+11	2.777E+05
Total	9.232E+12	6.179E+13	1.971E+07

Note: B_4C absorbers do not produce significant sources in the transport system.

which remain well below the exclusive use limit of 1000 mrem/hr. Maximum normal condition dose rate at the one foot radial detector (corresponding to the personnel barrier) is 63 mrem/hr. Azimuthal peaking at the personnel barrier is discussed in Section 5.8.10.3. Damaged dose rates are summarized in Table 5.8-50 and Table 5.8-51.

Nonfuel hardware may not be loaded in damaged fuel locations. NFHW may be loaded in any of the remaining 33 basket locations with the additional fuel requirements documented in Section 5.8.5.2. In order to accommodate the added source due to damaged fuel, some CE 14×14 and Westinghouse fuel types must be cooled slightly longer. Refer to Table 5.8-49 for the additional cool times required. When applicable, additional fuel cool times required to load NFHW must be combined with additional cool times due to damaged fuel. The baseline undamaged fuel minimum cool times are documented in Section 5.3 and contain data for low burnup (Table 5.8 14b), standard burnup (up to 45 GWd/MTU) and high burnup fuels.

In the model, no credit is taken for the thicker plates in the corner locations of the damaged fuel basket or the thickness of the damaged fuel cans themselves.

Note that CEA dose rates are not significant when compared to the fuel assembly results (see Table 5.8-34). Therefore, the combination of CEA and damaged fuel dose rates is not required and damaged fuel (maximum four assemblies) and CEAs (maximum nine assemblies) may both be loaded into damaged fuel baskets.

5.8.10.3 Damaged PWR Fuel Azimuthal Dose Rate Profiles

Data plots of dose rates versus axial location in the previous sections apply averaged dose rates over a given elevation. As the damaged fuel was evaluated at higher than undamaged source density, and the higher density source is located in four distinct basket locations, azimuthal (angular) dose rate peaking is addressed in the context of limiting dose rate locations. The limiting location for the package is the 2-meter boundary. Along with the 2-meter location an azimuthal detector was evaluated at the 1-foot location corresponding to the personnel barrier. Cask surface dose rates have significant margins to allowable and, therefore, azimuthal surface dose rate plots are not presented in this section, although bounding dose rates are shown in Table 5.8-50 and Table 5.8-51. At the fuel midplane axial location, 2-meter azimuthal (angular)-dependent data is extracted and plotted in Figure 5.8-60. As demonstrated in the azimuthal plot, there is no statistically resolvable dose rate peaking at the 2-meter, limiting dose rate location. The 1-foot azimuthal data is taken at the height of the top of the neutron shield assemblies and shown in Figure 5.8-60B. The plot shows a discernable shaping due to the four damaged fuel locations. The peaks are 30% greater than the radially averaged dose rates at 1 foot. Even after a 30% increase, the maximum 1-foot (personnel barrier) dose rates remain under 90 mrem/hr, well below the 200 mrem/hr limit for the personnel barrier.

Axial dose rate (cask lid and bottom) azimuthal divisions over the DF locations were not applied in the evaluations. Based on low dose rates in this region, the conservative cask model removing significant quantity of material from the impact limiter, and not modeling shielding or offset associated with the DF itself, the evaluation performed provides reasonable assurance that dose rate limits are met.

5.8.10.4 Sample Input Files

A sample input file for the normal condition cask and the active fuel damaged fuel scenario is provided in Figure 5.8-62. A sample input file for the accident event cask and the nonfuel hardware region damaged fuel scenario is provided in Figure 5.8-63.

Figure 5.8-47 **[DELETED] – was Figure 5.8-46 in Revision 12A**

[Deleted]

Figure 5.8-48 **[DELETED] – was Figure 5.8-47 in Revision 12A**

[Deleted]

Figure 5.8-49 **[DELETED] – was Figure 5.8-48 in Revision 12A**

[Deleted]

Figure 5.8-50 **[DELETED] – was Figure 5.8-49 in Revision 12A**

[Deleted]

Figure 5.8-51 **[DELETED] – was Figure 5.8-50 in Revision 12A**

[Deleted]

Figure 5.8-52 **[DELETED] – was Figure 5.8-51 in Revision 12A**

[Deleted]

Figure 5.8-53 Dose Rate Profile at 2m from Transport Vehicle of Normal Condition Cask – Damaged PWR Fuel

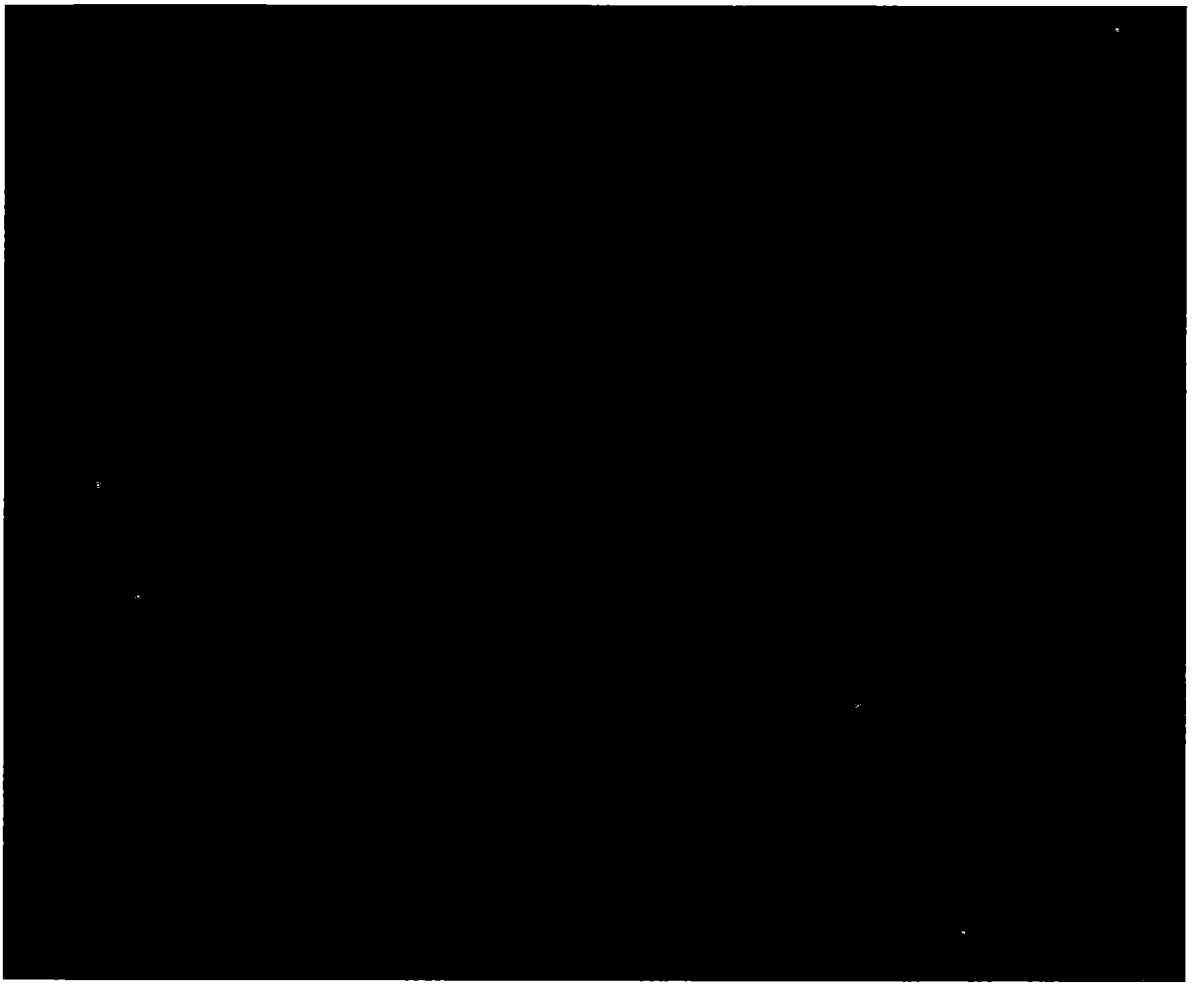

Figure 5.8-54 Dose Rate Profile at 2m from Top Surface of Normal Condition Cask – Damaged PWR Fuel

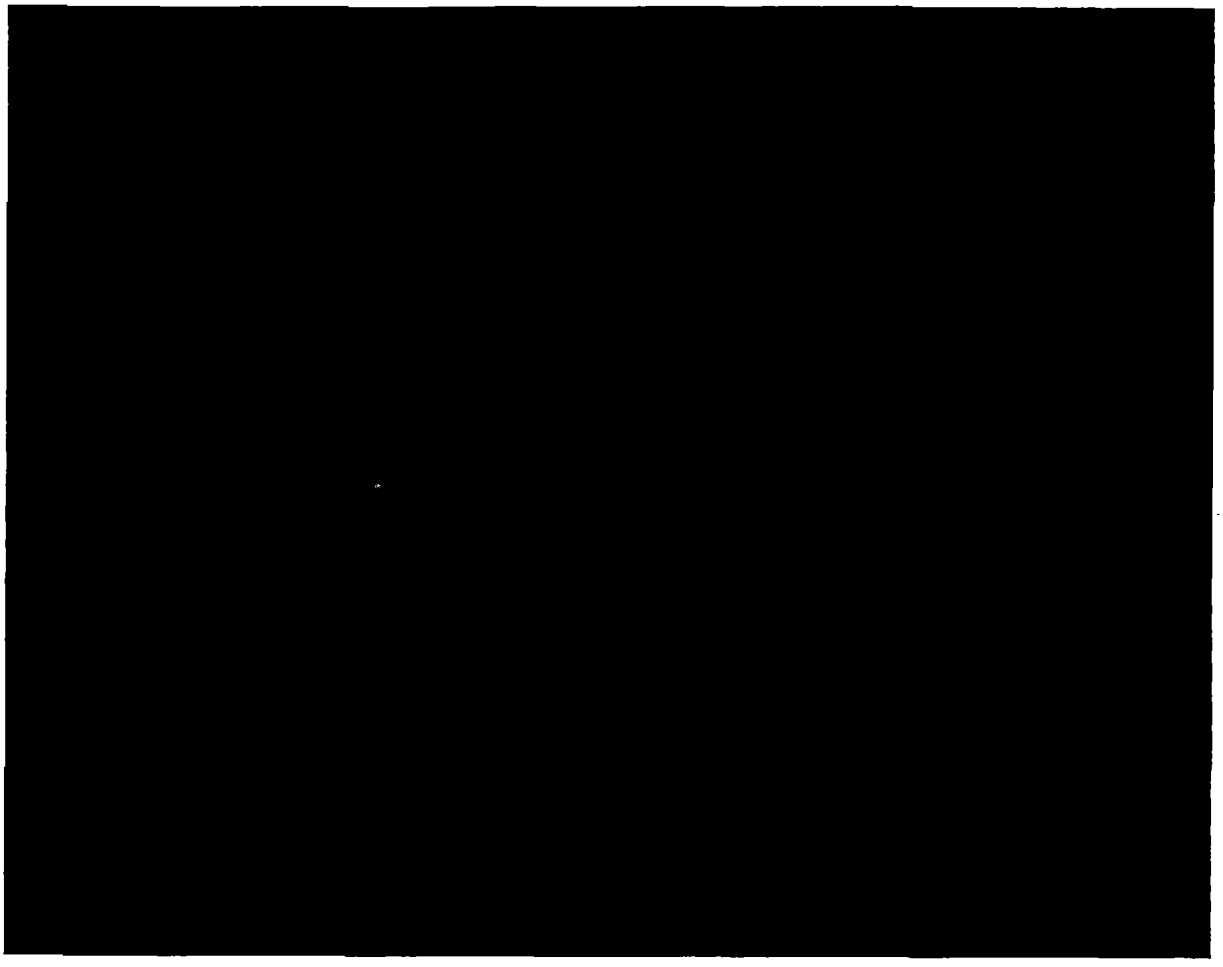

Figure 5.8-55 Dose Rate Profile at 2m from Bottom Surface of Normal Condition Cask – Damaged PWR Fuel

[redacted]

Figure 5.8-56 Dose Rate Profile at 1m from Radial Surface of Accident Event Cask – Damaged PWR Fuel

[redacted]

Figure 5.8-57 Dose Rate Profile at 1m from Top Surface of Accident Event Cask – Damaged PWR Fuel

[redacted]

Figure 5.8-58 Dose Rate Profile at 1m from Bottom Surface of Accident Event Cask – Damaged PWR Fuel

[redacted]

Figure 5.8-59 [DELETED] – was Figure 5.8-58 in Revision 12A

[Deleted]

Figure 5.8-60 Damaged Fuel Azimuthal Dose Rate Profile at Transport Cask Radial 2-Meter Distance – Normal Conditions – Active Fuel Midplane

[redacted]

Figure 5.8-60B Damaged Fuel Azimuthal Dose Rate Profile at Transport Cask Radial 1-Foot Distance – Normal Conditions – Top of Neutron Shield

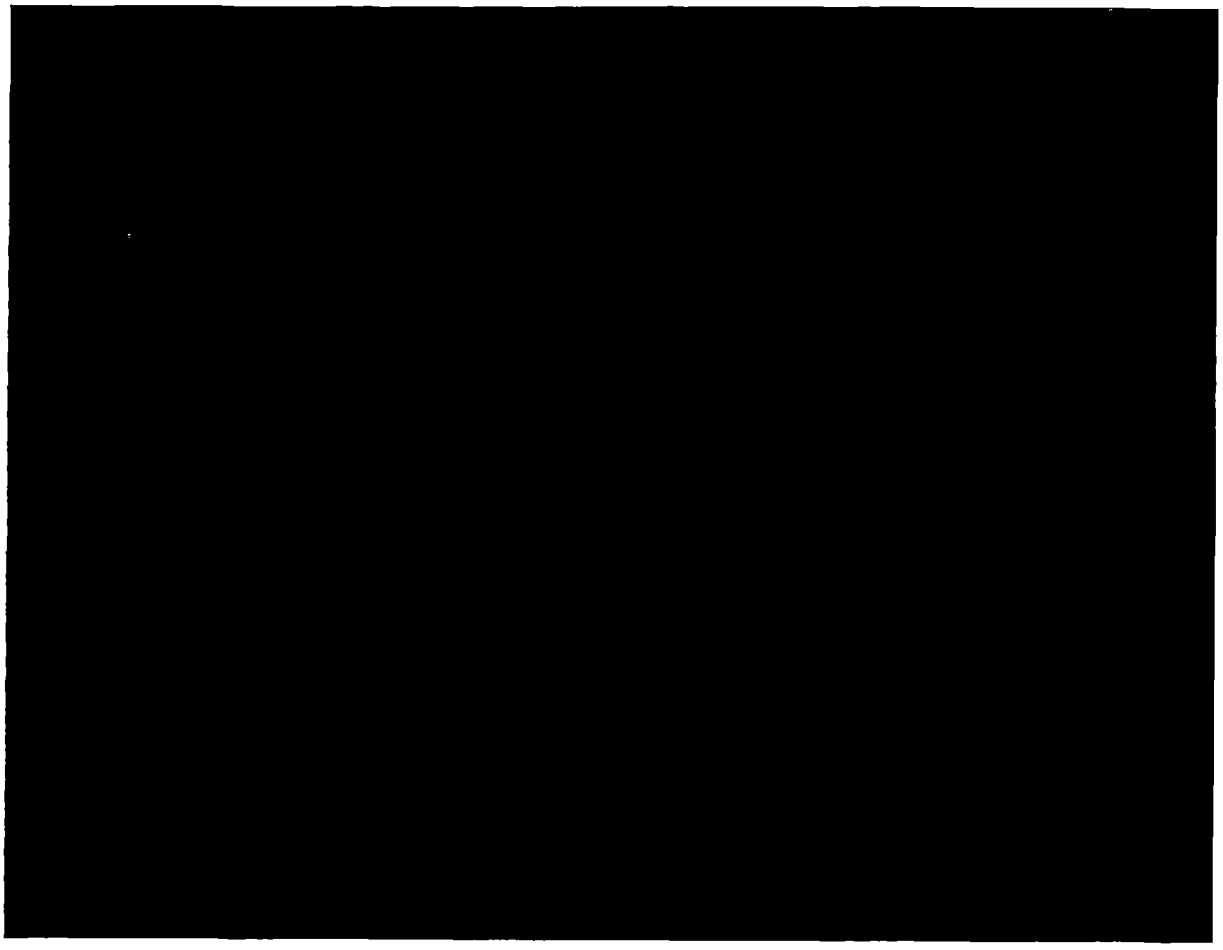

Figure 5.8-61 [DELETED] – was Figure 5.8-60 in Revision 12A

[Deleted]

Figure 5.8-62 Normal Condition Cask Sample Input File – Damaged PWR Fuel TSC – Active Fuel Damaged Fuel

[redacted]

Figure 5.8-62 Normal Condition Cask Sample Input File – Damaged PWR Fuel TSC – Active Fuel Damaged Fuel (cont'd)

[redacted]

Figure 5.8-62 Normal Condition Cask Sample Input File – Damaged PWR Fuel TSC – Active Fuel Damaged Fuel (cont'd)

[redacted]

Figure 5.8-62 Normal Condition Cask Sample Input File – Damaged PWR Fuel TSC – Active Fuel Damaged Fuel (cont'd)

[redacted]

Figure 5.8-62 Normal Condition Cask Sample Input File – Damaged PWR Fuel TSC – Active Fuel Damaged Fuel (cont'd)

[redacted]

Figure 5.8-62 Normal Condition Cask Sample Input File – Damaged PWR Fuel TSC – Active Fuel Damaged Fuel (cont'd)

[redacted]

Figure 5.8-62 Normal Condition Cask Sample Input File – Damaged PWR Fuel TSC – Active Fuel Damaged Fuel (cont'd)

[redacted]

Figure 5.8-62 Normal Condition Cask Sample Input File – Damaged PWR Fuel TSC – Active Fuel Damaged Fuel (cont'd)

[redacted]

Figure 5.8-62 Normal Condition Cask Sample Input File – Damaged PWR Fuel TSC – Active Fuel Damaged Fuel (cont'd)

[redacted]

Figure 5.8-62 Normal Condition Cask Sample Input File – Damaged PWR Fuel TSC – Active Fuel Damaged Fuel (cont'd)

[redacted]

Figure 5.8-62 Normal Condition Cask Sample Input File – Damaged PWR Fuel TSC – Active Fuel Damaged Fuel (cont'd)

[redacted]

Figure 5.8-62 Normal Condition Cask Sample Input File – Damaged PWR Fuel TSC – Active Fuel Damaged Fuel (cont'd)

[redacted]

Figure 5.8-62 Normal Condition Cask Sample Input File – Damaged PWR Fuel TSC – Active Fuel Damaged Fuel (cont'd)

[redacted]

Figure 5.8-62 Normal Condition Cask Sample Input File – Damaged PWR Fuel TSC – Active Fuel Damaged Fuel (cont'd)

[redacted]

Figure 5.8-62 Normal Condition Cask Sample Input File – Damaged PWR Fuel TSC – Active Fuel Damaged Fuel (cont'd)

[redacted]

Figure 5.8-62 Normal Condition Cask Sample Input File – Damaged PWR Fuel TSC – Active Fuel Damaged Fuel (cont'd)

[redacted]

Figure 5.8-62 Normal Condition Cask Sample Input File – Damaged PWR Fuel TSC – Active Fuel Damaged Fuel (cont'd)

[redacted]

Figure 5.8-62 Normal Condition Cask Sample Input File – Damaged PWR Fuel TSC – Active Fuel Damaged Fuel (cont'd)

[redacted]

Figure 5.8-62 Normal Condition Cask Sample Input File – Damaged PWR Fuel TSC – Active Fuel Damaged Fuel (cont'd)

[redacted]

Figure 5.8-62 Normal Condition Cask Sample Input File – Damaged PWR Fuel TSC – Active Fuel Damaged Fuel (cont'd)

[redacted]

Figure 5.8-62 Normal Condition Cask Sample Input File – Damaged PWR Fuel TSC – Active Fuel Damaged Fuel (cont'd)

[redacted]

Figure 5.8-62 Normal Condition Cask Sample Input File – Damaged PWR Fuel TSC – Active Fuel Damaged Fuel (cont'd)

[redacted]

Figure 5.8-62 Normal Condition Cask Sample Input File – Damaged PWR Fuel TSC – Active Fuel Damaged Fuel (cont'd)

[redacted]

Figure 5.8-62 Normal Condition Cask Sample Input File – Damaged PWR Fuel TSC – Active Fuel Damaged Fuel (cont'd)

[redacted]

Figure 5.8-62 Normal Condition Cask Sample Input File – Damaged PWR Fuel TSC – Active Fuel Damaged Fuel (cont'd)

[redacted]

Figure 5.8-62 Normal Condition Cask Sample Input File – Damaged PWR Fuel TSC – Active Fuel Damaged Fuel (cont'd)

[redacted]

Figure 5.8-62 Normal Condition Cask Sample Input File – Damaged PWR Fuel TSC – Active Fuel Damaged Fuel (cont'd)

[redacted]

Figure 5.8-62 Normal Condition Cask Sample Input File – Damaged PWR Fuel TSC – Active Fuel Damaged Fuel (cont'd)

[redacted]

Figure 5.8-62 Normal Condition Cask Sample Input File – Damaged PWR Fuel TSC – Active Fuel Damaged Fuel (cont'd)

[redacted]

Figure 5.8-62 Normal Condition Cask Sample Input File – Damaged PWR Fuel TSC – Active Fuel Damaged Fuel (cont'd)

[redacted]

Figure 5.8-63 Accident Event Cask Sample Input File – Damaged PWR Fuel TSC – Nonfuel Hardware Region Damaged Fuel

[redacted]

Figure 5.8-63 Accident Event Cask Sample Input File – Damaged PWR Fuel TSC – Nonfuel Hardware Region Damaged Fuel (cont'd)

[redacted]

Figure 5.8-63 Accident Event Cask Sample Input File – Damaged PWR Fuel TSC – Nonfuel Hardware Region Damaged Fuel (cont'd)

[redacted]

Figure 5.8-63 Accident Event Cask Sample Input File – Damaged PWR Fuel TSC – Nonfuel Hardware Region Damaged Fuel (cont'd)

[redacted]

Figure 5.8-63 Accident Event Cask Sample Input File – Damaged PWR Fuel TSC – Nonfuel Hardware Region Damaged Fuel (cont'd)

[redacted]

Figure 5.8-63 Accident Event Cask Sample Input File – Damaged PWR Fuel TSC – Nonfuel Hardware Region Damaged Fuel (cont'd)

[redacted]

Figure 5.8-63 Accident Event Cask Sample Input File – Damaged PWR Fuel TSC – Nonfuel Hardware Region Damaged Fuel (cont'd)

[redacted]

Figure 5.8-63 Accident Event Cask Sample Input File – Damaged PWR Fuel TSC – Nonfuel Hardware Region Damaged Fuel (cont'd)

[redacted]

Figure 5.8-63 Accident Event Cask Sample Input File – Damaged PWR Fuel TSC – Nonfuel Hardware Region Damaged Fuel (cont'd)

[redacted]

Figure 5.8-63 Accident Event Cask Sample Input File – Damaged PWR Fuel TSC – Nonfuel Hardware Region Damaged Fuel (cont'd)

[redacted]

Figure 5.8-63 Accident Event Cask Sample Input File – Damaged PWR Fuel TSC – Nonfuel Hardware Region Damaged Fuel (cont'd)

[redacted]

Figure 5.8-63 Accident Event Cask Sample Input File – Damaged PWR Fuel TSC – Nonfuel Hardware Region Damaged Fuel (cont'd)

[redacted]

Figure 5.8-63 Accident Event Cask Sample Input File – Damaged PWR Fuel TSC – Nonfuel Hardware Region Damaged Fuel (cont'd)

[redacted]

Figure 5.8-63 Accident Event Cask Sample Input File – Damaged PWR Fuel TSC – Nonfuel Hardware Region Damaged Fuel (cont'd)

[redacted]

Figure 5.8-63 Accident Event Cask Sample Input File – Damaged PWR Fuel TSC – Nonfuel Hardware Region Damaged Fuel (cont'd)

[redacted]

Figure 5.8-63 Accident Event Cask Sample Input File – Damaged PWR Fuel TSC – Nonfuel Hardware Region Damaged Fuel (cont'd)

[redacted]

Figure 5.8-63 Accident Event Cask Sample Input File – Damaged PWR Fuel TSC – Nonfuel Hardware Region Damaged Fuel (cont'd)

[redacted]

Figure 5.8-63 Accident Event Cask Sample Input File – Damaged PWR Fuel TSC – Nonfuel Hardware Region Damaged Fuel (cont'd)

[redacted]

Figure 5.8-63 Accident Event Cask Sample Input File – Damaged PWR Fuel TSC – Nonfuel Hardware Region Damaged Fuel (cont'd)

[redacted]

Figure 5.8-63 Accident Event Cask Sample Input File – Damaged PWR Fuel TSC – Nonfuel Hardware Region Damaged Fuel (cont'd)

[redacted]

Figure 5.8-63 Accident Event Cask Sample Input File – Damaged PWR Fuel TSC – Nonfuel Hardware Region Damaged Fuel (cont'd)

[redacted]

Figure 5.8-63 Accident Event Cask Sample Input File – Damaged PWR Fuel TSC – Nonfuel Hardware Region Damaged Fuel (cont'd)

[redacted]

Figure 5.8-63 Accident Event Cask Sample Input File – Damaged PWR Fuel TSC – Nonfuel Hardware Region Damaged Fuel (cont'd)

[redacted]

Figure 5.8-63 Accident Event Cask Sample Input File – Damaged PWR Fuel TSC – Nonfuel Hardware Region Damaged Fuel (cont'd)

[redacted]

Figure 5.8-63 Accident Event Cask Sample Input File – Damaged PWR Fuel TSC – Nonfuel Hardware Region Damaged Fuel (cont'd)

[redacted]

Figure 5.8-63 Accident Event Cask Sample Input File – Damaged PWR Fuel TSC – Nonfuel Hardware Region Damaged Fuel (cont'd)

[redacted]

Figure 5.8-63 Accident Event Cask Sample Input File – Damaged PWR Fuel TSC – Nonfuel Hardware Region Damaged Fuel (cont'd)

[redacted]

Figure 5.8-63 Accident Event Cask Sample Input File – Damaged PWR Fuel TSC – Nonfuel Hardware Region Damaged Fuel (cont'd)

[redacted]

Figure 5.8-63 Accident Event Cask Sample Input File – Damaged PWR Fuel TSC – Nonfuel Hardware Region Damaged Fuel (cont'd)

[redacted]

Table 5.8-47 Damaged Fuel Material Summary – 14a PWR Fuel

Material Description	Element/ Isotope	Density [atom/b-cm]	Density [g/cm³]
Damaged Fuel (Active Fuel)	Zirconium	4.1417E-03	9.9151
	Chromium	7.3976E-06	
	Tin	4.8602E-05	
	Nitrogen	1.3734E-05	
	Iron	8.6093E-06	
	Uranium 235	4.1900E-04	
	Uranium 238	2.0272E-02	
	Oxygen	4.1388E-02	
Damaged Fuel (Lower Nozzle)	Chromium	3.6218E-03	9.8996
	Manganese	3.6083E-04	
	Iron	1.2335E-02	
	Nickel	1.6043E-03	
	Uranium 235	3.7282E-04	
	Uranium 238	1.8037E-02	
	Oxygen	3.6824E-02	
Damaged Fuel (Upper Plenum)	Zirconium	1.0830E-03	10.0830
	Chromium	1.6340E-03	
	Tin	1.2710E-05	
	Nitrogen	3.5916E-06	
	Manganese	1.6259E-04	
	Iron	5.5604E-03	
	Nickel	7.2289E-04	
	Uranium 235	4.1440E-04	
	Uranium 238	2.0049E-02	
	Oxygen	4.0931E-02	
Damaged Fuel (Upper Nozzle)	Chromium	3.9541E-03	9.8526
	Manganese	3.9393E-04	
	Iron	1.3466E-02	
	Nickel	1.7515E-03	
	Uranium 235	3.6388E-04	
	Uranium 238	1.7065E-02	
	Oxygen	3.5941E-02	

Table 5.8-48 PWR Damaged Fuel Comparison – Normal Conditions 2 Meter Radial Dose Rates

[redacted]

Table 5.8-49 Additional Cool Time Required for 23 kW Damaged PWR Fuel Contents

Max. Burnup [GWd/MTU]	Min. Enr. [wt% U-235]	CE 14x14 Δ Cool Time [years]	WE 14x14 Δ Cool Time [years]	WE 15x15 Δ Cool Time [years]	WE 17x17 Δ Cool Time [years]
35	2.1	N/A	N/A	2.5	N/A
	2.3	0.0	0.6	0.8	0.3
40	2.5	1.9	2.4	3.3	2.8
	2.7	0.3	2.1	1.2	0.8
	2.9	0.0	0.6	0.0	0.0
45	2.7	3.9	2.6	4.5	4.2
	2.9	2.5	2.6	2.7	2.2
	3.1	0.6	2.5	0.7	0.1
	3.3	0.0	1.0	0.0	0.0
50	2.7	N/A	N/A	4.8	N/A
	2.9	3.6	2.8	3.5	2.8
	3.1	1.7	2.8	1.2	0.5
	3.3	0.0	1.2	0.0	0.0
55	3.1	4.2	2.9	4.0	3.6
	3.3	2.2	3.0	1.9	1.5
	3.5	0.2	2.0	0.0	0.0
60	3.1	N/A	N/A	5.0	N/A
	3.3	4.6	3.0	4.9	4.1
	3.5	3.1	3.1	2.9	2.1
	3.7	1.3	2.8	0.8	0.0
	3.9	0.0	0.9	0.0	0.0

Table 5.8-50 Normal Condition Maximum Damaged PWR Fuel Dose Rates

[redacted]

Table 5.8-51 Accident Event Maximum Damaged PWR Fuel Dose Rates

[redacted]

5.8.11 Greater than Class C (GTCC) Waste Shielding Evaluation

Greater than Class C (GTCC) waste may be transported in MAGNATRAN. The shielding evaluation of GTCC waste is based on quantities of waste from the decommissioning of Zion Nuclear Power Station (ZNPS). Bounding source terms were generated based on 32,000 lbs. of GTCC waste being loaded per TSC. This weigh is bounded by the maximum amount of weight that could be loaded in the TSC determined by the structural analysis (55,000 lbs).

5.8.11.1 Source Term

The source term for the GTCC waste is based on measured specific activities of three key isotopes at a characterization date of January 2008: Ni-63 (6 Ci/lb), Co-60 (13 Ci/lb), and Fe-55 (5 Ci/lb). Additional radionuclide isotopes typical of GTCC material do not significantly attribute to cask dose rates. Of the three isotopes included in the source generation model, Co-60 is the dominant isotope due to its combination of high source magnitude and high energy lines (>1 MeV). These specific activities were input into ORIGEN-S and decayed 12 years, which is assumed to be the minimum time between the measurement of the activity of the ZNPS waste and actual transport offsite. The ORIGEN-S file used to generate the source term is presented in Figure 5.8-64. The resulting specific source term is multiplied by the total mass of GTCC waste in the basket (32,000 lbs). The primary source of cask dose rates is the Co-60 component of the GTCC inventory, which at the decayed time represents a source of 2.68 Ci/lb. The resultant source spectrum is summarized in Table 5.8-52.

5.8.11.2 Shielding Model

The shielding model is based on a specialized basket that can be fit into a standard short TSC and MAGNATRAN transport cask. The basket is assumed to obtain a homogenized mix of stainless steel GTCC waste that has reduced density to account for the maximum loading within the basket (see Table 5.8-53). The canister model is identical to the composite lid canister model employed for the short MAGNATRAN TSC, with a 2-inch radial stainless steel liner added to shield the contents. Similarly, the normal condition and accident event cask models, including the streaming paths, are similar to those described in Section 5.5.1.2. For GTCC analysis the impact limiters are conservatively not included in the shielding model. The Section 5.5 model also contains shield material reductions on the top forging of the cask (attachment area for impact limiter). These reductions are not included in the GTCC model. Dose rates in this region of the cask are negligible (~0.1 mrem/hr on surface). Material reduction compensated for by the presence of the impact will not affect the safety conclusions of the analysis. The GTCC evaluation also used nominal, rather than minimum material thickness). The primary shield for the GTCC source is the lead cask shield. The lead shield of the MAGNATRAN cask is dimensioned to maintain the evaluated (nominal) size with all tolerances result in increases to

lead shielding. The evaluated system, when combined with the low calculated dose rates, provides reasonable assurance that dose rate limits will be met. GTCC models use the same detector descriptions as the fuel assembly contents. The canister and cask materials are the same as those summarized in Section 5.5.2.

A dimensioned sketch of the model is shown in Figure 5.8-65, with a VISED sketch shown in Figure 5.8-66. A sample input file is provided in Figure 5.8-67.

5.8.11.3 Dose Rates and Decay Heat

Maximum dose rates are computed for the GTCC waste in the MAGNATRAN system and presented in Table 5.8-54 for the normal condition and Table 5.8-55 for the accident condition. As shown in the tables, the dose rates are well below the 10 CFR 71 limits. The 1-meter normal condition maximum dose rate, which defines the transport index (TI) for the cask, is 2.4 mrem/hr.

Based on the analyzed weight of 32,000 lbs of stainless steel, the total decay heat of the GTCC waste is 1.7 kW, which is much less than the allowed loading of 23 kW in the PWR MAGNATRAN system.

Table 5.8-52 GTCC Source Spectrum

E Lower [MeV]	E Upper [MeV]	Source [γ/sec/lb]
1.00E-02	2.00E-02	2.109E+09
2.00E-02	5.00E-02	1.602E+09
5.00E-02	1.00E-01	5.363E+08
1.00E-01	2.00E-01	1.293E+08
2.00E-01	3.00E-01	6.421E+06
3.00E-01	4.00E-01	8.425E+06
4.00E-01	6.00E-01	5.325E+05
6.00E-01	8.00E-01	1.849E+05
8.00E-01	1.00E+00	6.973E+06
1.00E+00	1.22E+00	1.047E+11
1.22E+00	1.44E+00	9.937E+10
1.44E+00	1.66E+00	2.788E-01
1.66E+00	2.00E+00	0.000E+00
2.00E+00	2.50E+00	1.049E+06
2.50E+00	3.00E+00	1.627E+03
3.00E+00	4.00E+00	0.000E+00
4.00E+00	5.00E+00	0.000E+00
5.00E+00	6.50E+00	0.000E+00
6.50E+00	8.00E+00	0.000E+00
8.00E+00	1.00E+01	0.000E+00
1.00E+01	1.20E+01	0.000E+00
1.20E+01	1.40E+01	0.000E+00
Total		2.085E+11

Table 5.8-53 GTCC Material Description

Material	Density [g/cm³]	Nuclide / Element	Density [atom/barn-cm]
GTCC	1.49	CHROMIUM	3.2818E-03
		MANGANESE	3.2696E-04
		IRON	1.1177E-02
		NICKEL	1.4537E-03

Table 5.8-54 Normal Condition Maximum GTCC Waste Dose Rates

[redacted]

Table 5.8-55 Accident Condition Maximum GTCC Waste Dose Rates

[redacted]

5.8.12 Localized Dose Rate Evaluation using Mesh Tallies

Surface (F2) tallies are employed in the loading tables to determine maximum dose rates. The surface tallies average the dose rates around the circumference of the tally surface which may result in underestimating dose rate peaks. Additional cases were evaluated with cell-based mesh (fmesh) tallies at features of the cask which may allow localized streaming. The locations identified as potential streaming paths are:

- The cooling fins, neutron shield bolts, and expansion foam at the bolt locations;
- The bottom rotation trunnion locations.

There are multiple fuel types and source terms which produce dose rates at or near the 2 meter normal condition limits. The source chosen is a Westinghouse 14×14 with 40 GWd/MTU burnup, 2.5 wt. % ^{235}U, and 11.9 year cool time which is the source providing maximum radial dose rates for this fuel type. The source and assembly type chosen will not significantly affect the conclusions. The dose rates from the surface tallies are summarized in Table 5.8-56. The surface tallies apply 2.4 cm axial splitting at the surface, and 4.3 cm for the 2 meter from conveyance vehicle detectors.

The maximum surface dose rates calculated using the loading tables are above the neutron shield. An azimuthal detector is included in Section 5.8.3.2 that demonstrates increased dose rates on the cask surface, maximum of 241 mRem/hr for this assembly type, but minor azimuthal effects at that location. The section also includes an azimuthal detector at the rotation trunnions. This detector could potentially smear axial effects as the rotation trunnion height is significant. Therefore, a finer mesh that examines axial effects and azimuthal effects is necessary. The evaluation of the bottom trunnion location also shifts the cask interior components to the bottom of the cask cavity aligning the fuel assembly source adjacent to the trunnions, maximizing dose rates at this location.

Exponential transforms and weight windows are applied for variance reduction. Accident conditions are not evaluated as the combustion of gaseous elements in the transport cask neutron shield is the primary contributor to the increase in dose rates for that condition. Minor gamma shielding differences and complete removal of neutron shield in localized areas will not result in significant dose rate increases for accident conditions.

5.8.12.1 Cooling Fins, Shield Bolts, and Expansion Foam Locations

The cooling fins, bolt holes, and expansion foam surrounding the bolt holes could result in azimuthal and axial variations in dose rates. The expansion foam, modeled as void, are prominent in the radial dose rate profiles provided by the surface tallies. Surface tallies at this

location could underestimate dose rates as azimuthal effects are averaged over the entire circumference and small axial effects could be averaged over a larger axial band. Fine mesh tallies are evaluated to compare dose rates to those calculated with the surface tallies. All source types are considered as the cooling fins and neutron shield voids provide neutron and gamma shielding effects.

A superimposed mesh tally is applied on the surface. The mesh applies 1 cm axial splitting, 1° azimuthal splitting, and 1 cm depth. This detector size is significantly smaller than any physical detectors and will capture any local peaking on the cask surface. The area of interest is shown in Figure 5.8-68.

The fuel neutron surface dose rate profile is plotted in Figure 5.8-69. The surface and mesh tallies are compared in Figure 5.8-70. The dose rates spike significantly but remain below the peak above the neutron shield.

The fuel gamma surface dose rate profile is plotted in Figure 5.8-71. As shown in Figure 5.8-72, surface dose rates over the neutron shield are 24% higher than those averaged over the entire circumference.

The neutron induced gamma surface dose rate profile is plotted in Figure 5.8-73. The azimuthal dose rate effects are from the cooling fins. As shown in Figure 5.8-74, surface dose rates over the neutron shield are 14% higher than those averaged over the entire circumference.

The results from surface tallies in Table 5.8-56 are adjusted using the results from the surface mesh tallies and the relative increase for each source (i.e. hardware dose rates scaled using the fuel gamma increase). The estimated surface dose rates are provided in Table 5.8-57. The results demonstrate that the increase in surface dose rates remains below the calculated maximum dose rates above the neutron shield and are still significantly below the dose rate limit of 1,000 mRem/hr on the surface.

A superimposed mesh tally is used to evaluate the dose rates 2 meters from the conveyance vehicle. 2 cm axial splitting, 1° azimuthal splitting, and 2 cm depth is used for the mesh. This detector size will capture if any of the streaming effects demonstrated on the surface remain at 2 meters from the conveyance vehicle.

The fuel neutron 2 meter dose rate profile is plotted in Figure 5.8-75. The surface and mesh tallies are compared in Figure 5.8-76. Axial peaking is observable, but is distributed over a range that is adequately captured by the 4 cm axial detectors in the surface tallies. The azimuthal effects are visually indistinguishable based on geometric features, and an examination of the dose rates indicate that there are few statistical increases (i.e. no trends that would suggest

5.8.13 Reconstituted Fuel Assemblies

Reconstituted assemblies have fuel rods that have been replaced with an inert material. When this inert material is stainless steel, the activation source of these rods must be considered.

The number of stainless steel replacement rods is limited to five per assembly (13.90 kg) and a maximum exposure of 32.5 GWd/MTU. To maximize the neutron activation source, the fuel assembly into which the steel replacement rods are placed in the depletion/activation model is conservatively set to an initial enrichment of 2.1 wt % ^{235}U. Minimum cool (decay) time for the activated steel rods is 20 years. No credit is taken for the reduction in fuel (UO_2) source for the replaced fuel rods. The stainless steel replacement rod source was modeled in the basket periphery at the periphery of the fuel assembly, minimizing the effect of intra- and inter-assembly self-shielding. Direct MCNP cases are used to evaluate the reconstituted assemblies with stainless steel rods.

The fuel assembly dose rate profiles indicate that gamma sources in the fuel do not peak outside the fuel midplane region, and are relatively flat over the fuel height. Therefore, an azimuthal detector at the fuel midplane is sufficient for determination of the stainless steel rod contributions.

10 CFR 71 limits normal condition dose rates to 1,000 mrem/hr at the surface of the cask and 10 mrem/hr at 2 meters from the conveyance. The maximum surface dose rates occur above the neutron shield and are significantly below limits. The maximum surface dose rates from the reconstituted assemblies, shown in Figure 5.8-84, which occur at the fuel midplane will not affect the listed maximum surface dose rates.

Under normal conditions, at 2 meters from the conveyance vehicle the maximum dose rate from the reconstituted assemblies is 0.21 mRem/hr as shown in Figure 5.8-85. The margin to the 2 meter dose rate limit for fuel assemblies without hardware is small with the maximum dose rate occurring near the fuel midplane. To ensure that maximum dose rates remain below limits, the minimum cool time required for reconstituted fuel assemblies is extended by further restricting dose rates an additional 0.25 mrem/hr. The results indicate that all reconstituted fuel assemblies should be cooled an additional 1 year to ensure dose rates are below limits.

The 10 CFR 71 dose rate limit for accident conditions is 1,000 mRem/hr at 1 meter from the cask. The margin to this limit is large, and maximum dose rates are primarily a result of the loss of neutron shield gases. The dose rates for the stainless steel rods are shown in Figure 5.8-86 and are negligible compared to the maximum dose rate for fuel and the margin to the limit.

Initial analysis was performed on steel replacement rods in a WE15 fuel type. The WE15 fuel type does not represent a bounding fuel rod volume. As slightly higher sources could exist in

other fuel types (due to either larger rod diameter or activated length). Differences in radiation source associated with larger mass rods are accounted for with the additional dose rate applied for cool time addition (a 20% increase from 0.21 to 0.25 mrem/hr) and in rounding up the additional cool time to 1 year. A check was performed on the heat load produced by the other fuel type's steel replacement rods. The cool time required to be added as a result of the steel rod inclusion is significantly less than 1 year for all fuel types (e.g., 0.3 yr for BW15). Dose rate and heat load effects are conservatively addressed as neither calculations credits the reduction in fuel source from the removed rods.

A single reconstituted fuel assembly may be loaded into the MAGNATRAN system in any location in the basket. The reconstituted assembly can have up to five stainless steel rod replacements with the stainless steel rods being irradiated for up to 32.5 GWd/MTU with a minimum cool time of 20 years. The reconstituted fuel assemblies must be cooled an additional 1 year. The reconstituted assemblies may be loaded with non-fuel hardware.

List of Figures (cont'd)

Figure 6.8.1-29 Spent Fuel k_{eff} vs. $^{241}Pu/^{238}U$ Ratio 6.8.1-25
Figure 6.8.1-30 Spent Fuel k_{eff} vs. $^{242}Pu/^{238}U$ Ratio 6.8.1-25
Figure 6.8.1-31 Spent Fuel k_{eff} vs. $^{241}Am/^{238}U$ Ratio 6.8.1-26
Figure 6.8.1-32 LEU Fresh Fuel k_{eff} versus Fuel Enrichment for MCNP6.1 ..... 6.8.1-26
Figure 6.8.1-33 LEU Fresh Fuel k_{eff} versus Rod Pitch for MCNP6.1 ..... 6.8.1-27
Figure 6.8.1-34 LEU Fresh Fuel k_{eff} versus Fuel Pellet Diameter for MCNP6.1 ..... 6.8.1-27
Figure 6.8.1-35 LEU Fresh Fuel k_{eff} versus Fuel Rod Outside Diameter for MCNP6.1 6.8.1-28
Figure 6.8.1-36 LEU Fresh Fuel k_{eff} versus Hydrogen/^{235}U Atom Ratio for MCNP6.1 . 6.8.1-28
Figure 6.8.1-37 LEU Fresh Fuel k_{eff} versus Soluble Boron Concentration for MCNP6.1 ..... 6.8.1-29
Figure 6.8.1-38 LEU Fresh k_{eff} versus Cluster Gap Thickness for MCNP6.1 ..... 6.8.1-29
Figure 6.8.1-39 LEU Fresh Fuel k_{eff} versus ^{10}B Plate Loading for MCNP6.1 ..... 6.8.1-30
Figure 6.8.1-40 LEU Fresh Fuel k_{eff} versus Energy of Average Neutron Lethargy Causing Fission for MCNP6.1 ..... 6.8.1-30
Figure 6.8.2-1 [DELETED] 6.8.2-2
Figure 6.8.2-2 [DELETED] 6.8.2-2
Figure 6.8.2-3 [DELETED] 6.8.2-2
Figure 6.8.2-4 [DELETED] 6.8.2-2
Figure 6.10.1-1 PWR Fuel Tube 6.10.1-27
Figure 6.10.1-2 PWR Basket Structure 6.10.1-28
Figure 6.10.1-3 MCNP Analysis – Undamaged PWR Basket – 37-Assembly Basket 6.10.1-29
Figure 6.10.1-4 Nominal Tube Interface Width and Nominal Tube Outer Width 6.10.1-54
Figure 6.10.1-5 Nominal Tube Interface Width and Minimum Tube Outer Width 6.10.1-54
Figure 6.10.1-6 Minimum Tube Interface Width and Maximum Tube Outer Width ... 6.10.1-55
Figure 6.10.1-7 Minimum Tube Interface Width and Minimum Tube Outer Width 6.10.1-55
Figure 6.10.1-8 TRITON Actinide and Fission Product Isotopics Generation Sample Input 6.10.1-56
Figure 6.10.1-9 Bounding Loading Curve Generation – CE14 – 0.036 g/cm^2 ^{10}B 6.10.1-59
Figure 6.10.1-10 Bounding Loading Curve Generation – CE16 – 0.036 g/cm^2 ^{10}B 6.10.1-59
Figure 6.10.1-11 Bounding Loading Curve Generation – WE14 – 0.036 g/cm^2 ^{10}B 6.10.1-60
Figure 6.10.1-12 Bounding Loading Curve Generation – WE15 – 0.036 g/cm^2 ^{10}B 6.10.1-60
Figure 6.10.1-13 Bounding Loading Curve Generation – WE17 – 0.036 g/cm^2 ^{10}B 6.10.1-61
Figure 6.10.1-14 Bounding Loading Curve Generation – BW15 – 0.036 g/cm^2 ^{10}B 6.10.1-61
Figure 6.10.1-15 Bounding Loading Curve Generation – BW17 – 0.036 g/cm^2 ^{10}B 6.10.1-62
Figure 6.10.1-16 [DELETED] 6.10.1-62
Figure 6.10.1-17 Schematic of Optional PWR Basket Configurations 6.10.1-63
Figure 6.10.1-18 RCCA Unit Cell and 1/4 Assembly Model for TRITON/NEWT Depletion 6.10.1-64
Figure 6.10.1-19 RCCA Allowed Basket Location (Zone A) 6.10.1-65

List of Figures (cont'd)

Figure 6.10.1-20 RCCA Depletion Input (TRITON) 6.10.1-66
Figure 6.10.1-21 [DELETED] 6.10.1-78
Figure 6.10.1-22 [DELETED] 6.10.1-78
Figure 6.10.1-23 [DELETED] 6.10.1-78
Figure 6.10.1-24 [DELETED] 6.10.1-78
Figure 6.10.1-25 [DELETED] 6.10.1-78
Figure 6.10.1-26 [DELETED] 6.10.1-78
Figure 6.10.1-27 [DELETED] 6.10.1-78
Figure 6.10.1-28 Undamaged PWR Basket Moderator Density Study 6.10.1-79
Figure 6.10.1-29 Reactivity vs. Burnup for WE 15×15 Fuel Assembly 6.10.1-79
Figure 6.10.1-30 Reactivity vs. Enrichment for WE 15×15 Fuel Assembly 6.10.1-80
Figure 6.10.1-31 k_{eff} Distribution for RCCA (Ag-In-Cd) Benchmarking 6.10.1-80
Figure 6.10.1-32 Histogram of Reactivity Results for Additional Insert Bands in Fuel Depletion Analysis 6.10.1-81
Figure 6.10.1-33 Histogram of Reactivity Results for Mixed-Mode Depletion in Fuel Depletion Analysis 6.10.1-82
Figure 6.10.2-1 PWR Damaged Fuel Basket Sketch 6.10.2-8
Figure 6.10.2-2 Damaged Fuel Basket Moderator Density Study 6.10.2-9
Figure 6.10.3-1 BWR Fuel Tubes 6.10.3-10
Figure 6.10.3-2 BWR Basket Structure 6.10.3-11
Figure 6.10.3-3 BWR 87-Assembly Basket Optional Neutron Absorber Sheet Locations 6.10.3-12
Figure 6.10.3-4 BWR 82-Assembly Basket Optional Neutron Absorber Sheet Locations 6.10.3-13
Figure 6.10.3-5 MCNP Transport Cask Model – BWR 87-Assembly Basket 6.10.3-14
Figure 6.10.3-6 MCNP Transport Cask Model – BWR 82-Assembly Basket 6.10.3-38
Figure 6.10.3-7 Maximum Tube Interface Width & Maximum Tube Corner Grind 6.10.3-56
Figure 6.10.3-8 Maximum Tube Interface Width & Minimum Tube Corner Grind 6.10.3-56
Figure 6.10.3-9 Minimum Tube Interface Width & Maximum Tube Corner Grind 6.10.3-57
Figure 6.10.3-10 Minimum Tube Interface Width & Minimum Tube Corner Grind 6.10.3-57
Figure 6.10.3-11 Maximum Reactivity Moderation Graphical Results 6.10.3-58

List of Tables

Table 6.1.1-1 Effective Areal Density as a Function of Absorber Credit 6.1.1-5
Table 6.1.2-1 PWR Fuel Assembly Loading Criteria (Assembly Description) 6.1.2-2
Table 6.1.2-2 BWR Fuel Assembly Loading Criteria (Assembly Description) 6.1.2-3
Table 6.1.2-3 Undamaged BWR Fuel Assembly Loading Criteria (Enrichment Limits for Fuel with Axial Blanket) 6.1.2-4
Table 6.1.2-4 Undamaged BWR Fuel Assembly Loading Criteria (Enrichment Limits for Fuel without Axial Blanket) 6.1.2-5
Table 6.1.2-5 [DELETED] 6.1.2-6
Table 6.2.1-1 PWR Fuel Assembly Characteristics 6.2.1-3
Table 6.2.1-2 BWR Fuel Assembly Characteristics 6.2.1-4
Table 6.3.2-1 Fuel Assembly Material Densities and Compositions 6.3.2-2
Table 6.3.2-2 Basket, TSC and Cask Material Densities and Compositions 6.3.2-3
Table 6.4.2-1 [DELETED] 6.4.2-2
Table 6.5.2-1 [DELETED] 6.5.2-2
Table 6.6.3-1 [DELETED] 6.6.3-4
Table 6.6.3-2 [DELETED] 6.6.3-4
Table 6.6.3-3 [DELETED] 6.6.3-4
Table 6.8.1-1 LEU Range of Applicability for Complete Set of 186 Benchmark Experiments 6.8.1-31
Table 6.8.1-2 MCNP5 v1.3 LEU Correlation Coefficients and USLs for Benchmark Experiments 6.8.1-31
Table 6.8.1-3 LEU MCNP Validation Statistics 6.8.1-32
Table 6.8.1-4 [DELETED] 6.8.1-53
Table 6.8.1-5 [DELETED] 6.8.1-53
Table 6.8.1-6 [DELETED] 6.8.1-53
Table 6.8.1-7 Spent Fuel Range of Applicability for Complete Set of 215 Benchmark Experiments 6.8.1-54
Table 6.8.1-8 Spent Fuel Correlation Coefficients and USLs for Benchmark Experiments 6.8.1-55
Table 6.8.1-9 Spent Fuel MCNP Validation Statistics 6.8.1-56

List of Tables (cont'd)

Table 6.8.1-10 LEU Fresh Fuel Correlation Coefficients and USLs for Benchmark Experiments for MCNP6.1 ..... 6.8.1-66
Table 6.8.1-11 Set of Nuclides for Actinide-Only Burnup Credit 6.8.1-66
Table 6.8.1-12 Set of Additional Nuclides for Actinide and Fission Product Burnup Credit 6.8.1-66
Table 6.8.1-13 LEU Fresh Fuel MCNP6.1 Validation Statistics 6.8.1-67
Table 6.8.2-1 [DELETED] 6.8.2-2
Table 6.8.2-2 [DELETED] 6.8.2-2
Table 6.8.2-3 [DELETED] 6.8.2-2
Table 6.8.2-4 [DELETED] 6.8.2-2
Table 6.8.2-5 [DELETED] 6.8.2-2
Table 6.8.2-6 Isotopic k_{eff} Bias Uncertainty for Actinides and Fission Product Burnup Credit Evaluations of PWR SNF 6.8.2-3
Table 6.10.1-1 PWR Nonfuel Insert Study (Guide and Instrument Tube Insertion) ... 6.10.1-83
Table 6.10.1-2 PWR Basket Component Tolerance and Shift Study Results (Independent Variations) 6.10.1-84
Table 6.10.1-3 PWR Basket Component Tolerance and Shift Study Results (Combined Variations; Radial In Shift) 6.10.1-85
Table 6.10.1-4 Depletion Analysis Analyzed Parameters 6.10.1-86
Table 6.10.1-5 Axial Profile Shape for Depletion Analysis 6.10.1-87
Table 6.10.1-6 Isotopes Extracted from TRITON Runs 6.10.1-87
Table 6.10.1-7 TRITON Parameter Trends (Cask Analysis – NUREG/CR-6665) 6.10.1-89
Table 6.10.1-8 NUREG "Reasonably" Bounding Parameters 6.10.1-90
Table 6.10.1-9 Undamaged PWR Fuel - Fresh Fuel Maximum Enrichments 6.10.1-91
Table 6.10.1-10 Undamaged PWR Fuel Hypothetical End-Drop Accident Evaluation 6.10.1-91
Table 6.10.1-11 [DELETED] 6.10.1-91
Table 6.10.1-12 Maximum Initial Enrichment – 37 Assembly Undamaged Fuel Configuration – 0.036 g/cm^2 ^{10}B Absorber 6.10.1-92
Table 6.10.1-13 Maximum Initial Enrichment – 37 Assembly Undamaged Fuel Configuration – 0.030 g/cm^2 ^{10}B Absorber 6.10.1-92
Table 6.10.1-14 Maximum Initial Enrichment – 37 Assembly Undamaged Fuel Configuration – 0.027 g/cm^2 ^{10}B Absorber 6.10.1-93
Table 6.10.1-15 [DELETED] 6.10.1-93

List of Tables (cont'd)

Table 6.10.1-16 Maximum Initial Enrichment – Undamaged Fuel Configuration WE15 – Optional Configurations 6.10.1-94
Table 6.10.1-17 RCCA Geometry 6.10.1-94
Table 6.10.1-18 RCCA Calculated Isotopic Composition 6.10.1-95
Table 6.10.1-19 RCCA Input Composition (atom/b-cm) 6.10.1-96
Table 6.10.1-20 [DELETED] 6.10.1-96
Table 6.10.1-21 [DELETED] 6.10.1-96
Table 6.10.1-22 Undamaged Fuel Basket - RCCA Controlled / Spent Fuel Comparison 6.10.1-97
Table 6.10.1-23 [DELETED] 6.10.1-97
Table 6.10.1-24 [DELETED] 6.10.1-97
Table 6.10.1-25 [DELETED] 6.10.1-97
Table 6.10.1-26 [DELETED] 6.10.1-97
Table 6.10.1-27 [DELETED] 6.10.1-98
Table 6.10.1-28 [DELETED] 6.10.1-98
Table 6.10.1-29 [DELETED] 6.10.1-98
Table 6.10.1-30 Single Assembly Misload – Most Reactive Fuel Assemblies 6.10.1-98
Table 6.10.1-30a Babcock & Wilcox Single Misload Assembly Results 6.10.1-99
Table 6.10.1-30b Combustion Engineering Single Misload Assembly Results 6.10.1-99
Table 6.10.1-30c Westinghouse Single Misload Assembly Results 6.10.1-100
Table 6.10.1-30d 0.030 g/cm^2 ^{10}B Content – 75% Effective Absorber Sheet 6.10.1-100
Table 6.10.1-30e 0.027 g/cm^2 ^{10}B Content – 67.5% Effective Absorber Sheet 6.10.1-101
Table 6.10.1-31 Undamaged PWR Basket Reactivity Summary 6.10.1-102
Table 6.10.1-32 Power Density Bias Calculation for Depletion Analysis 6.10.1-103
Table 6.10.1-33 Fission Product and Minor Actinide Worth and Bias 6.10.1-104
Table 6.10.1-34 Burnup Credit Depletion Bias Uncertainty 6.10.1-105
Table 6.10.1-35 Burnup and Enrichment Ranges for Loading Curve Data 6.10.1-106
Table 6.10.1-36 MCNP6.1 Validation – Range of Applicability for PWR Fresh and Spent Fuel Evaluations 6.10.1-107
Table 6.10.1-37 MCNP Criticality Results RCCA (Ag-In-Cd) 6.10.1-108
Table 6.10.1-38 USLSTATS Method 1 Results for Correlated Variables at 5% MMS – RCCA (Ag-In-Cd) 6.10.1-109
Table 6.10.1-39 Reactivity Results for CE Absorber Material Effects in Fuel Depletion Analysis 6.10.1.109

List of Tables (cont'd)

Table 6.10.1-40 Reactivity Results for CEAs Partially Inserted in Fule Dpeletion Analysis 6.10.1-110
Table 6.10.1-41 Reactivity Results for CEAs Fully Inserted for 5 GWd/MTU in Fuel Depletion Analysis 6.10.1-110
Table 6.10.1-42 Reactivity Results for Additional Insert Bands in Fuel Dpeletion Analysis 6.10.1-111
Table 6.10.1-43 Reactivity Results for Mixed-Mode Depletion in Fuel Depletion Analysis 6.10.1-112
Table 6.10.1-44 Reactivity Results for Additional Depletion Bands and Mixed-Mode Depletion in RCCA Depletion Analysis 6.10.1-112
Table 6.10.2-1 Damaged to Undamaged Basket Reactivity Comparison 6.10.2-10
Table 6.10.2-2 Damaged Fresh Fuel Mixture Height Reactivity Study – 0.036 g/cm^2 ^{10}B 6.10.2-11
Table 6.10.2-3 Damaged Fresh Fuel Reactivity – 0.036 g/cm^2 ^{10}B 6.10.2-12
Table 6.10.2-4 Undamaged with Burnup Credit and Damaged Fuel Reactivity Comparison – 0.036 g/cm^2 ^{10}B 6.10.2-12
Table 6.10.2-5 Damaged Fuel Basket Loading Curve Summary – 0.036 g/cm^2 ^{10}B ... 6.10.2-13
Table 6.10.2-6 Damaged Fuel Basket Loading Curve Summary – 0.030 g/cm^2 ^{10}B ... 6.10.2-13
Table 6.10.2-7 Damaged Fuel Basket Loading Curve Summary – 0.027 g/cm^2 ^{10}B ... 6.10.2-14
Table 6.10.2-8 Damaged Fuel Maximum Reactivity Moderation Study 6.10.2-15
Table 6.10.2-9 Damaged Fuel Missing Rod Study 6.10.2-16
Table 6.10.2-10 Undamaged Fuel Basket - RCCA Controlled / Spent Fuel Comparison 6.10.2-16
Table 6.10.2-11 Maximum Initial Enrichment – Damaged Fuel Configuration WE15 – Optional Configurations 6.10.2-17
Table 6.10.2-12 Burnup and Enrichment Ranges for Damaged Basket Loading Curve Data 6.10.2-18
Table 6.10.3-1 Overpack Comparison Results – 87 Assemblies 6.10.3-59
Table 6.10.3-2 Overpack Comparison Results – 82 Assemblies 6.10.3-60
Table 6.10.3-3 System Reactivity Response to BWR Fuel Type and Pellet-to-Clad Condition 6.10.3-61
Table 6.10.3-4 System Reactivity Response to BWR Fuel Type and Channel Thickness 6.10.3-62
Table 6.10.3-5 BWR Lattice Parameter Reactivity Study (Increased Variance) 6.10.3-63
Table 6.10.3-6 BWR Heterogeneous vs. Homogeneous Enrichment Analysis Results 6.10.3-64

List of Tables (cont'd)

Table 6.10.3-7 BWR 87-Assembly Basket Component Tolerance and Shift Study Results (Independent Variations) 6.10.3-66
Table 6.10.3-8 BWR 87-Assembly Basket Component Tolerance and Shift Study Results (Combined Variations; Radial In Shift) 6.10.3-67
Table 6.10.3-9 BWR 82-Assembly Basket Component Tolerance and Shift Study Results (Combined Variations; Radial In Shift) 6.10.3-68
Table 6.10.3-10 Tube Dimensioning / Tolerancing Study Results 6.10.3-69
Table 6.10.3-11 Top End Drop Results, No Axial Blanket – 87 Assembly 6.10.3-70
Table 6.10.3-12 Top End Drop Results, No Axial Blanket – 82 Assembly 6.10.3-71
Table 6.10.3-13 Top End Drop Results, 6" Axial Blanket – 87 Assembly 6.10.3-72
Table 6.10.3-14 Top End Drop Results, 6" Axial Blanket – 82 Assembly 6.10.3-73
Table 6.10.3-15 Top End Drop Results, 6" No Bale Crush – No Axial Blanket – 87 Assembly 6.10.3-74
Table 6.10.3-16 Top End Drop Results, 6" Axial Blanket – 82 Assembly 6.10.3-75
Table 6.10.3-17 Top End Drop Results, No Blanket, Reduced Enrichment – 87 Assembly (0.027 g/cm2 10B Absorber) 6.10.3-76
Table 6.10.3-18 Top End Drop Results, No Blanket, Reduced Enrichment – 82 Assembly (0.027 g/cm2 10B Absorber) 6.10.3-77
Table 6.10.3-19 87 Assembly – Maximum Enrichment Fuel with and without Axial End Blanket (0.027 g/cm2 10B Absorber) 6.10.3-78
Table 6.10.3-20 82 Assembly – Maximum Enrichment Fuel with and without Axial End Blanket 6.10.3-79
Table 6.10.3-21 BWR Maximum Reactivity Moderation Results 6.10.3-80
Table 6.10.3-22 BWR Maximum System Reactivity Results (Infinite Array) 6.10.3-80
Table 6.10.3-23 BWR Single Cask Result Summary 6.10.3-81
Table 6.10.3-24 Maximum Allowed Enrichment – 0.0225 g/cm2 Effective 10B – 87 Assembly 6.10.3-82
Table 6.10.3-25 Maximum Allowed Enrichment – 0.0225 g/cm2 Effective 10B - 82 Assembly 6.10.3-83
Table 6.10.3-26 Maximum Allowed Enrichment – 0.020 g/cm2 Effective 10B – 87 Assembly 6.10.3-84
Table 6.10.3-27 Maximum Allowed Enrichment – 0.020 g/cm2 Effective 10B – 82 Assembly 6.10.3-85
Table 6.10.3-28 MCNP Validation – Range of Applicability for BWR Evaluations 6.10.3-86

31. NUREG/CR-6665, ORNL/TM-1999/303, Review and Prioritization of Technical Issues Related to Burnup Credit for LWR Fuel.
32. Technical Bases to Support Recommendations and Proposed Guidance for Expanded Use of Burnup Credit in PWR Transport and Storage Applications, JC. Wagner, C.V. Parks, I.C Gauld ORNL December 2000, Draft Report.
33. C.V. PARKS, C.J. WITHEE, and J.C. WAGNER, "U.S. Regulatory Recommendations for Actinide-Only Burnup Credit in Transport and Storage Casks," Proceedings of the IAEA Technical Meeting on Advances in Applications of Burnup Credit to Enhance Spent Fuel Transportation, Storage, Reprocessing and Disposition, August 29-October 2, 2005, London, U.K., IAEA-TECDOC-1547, ISBN 92-0-103307-9, Date of Issue: June 21, 2007.
34. ORNL/TM-2001/273, Recommendations for Addressing Axial Burnup in PWR Burnup Credit Analysis, NUREG/CR-6801.
35. DeHart, M.D. and Hermann, O.W. 1996. An Extension of the Validation of SCALE (SAS2H) Isotopic Predictions for PWR Spent Fuel. ORNL/TM-13317. Oak Ridge, Tennessee Oak Ridge National Laboratory.
36. DOE (U.S. Department of Energy) 1997. Isotopic and Criticality Validation for PWR Actinide-Only Burnup Credit. DOE/RW-0497. Washington, D.C.: U.S. Department of Energy, Office of Civilian Radioactive Waste Management.
37. NUREG/CR-6798, ORNL/TM-2001/259, "Isotopic Analysis of High-Burnup PWR Spent Fuel Samples From the Takahama-3 Reactor", C. E. Sanders, I. C. Gauld, Oak Ridge National Laboratory, Oak Ridge, Tennessee, May 2002.
38. Hermann, O.W.; Bowman, S.M.; Brady, M.C.; and Parks, C.V. 1995. Validation of the Scale System for PWR Spent Fuel Isotopic Composition Analyses. ORNL/TM-12667. Oak Ridge, Tennessee: Oak Ridge National Laboratory.
39. DOE/RW-0472, Rev. 2,"Topical report on Actinide-Only Burnup Credit for PWR Spent Nuclear Fuel Packages."
40. [Deleted].
41. "MCNP6 User's Manual," LA-CP-13-00634, Version 1.0, Manual Rev. 0, May 2013.
42. NUREG/CR-7041, ORNL/TM-2011/21, SCALE/TRITON Primer: A Primer for Light Water Reactor Lattice Physics Calculations.

6.10.1.4.2 Bounding Input Variable Determination

Key input into the TRITON analysis are the core operating parameters and conditions applied to the fuel assemblies being evaluated. Oak Ridge National Laboratory (ORNL) staff has issued several reports and papers on the various parameters used in burnup credit analysis for large cask transport systems.

Primary Inputs required are:

- Moderator temperature (fixing moderator density at a fixed PWR system pressure)
- Fuel temperature
- UO_2 density
- Power density
- Moderator boron concentration
- Minimum cool time
- Fuel inserts/absorber (CEAs, BPRAs, IFBAs, Burnable Absorbers)

Secondary inputs are required as input to the analysis but are not critical to analysis results, are associated with the clad. They do not affect results significantly as the clad is a zirconium alloy and zirconium's cross-section to neutrons is small. These variables are:

- Clad temperature
- Clad density

NUREG Discussion

The primary reports issued by ORNL as NUREGs are discussed in sequence and cover IFBAs, BPRAs, CEAs, and cool time. Each of the reports also contains a discussion of the bounding in-core parameters used (e.g., moderator conditions, temperature, power). ORNL also published a NUREG containing a summary of the individual reports.

Study of the Effect of Integral Burnable Absorbers for PWR Burnup Credit, NUREG/CR-6760

The study conclusion separated effects of integral fuel burnable absorber rods (IFBAs) comprised of UO_2-Gd_2O_3, UO_2-Er_2O_3, or Al_2O_3-B_4C from those of ZrB coated fuel rods. Assemblies with IFBA rods comprised of UO_2-Gd_2O_3, UO_2-Er_2O_3, or Al_2O_3-B_4C were determined to be less reactive throughout burnup than their corresponding designs without IFBA. ZrB coated fuel rods, more typical of WE and B&W core fuel designs, were determined to potentially increase reactivity for the burnup credit cask and were studied in significant detail. The analysis summary indicates that for 3-D cask calculations with the axial burnup included,

assemblies with IFBA rods are generally less reactive than corresponding assemblies without IFBA rods. This is the result of unburned absorber in the end regions of the fuel which controls reactivity in the burnup credit basket design. IFBA rods without full length coverage (i.e., no absorber in the fuel axial end-region) may have a small positive reactivity effect. IFBA rods are typically not (or minimally) used in conjunction with heavy BPRA use. Comparison of the reactivity effect of IFBA rods to the effect of BPRAs clearly demonstrate that the reactivity effect of the IFBA rods is significantly less than the reactivity effect due to BPRAs. Modeling maximum BPRA content is therefore bounding for IFBAs. This conclusion does not change based on the type of burnup credit.

The NUREG evaluates Westinghouse Pyrex Burnable Absorber Assemblies (BAAs) and Westinghouse Wet Annular Burnable Absorbers (WABAs). The reactivity effect for the WABAs is less than that of the BAAs due to the absence of water in the center region of the BAAs.

Parametric Study of the Effect of Burnable Poison Rods for PWR Burnup Credit, NUREG/CR-6761

The summary of the BPRA NUREG indicates a 2 to 3% Δk effect of a maximum BPRA loading inserted for the full burnup. The report suggests that an option to reduce this effect is to limit BPRA exposure to one cycle insertion with administrative controls for cask loading. Per the final discussion and implications section, using full exposure may be used to "account for the effect of temporary control rod insertions." The MAGNATRAN burnup credit analysis includes BPRAs for the full credited burnup to minimize administrative controls. This conclusion does not change based on the type of burnup credit.

ORNL/TM-2001/69, Parametric Study of the Effect of Control Rods for PWR Burnup Credit, NUREG/CR-6759

The NUREG documents that even for significant burnup exposures, minor axial control rod (CR) insertion (e.g., < 20 cm) results in an insignificant effect on the k_{eff} of the cask. Typical operation for US reactors is all rods out. Therefore, CR insertion is not considered critical for US burnup credit analysis. Should CRs (CEAs) be inserted beyond this stage, the insertion needs to be considered in the analysis (or alternatively be bounded by BPRA depletion modeling such as extended insertion of the BPRA beyond its typical, one-cycle, use).

ORNL/TM-2001/272, Recommendations on the Credit for Cooling Time in PWR Burnup Credit Analysis, NUREG/CR-6781

This report indicates a reduction in k_{eff} for cool times out to 100 years. The report suggests a use of 5 years as it bounds any later increase (i.e., later increase/peak is lower than the 5-year value). This conclusion does not change based on the type of burnup credit.

ORNL/TM-1999/303, Review and Prioritization of Technical Issues Related to Burnup Credit for LWR Fuel, NUREG/CR-6665

This NUREG contains a summary of each of the primary areas requiring input into a TRITON analysis. The effect of each input variable is discussed, thereby providing a conservative direction for adjusting the input parameters. The summary table resulting from these discussions is duplicated in Table 6.10.1-7.

With the exception of power density, all of the trends are related to spectral hardening. Conditions that harden the neutron spectrum (i.e., increase the average neutron energy in the assembly) result in increased plutonium production and the diminished fission of ^{235}U fission due to increased plutonium fission. This has the effect of increasing the reactivity of the fuel.

Fuel Temperature (NUREG Section 4.2.1)

There is an increased k_{eff} corresponding to an increased fuel temperature on the order of about 4 to 5 pcm/K (pcm = percent mill = $10^{-5}\Delta k/k$). 1000K is an appropriately conservative fuel temperature. This conclusion is not affected by crediting minor actinides and fission products.

Moderator Temperature (NUREG Section 4.2.2)

The upper bound moderator temperature is most conservative (e.g., core outlet temperature, 600K). For PWR in cask analysis the effect is approximately 35 pcm/K. This conclusion is not affected by crediting minor actinides and fission products.

Soluble Boron (NUREG Section 4.2.3)

Soluble boron of 1000-1500 ppm is typical at beginning of cycle with an end of cycle value of 0-200 ppm. Modeling may be either the average concentration or a step function over the cycle. The effect of the soluble boron level is approximately 3.5 pcm/ppm in cask models. A boron concentration of 750 ppm should be adequately bounding. This conclusion is not affected by crediting minor actinides and fission products.

Power History (NUREG Section 4.2.4)

For actinide-only burnup credit calculations, high power operation is conservative at EOL. For high burnup fuel, an additional study may be needed as intermediate power peak produces maximum k_{eff}. A simple continuous-power operating history at maximum power density was used for actinide-only burnup credit for conservatism.

For crediting minor actinides and fission products, a lower power density might be conservative. A power density study was performed to assess the effect of power density. The result of this study is shown in Table 6.10.1-32. A 0.005 bias is applied to the USL during loading curve generation to account for the potential non-conservatism of having generated the isotopes at high power density.

Fixed Burnable Absorbers (NUREG Section 4.2.5)

Insert BPRAs full time for conservative analysis. Concluded that additional studies are needed. Previously referenced reports support modeling full BPRA insertion. This conclusion does not change based on the type of burnup credit.

6.10.1.4.3 Depletion Parameter Summary Papers

ORNL published several papers summarizing the bases for choosing a conservative set of input parameters for depletion modeling. Two of these papers are outlined as follows.

Technical Bases to Support Recommendations and Proposed Guidance for Expanded Use of Burnup Credit in PWR Transport and Storage Applications.

- Cool time analysis based on NUREG/CR-6781 indicates recommended cool time of 1 to 40 years. The 40-year cool time is conservative for analysis out to 200 years. Reactivity decreases from 1 to 40 years.
- Burnable absorbers (BPRA and IFBA) are evaluated in detail in NUREG/CR-6760 and NUREG/CR-6761. Recommendation includes full BPRA exposure to minimize administrative control and bounding IFBA by BPRA.

U.S. Regulatory Recommendations for Actinide-Only Burnup Credit in Transport and Storage Casks," IAEA-TECDOC-1547.

- Maximum cool time credited should be limited to 40 years.
- Use of YAEC-1937 for axial burnup profile sufficient.
- Burnable Absorber/CEA - Effects characterized in NUREG/CR-6759, -6760 and -6761 reports.

These conclusions do not change based on the type of burnup credit.

6.10.1.4.4 Reference Bounding Depletion Parameters

The bounding parameter approach for depletion input is implemented in the NUREGs studying the effect of various nonfuel hardware insertion. Baseline parameters for a bounding analysis are, therefore, directly copied from two of the NUREGs, NUREG/CR-6759 and NUREG/CR-6761, and listed in Table 6.10.1-8. Based on the trends demonstrated in Table 6.10.1-7, the values in Table 6.10.1-8 are adjusted in a conservative direction to arrive at the analysis

parameters in Table 6.10.1-4. As documented in Section 6.10.1.4.2, a 0.005 Δk_{eff} bias is applied to the USL during loading curve generation to account for using a power density of 60 MW/MTU for actinide and fission product burnup credit analysis.

6.10.1.4.5 The Effect of Inserts in the Fuel Depletion Calculation

Discussion of Modeled Inserts

Per NUREG/CR-6759, 6760, and 6761 [27, 28, 29], the presence of absorbers (CEAs, IFBA, and BPRAs) during depletion hardens the neutron spectrum, resulting in lower ^{235}U depletion and higher production of fissile plutonium isotopes. The simultaneous increase in plutonium production and decrease in fission of ^{235}U may increase the reactivity of the fuel at discharge and beyond. Consequently, an assembly exposed to absorbers may have a higher reactivity for a given burnup than an assembly that has not been exposed to absorbers. The reference NUREGs are summarized in Section 6.10.1.4.2. Table 6.10.1-4 identifies the inserts utilized during the fuel depletion calculations. The inserts applied were determined using the referenced NUREGs.

For Westinghouse fuel assemblies, a full loading of BAA BPRAs are fully inserted. NUREG/CR-6761 demonstrates that a full loading of BAA BPRAs bounds WABA BPRAs for fuel depletion calculations. NUREG/CR-6760 concludes that the reactivity effect of IFBA rods is significantly less than the reactivity effect due to BPRs. NUREG/CR-6759 concludes that the effect of CEAs on discharge reactivity is relatively small, based on an assumption of minor axial insertion during typical operations.

For CE fuel assemblies, a full loading of CEAs are fully inserted for the full burnup credited. Per NUREG/CR-6761, CE fuel assemblies have BPRs that are best treated as IFBAs, as they are integral and non-removable. NUREG/CR-6760 concludes that CE IFBAs do not produce an increase in k_{eff} and can therefore be neglected in depletion calculations. CE CEAs consists of predominantly B_4C pellets. The lower 8 in. of the CEA finger consists of Ag-In-Cd material. As the CEAs are considered fully inserted during the fuel depletion, B_4C was utilized for the absorber material. The differences in k_{eff} as a result of the absorber material are calculated using six sample cases. The B_4C absorber material is replaced with Ag(80%)-In(15%)-Cd(5%) material. The results shown in Table 6.10.1-39 demonstrate no statistical reactivity increase from the material change.

For B&W fuel assemblies, a full loading of BPRAs are fully inserted. NUREG/CR-6761 demonstrates that a full loading of BPRAs increases k_{eff}. NUREG/CR-6760 concludes that IFBAs do not produce an increase in k_{eff} and can therefore be neglected in depletion calculations. NUREG/CR-6759 concludes that the effect of CEAs on discharge reactivity is relatively small, based on an assumption of minor axial insertion during fuel depletion.

Depletion with CEA Insertion

Per DOE/RW-0472 [39], the control rods in PWRs are normally reserved to maintain shutdown margins. The control rods must remain above a certain height, the rod insertion limit, so that in the event a trip occurs the full insertion of the rods will add at least a prescribed amount of negative reactivity. For this reason, the control rods are normally at their fully withdrawn positions during fuel depletion. However, some control rods may be inserted to their "bite positions" so that the rate of a negative reactivity introduction is large enough to aid response to power demand. The bite position is generally no deeper than the top node (approximately 20 cm) of a uniform 18 node analysis.

Control rod insertion effects the system by hardening of the neutron spectrum in the vicinity of the insertion. NUREG-6759 demonstrates for a generic cask that minor axial insertion (e.g. < 20 cm) during fuel depletion has no significant effect on reactivity. To demonstrate that BPRAs provide a bounding fuel depletion model for the MAGNATRAN system, Δk_{eff}'s were calculated. A single top node (approximately 20 cm) was modeled with CEA inserted for the full depletion cycle. The remaining 17 nodes were modeled with no inserts (e.g. water). Critical CEA dimensions were retrieved from NUREG-6759. Table 6.10.1-40 provides results of the study. There is no significant increase of k_{eff} as a result of partial CEA insertion.

During start-up or low power operations limited depletion could occur with significant CEA insertion. NUREG-6759 concludes this could be acceptable as the effects of minor depletion with full insertion of CEAs will be bounded by the full insertion of BPRAs for the full burnup. This is supported by the data in the referenced NUREG. Reactivity effects the fuel depletion with CEA insertion ($\leq$ 5 GWd/MTU) are negligible at lower burnups and equivalent to BPRA insertion (NUREG-6761) at any point in the depletion sequence. If the fuel was depleted with BPRA in the first cycle then followed by insertion into the control bank in the second cycle, the overall reactivity increase would be equivalent to BPRA insertion for the full depletion. The expected depletion during start-up is significantly less than 5 GWd/MTU which is approximately equivalent to 5 months of insertion in an 18 month cycle. Extended low power operations are not typical in commercial power reactors.

The NUREG only presents data at 4.0 wt.% ^{235}U and concludes that more information on CEA operations is needed to make a strong recommendation. To support the NUREG conclusions with data from the MAGNATRAN system, Δk_{eff}'s are calculated for fuel assemblies with CEAs inserted for 5 GWd/MTU. The CEAs are replaced by water following the 5 GWd/MTU depletion step. The results shown in Table 6.10.1-41 demonstrate that after one cycle, the Δk_{eff} is negligible. A fuel assembly with 5GW/MTU burnup and low enrichment is not expected in spent fuel inventories. Therefore, the conclusions of NUREG-6759 are supported by the results.

Full insertion of BPRAs for the full burnup is expected to bound any reasonable CEA insertion for fuel depletion calculations.

Furthermore, CEA insertion during start-up is limited to the lead control bank, and therefore only a small number of fuel assemblies would be affected by CEA insertion. All fuel assemblies have been depleted with inserts in the burnup credit evaluation. This evaluation is expected to be bounding for all fuel assemblies.

Insert Depletion Methods

For the TRITON fuel depletion models, a single depletion band was utilized for the inserts and all inserts were depleted using the fuel assembly specific power. A single depletion band was utilized to reduce computational time. The fuel was depleted using constant power in the fuel as this is generally a good representation for a fuel element in commercial reactor operations.

The SCALE/TRITON Primer [42] recommends at least five bands for burnable absorber fuel pins (i.e. gadolinia containing fuel pins common in BWRs or IFBAs common in PWRs). The fuel depletion calculation modeled BPRAs and CEAs in the hardware locations. As this hardware is external to the fuel, the effects are expected to be less than those shown in the Primer. This was demonstrated by calculating Δk_{eff}'s for inserts with up to five depletion bands. Six cases for each of the fuel insert types (WE BAA BPRAs, B&W BPRAs, and CE CEAs) were utilized. Volume-equivalent bands were modeled. Each band was given their own material in TRITON, and was depleted accordingly. The TRITON calculation results in new material definitions for the fuel in the MCNP model. The MCNP results are compared in Table 6.10.1-42. A histogram of the results are plotted in Figure 6.10.1-32. The average Δk_{eff} is approximately 0.00001. This is insignificant to the criticality evaluations.

The SCALE/TRITON Primer suggests allowing mixed-mode depletion to avoid forcing a constant power in nonfuel elements. The Primer is unclear about whether this effect is primarily for constant power with the basis being the absorber material. The TRITON depletion models in this evaluation provided the constant power basis as the fuel. To further examine the effect of using a constant power only depletion model, the cases from the previous depletion band study were modified to deplete the inserts using constant flux. The basis remained a constant power in the fuel elements. This is described as mixed-mode depletion within TRITON. The MCNP results are compared against the results from the previous study in Table 6.10.1-43. As these cases contain both additional depletion bands and mixed-mode depletion, comparing against the results with the depletion bands isolates the Δk_{eff} differences due to the mixed-mode depletion. The results are plotted in Figure 6.10.1-33. The average Δk_{eff} is approximately 0.00011. This is insignificant to the criticality evaluations.

6.10.1.5 Criticality Evaluation for Fresh and Depleted Fuel Materials

Based on initial scoping evaluations for the system under various moderator conditions, the most reactive credible configuration for criticality analysis is one in which the cask is modeled under hypothetical accident conditions (i.e., neutron shield removed) and maximum neutronic coupling between casks in an infinite array (void cask exterior and TSC to cask gap). The majority of the criticality analyses demonstrating compliance with 10 CFR 71.55 and 10 CFR 71.59 are, therefore, performed on the no neutron shield cask array configuration. Loading curves are constructed in two phases. In the first phase the maximum fresh, unirradiated, fuel enrichment is calculated based on the fresh fuel USL of 0.9376 for MCNP5 v1.3 with ENDF/B-VI. In the next phase, the maximum initial enrichment as a function of assembly average burnup is provided. The burnup credit is evaluated using actinides and fission products. Application of a USL and other uncertainties for the burnup credit analysis are described in Section 6.10.1.5.2. All criticality analysis for PWR fuel with burnup credit is performed with MCNP6.1 and the ENDF/B-VII cross-section library.

After completion of the loading curve generation for each fuel type, a limited set of single cask (package) cases is executed to confirm the accident condition array results in maximum reactivity and to demonstrate compliance with regulatory requirements. Single cask cases are generated by removing the reflective boundary condition. Full water reflection is achieved by surrounding the cask by 20 cm of water.

6.10.1.5.1 Fresh Fuel Maximum Enrichment

Using the maximum reactivity model description from Section 6.10.1.2, the maximum initial enrichments for unburned PWR fuel are calculated. The maximum initial enrichments are calculated for each fuel hybrid by increasing enrichments by 0.1 wt % until the calculated reactivities in the maximum reactivity configuration meet or remain below the fresh fuel USL. The MCNP5 v1.3 fresh UO_2 fuel USL of 0.9376 was used to generate the maximum enrichments. The maximum enrichments are summarized in Table 6.10.1-9 for each of the evaluated effective neutron absorber loadings (0.036, 0.030, and 0.027 g $^{10}B/cm^2$).

The MCNP analysis is performed without inserts (BPRAs/CEAs) in the guide tubes as previous evaluations have demonstrated that inserts displace moderator in the assembly and reduce reactivity in the under-moderated fuel rod lattice.

In addition to the fresh fuel maximum enrichment determinations, the fresh fuel models are also used to establish any potential effects associated with the postulated drops of the transport cask. As the neutron absorber extends essentially the full length of the fuel tube (delta less than 1.5 inches) and the fuel tube extends the canister cavity (minus 3 inch axial plenum spacers), fuel assembly hardware provides sufficient offset that minimal active fuel exposure occurs as a result

of the evaluated transport cask accidents. No accident condition results in permanent deformation of the basket structure. No reactivity increases are therefore expected as a result of the transport cask end-drop accidents which is confirmed by the results shown in Table 6.10.1-10. Only B&W type fuel is evaluated for the bottom drop as it is the only fuel evaluated with a bottom plenum/spring that would result in a change from a pre to post drop condition. PWR fuel nozzles/end-fittings are not deformed as a result of the drop condition.

6.10.1.5.2 PWR Loading Curve Generation

For the burnup credit criticality evaluations using MCNP6.1, the minimum of either the fresh fuel USL (0.9427 for ENDF/B-VII) or spent fuel USL (0.9400) is applied. Fresh fuel benchmarks remain applicable as low burnup fuel material compositions will be more comparable to fresh fuel than the spent fuel material compositions. The minimum USL for MCNP 6.1 (ENDF/B-VII cross sections) is the spent fuel USL of 0.9400.

The spent fuel USL is calculated from critical benchmark cases containing only major actinides. Additional bias in the k_{eff} calculation for additional minor actinides and fission products is included in the generation of loading curves. This bias is dependent on the minor actinide and fission product worth as is described in Section 6.8.1.2.3. 3% of the worth is credited against the USL for the additional bias. The worth is calculated for a representative case set containing 37 fuel assemblies and an absorber boron content of 0.036 g/cm^2 ^{10}B. The results and applied biases for the minor actinides and fission products are provided in Table 6.10.1-33.

The depletion bias uncertainty listed in Table 6.10.1-34, and discussed in Section 6.8.2, is also applied against the USL. The bias uncertainties for the MCNP code and depletion code are not statistically combined, but rather summed. All loading curves are generated up to the USL, adjusted for bias and bias uncertainties listed in Tables 6.10.1-32 through 6.10.1-34. The resulting maximum allowed k_{eff}'s (k_{eff} including 2σ and linear fit bias) are listed in Table 6.10.1-34.

The system k_{eff}, as a function of initial enrichment and burnup, are calculated for various state points (see Table 6.10.1-35) and fit using the least squares method for multiple linear regression analysis. A minimum 15 year cool time is applied to these calculations. The functions are defined by burnup profile (i.e. < 18 GWd/MTU, etc.) due to discontinuities associated with the varying burnup profiles. The relationships are observed to be linear within their ranges by calculating correlation coefficients (R) for each variable for a limited set of fuel assemblies and for the multiple linear regression fit. A bias for the linear fits is applied that accounts for the maximum under-prediction of k_{eff} for that particular fit (i.e. fuel type, burnup range, and basket and absorber loading). This bias assures that no under-prediction in k_{eff} occurs, regardless of linearity in the data fit or lack thereof.

Sample plots for a limited set of data are shown in Figure 6.10.1-29 and Figure 6.10.1-30 for a WE 15×15 fuel assembly in a fully loaded basket (i.e. 37 assemblies) with 0.036 g/cm^2 ^{10}B absorber

content. The linear fits, and their correlations of determination (R^2), demonstrate that the relationships are linear within the evaluated ranges.

Note that the TRITON bias uncertainty represents a significant reactivity penalty (i.e., once burnup credit is invoked, a certain amount of burnup is required to overcome the bias prior to any allowed initial enrichment increase). Further, it must be noted that the burnup profile has unique breakpoints at 18 and 30 GWd/MTU. A flattening of the burnup profile increases the burnup of the underburned axial end-region that controls system reactivity. These breakpoints directly translate to jumps in the allowed initial enrichment (i.e., a fuel assembly evaluated at 30 GWd/MTU with the 18-30 GWd/MTU profile would require a lower initial enrichment, or conversely require more burnup than the same fuel evaluated at the 30+ GWd/MTU profile). The increase of the depletion bias and bias uncertainties with burnup, as shown in Table 6.10.1-34, counter the burnup profile effects by reducing the allowed initial enrichment, or conversely requiring more burnup.

To limit the number of loading curves generated, the number of fuel assembly hybrids was collapsed to one per core / lattice configuration. Load table/curves are therefore generated for WE14, WE15, WE17, CE14, CE16, BW15, and BW17 fuel types. Preliminary loading curves were constructed for each fuel type to assure that the one chosen for licensing is bounding across all burnup and enrichment (e.g., curves were constructed for WE17H1 and WE17H2 and the bounding type, the one allowing the minimum enrichment at a given burnup, is applied as WE17).

Loading curves are generated by producing MCNP results at initial enrichment and assembly average burnup intervals bracketing the USL. The data ranges are shown in Table 6.10.1-35. Linear fits are then created for the three burnup ranges specified by the axial burnup profile: burnup < 18 GWd/MTU, 18 GWd/MTU ≤ burnup ≤ 30 GWd/MTU, and burnup > 30 GWd/MTU. These linear fits use bounding intercepts, based on the linear fit bias, to ensure that they bound the actual data. Resulting data plots for the 0.036 g/cm^2 ^{10}B are shown in Figure 6.10.1-9 through Figure 6.10.1-15. Summarized load limitations in tabular form are listed in Table 6.10.1-12 for the 0.036 g/cm^2 ^{10}B absorber. The same approach is applied to the 0.030g/cm^2 ^{10}B absorber with results shown in Table 6.10.1-13 and the 0.027g/cm^2 ^{10}B absorber with results listed in Table 6.10.1-14. Load limitations presented in tabular form are applicable to a 5 wt.% ^{235}U maximum fresh fuel enrichment.

Cavity interior moderator in all cases is set to maximum density (0.9982 g/cm^3) representing the maximum reactivity condition for the undermoderated PWR assemblies. Cask exterior moderator condition and cask to canister annulus condition were set to void conditions to

maximize interaction between casks in the array. Various moderator conditions are examined in Section 6.10.1.11.

6.10.1.6 Optional Load Cask Configurations

Underloaded assembly configurations (i.e., reducing the number of fuel assemblies allowed in the cask) is evaluated using a 15-year cool time for the WE 15 fuel type. Only WE15 assemblies are evaluated for the underloaded configuration. Empty fuel cell locations for 36, 35, and 33-assembly patterns are defined in Figure 6.10.1-17. Reducing assemblies in the fixed 37-slot basket structure removes fissile material from the system while simultaneously creating flux traps (regions with significant quantities of moderator to thermalize fission neutron for absorption in the neutron absorber sheets attached to the fuel tubes). This combined effect significantly reduces the burnup credit required for loading. Loading curves for the underloaded configuration are listed in Table 6.10.1-16.

6.10.1.7 Reactivity Control Using Fuel Assembly Inserts

6.10.1.7.1 Depletion and System k_{eff} Evaluation for Nine RCCA Controlled Assemblies

Undamaged fuel discharged from the core due to non-standard circumstances, such as early reactor decommissioning, may result in a fuel assembly requiring transport with enrichment designed for multiple cycle operation but only having been used for one or two cycles. These types of fuel assemblies, referred to in this section as significantly under-burned, may not be loadable in the previously discussed reduced capacity cask configuration without significant additional capacity reductions. An alternate approach for these assemblies is evaluated in this section.

[redacted]

[redacted]

6.10.1.7.2 Criticality Benchmarking for MCNP6.1 with RCCAs

[redacted]

[redacted]

6.10.1.7.3 Depletion Code Benchmarking for RCCAs

[redacted]

[redacted]

[redacted]

6.10.1.8 [DELETED]

[Deleted]

6.10.1.9 Horizontal Burnup Tilt

[redacted]

6.10.1.10 Misload

Reactivity control of the PWR system is ensured by fuel assemblies meeting the required burnup credit. Redundant preparation/check procedures in place during fuel movement and loading ensure that the correct fuel assembly is loaded into the system prior to transport. Procedures are outlined in Chapter 7, Package Operations, with detailed site-specific procedures developed from the general SAR procedure set.

[redacted]

The misload analysis evaluated for the MAGNATRAN system matches the recommendations of ISG 8 revision 3 and considers:

[redacted]

[redacted]

6.10.1.11 Evaluation of Single Cask and Package Arrays

Considering Monte Carlo statistics, no single fuel assembly at any given enrichment represents the maximum reactivity configuration, as the loading curves are designed to set maximum enrichment to USL with bias and bias uncertainties for all assembly types and enrichments at flooded cask conditions. To demonstrate that 10 CFR 71.55 and 10 CFR 71.59 (NCT array) conditions do not produce statistically higher reactivity's then those generated by the 10 CFR 71.59 accident array configuration applied in previous sections additional cases are generated. Summarized are reactivities for the single cask to satisfy 10 CFR 71.55 requirements and normal and accident condition arrays to provide 10 CFR 71.59 criticality safety index (CSI) results. All array cases are based on infinite array calculations for a CSI of 0. Maximum reactivity summaries for the PWR undamaged basket are provided in Table 6.10.1-31.

Differences in cask configuration between normal and accident condition analysis are limited to the removal of the neutron shield and impact limiters. As the neutron shield contains a solid high hydrogen material and boron carbide, the neutrons entering this region from the cask cavity are substantially moderated and absorbed. This isolates the canister contents from cask exterior reflecting moderator or other casks in the array. Therefore, applying accident conditions in lieu of normal conditions of transport is acceptable for determination of maximum reactivity.

10 CFR 71.55 (b) evaluations for a containment reflected cask are not evaluated for undamaged PWR fuel. The condition was evaluated for damaged fuel in Section 6.10.2.4 and it was determined that removing the lead reflector reduces reactivity. Exterior conditions are shown to have negligible impact in the results. Therefore, the containment reflected conditions are not required here to demonstrate maximum reactivity.

All maximum reactivity configurations are based on fully flooded conditions as the fuel assembly was documented to be under-moderated by insert and fuel parameter studies. Confirmation that a fully flooded cask is bounding and that exterior condition has no significant effect is demonstrated by plotting reactivity trends versus both cask interior and exterior moderator conditions in Figure 6.10.1-28.

The results in Table 6.10.1-31 demonstrate the flooded fuel pellet to clad gap is appropriate and that the cask to canister annulus condition results in negligible reactivity differences.

6.10.1.12 MCNP Range of Applicability

A comparison of the analyzed case parameters to the MCNP6.1 ranges validated in Section 6.8 is shown in Table 6.10.1-36. The spent fuel comparison is limited to the energy of average neutron lethargy causing fission (EALCF) and water-to-fuel volume ratio. Correlations for the isotopic ratios are skewed towards the lower end of the range because of zero or nearly zero values for many of the uranium and plutonium isotopes. Therefore, the isotopic ranges are not included in the range of applicability comparison.

The majority of the analyzed variables fall within the validated ranges. The analyzed variables outside of the validated ranges are discussed below.

UO_2 Validation

PWR load tables indicate maximum fresh fuel enrichment allowed is as low as 1.8 wt % ^{235}U. This is less than the minimum validated value of 2.35 wt % ^{235}U. A review of the validation shows no statistical trend of k_{eff} vs. enrichment. Any trending observed in the plot is for a higher predicted k_{eff} (i.e., higher USL) as ^{235}U weight percent is decreased. Therefore, applying a fresh fuel enrichment below the validated range is acceptable. System may be loaded with fuel as low as 1.3 wt % ^{235}U. System reactivity drops quickly as enrichment is reduced below maximum allowable providing additional conservatism for the lower enriched material. The same arguments provided in this section also apply to the damaged fuel basket.

The minimum analyzed fuel rod pitch, 1.2598 cm, is less than the minimum validated value of 1.30 cm. The maximum analyzed value falls within the validated range. Similar to enrichment, the validation shows essentially no trend of k_{eff} vs. fuel rod pitch. Therefore, having the minimum fuel rod pitch outside of the validated range will not affect the USL.

The minimum analyzed fuel pellet outer diameter, 0.7844 cm, is less than the minimum validated value of 0.790 cm. The maximum analyzed value falls within the validated range. The validation shows a slightly upward trend of k_{eff} vs. fuel pellet outer diameter. Because the difference in fuel pellet outer diameter is only 0.0056 cm (less than 1% of 0.790 cm), having the minimum fuel pellet outer diameter outside of the validated range will not significantly affect the USL.

The minimum analyzed fuel rod diameter, 0.9144 cm, is less than the minimum validated value of 0.9400 cm. The maximum analyzed value falls within the validated range. The validation shows a slightly upward trend of k_{eff} vs. fuel rod diameter. Because the difference in fuel rod diameter is only 0.0256 cm (less than 3% of 0.9400 cm), having the minimum fuel rod diameter outside of the validated range will not significantly affect the USL.

Figure 6.10.1-1 PWR Fuel Tube

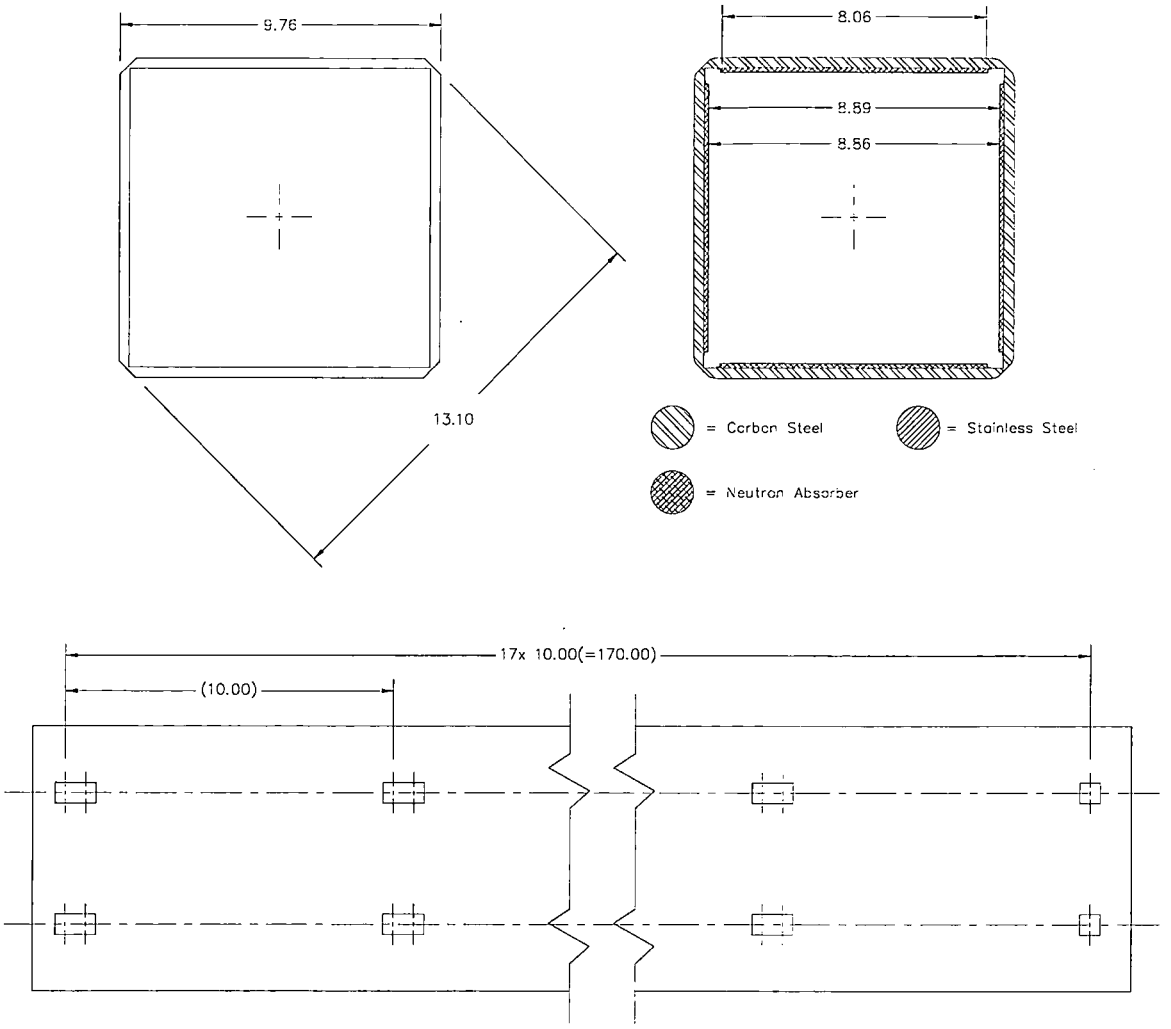

Note:
Dimensions in inches.

Figure 6.10.1-2 PWR Basket Structure

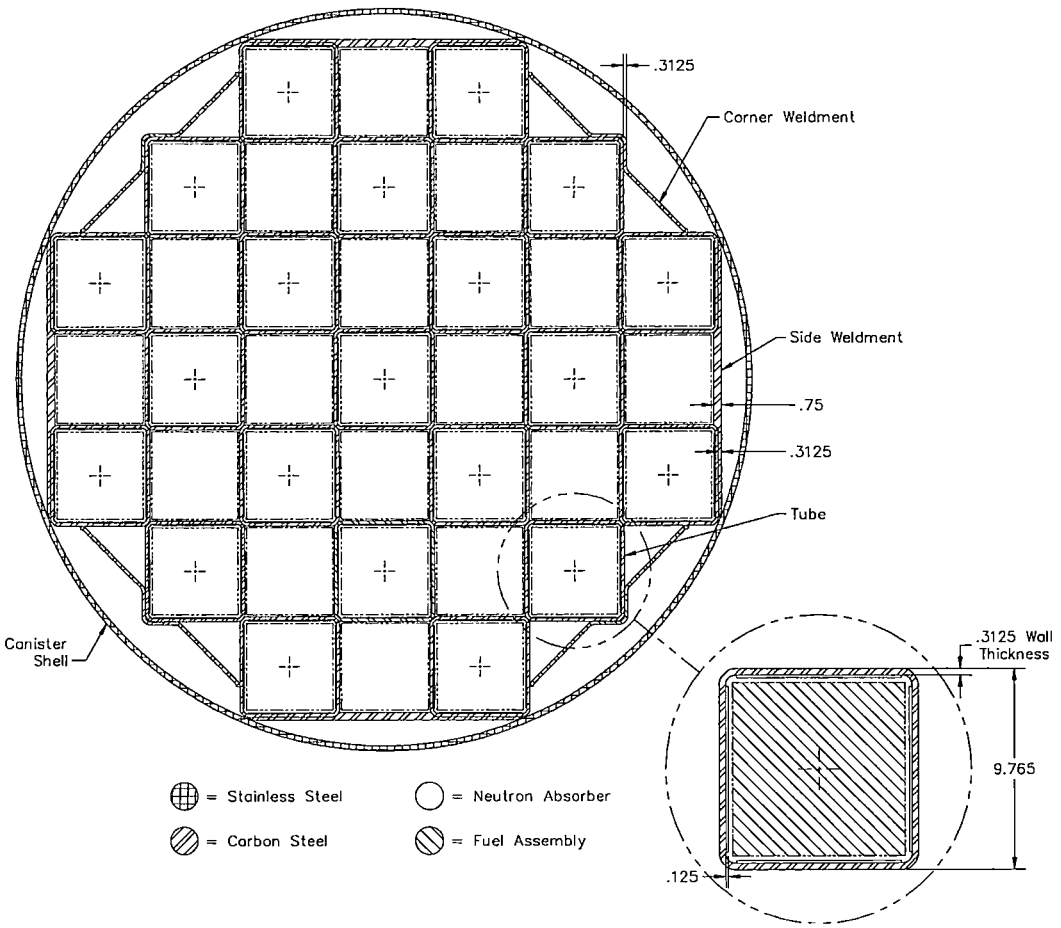

Notes:

- Dimensions in inches.
- Assembly fuel pin array is explicitly modeled. Shown as homogenized area for illustration purposes only.
- Neutron absorber is shown in figure, but is conservatively neglected from the maximum reactivity models.

Figure 6.10.1-3 MCNP Analysis – Undamaged PWR Basket – 37-Assembly Basket

[redacted]

Figure 6.10.1-3 MCNP Analysis – Undamaged PWR Basket – 37-Assembly Basket (cont'd)

[redacted]

Figure 6.10.1-3 MCNP Analysis – Undamaged PWR Basket – 37-Assembly Basket (cont'd)

[redacted]

Figure 6.10.1-3 MCNP Analysis – Undamaged PWR Basket – 37-Assembly Basket (cont'd)

[redacted]

Figure 6.10.1-3 MCNP Analysis – Undamaged PWR Basket – 37-Assembly Basket (cont'd)

[redacted]

Figure 6.10.1-3 MCNP Analysis – Undamaged PWR Basket – 37-Assembly Basket (cont'd)

[redacted]

Figure 6.10.1-3 MCNP Analysis – Undamaged PWR Basket – 37-Assembly Basket (cont'd)

[redacted]

Figure 6.10.1-3 MCNP Analysis – Undamaged PWR Basket – 37-Assembly Basket (cont'd)

[redacted]

Figure 6.10.1-3 MCNP Analysis – Undamaged PWR Basket – 37-Assembly Basket (cont'd)

[redacted]

Figure 6.10.1-3 MCNP Analysis – Undamaged PWR Basket – 37-Assembly Basket (cont'd)

[redacted]

Figure 6.10.1-3 MCNP Analysis – Undamaged PWR Basket – 37-Assembly Basket (cont'd)

[redacted]

Figure 6.10.1-3 MCNP Analysis – Undamaged PWR Basket – 37-Assembly Basket (cont'd)

[redacted]

Figure 6.10.1-3 MCNP Analysis – Undamaged PWR Basket – 37-Assembly Basket (cont'd)

[redacted]

Figure 6.10.1-3 MCNP Analysis – Undamaged PWR Basket – 37-Assembly Basket (cont'd)

[redacted]

Figure 6.10.1-3 MCNP Analysis – Undamaged PWR Basket – 37-Assembly Basket (cont'd)

[redacted]

Figure 6.10.1-3 MCNP Analysis – Undamaged PWR Basket – 37-Assembly Basket (cont'd)

[redacted]

Figure 6.10.1-3 MCNP Analysis – Undamaged PWR Basket – 37-Assembly Basket (cont'd)

[redacted]

Figure 6.10.1-3 MCNP Analysis – Undamaged PWR Basket – 37-Assembly Basket (cont'd)

[redacted]

Figure 6.10.1-3 MCNP Analysis – Undamaged PWR Basket – 37-Assembly Basket (cont'd)

[redacted]

Figure 6.10.1-3 MCNP Analysis – Undamaged PWR Basket – 37-Assembly Basket (cont'd)

[redacted]

Figure 6.10.1-3 MCNP Analysis – Undamaged PWR Basket – 37-Assembly Basket (cont'd)

[redacted]

Figure 6.10.1-3 MCNP Analysis – Undamaged PWR Basket – 37-Assembly Basket (cont'd)

[redacted]

Figure 6.10.1-3 MCNP Analysis – Undamaged PWR Basket – 37-Assembly Basket (cont'd)

[redacted]

Figure 6.10.1-3 MCNP Analysis – Undamaged PWR Basket – 37-Assembly Basket (cont'd)

[redacted]

Figure 6.10.1-3 MCNP Analysis – Undamaged PWR Basket – 37-Assembly Basket (cont'd)

[redacted]

Figure 6.10.1-4 Nominal Tube Interface Width and Nominal Tube Outer Width

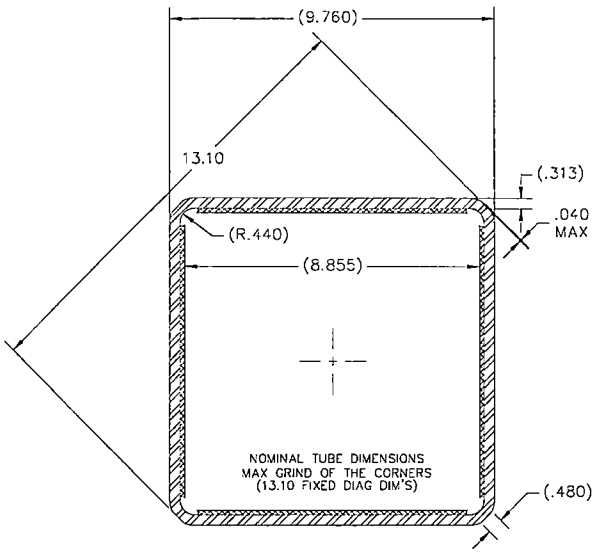

Figure 6.10.1-5 Nominal Tube Interface Width and Minimum Tube Outer Width

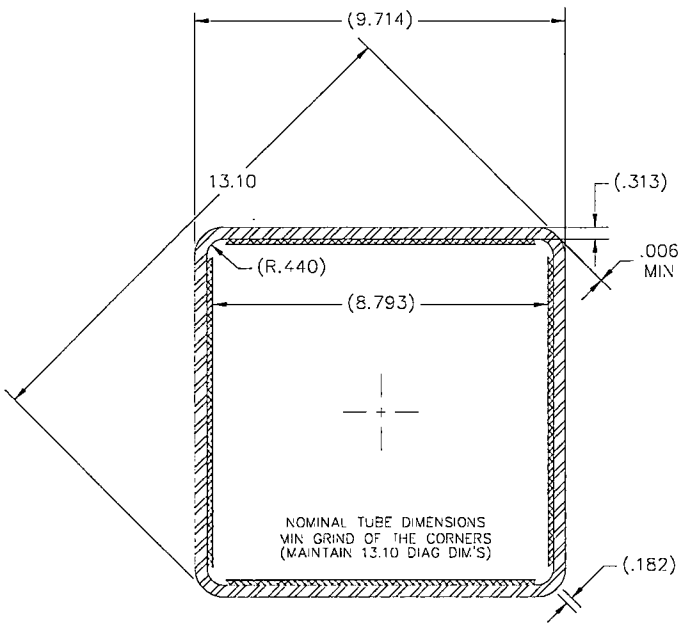

Figure 6.10.1-6 Minimum Tube Interface Width and Maximum Tube Outer Width

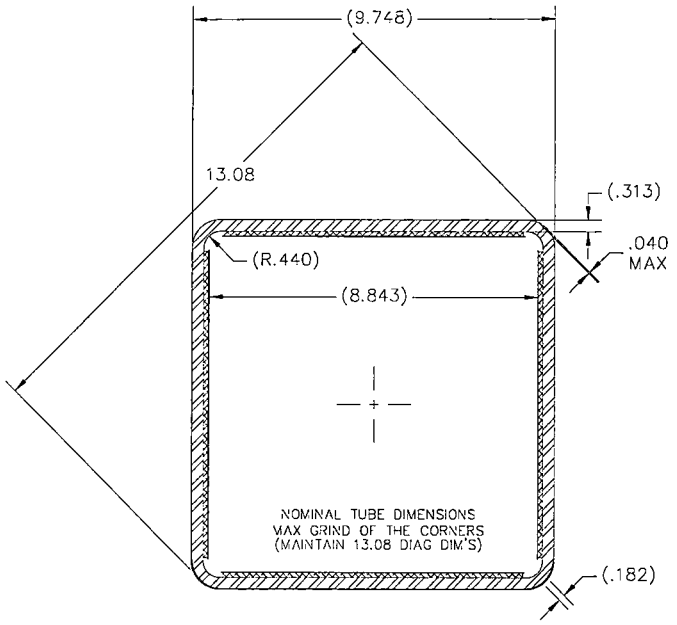

Figure 6.10.1-7 Minimum Tube Interface Width and Minimum Tube Outer Width

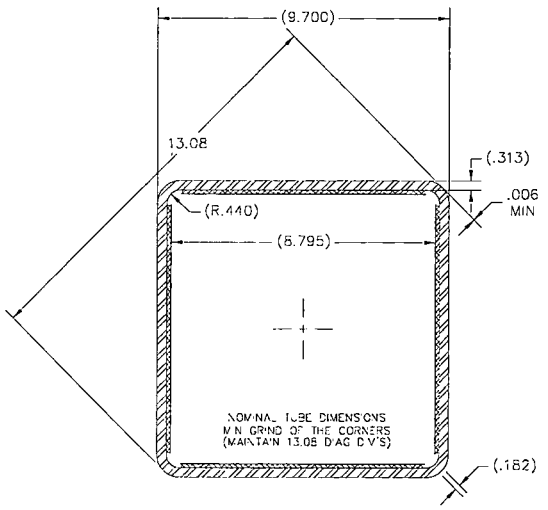

Figure 6.10.1-8 TRITON Actinide and Fission Product Isotopics Generation Sample Input

[redacted]

Figure 6.10.1-8 TRITON Actinide and Fission Product Isotopics Generation Sample Input (cont'd)

[redacted]

Figure 6.10.1-8 TRITON Actinide and Fission Product Isotopics Generation Sample Input (cont'd)

[redacted]

Figure 6.10.1-9 Bounding Loading Curve Generation – CE14 – 0.036 g/cm^2 ^{10}B

[redacted]

Figure 6.10.1-10 Bounding Loading Curve Generation – CE16 – 0.036 g/cm^2 ^{10}B

[redacted]

Figure 6.10.1-11 Bounding Loading Curve Generation – WE14 – 0.036 g/cm^2 ^{10}B

[redacted]

Figure 6.10.1-12 Bounding Loading Curve Generation – WE15 – 0.036 g/cm^2 ^{10}B

[redacted]

Figure 6.10.1-13 Bounding Loading Curve Generation – WE17 – 0.036 g/cm^2 ^{10}B

[redacted]

Figure 6.10.1-14 Bounding Loading Curve Generation – BW15 – 0.036 g/cm^2 ^{10}B

[redacted]

Figure 6.10.1-15 Bounding Loading Curve Generation – BW17 – 0.036 g/cm^2 ^{10}B

[redacted]

Figure 6.10.1-16 [DELETED]

[Deleted]

Figure 6.10.1-17 Schematic of Optional PWR Basket Configurations

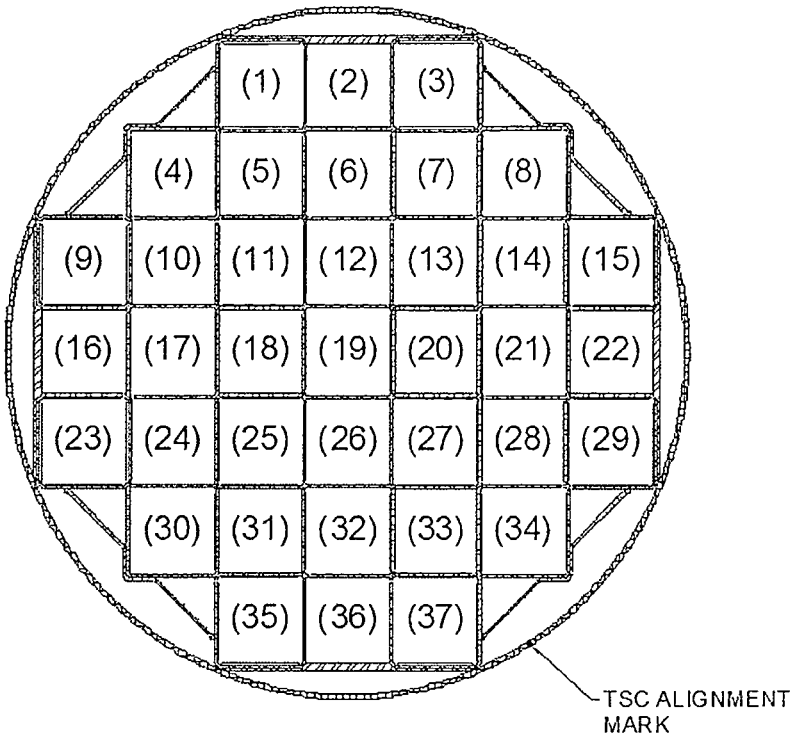

- 36 assembly loading: remove 19
- 35 assembly loading: remove 19, 18
- 33 assembly loading: remove 19, 18, 20, 12

Figure 6.10.1-18 RCCA Unit Cell and 1/4 Assembly Model for TRITON/NEWT Depletion

[redacted]

Figure 6.10.1-19 RCCA Allowed Basket Location (Zone A)

		ZONE C Location 01	ZONE C Location 02	ZONE C Location 03		
	ZONE C Location 04	ZONE B Location 05	ZONE B Location 06	ZONE B Location 07	ZONE C Location 08	
ZONE C Location 09	ZONE B Location 10	ZONE A Location 11	ZONE A Location 12	ZONE A Location 13	ZONE B Location 14	ZONE C Location 15
ZONE C Location 16	ZONE B Location 17	ZONE A Location 18	ZONE A Location 19	ZONE A Location 20	ZONE B Location 21	ZONE C Location 22
ZONE C Location 23	ZONE B Location 24	ZONE A Location 25	ZONE A Location 26	ZONE A Location 27	ZONE B Location 28	ZONE C Location 29
	ZONE C Location 30	ZONE B Location 31	ZONE B Location 32	ZONE B Location 33	ZONE C Location 34	
		ZONE C Location 35	ZONE C Location 36	ZONE C Location 37		

Figure 6.10.1-20 RCCA Depletion Input (TRITON)

[redacted]

Figure 6.10.1-20 RCCA Depletion Input (TRITON) (cont'd)

[redacted]

Figure 6.10.1-20 RCCA Depletion Input (TRITON) (cont'd)

[redacted]

Figure 6.10.1-20 RCCA Depletion Input (TRITON) (cont'd)

[redacted]

Figure 6.10.1-20 RCCA Depletion Input (TRITON) (cont'd)

[redacted]

Figure 6.10.1-20 RCCA Depletion Input (TRITON) (cont'd)

[redacted]

Figure 6.10.1-20 RCCA Depletion Input (TRITON) (cont'd)

[redacted]

Figure 6.10.1-20 RCCA Depletion Input (TRITON) (cont'd)

[redacted]

Figure 6.10.1-20 RCCA Depletion Input (TRITON) (cont'd)

[redacted]

Figure 6.10.1-20 RCCA Depletion Input (TRITON) (cont'd)

[redacted]

Figure 6.10.1-20 RCCA Depletion Input (TRITON) (cont'd)

[redacted]

Figure 6.10.1-20 RCCA Depletion Input (TRITON) (cont'd)

[redacted]

Figure 6.10.1-21 [DELETED]

[Deleted]

Figure 6.10.1-22 [DELETED]

[Deleted]

Figure 6.10.1-23 [DELETED]

[Deleted]

Figure 6.10.1-24 [DELETED]

[Deleted]

Figure 6.10.1-25 [DELETED]

[Deleted]

Figure 6.10.1-26 [DELETED]

[Deleted]

Figure 6.10.1-27 [DELETED]

[Deleted]

Figure 6.10.1-28 Undamaged PWR Basket Moderator Density Study

[redacted]

Figure 6.10.1-29 Reactivity vs. Burnup for WE 15×15 Fuel Assembly

[redacted]

Figure 6.10.1-30 Reactivity vs. Enrichment for WE 15×15 Fuel Assembly

[redacted]

Figure 6.10.1-31 k_{eff} Distribution for RCCA (Ag-In-Cd) Benchmarking

[redacted]

Figure 6.10.1-32 Histogram of Reactivity Results for Additional Insert Bands in Fuel Depletion Analysis

[redacted]

Figure 6.10.1-33 Histogram of Reactivity Results for Mixed-Mode Depletion in Fuel Depletion Analysis

[redacted]

Table 6.10.1-1 PWR Nonfuel Insert Study (Guide and Instrument Tube Insertion)

[redacted]

[a] Based on comparison to the same cask configuration case with no insert.

Table 6.10.1-2 PWR Basket Component Tolerance and Shift Study Results (Independent Variations)

[redacted]

Table 6.10.1-3 PWR Basket Component Tolerance and Shift Study Results (Combined Variations; Radial In Shift)

[redacted]

Table 6.10.1-4 Depletion Analysis Analyzed Parameters

Parameter	Analyzed
Moderator Temperature (K)	610
Fuel Temperature (K)	1100
UO_2 Density (g/cm^3)	10.5216
Power Density (MW/MTU)	60 [a]
Moderator Boron Concentration (ppm)	1000
IFBA / Burnable Absorber Rods	Bounded by BPRA/CEA Models
CE Assembly Type CEA	Full Insertion for Full Burnup Credited
B&W and WE CEA	≤ 20 cm Insertion Full Burnup and/or Partial to Full Insertion Allowed at Low Power or Start-Up Operations
B&W and WE Fuel BPRA	Included for Full Burnup Credited

[a] Basis for TRITON isotope generation. While high power density produces a bounding set of isotopes for actinide credit a lower power density may produce a bounding configuration when considering both actinide and fission product credit. Table 6.10.1-32 contains Δk_{eff} analysis for low power density and a bias is applied to account for the non-conservative power density listed in this table.

Table 6.10.1-5 Axial Profile Shape for Depletion Analysis

Axial Zone	Fraction of Core Height	< 18 GWd/MTU	18-30 GWd/MTU	> 30 GWd/MTU
1	0.0278	0.649	0.668	0.652
2	0.0833	1.044	1.034	0.967
3	0.1389	1.208	1.150	1.074
4	0.1944	1.215	1.094	1.103
5	0.2500	1.214	1.053	1.108
6	0.3056	1.208	1.048	1.106
7	0.3611	1.197	1.064	1.102
8	0.4169	1.189	1.095	1.097
9	0.4722	1.188	1.121	1.094
10	0.5278	1.192	1.135	1.094
11	0.5833	1.195	1.140	1.095
12	0.6389	1.190	1.138	1.096
13	0.6944	1.156	1.130	1.095
14	0.7500	1.022	1.106	1.086
15	0.8056	0.756	1.049	1.059
16	0.8611	0.614	0.933	0.971
17	0.9167	0.481	0.669	0.738
18	0.9722	0.284	0.373	0.462

Table 6.10.1-6 Isotopes Extracted from TRITON Runs

^{234}U	*^{235}U*	^{236}U	*^{238}U*	^{237}Np	*^{238}Pu*	*^{239}Pu*
^{240}Pu	*^{241}Pu*	*^{242}Pu*	*^{241}Am*	^{242m}Am	^{243}Am	^{95}Mo
^{99}Tc	^{101}Ru	^{103}Rh	^{109}Ag	^{133}Cs	^{143}Nd	^{145}Nd
^{147}Sm	^{149}Sm	^{150}Sm	^{151}Sm	^{152}Sm	^{151}Eu	^{153}Eu
^{155}Gd						

Note: The isotopes shown in italics are those applied to the actinide-only burnup credit analysis. The isotopes shown as underlined represent the balance of actinides and fission products used in the actinide and fission product burnup credit analysis. ^{242m}Am is not included in the recommended set of isotopes in ISG-8 Rev. 3 and not used in the MCNP evaluations.

^{234}U	*^{235}U*	^{236}U	*^{238}U*	^{237}Np	*^{238}Pu*	*^{239}Pu*
^{240}Pu	*^{241}Pu*	*^{242}Pu*	*^{241}Am*	^{243}Am	^{95}Mo	^{99}Tc
^{101}Ru	^{103}Rh	^{109}Ag	^{133}Cs	^{143}Nd	^{145}Nd	^{147}Sm
^{149}Sm	^{150}Sm	^{151}Sm	^{152}Sm	^{151}Eu	^{153}Eu	^{155}Gd

Note: The isotopes shown in italics are those applied to the actinide-only burnup credit analysis. The isotopes shown as underlined represent the balance of actinides and fission products used in the actinide and fission product burnup credit analysis. ^{242m}Am is not included in the recommended set of isotopes in ISG-8 Rev. 3 and not used in the MCNP evaluations.

Table 6.10.1-7 TRITON Parameter Trends (Cask Analysis – NUREG/CR-6665)

Parameter	Bounding Condition	Estimated Sensitivity	Recommended Value/Model
Fuel temperature *(NUREG Sect. 4.2.1)*	Highest temperature	4 pcm/K	Maximum pellet-average temperature
Moderator temperature (PWR) *(NUREG Sect. 4.2.2)*	Highest temperature	35 pcm/K	Maximum core outlet temperature
Soluble boron concentration *(NUREG Sect. 4.2.3)*	Highest concentration	3.5 pcm/ppm	Maximum cycle-averaged concentration
Operating history *(NUREG Sect. 4.2.4)*	Low power late in life (actinide and fission product)	N/A	Assume simple operating history, with margin of 200 pcm or more
Specific power *(NUREG Sect. 4.2.4)*	Low specific power (actinide and fission product)	N/A	Low but credible specific power
Fixed/Integral burnable absorbers *(NUREG Sect. 4.2.5, 4.2.6)*	Burnable absorbers present during depletion	N/A	May not be excessive to assume fixed burnable absorbers present, but further study is warranted.

Table 6.10.1-8 NUREG "Reasonably" Bounding Parameters

Parameter	NUREG-6759	NUREG-6761
Moderator temperature (K)	600	600
Fuel temperature (K)	1000	1000
UO_2 density (g/cm^3)	10.44	10.5216
Clad temperature (K)	600	620
Clad density (g/cm^3)	5.78	6.56
Power density (MW/MTU) [a]	60	60
Moderator boron concentration (ppm)	650	650

[a] See note to Table 6.10.1-4.

Table 6.10.1-9 Undamaged PWR Fuel - Fresh Fuel Maximum Enrichments

[redacted]

Table 6.10.1-10 Undamaged PWR Fuel Hypothetical End-Drop Accident Evaluation

[redacted]

Table 6.10.1-11 [DELETED]

[Deleted]

Table 6.10.1-12 Maximum Initial Enrichment – 37 Assembly Undamaged Fuel Configuration – 0.036 g/cm² ^{10}B Absorber

Assembly ID	Zero (0) Burnup Max. Enr. (wt %)	Max Initial Enrichment (wt % ^{235}U) = C_4 × Burnup (GWd/MTU) + C_5					
		Burnup (GWd/MTU) < 18		18 ≤ Burnup (GWd/MTU) ≤ 30		Burnup (GWd/MTU) > 30	
		C_4	C_5	C_4	C_5	C_4	C_5
BW 15×15	1.9	0.0501	1.69	0.0693	1.65	0.0748	1.60
BW 17×17	1.9	0.0502	1.72	0.0687	1.70	0.0742	1.66
CE 14×14	2.1	0.0473	2.04	0.0675	2.03	0.0759	1.93
CE 16×16	2.1	0.0464	2.03	0.0657	2.06	0.0733	1.99
WE 14×14	2.2	0.0496	2.08	0.0672	2.21	0.0725	2.29
WE 15×15	1.9	0.0494	1.74	0.0683	1.72	0.0742	1.67
WE 17×17	1.9	0.0494	1.71	0.0685	1.68	0.0749	1.61

Table 6.10.1-13 Maximum Initial Enrichment – 37 Assembly Undamaged Fuel Configuration – 0.030 g/cm² ^{10}B Absorber

Assembly ID	Zero (0) Burnup Max. Enr. (wt %)	Max Initial Enrichment (wt % ^{235}U) = C_4 × Burnup (GWd/MTU) + C_5					
		Burnup (GWd/MTU) < 18		18 ≤ Burnup (GWd/MTU) ≤ 30		Burnup (GWd/MTU) > 30	
		C_4	C_5	C_4	C_5	C_4	C_5
BW 15×15	1.8	0.0507	1.61	0.0687	1.59	0.0745	1.48
BW 17×17	1.9	0.0503	1.66	0.0683	1.63	0.0733	1.59
CE 14×14	2.1	0.0468	1.95	0.0664	1.97	0.0738	1.90
CE 16×16	2.1	0.0470	1.95	0.0649	1.99	0.0727	1.90
WE 14×14	2.1	0.0492	2.03	0.0680	2.10	0.0728	2.19
WE 15×15	1.9	0.0503	1.67	0.0675	1.66	0.0747	1.54
WE 17×17	1.9	0.0494	1.64	0.0685	1.58	0.0737	1.53

Table 6.10.1-14 Maximum Initial Enrichment – 37 Assembly Undamaged Fuel Configuration – 0.027 g/cm^2 ^{10}B Absorber

Assembly ID	Zero (0) Burnup Max. Enr. (wt %)	Max Initial Enrichment (wt % ^{235}U) = C_4 × Burnup (GWd/MTU) + C_5					
		Burnup (GWd/MTU) < 18		18 ≤ Burnup (GWd/MTU) ≤ 30		Burnup (GWd/MTU) > 30	
		C_4	C_5	C_4	C_5	C_4	C_5
BW 15×15	1.8	0.0508	1.58	0.0686	1.52	0.0754	1.41
BW 17×17	1.8	0.0503	1.62	0.0683	1.59	0.0748	1.47
CE 14×14	2.1	0.0471	1.92	0.0666	1.92	0.0729	1.87
CE 16×16	2.1	0.0462	1.93	0.0657	1.92	0.0747	1.75
WE 14×14	2.1	0.0499	1.98	0.0667	2.10	0.0743	2.07
WE 15×15	1.9	0.0503	1.63	0.0677	1.60	0.0749	1.46
WE 17×17	1.9	0.0497	1.60	0.0683	1.54	0.0749	1.41

Table 6.10.1-15 [DELETED]

[Deleted]

Table 6.10.1-16 Maximum Initial Enrichment – Undamaged Fuel Configuration WE15 – Optional Configurations

# Assemblies	Zero (0) Burnup Maximum. Enrichment (wt % ^{235}U)	Max Initial Enrichment (wt % ^{235}U) = C_4 × Burnup (GWd/MTU) + C_5					
		Burnup (GWd/MTU) < 18		18 ≤ Burnup (GWd/MTU) ≤ 30		Burnup (GWd/MTU) > 30	
		C_4	C_5	C_4	C_5	C_4	C_5
0.036 g/cm² ^{10}B Absorber							
36	2.0	0.0497	1.93	0.0681	1.99	0.0747	2.00
35	2.1	0.0507	1.97	0.0673	2.08	0.0730	2.12
33	2.2	0.0504	2.12	0.0664	2.29	0.0745	2.32
0.030 g/cm² ^{10}B Absorber							
36	2.0	0.0494	1.87	0.0687	1.90	0.0737	1.93
35	2.0	0.0499	1.92	0.0688	1.97	0.0740	1.99
33	2.1	0.0497	2.06	0.0686	2.15	0.0724	2.29
0.027 g/cm² ^{10}B Absorber							
36	2.0	0.0501	1.83	0.0677	1.87	0.0741	1.84
35	2.0	0.0494	1.89	0.0675	1.94	0.0735	1.96
33	2.1	0.0492	2.03	0.0674	2.12	0.0730	2.21

Table 6.10.1-17 RCCA Geometry

WE15H1 RCCA Data	Dimension (inches)
Absorber Pellet Diameter	0.3925
RCCA Clad Inside Diameter	0.4005
RCCA Clad Outside Diameter	0.4390
Absorber Length	142.0

Table 6.10.1-18 RCCA Calculated Isotopic Composition

[redacted]

Table 6.10.1-19 RCCA Input Composition (atom/b-cm)

[redacted]

Table 6.10.1-20 [DELETED]

[Deleted]

Table 6.10.1-21 [DELETED]

[Deleted]

Table 6.10.1-22 Undamaged Fuel Basket - RCCA Controlled / Spent Fuel Comparison

[redacted]

Table 6.10.1-23 [DELETED]

[Deleted]

Table 6.10.1-24 [DELETED]

[Deleted]

Table 6.10.1-25 [DELETED]

[Deleted]

Table 6.10.1-26 [DELETED]

[Deleted]

Table 6.10.1-27 [DELETED]

[Deleted]

Table 6.10.1-28 [DELETED]

[Deleted]

Table 6.10.1-29 [DELETED]

[Deleted]

Table 6.10.1-30 Single Assembly Misload – Most Reactive Fuel Assemblies

[redacted]

Table 6.10.1-30a Babcock & Wilcox Single Misload Assembly Results

[redacted]

Table 6.10.1-30b Combustion Engineering Single Misload Assembly Results

[redacted]

Table 6.10.1-30c Westinghouse Single Misload Assembly Results

[redacted]

Table 6.10.1-30d 0.030 g/cm^2 ^{10}B Content – 75% Effective Absorber Sheet

[redacted]

Table 6.10.1-30e 0.027 g/cm^2 ^{10}B Content – 67.5% Effective Absorber Sheet

[redacted]

Table 6.10.1-31 Undamaged PWR Basket Reactivity Summary

[redacted]

Table 6.10.1-32 Power Density Bias Calculation for Depletion Analysis

[redacted]

Table 6.10.1-33 Fission Product and Minor Actinide Worth and Bias

[redacted]

Table 6.10.1-34 Burnup Credit Depletion Bias Uncertainty

[redacted]

Table 6.10.1-35 Burnup and Enrichment Ranges for Loading Curve Data

[redacted]

Table 6.10.1-36 MCNP6.1 Validation – Range of Applicability for PWR Fresh and Spent Fuel Evaluations

[redacted]

[a] As the MAGNATRAN system is not a normal flux trap system, the cluster gap is calculated as the difference between the tube outer width and the fuel width.

Table 6.10.1-37 MCNP Criticality Results RCCA (Ag-In-Cd)

[redacted]

Table 6.10.1-37 MCNP Criticality Results RCCA (Ag-In-Cd) (cont'd)

[redacted]

Table 6.10.1-38 USLSTATS Method 1 Results for Correlated Variables at 5% MMS – RCCA (Ag-In-Cd)

[redacted]

Table 6.10.1-39 Reactivity Results for CE Absorber Material Effects in Fuel Depletion Analysis

[redacted]

Table 6.10.1-40 Reactivity Results for CEAs Partially Inserted in Fuel Depletion Analysis

[redacted]

Table 6.10.1-41 Reactivity Results for CEAs Fully Inserted for 5 GWd/MTU in Fuel Depletion Analysis

[redacted]

Table 6.10.1-42 Reactivity Results for Additional Insert Bands in Fuel Depletion Analysis

[redacted]

Table 6.10.1-43 Reactivity Results for Mixed-Mode Depletion in Fuel Depletion Analysis

[redacted]

Table 6.10.1-44 Reactivity Results for Additional Depletion Bands and Mixed-Mode Depletion in RCCA Depletion Analysis

[redacted]

Chapter 7
Package Operations

Table of Contents

7 PACKAGE OPERATIONS 7-1

7.1 Package Loading 7.1-1
7.1.1 Receipt and Preparation for Loading 7.1-1
7.1.2 Loading of Contents 7.1-5
7.1.3 Preparation for Transport 7.1-10
7.1.4 Loading the Transportable Storage Canister with Spent Fuel Contents 7.1-11
7.1.5 Loading the Transportable Storage Canister with GTCC Waste Contents 7.1-14

7.2 Package Unloading 7.2-1
7.2.1 Receipt of Package from Carrier 7.2-1
7.2.2 Removal of Contents 7.2-3

7.3 Preparation of Empty Packaging for Transport 7.3-1

7.4 References 7.4-1

List of Tables

Table 7.1-1 Threaded Component Torque Values 7.1-4

7.1 Package Loading

This section describes the procedures for receipt of an empty MAGNATRAN transport cask (packaging), preparation of the cask for loading, loading of the contents, closure, and preparation of the loaded cask (package) for transport. For the transport of loaded TSCs, the MAGNATRAN nameplate identification shall be verified as correct, the cavity shall be dry, and the contents shall be verified to be in compliance with the applicable content conditions of the Certificate of Compliance (CoC). A cask loading inspection checklist may be utilized by the cask user to assist in identifying operating conditions and status. In addition, prior to use of a MAGNATRAN packaging, verification that the cask has been fabricated, inspected, tested and maintained in accordance with the Acceptance Test and Maintenance Program in Chapter 8 and the CoC shall be performed.

The MAGNATRAN transport configuration is detailed in the license drawings contained in Chapter 1 of this SAR. The MAGNATRAN closure includes a bolted lid and port cover, each of which is sealed by a metallic O-ring. Prior to the transport of a loaded TSC, the transport cask closure metallic O-ring seals shall be replaced and the containment closure verified to be leak tight using the test methods described in the procedures.

The generic operating procedures for the loading, closure and dry transfer of a TSC into a MAGNATRAN transport cask and preparation of the package for transport are provided in the following sections.

The generic operating procedures for the loading, closure and preparation for storage of a TSC, and for the removal of a loaded TSC from storage in a MAGNASTOR concrete cask (CC) at an ISFSI, are provided in the MAGNASTOR FSAR. Those procedures are outside the scope of these MAGNATRAN operating procedures.

7.1.1 Receipt and Preparation for Loading

1. Receive the empty MAGNATRAN transport cask (packaging) and transport vehicle at the loading facility.
2. Position the transport vehicle and cask in the designated cask unloading area. Set brakes or install chocks, as required.
3. Perform a radiation survey of the transport vehicle and cask.
4. Remove the personnel barrier. Verify the packaging nameplate displays the correct packaging identification and serial numbers.

5. Perform a radiation level and removable contamination survey of the empty cask and transport vehicle.

   Note: A receiving survey of the cask and transport vehicle must be performed as soon as practical after arrival at the site to ensure compliance with 10 CFR 20.1906 and that removable contamination and dose rates comply with the applicable limits of 49 CFR 173.428.

6. Perform a visual inspection of the transport vehicle and packaging, including impact limiters, to identify any transport damage. Record inspection results.

7. Clean the transport vehicle and cask, which includes the impact limiters, cask body, and cask copper fins, of road dirt and debris, as needed. Cleaning of the package exterior shall ensure that surfaces are cleaned of chloride-containing salts and other corrosive agents. The following procedures, materials and methods are required to be used for the cleaning of the MAGNATRAN exterior stainless steel surfaces. The cleaning procedure, inspection and examination and results of the cleaning and reports shall be maintained as part of the MAGNATRAN operating records.

   Note: MAGNATRAN external stainless steel plate surfaces are procured as hot-rolled and annealed, blast cleaned or pickled, and passivated. Stainless steel sheet is procured with a 2B surface finish.

   Note: The following shall not be used for cleaning of the stainless steel surfaces: steel pads, wire brushes, scrapers, or cleaning solutions containing chlorides or quaternary salts.

   a) Cleaning procedures shall be prepared in accordance with ASME NQA-1, Subpart 2.1 for cleanliness level B (Reference 8 in Section 7.4). Flush and cleaning agent mixing water shall meet the requirements for Fresh Water per Table 304.1, or better.

   b) Visually examine exterior surfaces of the package to identify general overall cleanliness levels following cleaning of road dirt and debris. Flush external surfaces of the cask with fresh water. If available, pressure cleaning can be utilized.

   c) Areas showing deposits following flushing shall be cleaned with non-abrasive soft plastic pads or soft clothes. Clean areas in direction (parallel) of polish lines or grain of the stainless steel plates and sheets. As required, chloride-free cleaning materials may be used.

   d) Perform final flush of external surfaces following the cleaning and wipe dry any standing water with soft clothes. After wiping allow surfaces to air dry.

8. Confirm the acceptable removal of chloride-containing salts and other corrosive agents by performing the following inspection. The acceptance criteria for confirmation of acceptable cleanliness level is as follows:

   a) Following cleaning the external surfaces shall appear metal clean and free of organic films and contaminants when examined in accordance with Paragraph 7.2.1 of ASTM A380-78 (Reference 9, Section 7.4), except light deposits of atmospheric dust are permissible.

   b) Following the visual examination, perform a wipe test per paragraph 7.2.2 of ASTM A 380-78. The test shall show no deleterious contamination. Surfaces shall be confirmed to comply with Table 302.5 for Class B corrosion-resistant alloys.

9. Attach slings to the upper impact limiter and take up slack. Remove jam and attachment nuts from the impact limiter retaining rods, and remove the retaining rods.

10. Remove the upper (front) impact limiter and store it in an upright position in a clean area.

11. Repeat steps 8 and 9 for the lower (rear) impact limiter.

12. Release the cask front tie-down assembly and remove the rear trunnion tie-downs.

13. Remove the two lifting trunnion plugs from the cask upper forging and store the plugs and bolts to prevent damage. Visually inspect the trunnion recesses.

14. Using a crane and slings, lift and position a lifting trunnion on the cask, install the attachment bolts, and torque the bolts to the value specified in Table 7.1-1. Repeat for second lifting trunnion.

    Note: At facilities requiring the transport vehicle to move to allow the cask to be uprighted and downloaded on the vehicle, the brakes and chocks may be removed for these operations, if the vehicle remains under the control of a driver or operator.

15. Attach the cask lift yoke to the cask handling crane hook. Verify proper operation of the yoke lift arm actuation system.

16. Position the yoke arms adjacent to the lifting trunnions and close the arms using the actuation system. Visually verify proper yoke arm engagement with the lifting trunnions

17. Lift the cask to a vertical orientation by rotating the cask on the rotation trunnions.

18. Lift the cask from the transport frame and position the cask in the designated loading area.

    Note: At facilities where a mobile crane or external structures and equipment not connected to the 10 CFR 50 facility are utilized to perform the cask off-loading from the

transport vehicle and TSC transfer operations, the TSC Handling and Transfer Facility criteria of the 10 CFR 72 CoC No. 1031 shall be satisfied.

19. Disengage the lift yoke from the cask lifting trunnions and remove it from the immediate area.

Table 7.1-1 Threaded Component Torque Values

Threaded Component (1)	Torque Value (2)
Lid Bolts – Loaded System	4,600, + 200, -200 ft-lb (3)
Lid Bolts – Empty System	1,300, + 100, -100 ft-lb (4)
Coverplate Bolts	300, + 30, -30 in-lb
Lid Test Port Plug	120, +5, -5 in-lb
Coverplate Test Port Plug	120, +5, -5 in-lb
Impact Limiter Retaining Rods	Hand tight
Impact Limiter Attachment Nuts	35, +2, -2 ft-lb
Impact Limiter Jam Nuts	75, + 5, -5 ft-lb
Trunnion Attachment Bolts	120, + 20, -20 ft-lb
Trunnion Cap Bolts	50, +5, -5 in-lb
Cask Cavity Spacer Attachment Bolts	300, + 20, -20 in-lb
TSC and Cask Lid Lifting Hoist Rings	100, + 50, -0 ft-lb (5)

Note: (1) Threaded fasteners should be lubricated with nuclear-grade Never-Seeze, or equivalent, as follows:
a. Apply lubricant to the threads of the fastener only.
b. Drive the fastener into and then out of mating threads to evenly lubricate the mating threads.
c. Lubricate the bottom surface of the head of the fastener.
d. Remove excess lubricant, reinstall and torque.

(2) Torque values for support components (i.e., transport frame components) not shown above are provided on the applicable Design Drawing.

(3) Lid bolts (loaded system) to be torqued at three intermediate levels of 500, 2,000 and 3,500 ft-lb prior to final torque. All bolts are to be verified as torqued to the intermediate value prior to proceeding to the next torque level.

(4) Lid bolts (empty system) to be torqued at an intermediate level of 500 ft-lb prior to final torque. All bolts are to be verified as torqued to the intermediate value prior to proceeding to the next torque level.

(5) Hoist ring torque values are valid for 2-½-inch hoist rings supplied by Jergens.

7.1.2 Loading of Contents

Note: The MAGNATRAN transport cask is dry loaded in the spent fuel building or facility, or at the onsite ISFSI using the MTC and attendant support hardware. Operation of the MTC is described in the approved site-specific procedures and the MAGNASTOR® FSAR. Site-specific procedures shall comply with the requirements of the SAR. Potential alternate procedures and site-specific hardware are described when necessary.

1. Install appropriate work platforms, scaffolding or lifts to allow access to the top of the MAGNATRAN transport cask.
2. Detorque and remove the lid port coverplate bolts and store the coverplate and associated bolts to prevent damage.
3. Detorque the cask lid bolts in the reverse order of the torquing sequence indicated on the lid.
4. Remove the lid bolts, inspect the bolts for thread damage and store to prevent damage.
5. Install the two lid alignment pins in their designated threaded holes (#s 14 and 36) and hand-tighten.
6. Install and tighten the swivel hoist rings (or equivalent approved site-specific lifting system) in the four threaded lifting holes in the cask lid and torque to the values specified in Table 7.1-1.
7. Attach an appropriate lifting sling set to the swivel hoist rings and to a crane hook. Lift the lid from the cask and store it to prevent damage.
8. Remove the two alignment pins. Using a crane and suitable slings, install the transfer shield ring into the lid recess.

   Note: The transfer shield ring aligns the transfer cask adapter to the cask cavity, provides additional side shielding and protects the cask lid seating surface from damage.

   Note: The following loading procedures are based on the dry transfer of a loaded and closed TSC containing spent fuel assemblies or a loaded and closed TSC containing GTCC waste. All TSCs shall be independently verified to be in compliance with the CoC content conditions.

   Note: An evaluation of TSCs containing spent nuclear fuel shall be performed to verify that the installed neutron absorbing materials required to assure criticality safety are acceptable for transport conditions.

   Note: TSCs containing spent nuclear fuels that are to be retrieved from storage for off-site transport in the MAGNATRAN transport cask will be evaluated to ensure that the specific TSC stored in the storage overpack, which may have been subject to 10 CFR 72 normal and off-normal, accident and natural phenomena events, retains its ability

to satisfy functional and performance requirements of the MAGNATRAN packaging certified content conditions. Dry storage systems that have been maintained within an Aging Management Program will include system specific review and assessment of this information record as part of the off-site transport evaluation to ensure that the MAGNATRAN packaging certified content conditions are validated.

TSCs containing spent nuclear fuel and experiencing only normal or off-normal events during storage will be evaluated for potential corrosion at the welds and any damage caused by removal of the TSC from the storage overpack.

In addition to the evaluation done for normal/off-normal storage, TSCs containing spent nuclear fuel that have experienced accident or natural phenomena events must be evaluated for potential degradation of the fuel, basket, and neutron absorbers. This evaluation will be performed for each TSC as part of the preparation for loading for off-site transport using: 1) the annual inspection and surveillance records and off-normal and accident event reports that are maintained by the licensee for each loaded MAGNASTOR system in compliance with 10 CFR 72 requirements; and 2) in the case of storage accidents and natural phenomena events, any necessary examinations performed at the time of transfer to ensure the condition of the TSC and contents.

Maximum assembly average burnup for fuel assemblies to be transported off-site as undamaged is limited to ≤ 45,000 MWd/MTU. A fuel assembly to be transported off-site having a maximum assembly average burnup > 45,000 MWd/MTU but ≤ 60,000 MWd/MTU shall be loaded in a MAGNASTOR damaged fuel can (DFC).

TSC loading into the MAGNATRAN transport cask will be observed by operations staff noting any system interferences that occur during TSC retrieval from the storage overpack and during placement of the TSC into the transport cask. The cause of the interference and potential damage caused by the interference will be determined prior to shipment. Noted interferences will be made part of the TSC evaluation record to the extent required to validate that MAGNATRAN packaging content conditions are satisfied when the spent fuel canister is placed within the MAGNATRAN transport cask containment boundary for off-site transport.

9. Remove the loaded TSC from the concrete cask (CC) and close the MTC shield doors. Record the time the TSC is lifted off the CC pedestal. Install the shield door locking devices. **Caution:** In order to ensure that the spent fuel clad temperatures do not exceed 400°C in accordance with ISG-11, Revision 3, the time allowed for transfer of a loaded TSC containing spent fuel to the MAGNATRAN cask is limited. The following time limits apply as noted:

Condition 1) For the maximum transportable fuel TSC heat loads of 23 kW for PWR and 22 kW for BWR, the maximum time from lifting the TSC off the CC pedestal (Section 7.1.2, Step 9) for placement in the MTC through completion of the preparation of the MAGNATRAN for transport and placement in a horizontal orientation on the transport vehicle (Section 7.1.3, Step 4) shall be < 41 hours;

Condition 2) For maximum heat load fuel TSCs loaded immediately prior to loading into the MAGNATRAN cask, the maximum time from completion of TSC closure operations, including helium backfill time and termination of external cooling (for 24 hours) of the TSC (Section 7.1.5, Step 17) through completion of the preparation of the MAGNATRAN for transport and placement in a horizontal orientation on the transport vehicle (Section 7.1.3, Step 4), shall be < 65 hours. These maximum transfer and preparation times are not applicable to the loading of GTCC waste TSCs as the ISG-11 temperature limits are not applicable.

In the event that the transfer and MAGNATRAN preparation procedures through placement of the cask in a horizontal orientation are not completed within the specified time period, corrective actions shall be implemented to return the TSC to the MAGNASTOR Transfer Cask (MTC) where active cooling of the TSC can be completed in accordance with procedures established in the MAGNASTOR FSAR and Operating Manual. The corrective actions shall be implemented with sufficient time to ensure that the maximum transfer and preparation times are not exceeded. The external cooling of the TSC shall be continued for a minimum of 24 hours to reduce the fuel clad and TSC internal component temperatures to allow re-start of MAGNATRAN loading procedures. The maximum time limit is 31 hours for both Condition 1 and 2 for each subsequent TSC transfer and transport preparation activity.

Note: The time limits specified in Step 9 are for the maximum allowable heat loads in the MAGNATRAN transport cask. Although transfer and cask preparation times would be longer for lower content decay heat loads, the limits for the maximum heat loads (PWR - 23 kW; BWR - 22 kW) will be conservatively implemented to all content decay heat loads.

10. Connect lift slings to the transfer adapter, lift the adapter, and place it on the top of the MAGNATRAN cask. Visually verify proper fit-up with the transfer shield ring positioned in the lid recess.
11. Connect and verify operation of the transfer adapter auxiliary hydraulic system.
12. Install the TSC lifting hoist rings and sling set (or equivalent TSC lifting system meeting the facility's heavy load program) in the TSC closure lid threaded holes. Torque the hoist rings to the torque specified in Table 7.1-1.

13. Using the MTC lift yoke, engage the lifting trunnions and position the MTC containing the loaded TSC on the transfer adapter positioned on the MAGNATRAN transport cask. Remove the shield door stops.
14. Install a stabilization system for the MTC, if required by the facility heavy load handling or seismic analysis programs.
15. Disengage the MTC lift yoke from the MTC trunnions and move the lift yoke from the area.
16. Connect TSC sling set(s) (or site-specific approved TSC lifting system meeting the facility's heavy load program) to the crane hook. Verify that the MTC retaining components are in the engaged position.
17. Lift the TSC off the MTC shield doors (approximately ½ inch) and open the doors using the auxiliary hydraulic system.
18. Lower the loaded TSC into the MAGNATRAN cask until the TSC rests on the bottom of the cask cavity.
19. Disengage the lifting sling set(s) from the hook or disengage the site-specific approved lifting system meeting the facility's heavy load program from the TSC. Close the MTC shield doors and install the door stops.
20. Retrieve the MTC lift yoke, engage the lifting trunnions, remove the stabilization system (if used), and lift the MTC off the top of the MAGNATRAN cask. Move the MTC and lift yoke from the area and store.
21. Disconnect the auxiliary hydraulic system connections, attach lifting slings to the transfer adapter and lift and move the transfer adapter from the area and store.
22. Remove the TSC lifting sling set(s), hoist rings or other site-specific approved TSC lifting system components from the top of the TSC.
23. Attach lifting slings, lift and remove the transfer shield ring. Inspect the cask lid O-ring seating surface for cleanliness and integrity.
24. Engage the cask lid lifting sling set to the crane and position the lid for seal inspection and replacement.
25. Remove and replace the lid metallic O-ring with an approved spare. Inspect the lid outer O-ring seal and, if it is damaged, replace it with an approved spare. Ensure that the replaced O-rings are properly installed and seated.
26. For the transport of shorter length TSCs install the cask cavity spacer to the bottom side of the lid with the four attachment bolts and lock washers. Torque the attachment bolts to the value specified in Table 7.1-1.

27. Install the two lid alignment pins in their designated threaded hole locations (#s 14 and 36) in the cask and hand-tighten.
28. Lift the cask lid and position the lid to engage the alignment pins. Slowly lower the lid into position. Remove the lid lifting equipment and alignment pins.
29. Inspect the 48 lid bolts for damage and replace, as required, with approved spares. Lubricate the bolts with nuclear-grade Never-Seeze, or equivalent, and install the lid bolts to hand tight. In a minimum of four passes of increasing torque, torque the 48 lid bolts to the final value specified in Table 7.1-1 following the torquing sequence pattern marked on the lid.
30. Connect a vacuum pump and helium gas backfill system to the lid port quick-disconnect valve. Evacuate the cask cavity to a vacuum pressure of < 3 torr and backfill the cavity with helium gas to a pressure of 17.5, +2.5,-0 psia.
31. Disconnect the vacuum pump and backfill system from the lid port quick-disconnect valve.
32. Remove and replace the port coverplate metallic O-ring with an approved spare. Inspect the coverplate outer O-ring seal and, if damaged, replace it with an approved spare. Ensure that the replaced O-rings are properly installed and seated.
33. Install the coverplate in the lid port recess, purge the volume under the coverplate with helium prior to final seating, and torque the coverplate bolts to the value specified in Table 7.1-1.
34. Remove the cask lid test port plug and connect a Helium Mass Spectrometer Leak Detector (He MSLD) to the test port to perform the helium leakage test.
35. Using the He MSLD evacuate the volume between the cask lid metallic inner O-ring and the outer O-ring to a vacuum of < 0.1 torr. Operate the He MSLD to detect for helium in the evacuated volume to confirm the lid leakage rate is less than or equal to 2.0×10^{-7} cm^3/s, helium with a minimum test sensitivity of 1.0×10^{-7} cm^3/s, helium.
36. Upon completion of an acceptable lid helium leakage test, disconnect the He MSLD from the lid test port connection. Replace test port plug metallic seal with an approved spare, install the lid test port plug and torque to the value specified in Table 7.1-1.
37. Remove the coverplate test port plug and connect the He MSLD to the port to perform the helium leakage test.
38. Using the He MSLD evacuate the volume between the coverplate metallic inner O-ring and the outer O-ring to a vacuum of < 0.1 torr. Operate the He MSLD to detect for helium in the evacuated volume to confirm the lid port coverplate leakage rate is less than or equal to 2.0×10^{-7} cm^3/s, helium with a minimum test sensitivity of 1.0×10^{-7} cm^3/s.

    Note: If a helium leakage rate exceeding the specified leakage rate is measured during either the lid or lid port coverplate leakage test, determine the source of the leak,

repair (i.e., replace O-ring with approved spare, clean seating surfaces), reinstall and torque, and retest to original acceptance criteria.

39. Upon completion of an acceptable lid port coverplate leakage test, disconnect the He MSLD from the coverplate test port connection. Replace test port plug metallic seal with an approved spare, install the coverplate test port plug and torque to the value specified in Table 7.1-1.

7.1.3 Preparation for Transport

1. Remove scaffolding or work platforms from around the top of the MAGNATRAN transport cask.
2. Connect the cask lift yoke to the cask handling crane and engage the lift yoke arms to the two transport cask lifting trunnions.
3. Lift the cask and move it into position over the transport frame/vehicle rear support structure.
4. Lower the cask to engage the rotation trunnions in the transport frame/vehicle rear support structure, rotate the cask to the horizontal orientation and disengage the lift yoke.

   Note: The rotation trunnions are offset from the centerline to ensure rotation of the cask in the proper direction.

5. Using slings and a suitable crane, detorque and remove the nine lifting trunnion attachment bolts from one trunnion. Remove, clean and inspect the trunnion and bolts, observing for damage/wear. Repeat for the second lifting trunnion and bolts and store the trunnions and trunnion bolts.
6. Clean and inspect the trunnion recess and bolt holes. Position and install the trunnion plug. Apply nuclear-grade lubricant, such as Never-Seeze, or equivalent, to the three trunnion plug bolts, and torque the bolts to the value specified in Table 7.1-1. Repeat for the second trunnion recess and plug.
7. Decontaminate and clean the surfaces of the transport cask to ensure removable contamination limits for transport are met.
8. Install the transport tie-downs over the top forging and on the rotation trunnions.
9. Using the impact limiter lifting sling set, lift and install the lower (rear) impact limiter. Install retaining rods and attachment and jam nuts, and torque all the components to the values specified in Table 7.1-1. Install the retaining rod lock wires.
10. Repeat the installation sequence for the upper (front) impact limiter.
11. Install a tamper indicating device (TID) to the upper impact limiter attachment rods. Record the TID identification numbers on the cask loading checklist and shipping papers.

12. Perform final visual inspection of the cask to ensure proper package assembly in accordance with the CoC.
13. Complete radiation and contamination surveys of the package external surfaces and record the data. Ensure removable contamination and radiation dose rates survey results comply with the limits specified in 10 CFR 71.87(i) and (j) to verify removable contamination levels are in compliance with 49 CFR 173.443 and radiation dose rates comply with 10 CFR 71.47, respectively.
14. Measure the dose rate in millirems per hour at one meter from the package surface to determine the Transport Index (TI). Indicate the TI on the Radioactive Material labels applied to the package in accordance with 49 CFR 172, Subpart E.
15. Determine the appropriate Criticality Safety Index (CSI) assigned to the package contents in accordance with the CoC, and indicate the correct CSI on the Fissile Material label applied to the package per 49 CFR 172, Subpart E.
16. Measure and record the temperature of the MAGNATRAN shield shell outer surface at the top center of the package in the horizontal position and verify that the measured package external temperature meets the exclusive use shipment temperature limit of 85°C (185°F) per 10 CFR 71.43(g).
17. Install the personnel barrier to the transport vehicle and verify all access points are locked.
18. Perform a radiation survey of the package and the transport vehicle to assure radiation levels are in compliance with 49 CFR 173.441.
19. Apply placards to the transport vehicle in accordance with 49 CFR 172 Subpart F.
20. Review the cask loading inspection checklist and verify all required steps, tests and verifications have been satisfactorily completed, and all routine determinations have been satisfactorily completed in accordance with 10 CFR 71.87.
21. Complete the shipping documentation for an Exclusive Use Shipment and provide special instructions to the carrier to maintain an Exclusive Use Shipment.
22. The MAGNATRAN transport cask (package) is now ready for release and transport.

7.1.4 Loading the Transportable Storage Canister with Spent Fuel Contents

1. Visually inspect the TSC to ensure that it is clean and free of debris.
2. Place the TSC in the MTC.
3. Place the MTC containing the TSC into the spent fuel pool.

4. Load the previously designated fuel assemblies into the TSC in accordance with applicable CoC requirements.

   Note: The fuel assemblies and authorized nonfuel hardware shall be selected in compliance with the requirements of the approved contents specified in the CoC including limitations on fuel assembly, damaged fuel assemblies in Damaged Fuel Cans (DFCs), and nonfuel hardware positions within the basket. Assembly, DFC, and nonfuel hardware selection and placement within the basket shall be independently verified.

   Note: Verification of the location of high reactivity fuel (i.e., fresh or severely underburned fuel) in the spent fuel pool shall be performed prior to and after TSC loading to ensure appropriate fuel assemblies have been loaded.

   Note: A qualitative visual verification that a fuel assembly has been burned shall be performed prior to or during TSC loading operations.

   Note: A verification of the TSC or package fuel inventory and loading records shall be performed under a 10 CFR 71 quality assurance program prior to shipment for previously loaded (i.e., TSCs transferred from 10 CFR 72 storage facilities) TSCs.

   Note: Fuel assemblies without visible identification shall only be loaded after quantitative measurement of the fuel assembly.

   Note: Fuel assemblies may use burnup credit to demonstrate criticality acceptability. When applying burnup credit the documented fuel assembly burnup must be adjusted downward (decreased) to account for reactor record or measurement uncertainty prior to comparison to CoC minimum requirements

   Note: Nonfuel hardware is defined as reactor control components (RCCs), burnable poison absorber assemblies (BPAAs), guide tube plug devices (GTPDs), neutron sources/neutron source assemblies (NSAs), hafnium absorber assemblies (HFRAs), instrument tube tie components, guide tube anchors or other similar devices, in-core instrument thimbles, steel rod inserts (used to displace water from lower section of guide tube), and components of these devices such as individual rods. All nonfuel hardware, with the exception of instrument tube tie components, guide tube anchors or other similar devices, and steel rod inserts, may be activated during in-core operations.

   Note: Up to four DFCs containing authorized PWR contents may be loaded in a TSC with a DF Basket Assembly. A DFC spacer is required to be positioned in the designated DF Basket Assembly corner locations for the shorter length DFCs. Independently, visually verify proper placement and correct orientation of each required DFC spacer.

Note: At the option of the user, install fuel assembly spacers for the axial positioning of the PWR fuel assembly types to be loaded.

Note: For fuel spacer use mandated by the CoC content conditions, verify spacer identification and install fuel spacers in each intended fuel loading location based on the fuel spacer plan prepared, which is based on the fuel assembly inventory and nonfuel hardware to be loaded. Independently, visually verify proper placement and correct orientation of each required fuel spacer.

5. Place the closure lid on top of the loaded TSC.
6. Remove the MTC with the loaded TSC from the spent fuel pool.
7. Insert the drain tube assembly, torque to 200 ± 25 ft-lb (115, ± 5 ft-lb for DF 1" drain tube) and remove approximately 70 gallons of water. Attach a hydrogen detector to the vent line. Ensure that the vent line does not interfere with the operation of the weld machine. Sample the gas volume below the closure lid and observe hydrogen detector for H_2 concentration prior to commencing closure lid welding operations. Monitor H_2 concentration in the TSC until the root pass of the closure lid-to-shell weld is completed.

   Note: If H_2 concentration exceeds 2.4% prior to or during root pass welding operations, immediately stop welding operations. Evacuate the TSC gas volume or purge the gas volume with helium. Verify H_2 levels are <2.4% prior to restarting welding operations.

   Note: In place of continuous H_2 monitoring, continuous gas purging of the volume below the lid may be used in concert with initial (prior to start of welding) and intermittent H_2 monitoring (upon termination of gas purging and prior to re-starting welding operations).

8. Weld the closure lid in place and verify the adequacy of welds with root, mid-plane, and final surface visual and liquid penetrant examinations. Record results of examinations as required.
9. Refill TSC and hydrostatically test the TSC.
10. Release the pressure and drain the cavity water from the TSC by pumping or helium gas blowdown ensuring fuel cladding is not exposed to air.
11. Vacuum dry the TSC using vacuum drying methods as follows.

    Note: Ensure heat load-dependent vacuum drying time limits are not exceeded so that fuel cladding temperatures are maintained below 752°F.

    a. Connect the vacuum drying system to the vent and drain port openings.
    b. Operate the vacuum pump until a vapor pressure of < 10 torr is achieved in the TSC.

c. Isolate the vacuum pump from the TSC and turn off the vacuum pump. Observe the vacuum gauge connected to the TSC for an increase in pressure for a minimum period of 10 minutes. If the TSC pressure is ≤ 10 torr at the end of 10 minutes, the TSC is dry of free water. If pressure is > 10 torr at end of 10 minutes, continue vacuum drying until dryness criteria are met.

12. Following successful completion of drying verification, evacuate TSC to a vacuum of < 3 torr and immediately backfill the TSC with the required mass of high purity helium (99.995% minimum). Disconnect drying and helium backfill system from vent and drain ports.

13. Install inner vent and drain port covers purging volume behind the port cover with helium gas prior to completion of welding inner port covers in place, and perform visual and liquid penetrant examinations of final weld surface. Perform leakage test of inner port cover to verify the leakage rate is $\leq 2.0 \times 10^{-7}$ cm^3/s, helium to a sensitivity of $\leq 1.0 \times 10^{-7}$ cm^3/s, helium. Record results of examinations as required.

14. Install closure ring and weld the closure ring to the closure lid and TSC shell. Verify the adequacy of welds with final surface visual and liquid penetrant examinations. Record results of examinations as required.

15. Install outer vent and drain port covers, weld port covers in place, and perform visual and liquid penetrant examinations of final weld surface.

16. Install the MTC retaining device.

17. Decontaminate the external surface of the MTC and TSC to the limits established for the site, as required, and terminate TSC external cooling operations.

Note: The loaded TSC is now properly loaded for transfer either directly to the MAGNATRAN transport cask in accordance with CoC No. 9356 or to the MAGNASTOR concrete cask (CC) for interim storage in accordance with CoC No. 1031.

7.1.5 Loading the Transportable Storage Canister with GTCC Waste Contents

1. Visually inspect the GTCC waste TSC and GTCC waste basket liner to ensure that they are clean and free of debris.

2. Place the GTCC waste basket liner into the flooded reactor cavity or other designated waste loading location.

3. Load the authorized quantity of GTCC waste into the GTSC waste basket liner in accordance with CoC No. 9356 content limits and requirements.
4. Place the MTC containing the TSC into the flooded reactor cavity or other designated waste loading location.
5. Using the crane and slings installed on the loaded GTCC waste basket liner lift the GTCC waste basket liner and position it over the MTC/TSC.
6. Lower the GTCC waste basket liner into the TSC until it seats on the TSC baseplate.
7. Place the closure lid on top of the loaded GTCC waste TSC.
8. Remove the MTC with the loaded TSC from the flooded reactor cavity or other designated waste loading location.
9. Insert the GTCC waste TSC drain tube assembly through the drain port opening and torque to 200 ± 25 ft-lb. Drain approximately 70 gallons of water from the cavity.
10. Weld the closure lid in place and verify the adequacy of the weld root and final weld passes with visual and liquid penetrant examinations. Record results of examinations as required. Install the closure ring and weld the closure ring to the closure lid and TSC shell. Verify the adequacy of the welds with final surface visual and liquid penetrant examinations. Record results of examinations.
11. Drain the cavity water from the TSC.
12. Vacuum dry the TSC and verify dryness as follows:
    a) Connect the vacuum drying system to the vent and drain port openings.
    b) Operate the vacuum pump until a vapor pressure of < 10 torr is achieved in the TSC.
    c) Isolate the vacuum pump from the TSC and turn off the vacuum pump. Observe the vacuum gauge connected to the TSC for an increase in pressure for a minimum period of 10 minutes. If the TSC pressure is ≤ 10 torr at the end of 10 minutes, the TSC is dry of free water. If pressure is > 10 torr at end of 10 minutes, continue vacuum drying until dryness criteria are met.
13. Evacuate the TSC to a vacuum of less than 3 torr and backfill the TSC with high purity (≥ 99.9% pure) helium to 15.0 + 2, - 0 psig. Disconnect the drying and helium backfill system from the vent and drain ports.
14. Install inner vent and drain inner port covers, weld port covers in place, and perform visual and liquid penetrant examinations of final weld surfaces. Install outer vent and drain port covers, weld port covers in place, and perform liquid penetrant examinations of the final weld surfaces. Record results of examinations as required.

15. Install the TSC retaining device in the MTC.
16. Decontaminate the external surface of the MTC and TSC to the limits established for the site, as required.

    Note: The loaded GTCC waste TSC is now properly loaded for transfer directly to the MAGNATRAN transport cask in accordance with CoC No. 9356.

7.2 Package Unloading

This section describes the procedures for receiving a loaded MAGNATRAN transport cask (package) and preparing it for unloading operations. A cask unloading inspection checklist may be utilized by the cask user to assist in identifying operating conditions and status. Operation of the MTC is described in the approved site-specific procedures and the MAGNASTOR® FSAR. Site-specific procedures shall comply with the requirements of the SAR as provided herein. The procedures provided herein are based on utilizing the unloading facility cask handling crane, the transfer adapter, and the MTC to lift and shield the loaded TSC during removal from the transport cask. Potential alternate procedures and site-specific hardware are described when necessary.

7.2.1 Receipt of Package from Carrier

The procedures for the dry unloading of the loaded TSC from the MAGNATRAN transport cask are as follows:

1. Upon receipt of the loaded MAGNATRAN transport cask at the unloading facility, perform and record radiation and removable contamination surveys on the transport vehicle, personnel barrier and package surfaces to verify that radiation dose rates and contamination levels comply with the requirements of 10 CFR 20.1906. If contamination levels exceed the limits of 10 CFR 71.87(i) or radiation levels exceed the limits of 10 CFR 71.47, the licensee/user shall notify the NRC Operations Center.
2. Remove the personnel barrier and complete radiation and contamination surveys of the now-accessible package surfaces to verify that radiation dose rates and contamination levels comply with the requirements of 10 CFR 20.1906. If contamination levels exceed the limits of 10 CFR 71.87(i) or radiation levels exceed the limits of 10 CFR 71.47, the licensee/user shall notify the NRC Operations Center.
3. Perform a visual receipt inspection of the vehicle and package to identify any transport damage. Clean the vehicle and cask of road dirt and debris. Cleaning of the package exterior shall ensure that surfaces are cleaned of chloride-containing salts and other corrosive agents. The following procedures, materials and methods are required to be used for the cleaning of the MAGNATRAN exterior stainless steel surfaces. The cleaning procedure, inspection and examination and results of the cleaning and reports shall be maintained as part of the MAGNATRAN operating records.

   Note: MAGNATRAN external stainless steel plate surfaces are procured as hot-rolled and annealed, blast cleaned or pickled, and passivated. Stainless steel sheet is procured with a 2B surface finish.

Note: The following shall not be used for cleaning of the stainless steel surfaces: steel pads, wire brushes, scrapers, or cleaning solutions containing chlorides or quaternary salts.

a. Cleaning procedures shall be prepared in accordance with ASME NQA-1, Subpart 2.1 for cleanliness level B (Reference 8 in Section 7.4). Flush and cleaning agent mixing water shall meet the requirements for Fresh Water per Table 304.1, or better.
b. Visually examine exterior surfaces of the package to identify general overall cleanliness levels following cleaning of road dirt and debris. Flush external surfaces of the cask with fresh water. If available, pressure cleaning can be utilized.
c. Areas showing deposits following flushing shall be cleaned with non-abrasive soft plastic pads or soft clothes. Clean areas in direction (parallel) of polish lines or grain of the stainless steel plates and sheets. As required, chloride-free cleaning materials may be used.
d. Perform final flush of external surfaces following the cleaning and wipe dry any standing water with soft clothes. After wiping allow surfaces to air dry.

4. Confirm the acceptable removal of chloride-containing salts and other corrosive agents by performing the following inspection. The acceptance criteria for confirmation of acceptable cleanliness level is as follows:

   a) Following cleaning the external surfaces shall appear metal clean and free of organic films and contaminants when examined in accordance with Paragraph 7.2.1 of ASTM A380-78 (Reference 9, Section 7.4), except light deposits of atmospheric dust are permissible.

   b) Following the visual examination, perform a wipe test per paragraph 7.2.2 of ASTM A 380-78. The test shall show no deleterious contamination. Surfaces shall be confirmed to comply with Table 302.5 for Class B corrosion-resistant alloys.

5. Verify the TID installed on the upper impact limiter is intact and the identification number matches the number documented on the shipping papers. Make appropriate notifications if tampering is suspected. Remove the TID.
6. Move the transport vehicle to the cask unloading area.
7. Secure the vehicle by applying the brakes or chocking the wheels.

   Note: At facilities requiring the vehicle to move in order to upright or download the cask on the vehicle, the brakes and chocks can be removed and vehicle movement allowed during the process if the vehicle is maintained under the control of an authorized driver or operator.

8. Attach impact limiter slings to the upper impact limiter and a suitable crane hook and take up the slack in the slings.
9. Remove the impact limiter lock wires and the jam and attachment nuts. Remove the impact limiter retaining rods.
10. Remove the upper impact limiter and store it in the upright position in a clean area.
11. Repeat Steps 7-9 for the lower impact limiter.
12. Release the front tie-down assembly from the top forging of the cask and remove the rotation trunnion tie-downs.
13. Remove the two trunnion plugs and store the plugs and bolts to prevent damage. Visually inspect the trunnion recesses for any damage.
14. Using a crane and slings, lift and position a lifting trunnion, install the attachment bolts, and torque the bolts to the value specified in Table 7.1-1. Repeat for the second lifting trunnion.
15. Attach the cask lifting yoke to the cask handling crane hook. Verify the proper operation of the lift arm pneumatic actuation system.
16. Position the cask lifting yoke arms adjacent to the lifting trunnions and close the arms using the actuation system. Visually verify proper yoke arm engagement.
17. Lift and rotate the cask to the vertical orientation on the rotation trunnions. Lift the cask from the transport frame/vehicle rear support structure and position the cask vertically in the designated unloading area.
18. Disengage the yoke from the cask lifting trunnions and remove it from the immediate area.
19. Install appropriate work platforms, scaffolding or lifts to facilitate access to the top of the cask.

7.2.2 Removal of Contents

1. Detorque and remove the lid port coverplate bolts. Visually inspect the bolt threads for damage and store them. Remove the coverplate and store it.
2. Attach a pressure fixture, including a pressure gauge, evacuated gas sample bottle and a valve to the lid port quick-disconnect valve. Measure the cask internal pressure.
3. Withdraw a sample of the cavity gas using the evacuated sample bottle and determine the cask cavity's gaseous activity. If activity and pressure levels are acceptable per facility criteria, vent the cavity gas to an appropriate filter/system.
4. Disconnect the pressure fixture from the lid port.
5. Detorque and remove the cask lid bolts using the reverse of the torquing sequence shown on the lid. Clean and inspect the bolt threads for damage and store them.

6. Install and torque swivel hoist rings to the value specified in Table 7.1-1 (or equivalent lid lifting device) in the four threaded lifting holes in the cask lid.
7. Install and hand-tighten the lid alignment pins in their designated hole locations (#s 14 and 36).
8. Attach an appropriate lid sling set to the swivel hoist rings (or equivalent site-specific approved lid lifting system) and a suitable crane.
9. Lift and remove the cask lid. Decontaminate and store the lid to prevent damage to the seal surfaces and cask cavity spacer, if installed. Record the time the lid is removed.
   Caution: In order to ensure that the fuel clad temperatures do not exceed 400°C, as established by ISG-11, Revision 3, a fuel TSC containing maximum heat load contents (i.e., PWR - 23 kW; BWR - 22 kW) shall be removed from the MAGNATRAN following cask lid removal and placed in a safe condition (i.e., in a MTC or equivalent transfer device). The maximum time to complete the operational sequence from Section 7.2.2, Step 9 through Step 18 shall be < 6 hours. This maximum transfer and preparation time is not applicable to the loading of GTCC waste TSCs as the ISG-11 temperature limits are not applicable.
   In the event that the MAGNATRAN unloading procedure, through removal of the TSC from the cavity, is not completed within the specified time period, corrective actions shall be implemented to cool the TSC in the MAGNATRAN cask through introduction of demineralized water into the cask cavity either directly into the cask or through the vent port if the lid is still installed. The corrective actions shall be implemented with sufficient time to ensure that the maximum TSC unloading time is not exceeded. The external cooling of the TSC shall be continued for a minimum of 24 hours to reduce the fuel clad and TSC internal component temperatures to allow re-start of MAGNATRAN unloading procedures. The maximum time limits of < 6 hours is in effect for each attempted unloading sequence. If cooling of the TSC is required while the TSC is in the MAGNATRAN cask, the cask cavity shall be appropriately drained and dried prior to returning the cask to service.

   Note: The time limits specified in Step 9 are for the maximum allowable heat loads in the MAGNATRAN transport cask. Although TSC unloading times would be longer for lower content decay heat loads, the limits for the maximum heat loads (PWR - 23 kW; BWR - 22 kW) will be conservatively implemented to all content decay heat loads.
10. Remove the lid alignment pins, and using a suitable crane and sling set, install the transfer shield ring in the lid recess.

    Note: The transfer shield ring aligns the transfer adapter to the cask cavity, provides additional side shielding and protects the cask lid seating surface from damage.

11. Position the transfer adapter on the top of the transport cask and connect the shield door ancillary hydraulic actuation system.
12. Install the TSC lifting system swivel hoist rings and lifting slings (or other appropriate TSC lifting system meeting the facility's heavy load program) to the threaded holes in the TSC closure lid and torque to the value specified in Table 7.1-1.
13. Using the MTC lift yoke, lift the empty MTC and place it on the transfer adapter on top of the transport cask. Ensure that the connector assemblies are in the engaged position. Remove the door stops.
14. Install a stabilization system for the MTC, if required by the facility heavy load handling or seismic analysis programs.
15. Disengage the MTC lift yoke and remove it from the area.
16. Open the MTC shield doors using the ancillary hydraulic actuation system.
17. Connect the handling crane to the TSC lifting sling set(s) or the site-specific approved lifting system meeting the facility's heavy load program. Verify that the MTC retaining device is in the engaged position and lift the loaded TSC from the transport cask cavity into the MTC.
18. Using the ancillary hydraulic actuation system, close the MTC shield doors and set the TSC down on the doors. Install the shield door stops.
19. Disengage the TSC lifting sling set(s) from the cask handling crane or disengage the site-specific approved lifting system meeting the facility's heavy load program.
20. Using the MTC lift yoke, engage the lift yoke to the MTC lifting trunnions. Remove the stabilization system from the MTC (if used).
21. Lift the MTC containing the loaded TSC and move it to the designated location for further processing, on-site storage or unloading.
22. Attach lifting slings to the transfer adapter, lift the transfer adapter from the top of the transport cask and move the adapter to a designated storage area.
23. Connect the handling slings and remove the transfer shield ring from the transfer cask lid recess. Store the transfer shield ring in a designated storage area.
24. Take removable contamination smears of the cask inner shell to verify that the package will meet the definition for an empty package in accordance with Department of Transportation (DOT) regulations per 49 CFR 173.428(d).
25. Install the two transport cask lid alignment pins in their designated hole locations (#s 14 and 36).
26. Using the cask lid lifting slings (or equivalent site-specific approved lid lifting system) lift and install the transport cask lid. Remove the lid lifting components.

Note: It is not necessary to replace the metallic seals on the cask lid and lid port coverplate for an empty shipment. The metallic seals will be replaced prior to the next loaded transport.

Note: Depending on the next planned shipment contents, the cask cavity spacer may be left installed on the lid or removed and shipped separately, as appropriate.

27. Remove the cask lid alignment pins.
28. Inspect the 48 lid bolts for damage and replace, as required, with approved spares. Lubricate the bolt with nuclear-grade Never-Seeze, or equivalent, and install the lid bolts to hand tight. In a minimum of four passes of increasing torque, torque the 48 lid bolts to the final value specified in Table 7.1-1 for an empty cask system transport following the torquing sequence pattern marked on the lid.
29. Install the lid port coverplate and bolts on the cask lid, and torque the bolts to the value specified in Table 7.1-1.
30. Remove scaffolding or work platforms from areas around the top of the cask.

7.3 Preparation of Empty Packaging for Transport

1. Using the cask lift yoke connected to the cask handling crane, lift the empty MAGNATRAN transport cask and position it over the rotation trunnion support structure.
2. Lower the cask to engage the rotation trunnions in the transport frame/vehicle rear support structure, rotate the cask to the horizontal orientation and disengage the lift yoke.

   Note: The rotation trunnions are offset from the centerline to ensure rotation of the cask in the proper direction.
3. Using slings and a suitable crane, detorque and remove the nine lifting trunnion attachment bolts from one trunnion. Remove, clean and inspect the trunnion and bolts, observing for damage/wear. Repeat for the second lifting trunnion and bolts. Store the trunnions and bolts.
4. Clean and inspect the trunnion recess. Position and install the trunnion plug. Apply nuclear-grade lubricant, such as Never-Seeze, or equivalent, to the three trunnion plug bolts, and torque the bolts to the value specified in Table 7.1-1. Repeat for the second trunnion recess and plug.
5. Decontaminate and clean the surfaces of the transport cask to ensure removable contamination limits for an empty packaging are met.
6. Install the transport tie-downs over the top forging and on the rotation trunnions.
7. Using the impact limiter lifting sling set, lift and install the lower impact limiter. Install retaining rods and attachment and jam nuts, and torque all the components to the values specified in Table 7.1-1. Install the retaining rod lock wires.
8. Repeat the installation sequence for the upper impact limiter.
9. Perform contamination and radiation surveys and record results. Verify results comply with the applicable requirements of 49 CFR 173.428.
10. Perform final visual inspection of the cask to ensure proper packaging assembly in accordance with the CoC.
11. Apply appropriate labels to the empty package in accordance with 49 CFR 173.428.
12. Install the personnel barrier to the transport frame/vehicle and lock all access points.
13. Review the cask loading inspection checklist and verify all required steps have been appropriately completed.
14. Complete the shipping documentation for an empty package transport.
15. Apply placards to the vehicle in compliance with 49 CFR 172.500 and 173.428 requirements.
16. Advise the carrier of any special instructions and release the empty MAGNATRAN transport cask for shipment.

7.4 References

1. Code of Federal Regulations Title 10, Part 20, "Standards for Protection Against Radiation."
2. Code of Federal Regulations Title 10, Part 71, "Packaging and Transportation of Radioactive Material."
3. Code of Federal Regulations Title 49, Part 173, "Shippers – General Requirements for Shipments and Packaging."
4. Code of Federal Regulations Title 49, Part 172, "Hazardous Materials Table, Special Provisions, Hazardous Materials Communications, Emergency Response Information, and Training Requirements."
5. Interim Staff Guidance (ISG)-11, "Cladding Considerations for the Transportation and Storage of Spent Fuel."
6. MAGNASTOR® Final Safety Analysis Report, current revision.
7. USNRC Certificate of Compliance No. 1031 for the MAGNASTOR® System, current revision.
8. ASME Code, ASME NQA-1-2008, "Quality Assurance Requirements for Cleaning of Fluid Systems and Associated Components for Nuclear Power Plants."
9. ASTM A380-78, "Standard Recommended Practice for Cleaning and Descaling Stainless Steel Parts, Equipment, and Systems."

external surface of the shell at 30° intervals and at five points along the height of the shield (a total of 60 measuring points). In addition, neutron and gamma dose rate measurements are made at the trunnion areas above the neutron shield, at four points below the neutron shield, and at the edges and center of the cask top and bottom surfaces. Dose rates at the top and bottom of the cask are measured with the impact limiters installed. The dose rates measured at contact and at 2.3 m are recorded on the test data sheet. Additional date recorded for the shielding effectiveness test include the total power of the loaded fuel assemblies; date, time and location of test; identification and calibration of instrumentation; and identification of test engineer and operators. To enable the measured dose rates to be evaluated, the burnup and cool time for the actual fuel assemblies loaded into the cask are determined and recorded. From this fuel history data, the total actual neutron and gamma source terms are estimated by using ORIGEN or similar calculations. Utilizing the neutron and gamma source terms estimated (i.e., calculated) gamma and neutron dose rates will be developed in order to properly evaluate the measured dose rates.

If the measured dose rates exceed the estimated dose rates corresponding to the MAGNATRAN fuel contents, the cask User shall notify the NRC in accordance with 10 CFR 71.95. Appropriate corrective measures shall be taken including unloading the TSC from the MAGNATRAN and correction of identified shielding deficiencies. Following corrective actions, the shield effectiveness test shall be re-performed to the original acceptance criteria prior to final cask acceptance for transport operations.

8.1.7 Thermal Acceptance Test

Prior to acceptance of each MAGNATRAN transport cask, a thermal test using electric heaters will be performed on a fabricated packaging to verify that the fabricated and assembled transport cask possesses the heat rejection capabilities evaluated in the thermal analyses in Chapter 3. The thermal test will be performed in accordance with approved written procedures.

8.1.7.1 Thermal Test Setup

A typical thermal test set-up is shown in Figure 8.1-1. As depicted, the thermal test will be performed with the cask positioned horizontally on a test frame. The transport impact limiter or equivalent insulating material will be installed on each end of the cask to simulate the transport configuration. The cask will be located in a covered building in a still environment. The contents heat will be simulated by using electric heaters to apply 23 kW to the inner surface of the transport cask. The electric heating elements will be mounted on a metallic shell and will extend for the full length of the cask cavity except for approximately 6 inches from each end. The metallic heater-mounted test shell will radiate and conduct heat to the inner surface of the cask cavity. The cask bottom or top will receive negligible heat. Due to the small radial gap

between the metallic heater-mounted test shell and the inner cask surface, the heat transfer by convection is negligible compared to the heat transfer by radiation and conduction. Electrical heaters are spaced to provide a uniform heat flux, circumferentially to the cask wall and permit power input to be measured for heating element.

As described below and Figure 8.1-1, six calibrated thermocouples will be installed on the inner surface of the MAGNATRAN transport cask and six calibrated thermocouples will be installed on the cask external surface at the same angular and axial locations as the thermocouples on the cask inner surface.

- Four thermocouples located at approximately 90° intervals (see Figure 8.1-1) on the inner shell surface 88 inches from the inner surface of the cask bottom
- One thermocouple at the upper region (180° location as shown in Figure 8.1-1) of the inner shell surface at 21 inches from the inner surface of the cask bottom
- One thermocouple at the upper region (180° location as shown in Figure 8.1-1) of the inner shell surface at 154 inches from the inner surface of the cask bottom
- Four thermocouples located at approximately 90° intervals (see Figure 8.1-1) on the neutron shell outer surface with the axial location at 88 inches from inner surface of cask bottom and at the thermocouples on the inner shell surface
- One thermocouple at the upper region of the neutron shield shell (180° location as shown in Figure 8.1-1) with the axial location at 154 inches from the inner surface of cask bottom and at the same angular location as the thermocouple on the inner shell surface
- One thermocouple at the upper region of neutron shield shell surface (180° location as shown in Figure 8.1-1) with the axial location at 154 inches from inner surface of cask bottom and at the same angular location as the thermocouple on the inner shell surface

An additional thermocouple is required to measure the ambient temperature. The thermocouples will be attached to strip chart recorders, which may have multiple input channels, or another similar device to allow for continuous monitoring and recording of temperatures during the test. These records will be part of the quality assurance acceptance records for the cask under test.

The nominal test conditions are ambient temperature and with the initial cask body temperatures being 70°F, no solar insolation, still air, and no external radiant heat sources. At these test conditions, the cask surface temperature will be bounded by the calculated steady-state equilibrium temperature of 178°F. It will take about 110 hours for the system to approach steady state condition. The thermal test procedure will provide a thermal transient heat-up curve to show the time at which equilibrium is expected to be established, and a table, or set of curves, that correlates equilibrium neutron shield assembly surface temperature with a range of ambient temperatures. For purposes of the thermal test, equilibrium temperature is assumed to be

established when the change in neutron shield assembly surface temperature no longer exceeds 2°F in a two-hour period.

8.1.7.2 Thermal Test Acceptance Criteria

The purpose of the thermal test is to confirm that the heat rejection capabilities of the as-built MAGNATRAN transport cask are acceptable. Cask thermal test acceptance is based on the demonstration that the measured temperature gradients are less than, or equal to, the thermal gradients calculated in the thermal analyses, as described in Section 8.1.7.3, and that the total heat rejection rate is equal to, or greater than, the cask design basis heat rejection rate.

8.1.7.3 Thermal Analyses for Thermal Test

A three dimensional half-symmetry model based on the full-length model described in Section 3.4.1.1.1 (Figure 3.4-13) is utilized to perform steady state and transient analyses for the usage of the thermal test. The steady state analysis evaluates the temperatures at the thermocouple locations of the thermal test, while the transient analysis identifies the duration for the system to reach a steady state condition.

The model boundary conditions described in Section 3.4.1.1.1 were modified to reflect the actual testing conditions of the transport cask. The main boundary conditions were listed below:

1) A uniform heat flux is applied to the entire inner surface of the cask inner shell based on the design heat load of 23kW.

2) Convection film coefficient for the model, as described in Section 3.2.3, is used.

3) No solar insolance is considered in this analysis.

4) An ambient temperature of 70°F is considered.

In order to compare the analytical results with the thermal test results, the maximum component temperatures and temperatures at three axial locations of the cask inner and outer surfaces are post processed for the steady state condition. The transient thermal analysis confirms that approximately 110 hours are needed for the cask to reach thermal steady state condition.

Figure 8.1-1 Thermal Test Arrangement

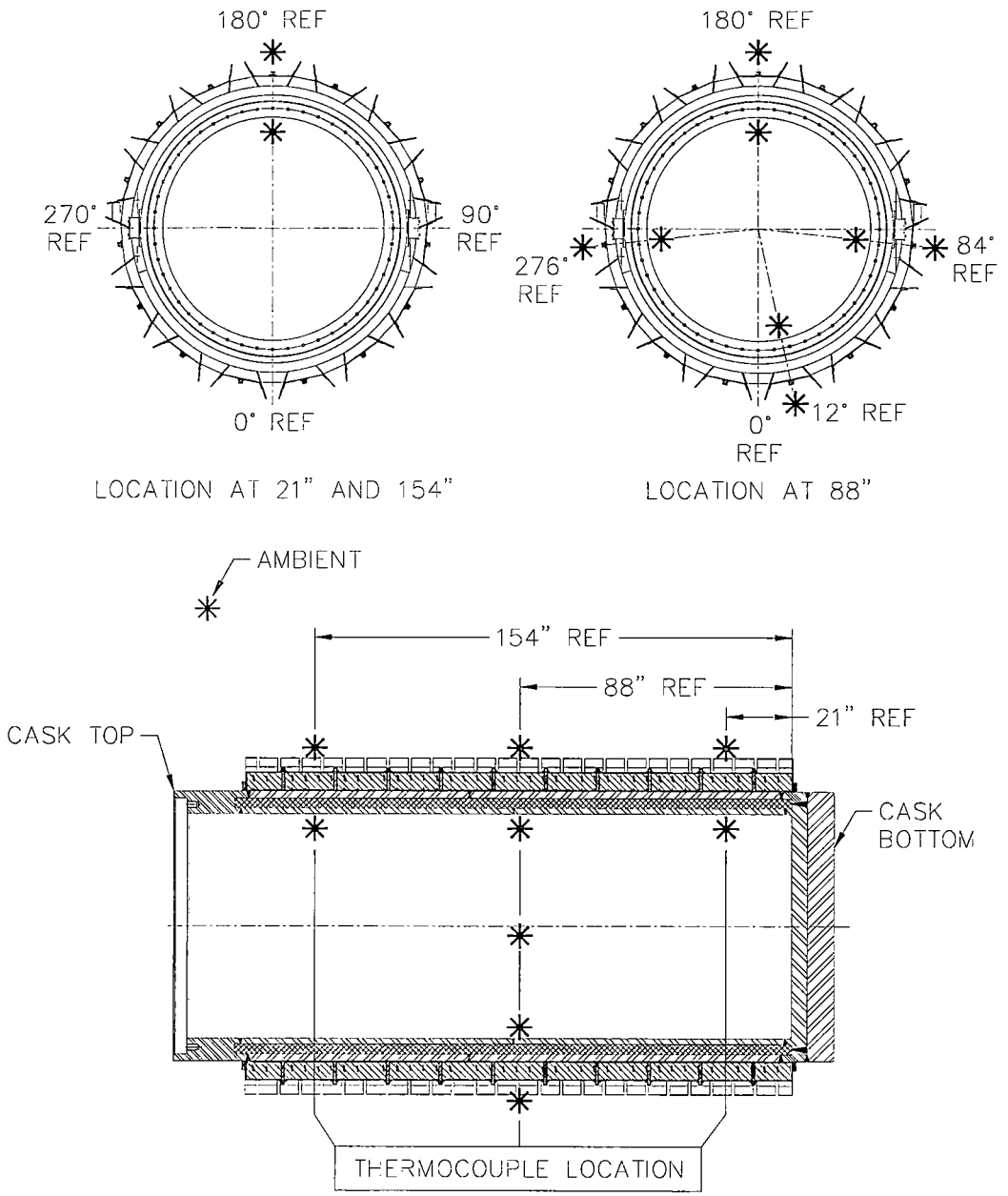

Table 8.2-1 MAGNATRAN Maintenance Schedule

Task/Activity	Frequency
Visual inspection of cavity	Prior to loading
Visual inspection of O-rings	Prior to loading
Visual inspection of neutron shield shell segments for structural or penetration damage	Prior to loading
Visual inspection of cask lid bolts and lid port coverplate bolts	Prior to installation (each use)
Visual and Proper Function Inspection of Cask	Prior to and during each use
Visual inspection of lifting trunnions and rotation trunnions	Prior to and during each use
Liquid penetrant inspection of lifting trunnion and rotation trunnion weld surfaces	Annually during use
Periodic leakage rate test of cask lid and lid port coverplate containment O-rings	Annually during use
Periodic Gamma and Neutron Shield Effectiveness Tests	Every 5 years during operation and use
Pre-shipment leakage rate test of cask lid and lid port coverplate containment O-rings	Prior to each loaded transport
Maintenance leakage rate test of containment system	After replacement or repair of containment boundary components
Replacement of lid and lid port coverplate metallic O-rings	Prior to each loaded transport
Visual inspection of impact limiters for structural or penetration damage	Prior to each loaded transport
Inspection of quick disconnect for proper function	Each cask use
Liquid penetrant inspection of impact limiter shell weld surfaces	Every five years or as required by visual inspection results during operation and use
Liquid penetrant inspection of neutron shield shell assemblies weld surfaces	Every five years or as required by visual inspection results during operation and use
Replacement of quick disconnect	Every two years or as required by performance during operations
Replacement of non-containment O-ring	Annually, or as required by inspection during operations
Replacement of lid port coverplate bolts	Every 20 years, or as required due to thread damage
Replacement of cask lid bolts	Every 20 years or after 350 applications of the specified torque, or as required due to thread damage

8.2.3 Component and Material Tests

Each MAGNATRAN transport cask impact limiter will be visually inspected for damage prior to each loaded transport and will be repaired, as required, using written procedures to return it to its licensed condition in accordance with the applicable License Drawing as referenced in the CoC.

The external surface of the MAGNATRAN transport cask neutron shield will be visually inspected for damage prior to each loading operation and will be repaired, as required, using written procedures to return the affected neutron shield segment to its licensed condition in accordance with the applicable License Drawing as referenced in the CoC.

No valves providing a containment function are present on the MAGNATRAN transport cask packaging. One quick-disconnect is provided in the cask lid port for ease of cask operation. The MAGNATRAN transport cask containment vessel has no rupture disks. The quick-disconnect will be inspected for proper performance and function during each cask use and will be replaced as necessary. The quick-disconnect shall be replaced every two years during transport operations.

The cask lid and lid port cover non-containment O-rings are visually inspected for damage during each cask closure operation. Any identified damage, or failure to seal, is cause for replacement of the O-ring. The cask lid and lid port cover containment boundary metallic O-rings are replaced and leak tested as specified in Table 8.2-1 prior to each loaded transport.

The cask lid and lid port cover bolts are inspected for damage during each cask use, and replaced as required. The cask lid and lid port cover bolts will be completely replaced every 20 years of service.

The gamma and neutron shields of the MAGNATRAN transport cask are not expected to degrade with time or usage. However, to confirm the continued effectiveness of the solid gamma and neutron shields, a separate gamma and neutron radiation shield effectiveness test will be performed on each MAGNATRAN transport cask every five (5) years as identified on Table 8.2-1 or prior to the next loaded transport. The gamma and neutron shield effectiveness test will be performed using approved written procedures and calibrated radiation measurement instrumentation utilizing the procedures, methods, equipment, and acceptance criteria as defined in Section 8.1.6.3. Utilizing the neutron and gamma source terms estimated (i.e., calculated) gamma and neutron dose rates will be developed in order to properly evaluate the measured dose rates. If the measured dose rates exceed the estimated dose rates corresponding to the MAGNATRAN fuel contents, the cask User shall notify the NRC in accordance with 10 CFR 71.95. Appropriate corrective measures shall be taken including unloading the TSC from the MAGNATRAN and correction of identified shielding deficiencies. Following corrective

actions, the shield effectiveness test shall be re-performed to the original acceptance criteria prior to returning the cask to service.

The sealed neutron shield assemblies and the impact limiters welded stainless steel enclosure welds shall be examined by dye penetrant examination every five years or after identification of potential damage to the component as identified on Table 8.2-1 and using the methods and acceptance criteria described in Section 8.1.8.

There are no other MAGNATRAN components or materials that are susceptible to degradation during normal conditions of transport activities.

8.2.4 Thermal Test

The heat transfer capability of the MAGNATRAN transport cask does not degrade over the lifetime of its use for normal conditions of transport. Therefore, no periodic thermal test is required.

8.2.5 Miscellaneous Tests

As summarized in the MAGNATRAN Maintenance Schedule, Table 8.2-1, a number of routine inspections and maintenance activities are performed on the MAGNATRAN cask during use and on defined frequencies. These inspections include visual inspection of the cask cavity and exterior surfaces for foreign material and damage, inspections of the lifting and rotation trunnions for damage prior to and after use. Foreign material and obstructions shall be discarded or appropriately removed. Damage to any containment boundary sealing surface on the cask lid or upper forging seal surface, or lid port cover and corresponding recessed seal surface, or inner shell shall be assessed and repaired, if necessary, including performance of a maintenance leakage rate test of the affected area or component in accordance with Section 8.2.2.2. All repairs and retesting shall be performed in accordance with approved procedures and an approved QA program. The final condition of the cask repaired areas shall be in compliance with the applicable License Drawing(s) as referenced in the CoC.

In addition, the maintenance schedule defines a periodic inspection, test and equipment replacement schedule for key operational components of the cask system and for components that may be damaged during use (e.g., impact limiters, neutron shield sections, lifting and rotation trunnions, etc.) to ensure continued proper functioning in accordance with the analyses in the SAR. For each MAGNATRAN transport cask loaded for transport, the following information is included in the cask loading report: results of the visual inspections; leak test results; shielding and radiological contamination surveys; identification information for the package contents; date, time, and location of the cask loading operations; and remarks regarding

replaced components. The specific requirements of a recommended cask loading report will be detailed in the MAGNATRAN transport cask operations and maintenance manual.